Functional analysis of cancer/testis antigens in human cancer

Anna Pagotto

A thesis submitted in fulfilment of the requirements for the degree of

Doctor of Philosophy

St Hilda's College

Ludwig Institute for Cancer Research, ORCRB

Nuffield Department of Clinical Medicine

University of Oxford

Trinity 2012

Declaration

All the work presented in this thesis is the result of my own work unless otherwise stated and does not constitute part of any other thesis. The work herein described was carried out while I was a graduate student at the Ludwig Institute for Cancer Research, under the supervision of Professor Xin Lu.

44,836 words

Functional analysis of cancer/testis antigens in human cancer

Anna Pagotto, St Hilda's College, DPhil in Clinical Medicine, Trinity 2012

Abstract

The cancer/testis (CT) antigens are a family of genes that are silenced in the majority of normal human tissues, except for the testes, but are specifically re-expressed in a number of human tumours. Interestingly, their expression is frequently found in only a subpopulation of cells in malignancies, but the reasons for this heterogeneous expression pattern have not yet been investigated. Since little is known about the regulation and the biological significance of the CT antigens, it is not yet clear whether they play an active role in tumourigenesis or whether their expression is a consequence of cancer progression. To address this question, attempts were made to develop an *in vitro* experimental model that mimics tumours expressing CT antigens. Twenty-one melanoma, small cell lung cancer (SCLC) and multiple myeloma (MM) cell lines were screened for the expression of three CT antigens: NY-ESO-1, its binding partner MAGE-C1, and a molecule that is closely related to MAGE-C1 called MAGE-C2. Intriguingly, some of these cell lines showed heterogeneous expression patterns that resembled those observed in tumour samples. Selected cell lines were treated with MG132, an inhibitor of the proteasome protein degradation pathway, to investigate the post-translational regulation of CT antigens. Insoluble MAGE-C1 and NY-ESO-1 were stabilised upon treatment, moreover MG132 caused accumulation of these two antigens at the centrosome. Interestingly, co-transfection experiments showed that NY-ESO-1 enhances the MG132-induced stabilisation of MAGE-C1 MAGE homology domain (MHD). In addition to proteasome degradation, SUMO-1 conjugation was also identified as a post-translational regulatory mechanism for MAGE-C1. Finally, MAGE-C1 knockdown experiments demonstrated that depletion of this antigen increases cell death in response to endoplasmic reticulum (ER) stress, while reducing the stability of the pro-survival protein Mcl-1. Thus, MAGE-C1 is a novel inhibitor of ER stress-induced apoptosis. As a whole, this study provides new insights into the expression, regulation and function of these CT antigens in cancer cells.

Acknowledgements

I would like to express my gratitude to my supervisor, Professor Xin Lu, whose guidance and expertise has enabled me to write this thesis, and to the Ludwig Institute for Cancer Research for the support it has provided. I would also like to thank Professor Colin Goding for all his help throughout the years of PhD, and Evelyn Harvey for the valuable suggestions regarding the thesis.

I am extremely grateful to our collaborators at the LICR New York branch Dr Andy Simpson, Dr Otavia Caballero and Dr Sylvie Devalle for providing many of the constructs utilised in this thesis and for the fruitful scientific discussions.

Massive thanks to all the members of the Lu group and the colleagues from the institute, in particular to the ones that have also become my good friends: the other Italians Luca and Mario, thanks to whom I never felt homesick, my colleagues from the "cool" corner Chris, Ewa and Emma for our quirky and funny conversations, Sofia for the unwavering enthusiasm, Jorge De la Mancha for the passion and excitement he transmits, Susana for her precious help with the project.

I would also like to thank my friends from outside the lab, Cristiano, Massimo and Mikey, my ex-flatmates Haibo and James and my great girlfriends Hilde and Fiona. Each of them is special to me. Special thanks go to Elise for sharing with me the PhD tribulations and simply being a great person, and to Eleonora for her warmth, her crazy stories and her invaluable friendship.

My 'old' Italian friends Chiara, Mena, Federico and Vico deserve a particular mention for always welcoming me every time I go back home and making my time there awesome.

Thanks to Enrico, who has taught me positivity and optimism, who always makes me laugh and who reminds me of the really important things in life.

Finally, I would like to dedicate this thesis to my family: my parents, my sister, my grandmas, my uncle Mauro and my cats; thanks for taking care of me, supporting me, scolding me when needed and always being proud of me.

Table of contents

Chapter I: Introduction 18

1.1 Tumourigenmesis 18

1.2 Apoptosis and cancer 22

1.2.1 Caspases 23

1.2.2 The extrinsic apoptotic pathway 24

1.2.3 The intrinsic apoptotic pathway: role of the organelles 26

1.2.3.1 Role of the mitochondrion 26

1.2.3.2 Role of the endoplasmic reticulum 26

1.2.4 The Bcl-2 family of proteins 30

1.2.5 Ubiquitination: a role in apoptosis and cancer 38

1.2.6 SUMOylation: a role in apoptosis and cancer 42

1.3 Tumour antigens 45

1.3.1 The cancer/testis antigens: classification 48

1.3.1.1 The MAGE family 50

1.3.1.2 The NY-ESO-1 family 52

1.3.1.3 The GAGE/PAGE/XAGE family 52

1.3.1.4 The SSX, SPANX, and CSAGE/TRAG-3 families 53

1.3.2 CT antigen expression 54

1.3.2.1 CT genes in normal tissues 54

1.3.2.2 CT genes in cancer 56

1.3.3 CT antigen regulation 59

1.3.4 CT antigens in cancer immunotherapy 63

1.3.4.1 MAGE-based cancer vaccines *66*

1.3.4.2 NY-ESO-1-based cancer vaccines *67*

1.3.5 Biological functions of CT antigens 69

1.3.5.1 Function of MAGE proteins *69*

1.3.5.2 Function of SSX proteins *75*

1.3.5.3 Function of other CT antigens *76*

1.4 Aim of study 82

Chapter II: Materials and Methods 83

2.1 Materials 83

2.1.1 Reagents 83

2.1.2 Antibodies 95

2.1.3 Plasmids 97

2.1.4 Cell lines 98

2.2 Methods 100

2.2.1 Tissue culture 100

2.2.2 DNA techniques 101

2.2.3 RNA manipulation 104

2.2.4 Protein manipulation 105

2.2.5 Cell based assays 109

2.2.6 Data analysis 111

Chapter III: NY-ESO-1, MAGE-C1 and MAGE-C2 are heterogeneously expressed in human cancer cell lines 112

3.1 Introduction 112

3.2 Results 116

3.2.1 NY-ESO-1, MAGE-C1 and MAGE-C2 expression patterns vary in different human melanoma cell lines 116

3.2.2 NY-ESO-1 and MAGE-C1 are not always co-expressed in the same cells 123

3.2.3 NY-ESO-1, MAGE-C1 and MAGE-C2 expression patterns vary in different human SCLC cell lines 123

3.2.4 NY-ESO-1, MAGE-C1 and MAGE-C2 expression patterns vary in different human MM cell lines 128

3.3 Summary and discussion 132

Chapter IV: NY-ESO-1 affects the stability of MAGE-C1 MAGE homology domain 134

4.1 Introduction 134

4.2 Results 136

4.2.1 Proteasome inhibitor MG132 induces insoluble MAGE-C1, which accumulates at the centrosome. 136

4.2.2 MAGE-C1 and NY-ESO-1 co-localise at the centrosome after MG132 treatment 139

4.2.3 Proteasome inhibitor MG132 induces insoluble MAGE-C2 142

4.2.4 MAGE-C1 and NY-ESO-1 centrosome localisation is specifically induced by proteasome inhibitors. 143

4.2.5 MAGE-C1 and NY-ESO-1 localise at the centrosome independently from each other 145

4.2.6 The MAGE homology domain of MAGE-C1 is stabilised by MG132 treatment 149

4.2.7 NY-ESO-1 deletion mutants 91-180 and 50-150 are stabilised and localise at the centrosome upon MG132 treatment. 152

4.2.8 Lysine 124 is not essential for NY-ESO-1 localisation at the centrosome. 157

4.2.9 NY-ESO-1 enhances the stabilisation of MAGE-C1 MHD upon MG132 treatment. 158

4.2.10 MAGE-C1 is SUMOylated. 162

4.3 Summary and discussion.....167

Chapter V: MAGE-C1 inhibits apoptosis and affects Mcl-1 stability in response to endoplasmic reticulum stress 171

5.1 Introduction.....171

5.2 Results.....175

5.2.1 MAGE-C1, but not NY-ESO-1, inhibits cell death in response to specific types of cellular stress. 175

5.2.2 MAGE-C1 does not affect p53 protein levels. 183

5.2.3 MAGE-C1 regulates affects Mcl-1 protein levels in response to tunicamycin treatment. 185

5.2.4 MAGE-C1 regulates Mcl-1 accumulation upon proteasome inhibition during ER stress. 188

5.2.5 MAGE-C1 binds Mcl-1. 189

5.2.6 MAGE-C1 binding with Mcl-1 is independent of NY-ESO-1. 190

5.2.7 MAGE-C1 binds to the N-terminus of Mcl-1. 192

5.2.8 MAGE-C1 is modified in mitosis. 194

5.3 Summary and discussion.....196

Chapter VI: Conclusions and future perspectives.....200

6.1 CT antigens are heterogeneously expressed in human cancer cell lines.....200

6.2 Modulating MAGE-C1 stability: a novel potential function for NY-ESO-1.....202

6.3 MAGE-C1 and Mcl-1: a role in ER stress-induced apoptosis 207

References.....211

List of figures and tables

Figure 1.1 The extrinsic and intrinsic apoptotic pathways 25

Figure 1.2 The unfolded protein response 28

Figure 1.3 The Bcl-2 family 31

Figure 1.4 Bcl-2 family role in apoptosis at the mitochondria and the ER 33

Figure 1.5 Schematic representation of Mcl-1 regulation 37

Figure 1.6 The proteasome pathway 41

Figure 1.7 The SUMOylation pathway 44

Figure 1.8 Schematic representation of some MAGE family members 51

Figure 1.9 CT antigen expression in normal tissues and tumours 57

Figure 1.10 Regulation of MAGE antigens 62

Figure 3.1 Analysis of CT antigen expression in melanoma cell lines 118

Figure 3.2 Immunofluorescence staining of endogenous CT antigens in human melanoma cell lines 122

Figure 3.3 Immunofluorescence double staining of endogenous MAGE-C1 and NY-ESO-1 in SK-MEL-14 123

Figure 3.4 Analysis of CT antigen expression in SCLC cell lines 124

Figure 3.5 Immunofluorescence staining of endogenous CT antigens in human SCLC cell lines 127

Figure 3.6 Analysis of CT antigen expression in MM cell lines 130

Figure 4.1 Proteasome inhibitor MG132 induces insoluble MAGE-C1, which accumulates at the centrosome 138

Figure 4.2 MAGE-C1 and NY-ESO-1 co-localise at the centrosome after MG132 treatment 140

Figure 4.3 Proteasome inhibitor MG132 induces insoluble MAGE-C2 142

Figure 4.4 MAGE-C1 and NY-ESO-1 centrosome localisation is specifically induced by proteasome inhibitors 144
Figure 4.5 MAGE-C1 and NY-ESO-1 localise at the centrosome independently from each other 146
Figure 4.6 The MAGE homology domain of MAGE-C1 is stabilised by MG132 treatment 150
Figure 4.7 Subcellular localisation of MAGE-C1 deletion mutants 151
Figure 4.8 NY-ESO-1 deletion mutants 91-180 and 50-150 are stabilised after MG132 treatment 153
Figure 4.9 Subcellular localisation of NY-ESO-1 deletion mutants in NIH3T3 cells 154
Figure 4.10 Subcellular localisation of NY-ESO-1 deletion mutants in SK-MEL-37 cells 155
Figure 4.11 Lysine 124 is not essential for NY-ESO-1 localisation at the centrosome 157
Figure 4.12 NY-ESO-1 modulates the stability of MAGE-C1 C-terminus 159
Figure 4.13 NY-ESO-1 enhances the stabilisation of MAGE-C1 MHD upon MG132 treatment 161
Figure 4.14 MAGE-C1 is not ubiquitinated or glycosylated upon MG132 treatment 163
Figure 4.15 MAGE-C1 is SUMO-1-conjugated 165
Figure 5.1 Characterisation of MAGE-C1 and NY-ESO-1 expression in U2OS and H1299 cancer cell lines 176
Figure 5.2 MAGE-C1 RNAi induces cell death in response to specific types of stress 178
Figure 5.3 MAGE-C1 RNAi does not affect the cell cycle 180
Figure 5.4 NY-ESO-1 RNAi does not affect apoptosis or the cell cycle 182
Figure 5.5 MAGE-C1 RNAi does not affect p53 protein levels 184
Figure 5.6 MAGE-C1 RNAi affects Mcl-1 protein levels upon tunicamycin treatment 186
Figure 5.7 MAGE-C1 RNAi affects Mcl-1 stabilisation in ER stress conditions 189
Figure 5.8 MAGE-C1 binds Mcl-1 190
Figure 5.9 MAGE-C1 binding with Mcl-1 is independent of NY-ESO-1 191
Figure 5.10 MAGE-C1 binds to the N-terminus of Mcl-1 193

Figure 5.11 MAGE-C1 is modified in mitosis 195

Figure 6.1 Model illustrating MAGE-C1 inhibition of ER stress-induced apoptosis and MAGE-C1 protein regulation 210

Table 1.1 Ubiquitin-proteasome pathway proteins affecting apoptosis 38

Table 1.2 CT-X antigen most studied families 49

Table 1.3 Published mRNA expression frequencies of some CT genes in various cancers 56

Table 1.4 Function of MAGE proteins in relation to their binding partners 75

Table 1.5 Function of CT antigens other than the MAGE family 81

Table 3.1 Summary of melanoma staining screening 119

Table 3.2 Summary of SCLC staining screening 125

Table 3.3 Summary of MM staining screening 131

Abbreviations

ADAM2	A disintegrin and metalloprotease domain 2
ADP	Adenosine diphosphate
AFP	Alphafetoprotein
AIF	Apoptosis inducing factor
AML	Acute myeloid leukaemia
AML1	Acute myeloid leukemia 1 protein
AMP	Adenosine monophosphate
AOS1	Activator of SUMO1
AP-1	Activator protein 1
Apaf-1	Apoptotic protease activating factor-1
APC	Adenomatous polyposis coli
APC	Anaphase-promoting complex
AR	Androgen receptor
Arf	Alternate reading frame of the INK4a/ARF locus
ASK1	Apoptosis-signal-regulating kinase 1
ATF	Activating transcription factor
ATP	Adenosine triphosphate
Bad	Bcl-2-associated death promoter
Bak	Bcl-2 homologous antagonist killer
Bax	Bcl-2-associated X protein
Bcl-2	B-cell lymphoma 2
Bcl-w	B-cell lymphoma w
Bcl-xL	B-cell lymphoma x large
BCR-ABL	Breakpoint cluster region- Abelson murine leukemia viral oncogene homolog
BF-1	Brain factor-1
bFGF	Basic fibroblast growth factor
BH	Bcl-2 homology
Bid	BH3-interacting domain death agonist
Bik	Bcl-2-interacting killer
Bim	Bcl-2 interacting mediator of cell death
Blk	B lymphocyte kinase
Bmf	Bcl2 modifying factor
BMP	Bone morphogenetic protein
BNIP3	BCL2/adenovirus E1B 19 kDa protein-interacting protein 3
Bok/Mtd	Bcl2-related ovarian killer/matador
BORIS	Brother of the regulator of imprinted sites
BRCA1	Breast cancer 1
BRDT	Bromodomain, testis-specific
CAGE	Cancer antigen
CAMEL	CTL-recognised antigen on melanoma
Caspase	Cysteine ASPartyl protease

Cdc20	Cell-division cycle protein 20
Cdk	Cyclin-dependent kinase
CEA	Carcinoembryonic antigen
Ced	Cell death protein
CHOP	C/EBP homologous protein
CK	Casein kinase
CLL	Chronic lymphocytic leukaemia
CSAGE/TRAG-3	Chondrosarcoma associated gene 1/ taxol resistance associated gene 3
CSC	Cancer stem cell
CT	Cancer/testis
CTCF	CCCTC-binding factor
CTL	Cytotoxic T Lymphocyte
CTLA-4	Cytotoxic T lymphocyte-associated protein 4
CYLD	Cylindromatosis
DAPI	4',6-diamidino-2-phenylindole
DAPI	4',6-diamidino-2-phenylindole
DAXX	Death-domain associated protein
DD	Death domain
DED	Death effector domain
DISC	Death inducing signalling complex
Dlx	Distal-less homeobox
DMSO	Dimethylsulphoxide
DMSO	Dimethyl sulfoxide
DNA	Deoxyribonucleic acid
dNTP	Deoxyribonucleotide phosphate
DR	Death receptor
DTT	Dithiotreitol
DTT	Dithiotreitol
E1A	Early region 1 A of adenovirus
EBNA	Epstein-Barr nuclear antigen 1
EDTA	Ethylene diamine tetraacetic acid
EGF	Epidermal growth factor
eIF	Eukaryotic Initiation Factor
ER	Endoplasmic reticulum
ERAD	ER-associated degradation
ERK	Extracellular signal-regulated kinase
ERV29	ER-derived vesicles protein
ESC	Embryonic stem cells
ESO3	Esophageal squamous cell carcinoma 3
ETO	Eight twenty one protein
Ets	E-twenty six
FADD	Fas-associated polypeptide with death domain
FAK	Focal adhesion kinase
Fbw7	F-box and WD repeat domain containing 7, E3 ubiquitin protein ligase
FDA	Food and Drug Administration

FITC	Fluorescein isothiocyanate
FL	Full length
FLIP	Fetal liver LKB1-interacting protein
FMRP	Fragile X mental retardation protein
FOXO4	Forkhead box O4
GADD34	Growth arrest and DNA damage-inducible protein 34
GADD45	Growth arrest and DNA damage-inducible protein 45
GAGE	X antigen family
GAPDH	Glyceraldehyde 3-phosphate dehydrogenase
GFP	Green fluorescent protein
GRP	Glucose-regulated protein
GSK-3	Glycogen synthase kinase-3
HAGE	Helical antigen
HAT	Histone acetyl-transferase
HDAC	Histone deacetlyases
HECT	Homologous to the E6-AP Carboxyl Terminus
HER-2	Human epidermal growth factor receptor 2
HIF	Hypoxia-inducible factor
HIPK2	Homeodomain interacting protein kinase 2
HRK	Harakiri
HSE	Heat shock elements
Hsp	Heat shock protien
HSR	Heat shock response
IAP	Inhibitor of apoptosis protein
IB	Immunoblot
ID1	Inhibitor of DNA binding 1
IFN-γ	Interferon-γ
IgG	Immunoglobulin
IKK	IκB kinase
IL	Interleukin
IP3R	Inositol triphosphate receptor
IRE1	Inositol-requiring enzyme 1
IRF1	Interferon regulatory factor 1
IκB	Inhibitor of NFκB
JAK	Janus kinase
JNK	Jun N-terminal kinase
KAP-1	Krüppel-associated protein
Ki67	Antigen identified by monoclonal antibody *Ki-67*
KRAB	Krueppel-associated box
KSP	Kinesin spindle protein
LAGE-1	L antigen family member 1
LMP	LIM mineralization protein
MAGE	Melanoma Antigen Genes
MALT-1	Mucosa-associated lymphoid tissue lymphoma translocation protein 1
MAP	Microtubule-associated protein

MAPK	Mitogen-activated protein kinase
Mcl-1	Myeloid cell leukemia 1
Mcl-1S	Myeloid cell leukemia 1 short isoform
Mdm2	Murine double mutant 2
MdmX	Murine double minute X
Melan-A/MART-1	Melanoma antigen recognised by T-cells 1
MHC	Major histocompatibility complex
MHD	MAGE homology domain
MIZ-1	Myc-interacting zinc finger protein 1
MM	Multiple myeloma
Msx	Msh homeobox
MTOC	Microtubule-organising centre
MUC-1	Mucin 1
Mule/ARF-BP1	Mcl-1 ubiquitin ligase E3/ARF binding protein 1
NEMO	NF-κB essential modulator
NFY	Nuclear transcription factor Y
NFκB	Nuclear factor of kappa light polypeptide gene enhancer in B-cells
Nix	Nip3-like protein X
NPM	Nucleophosmin
NRAGE	Neurotrophin receptor-interacting MAGE homolog
NSCLC	Non-small cell lung cancer
NXF2	Nuclear RNA export factor 2
NY-ESO-1	New York esophageal squamous cell carcinoma 1
p75NTR	p75 neurotrophin receptor
PAGE	P antigen family (prostete associated)
PARP	Poly ADP ribose polymerase
PAS	Per ARNT Sim
PAX9	Paired box gene 9
PCNA	Proliferating cell nuclear antigen
PCR	Polymerase chain reaction
PERK	Pancreatic ER kinase (PKR)-like ER kinase
PEST	Peptide sequence which is rich in proline (P), glutamic acid (E), serine (S), and threonine (T)
PHD	Prolyl hydroxylase
PI	Propidium Iodide
PI3K	Phosphoinoside-3 kinase
PIAS3	Protein inhibitor of activated STAT, 3
Piwil2	Piwi-like2
PKA	Protein kinase A
PKB	Protein kinase B (Akt)
PKC	Protein kinase C
PML	Promyelocytic leukaemia
PML	Promyelocytic leukemia
PNGase F	Peptide: N-Glycosidase F
PP1	Protein phosphatase 1

PRAME	Preferentially Expressed Antigen of Melanoma
PSA	Prostate-specific antigen
PT	Permeability transition
PTEN	Phosphatase and tensin homolog
Puma	p53 upregulated modulator of apoptosis
PUMA	p53 upregulated modulator of apoptosis
qRT-PCR	Quantitative reverse transcriptase PCR
RAR	Retinoic acid receptor
Rb	Retinoblastoma
RING	Really Interesting New Gene
RIP1	Receptor interacting protein 1
RNA	Ribonucleic acid
RNAi	RNA interference
RNAi	RNA-interference
ROS	Reactive oxygen species
ROS	Reactive oxygen species
SC35	Splicing component, 35 kDa
SCF	Skp1-Cul1-F-box protein
SCLC	Small cell lung cancer
SCP-1	Synaptonemal complex protein 1
SENP	SUMO1/sentrin specific peptidase
SERCA	Sarcoplasmic/endoplasmic reticulum Ca^{2+}-dependent ATPase
SIAH	Seven in absentia homolog 1
siRNA	Small interfering RNA
SKIP	SKI-interacting protein
SLCO6A1	Solute carrier organic anion transporter family, member 6A1
Smac/Diablo	Second mitochondria-derived activator of caspases/direct IAP binding protein with low pI
SMAD	Mothers against decapentaplegic homolog
Sp1	Specificity protein 1
Sp1	Specificity Protein 1
SPAG9	Sperm-associated antigen 9
SPANX	Sperm protein associated with the nucleus on the X chromosome
Spike	Small protein with inherent killing effect
Src	Sarcoma
SS18	Synovial sarcoma translocation, chromosome 18
SSX	Synovial sarcoma, X breakpoint
SSXRD	SSX repression domain
STAT3	Signal transducer and activator of transcription 3
SUSP4	SUMO specific peptidase 4
SV40 LT	Simian Vacuolating Virus 40 large T antigen
TAF7	TATA box binding protein (TBP)-associated factor 7
TAF7L	TATA box binding protein (TBP)-associated factor 7L
TAP	Transporters associated with antigen processing
TFIID	Transcription Factor II D
TGFβ	Transforming growth factor β

TNF	Tumour necrosis factor
TNFR	Tumour necrosis factor receptor
TPX1	Testis specific protein 1
TRADD	TNF receptor-associated death domain
TRAF2	TNF-receptor-associated factor 2
TRAIL	TNF-related apoptosis-inducing ligand
TRITC	Tetramethylrhodamine-5-(and 6)-isothiocyanate
TSP50	Testis-specific protease 50
UBA2	Ubiquitin-like modifier activating enzyme 2
UBC13	Ubiquitin-conjugating enzyme 13
UBC9	Ubiquitin-conjugating enzyme 9
UBCH5	Ubiquitin-conjugating enzyme H5
UNC5H1	UNC-5 homolog 1
UPR	Unfolded protein response
USP	Ubiquitin specific peptidase
USP9X	Ubiquitin specific peptidase 9, X-linked
UV	Ultraviolet
VEGF	Vascular endothelial growth factor
VHL	Von Hippel–Lindau
WT1	Wilms' tumour gene 1
XAGE	G antigen family
XBP1	X-box binding protein 1
XIAP	X-linked inhibitor of apoptosis
β-TrCP	β- transducin repeat containing E3 ubiquitin protein ligase

Chapter I: Introduction

1.1 Tumourigenesis

Tumour formation is a multistep process involving dynamic changes in the genome by which normal cells acquire malignant characteristics. The accumulation of genetic mutations and epigenetic alterations confers selective growth advantage to subclones of cells, resulting in uncontrolled cell division and ability to invade and destroy normal tissues.

Although there is much diversity and heterogeneity amongst various cancers, a few key alterations have been identified as being required for a cell to become cancerous, and are therefore considered the hallmarks of cancer: self-sufficiency in growth signals, insensitivity to growth-inhibitory signals, evasion of programmed cell death (apoptosis), limitless replicative potential, sustained angiogenesis, and tissue invasion and metastasis (Hanahan and Weinberg, 2000). More recently, two additional hallmarks have been added to the current concept of cancer, these are deregulation in cellular energetics and the capacity to evade immune destruction. The acquisition of the hallmarks in cancer cells is made possible by enabling traits, such as intrinsic genomic instability, which facilitates the generation of random mutations including chromosomal rearrangements, and the ability of the tumour to promote inflammation (Hanahan and Weinberg, 2011).

In most cases the DNA mutations involved in tumourigenesis arise spontaneously (non-inherited cancer), but they can also be inherited through parental genes (familial or hereditary cancer). For example, some breast and ovarian cancers are the consequences of familial mutations within the *BRCA1* gene (Narod et al., 1993), and a form of colon cancer is due to acquired mutations in the Adenomatous Polyposis (*APC*) gene (Kinzler and Vogelstein, 1996).

Viral infection is another common cause of cancer formation (Carrillo-Infante et al., 2007): some examples of well-known tumorigenic viruses are Human Papilloma virus (HPV), involved in the

onset of cervical cancer, Hepatitis B virus (HBV), which participates in the generation of liver cancer, and Epstein-Barr virus (EBV), which is associated with the induction of lymphoma (Geller, 2002; Pattle and Farrell, 2006; Walboomers et al., 1999). Viruses need the host cell machinery to survive and replicate, therefore they disrupt signalling pathways of the cellular host to their advantage. The investigation of their targets in the host cell led to the concept of proto-oncogenes.

Proto-oncogenes are genes critical for proliferation, survival, angiogenesis and normal homeostasis that become oncogenic due to increased expression or function (Todd and Wong, 1999). They are in general dominant genes, therefore the alteration of one allele is sufficient to increase their expression and function and confer their oncogenic activity.

The integration of a retroviral genome close to proto-oncogenes can lead to their activation, (e.g. avian leukaemia virus and *c-Myc* (Hayward et al., 1981)). Viruses can also carry in their genome transformed cellular genes supposedly integrated from abnormal splicing during the packaging of the new virion; this is the case for Rous Sarcoma virus, which causes sarcoma in chickens and presents a mutated form of the proto-oncogene *c-Src* which misses a C-terminal inhibitory phosphorylation site (Kmiecik and Shalloway, 1987). Other mechanisms of oncogene induction include point mutations within their sequence that affect activity or conformation (e.g., *Ras*), gene duplication (e.g., *c-Myc*) and chromosomal translocations causing either an increase in gene expression or the expression of a fusion protein (e.g., *BCR-ABL* fusion gene) (Bos, 1989; Ren, 2005; Wong et al., 1986).

In contrast to oncogenes, tumour suppressor genes are generally involved in the repression of the cell cycle or in the promotion of apoptosis. Most tumour suppressors are recessive as they usually require inactivation of both copies of the gene in order to cause cellular alteration (Stanbridge, 1990). However, some non-classical tumour suppressors such as *p53* and $p27^{Kip1}$ are haploinsufficient, meaning that the loss of one allele alone is sufficient to confer a selective advantage towards tumour growth (Cook and McCaw, 2000).

Tumour suppressor have been classified into three main subgroups (Kinzler and Vogelstein, 1998): the 'gatekeepers', the 'caretakers' and the 'landscapers'. The 'gatekeeper' genes, such as *p53*, *Rb*, *VHL* and *APC*, are directly involved in controlling cell growth. The 'caretakers' typically encode proteins involved in DNA repair after damage, therefore their inactivation leads to an increase in mutation rate. The 'landscapers' are genes which, when mutated, can increase the risk of alterations in the stromal environment, facilitating the onset of cancer.

In addition to mutations, tumourigenesis can arise from epigenetic alterations, namely heritable changes in gene expression that occur without alteration in DNA sequence (Egger et al., 2004). One common mechanism is based on DNA methylation, an event that in humans occurs almost exclusively at CpG dinucleotides. Most CpG sequences in the genome are methylated. The modification is generally repressive to transcription and helps to maintain silencing of transposable elements, thereby enhancing genome stability. In cancer, aberrant methylation of CG in CpG islands often results in silencing tumour suppressor genes, such as *BRCA1* and *APC* (Yang et al., 2006), whereas global hypomethylation leads to genome instability and inappropriate activation of oncogenes (Ehrlich, 2002). Interestingly, methylation seems to be specific to the tumour type and increased expression of DNA methyltransferase proteins is frequently observed (Park et al., 2006; Peng et al., 2006). Histone modifications, namely acetylation, methylation and phosphorylation, also play a role in transcriptional regulation and so each has the potential to be oncogenic if a deregulated deposition leads, for example, to loss of expression of a tumour suppressor gene. Many histone acetyltransferase (HAT) genes are altered in some way in a variety of cancers, for instance the *p300* HAT gene is mutated in a number of gastrointestinal tumours (Muraoka et al., 1996; Zhang and Dent, 2005).

Recently a class of non-coding small RNA, known as microRNAs (miRNAs), has been shown to be capable of deregulating gene expression and enhancing tumour formation (Garzon et al., 2010). MicroRNAs are involved in the regulation of cellular differentiation, proliferation and apoptosis by controlling the stability or the translation of target messenger RNAs (Bartel, 2004). To date, more than 200 microRNAs have been identified in humans and many studies of

malignant tissues reveal deregulated patterns of these miRNAs. For example, the mir-15a–mir-16-1 cluster is deleted or downregulated in the B cells of some patients affected by chronic lymphocytic leukaemia (CLL). These miRNAs target the pro-survival protein Bcl-2 mRNA, therefore their loss leads to an upregulation in this gene (Calin et al., 2002; Cimmino et al., 2005).

1.2 Apoptosis and cancer

Tissue homeostasis is dependent on the perfect balance between cell growth and programmed cell death (or apoptosis). Proliferation and apoptosis are intimately coupled, and an imbalance can result in pathological conditions linked with unwanted apoptosis, including neurodegenerative and autoimmune diseases. Conversely, evasion of programmed cell death is a hallmark of most and perhaps all types of cancer.

Cell proliferation occurs by means of the cell cycle or cell division, an essential physiological event in which the cell duplicates its genome and gives rise to two daughter cells.

The cell cycle is divided in four distinct phases: G1 phase, S phase (synthesis), G2 phase (collectively known as interphase) and M phase (mitosis). The G1 phase involves a high rate of biosynthesis and growth in preparation for the S phase, in which the DNA content is doubled as a result of chromosome replication; the G2 phase is another biosynthetic step mainly involving the production of microtubules, which are required during the process of mitosis. During the relatively brief M phase, cell growth stops and cellular energy is focused on the separation of chromosomes and the orderly division into two daughter cells (cytokinesis) (Norbury and Nurse, 1992). Activation of each phase is dependent on the proper progression and completion of the previous one. Cells that have temporarily or reversibly stopped dividing, for example upon growth factors or nutrient deprivation, are said to have entered a state of quiescence called G0 phase. These non-proliferative cells can upon appropriate external stimuli re-enter the cell cycle (Pardee, 1989).

The process of apoptosis is triggered in response to a diverse range of cell signals, which may originate either extracellularly (extrinsic inducers) or intracellularly (intrinsic inducers).

Apoptosis is characterised by a series of morphological changes such as membrane blebbing, cell shrinkage, chromatin condensation, DNA fragmentation (Wyllie, 1980a; Wyllie et al., 1980b) and randomisation of the distribution of phosphatidyl serine between the inner and the outer leaflets of the plasma membrane (Nicoletti et al., 1991). Ultimately cells disintegrate into membrane-bound apoptotic bodies, containing organelles and nuclear fragments, which are then phagocytosed and

rapidly degraded, thereby avoiding any inflammatory response in the surrounding environment. The absence of inflammation is one of the major differences between apoptosis and another form of cell death, necrosis, which is characterised by unregulated cell swelling and release of the cellular content into the extracellular space (Savill and Fadok, 2000). In addition to the morphological changes, apoptosis and necrosis differ in the fact that the former is tightly regulated at the genetic level.

The basis of current knowledge on programmed cell death has been provided by studies in *Caenorhabditis elegans*: this has been a particularly good model to study as extensive apoptosis takes place during its development (Brenner, 1974). Detailed studies revealed that two genes are absolutely required for cell death in *C. elegans*, named *ced-3* and *ced-4* (Ellis and Horvitz, 1986), whereas another gene called *ced-9* prevented apoptosis from occurring (Hengartner and Horvitz, 1994a, b). These genes are conserved through evolution and are found in humans, with the name of caspases.

1.2.1 Caspases

Caspases (Cysteine ASPartyl protease) are a family of cysteine proteases that recognise tetrapeptide motifs and cleave their substrate after an aspartate residue (Black et al., 1989). Each caspase has its distinct substrate specificity determined by the pattern of amino acid residues upstream of the aspartate. The activity of caspases is tightly regulated in order to prevent unwanted apoptosis: they are synthesised as an inactive precursor (procaspase), containing an N-terminal prodomain, a large subunit (~20kDa) and a small subunit (~10kDa). Upon apoptotic stimulation, the three domains are cleaved and they assemble as active heterotetramers composed of two large and two small subunits (Walker et al., 1994).

At least14 caspases have been identified in mammals (Alnemri et al., 1996) that have been divided in two classes: initiator caspases (e.g., caspase-8 and -9) and executioner caspases (e.g., caspase-3, -6 and -7). Initiator caspases are activated by contact with a dedicated adaptor or scaffold protein (Boatright et al., 2003) and are then responsible for initiation of the proteolytic

cascade by cleavage and activation of the effector caspases. The latter then are able to cleave multiple key cellular proteins, including DNA repair enzymes (e.g., PARP), structural proteins (e.g., actin, nuclear lamins) and cell cycle proteins (e.g., $p21^{Cip1/Waf1}$, $p27^{Kip1}$). As such, caspases are the final effectors of programmed cell death and the apoptotic signalling pathways that lead to their activation can be subdivided in two major routes that converge on caspase-3: the extrinsic (or death receptor) apoptotic pathway and the intrinsic (or mitochondrial) apoptotic pathway (Figure 1.1).

1.2.2 The extrinsic apoptotic pathway

Cell death can be triggered by external signals. This involves cell surface receptors, called death receptors, which transmit apoptotic signals after ligation with specific ligands. Death receptors belong to the tumour necrosis factor receptor (TNFR) gene superfamily, including TNFR-1, Fas/CD95 and the TRAIL receptors DR-4 and DR-5 (Ashkenazi, 2002). All members of the TNFR family present cysteine-rich extracellular domains which allow them to recognise their ligands with specificity, resulting in trimerisation and activation (Naismith and Sprang, 1998). Subsequent signalling is mediated by the cytoplasmic part of the death receptor, which contains a conserved sequence termed the death domain (DD). Adaptor molecules like FADD or TRADD themselves possess their own DDs by which they are recruited to the DDs of the activated death receptor, thereby forming the so-called death inducing signalling complex (DISC). In addition to its DD, the adaptor FADD also contains a death effector domain (DED) that through interaction with the DED of procaspase-8 sequesters it to the DISC. The local concentration of several procaspase-8 molecules at the DISC leads to their autocatalytic activation and release of active caspase-8. Caspase-8 then processes downstream effector caspases which subsequently cleave specific substrates resulting in cell death. Cells harbouring the capacity to induce such direct apoptosis pathway were classified as ‘type I cells’ (Scaffidi et al., 1998) (Figure 1.1a).

In type II cells, the signal coming from the activated receptor does not generate a caspase signalling cascade strong enough for the execution of cell death on its own. In this case, the signal

needs to be amplified via the mitochondria-dependent intrinsic apoptotic pathways. The link between the caspase signalling cascade and the mitochondria is provided by the Bcl-2 family member Bid. Bid is cleaved by caspase-8 and in its truncated form (tBID) translocates to the mitochondria where it stimulates the release of cytochrome c and other mitochondrial proapoptotic factors into the cytosol (Luo et al., 1998).

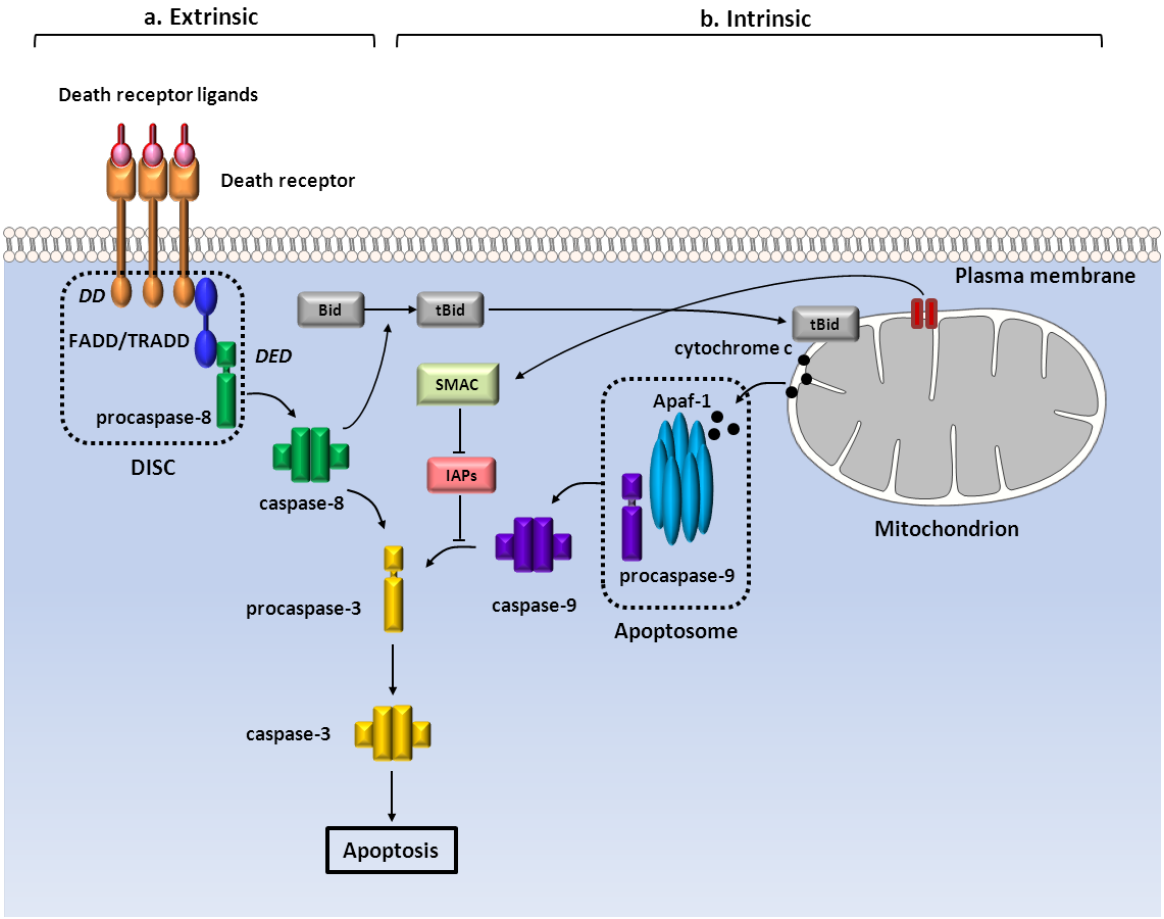

Figure 1.1 The extrinsic and intrinsic apoptotic pathways. Apoptosis is executed via death receptor (or extrinsic) and mitochondrial (or intrinsic) pathways, and it culminates with the activation of caspases. a. Death ligands, such as FASL, TRAIL or TNFα, engage their cognate receptors to recruit adaptor proteins FADD and TRADD via their death domains (DD), with formation of the death-inducing signalling complex (DISC). Adaptor molecules bind to procaspase-8 via their death effector domain (DED) resulting in the activation of caspase-8 and the subsequent activation of effector caspases-3 and -7 (type I cells). Caspase-8 also induces cleavage of Bid to tBid, which translocates to the mitochondrion and facilitate the release of proapoptotic factors (type II cells). b. The intrinsic pathway is activated by chemotherapeutic agents, irradiation or growth factor withdrawal, leading to the disruption of mitochondrial integrity. This causes the release of cytochrome c into the cytosol and the apoptosome-dependent activation of caspase-9. Other proapoptotic factors are also released from the mitochondrion including SMAC, which inhibits the inhibitor of apoptosis proteins (IAPs). This in turn leads to the activation of caspases-3 and, ultimately, to apoptosis.

1.2.3 The intrinsic apoptotic pathway: role of the organelles

Apoptosis might also be initiated by intrinsic signals, such as DNA damage, oxidative stress, and starvation (Kaufmann and Earnshaw, 2000). This is mainly achieved through two organelles, the mitochondrion and the endoplasmic reticulum (ER).

1.2.3.1 Role of the mitochondrion

Most apoptosis-inducing conditions involve the disruption of the mitochondrial transmembrane potential ($\Delta\psi$) as well as the so called permeability transition (PT), a sudden increase of the mitochondrial membrane permeability. Concomitantly, osmotic mitochondrial swelling has been observed by influx of water into the matrix with eventual rupture of the outer mitochondrial membrane, resulting in the release of pro-apoptotic proteins from the mitochondrial intermembrane space into the cytoplasm (Bernardi et al., 1999; Loeffler and Kroemer, 2000). Released proteins include cytochrome c and other apoptogenic proteins such as apoptosis inducing factor (AIF), Smac/Diablo and endonuclease G.

Once released, cytochrome c is able to bind and activate the Apaf-1 adaptor protein. The complex formed, called 'apoptosome' (Bao and Shi, 2007), is then able to cleave procaspase-9 (using ATP), which in turn activates effector caspases such as caspase-3, -6 and -7 ultimately resulting in cell death (Li et al., 1997; Slee et al., 1999). Smac/Diablo prevents the inhibitor of apoptosis proteins (IAPs) from directly inhibiting caspase activity, whereas endonuclease G and AIF are thought to contribute to nuclear DNA fragmentation (Saelens et al., 2004) (Figure 1.1b).

1.2.3.2 Role of the endoplasmic reticulum

The endoplasmic reticulum (ER) is the second organelle to take part in the intrinsic apoptotic pathway.

The ER has essential roles in multiple cellular processes required for cell survival. First of all it modulates calcium homeostasis, being the main site for storage of intracellular Ca^{2+}, and

accordingly it presents the highest concentration of calcium within the cell. Additionally, it regulates protein folding and secretion: the ER lumen is in fact an oxidative environment that is crucial for the formation of disulphide bonds and therefore for protein tertiary and quaternary structures. Because of its role in the secretory pathway, the ER is rich in calcium-dependent molecular chaperones, such as GRP78 and GRP94, which transiently stabilise incompletely folded proteins, assist protein folding, and dispatch misfolded proteins for degradation. Furthermore, the ER has a vital role in the biosynthesis of sterols and phospholipids that constitute the bulk of all biological membranes. Finally, various post-translational modifications occur in its lumen, including glycosylation and lipidation (Anelli and Sitia, 2008; Ma and Hendershot, 2004; Pizzo and Pozzan, 2007).

ER stress is the result of impairment in protein folding, which can be caused by disturbances in cellular redox regulation, diseases characterised by the formation of protein-inclusion bodies, and viral infection with ER overload of virus-encoding protein. Other inducers of ER stress include disruptions to ER Ca^{2+} stores, glucose deprivation, which interferes with protein glycosylation, and a variety of chemicals compounds that affect the ER function (e.g., thapsigargin that blocks Ca^{2+} ATPase pumps or tunicamycin that inhibits N-linked glycosylation) (Shore et al., 2011). The cell responds via a coordinated process called the unfolded protein response (UPR). The UPR consists of a global inhibition of protein synthesis while promoting the expression of ER chaperones and enhancing the degradation of misfolded proteins through a process called ER-associated degradation (ERAD) (Schroder and Kaufman, 2005).

The UPR is mediated through the activation of three ER transmembrane stress sensors, namely pancreatic ER kinase (PKR)-like ER kinase (PERK), activating transcription factor 6 (ATF6) and inositol-requiring enzyme 1 (IRE1) (Kim et al., 2008). In the absence of stress, the molecular chaperone GRP78 is bound to the luminal domain of these three stress sensors and maintains them in an inactive conformation; accumulation of unfolded proteins and alteration in the redox status within the ER lumen trigger the dissociation of GRP78 and their activation. PERK inhibits general protein biosynthesis by phosphorylating and inactivating the translational initiation factor

eIF2α; this enables translation of the ATF4 transcription factor through an alternative, eIF2α-independent pathway, and ATF4 in turn induces ER chaperones (GRP78 and GRP94) and proteins involved in metabolism and resistance to oxidative stress. ATF6 also regulates the expression of chaperones, besides it induces XBP1, another transcription factor that is processed by splicing through an IRE1-dependent mechanism and enhances the expression of chaperones and genes involved in protein degradation (Figure 1.2).

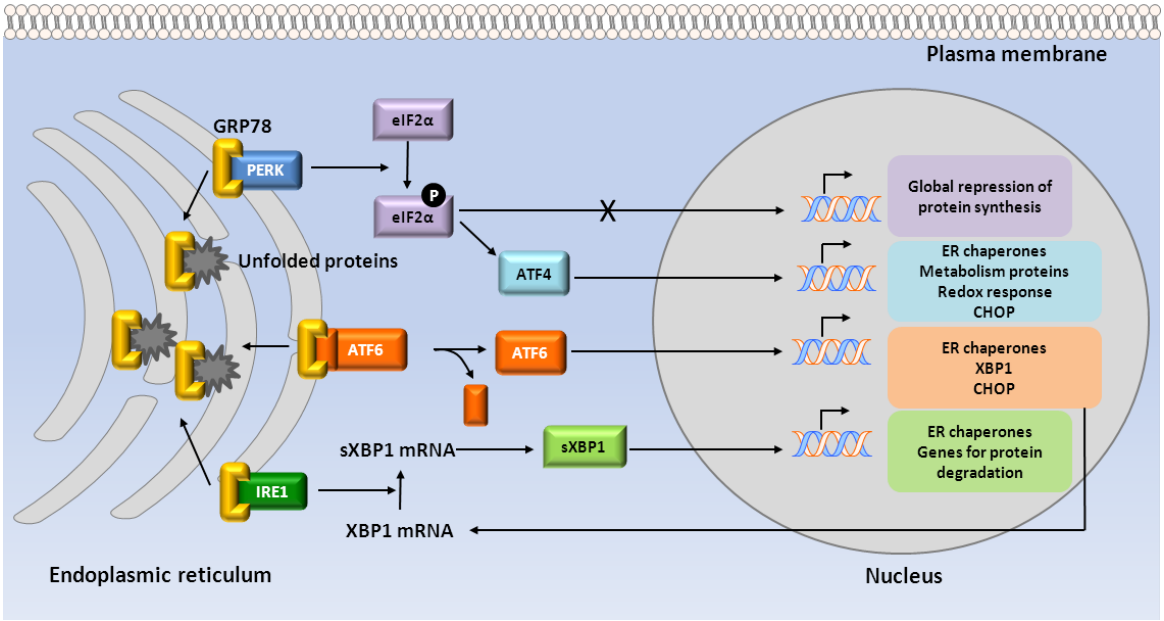

Figure 1.2 The unfolded protein response. On aggregation of unfolded proteins, GRP78 dissociates from the three endoplasmic reticulum (ER) stress receptors PERK, ATF6 and IRE1, allowing their activation. The activation of the receptors occurs sequentially, with PERK being the first, rapidly followed by ATF6, whereas IRE1 is activated last. Activated PERK blocks general protein synthesis by phosphorylating the initiation factor eIF2α. This phosphorylation enables translation of ATF4 transcription factor through an eIF2α-independent translation pathway.ATF4 translocates to the nucleus and induces the transcription of genes required to restore ER homeostasis. ATF6 is activated by proteolysis after its translocation from the ER to the Golgi apparatus. Active ATF6 is also a transcription factor and it regulates the expression of ER chaperones and XBP1, another transcription factor. To achieve its active form, XBP1 must undergo mRNA splicing, which is carried out by IRE1. Spliced XBP1 protein (sXBP1) translocates to the nucleus and controls the transcription of chaperones as well as genes involved in protein degradation. This concerted action aims to restore ER function by blocking further build-up of client proteins, enhancing the folding capacity and initiating degradation of protein aggregates.

As a whole, PERK, ATF6 and IRE1 initially promote pro-survival signalling. If activation of the UPR successfully removes the accumulation of misfolded proteins in the ER, normal translation is resumed and the cell recovers; in the event of prolonged or severe stress, the UPR responds

initiating apoptosis. This occurs mainly through the induction of the transcription factor C/EBP homologous protein (CHOP), which downregulates the pro-survival protein Bcl-2 while upregulating other apoptosis-related genes including DR5 and GADD34. The latter is a regulatory subunit of protein phosphatase 1 (PP1) which promotes eIF2α dephosphorylation and reverses attenuation of mRNA translation. IRE1 is also involved in ER stress-induced apoptosis, as it forms a complex with the adaptor molecule TNF-receptor-associated factor 2 (TRAF2) which recruits the apoptosis-signal-regulating kinase 1 (ASK1), leading to the activation of c-Jun-N-terminal kinase (JNK). This acts primarily by affecting the balance between pro-survival and pro-apoptotic Bcl-2 proteins (Szegezdi et al., 2006).

Caspase-12, a murine caspase not yet unequivocally identified in human tissue, is specifically involved in apoptosis that results from ER stress. Caspase-12 is localised at the ER and activated upon ER stress; accordingly, caspase-12 null mice are partially resistant to apoptosis induced by ER stress but not by other apoptotic stimuli (Nakagawa et al., 2000). The activation of caspase-12 may occur through ER stress-induced calpain or caspase-7 cleavage of procaspase-12 (Rao et al., 2002). ER stress-activated IRE1 may also aggregate procaspase-12 at the ER membrane surface through the cytosolic adaptor TRAF2 proteins, resulting in cleavage and activation (Yoneda et al., 2001). Once activated, caspase-12 is able to cleave caspase-9 leading to activation of caspase-3 (Morishima et al., 2002). Therefore, caspase-12 serves as a mediator of a novel intrinsic apoptosis pathway that is independent of Apaf-1, cytochrome c and mitochondria.

Cancer cells present high rates of growth and proliferation hence they require an increased amount of protein folding and assembly in the ER. Furthermore, the poorly organised vascularisation that characterises the tumour mass causes nutrient starvation, hypoxia and alteration in the redox environment. All these events are inducers of the UPR pathway and accordingly increased expression of UPR proteins has been reported in a number of cancers. For example, GRP78 chaperone overexpression is associated with drug resistance, as well as with higher grade, recurrence rate and poor survival (Lee, 2007). Similarly, XBP1 is overexpressed in a variety of cancers, including breast, liver and colon carcinoma (Fujimoto et al., 2003; Fujimoto

et al., 2007; Shuda et al., 2003), and increased levels of XBP1 induce the development of multiple myeloma (MM) in a transgenic mouse model (Carrasco et al., 2007). MM is a plasma cell malignancy characterised by excessive production of monoclonal antibodies which requires a strict control at the endoplasmic reticulum, hence blockade of XBP1 splicing with IRE1 inhibitors represents a potential therapeutic option for this type of tumour (Mimura et al., 2012).

Communication between mitochondria and the ER to trigger apoptosis is widely reported. This is mostly achieved by the Bcl-2 family of proteins of which several members were shown to be present both at the ER and at mitochondria.

1.2.4 The Bcl-2 family of proteins

B cell lymphoma 2 (*Bcl-2*), an oncogene that is frequently overexpressed in follicular lymphoma due to chromosomal translocation to an immunoglobulin locus, was the first example of oncoprotein that acts by promoting cell survival rather than by driving cell proliferation (Vaux et al., 1988). Since then, a growing number of proteins with structural similarities to Bcl-2 have been identified in mammalian cells, defined by the presence of conserved sequence motifs known as Bcl-2 homology (BH) domains (BH1 to BH4). Most members also contain a C-terminal transmembrane domain that allows them to anchor to the outer mitochondrial membrane and ER.

The Bcl-2 family of proteins is generally divided into two groups, the pro-survival group and the pro-apoptotic group (Cory et al., 2003). The first subfamily is composed of Bcl-2 and its closest relatives Bcl-xL, Bcl-w, Mcl-1 and A1. Members of this group contain three to four BH domains and function as inhibitors of stress-induced apoptosis. The pro-apoptotic Bcl-2 members can be further divided into two subgroups: the Bax subfamily consists of Bax, Bak and Bok/Mtd that all possess the domains BH1, BH2 and BH3, whereas the BH3-only proteins (Bid, Bad, Bim, Bik, Blk, Bmf, BNIP3, HRK, Nix, Noxa, Puma and Spike) only present the short BH3 motif (Cory et al., 2003; Walensky, 2006) (Figure 1.3). Both pro-apoptotic subgroups promote cell death, but differ greatly in how they participate in apoptosis.

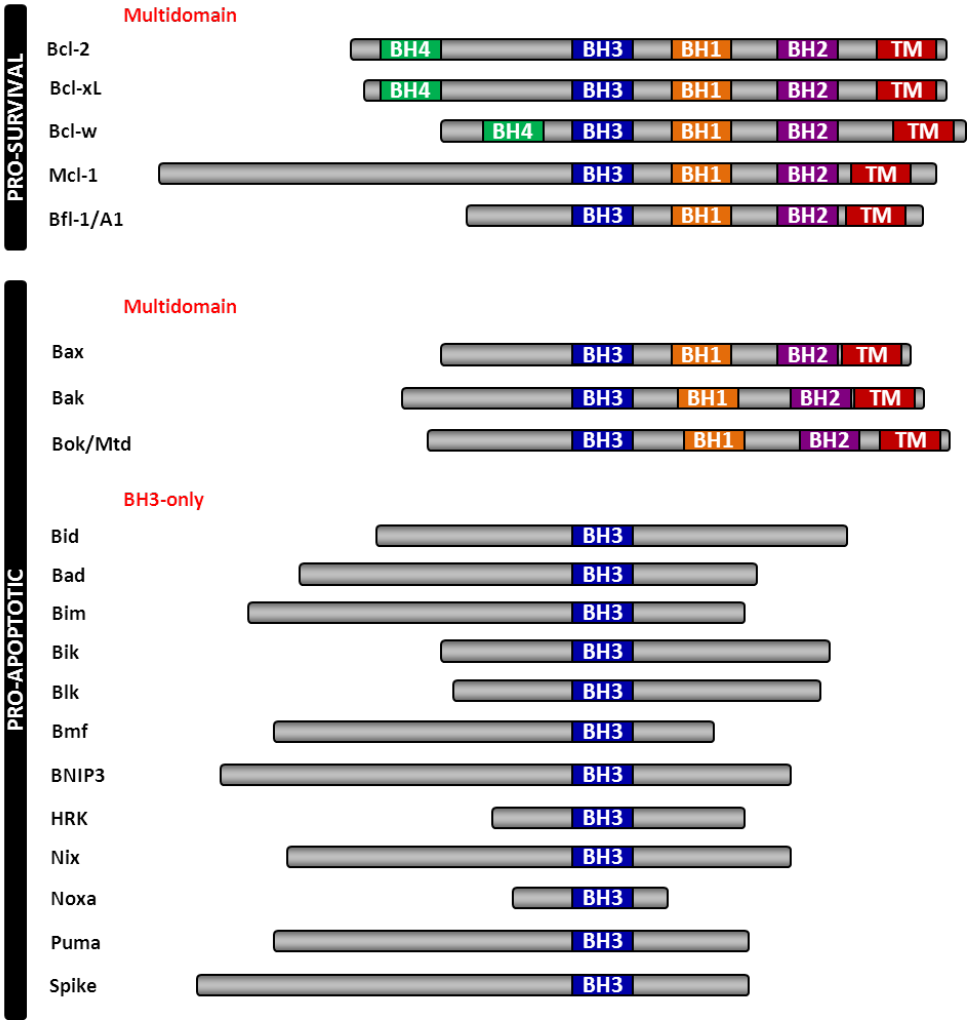

Figure 1.3 The Bcl-2 family. Bcl-2 family proteins are structurally defined by their Bcl-2 homology domains (BH domains) and functionally categorised by their ability to inhibit or activate cell death. Human Bcl-2 family proteins are drawn to scale based upon polypeptide length and aligned by their BH3 domains.

In response to a variety of physiological and pathological death signals the cell's decision to initiate cell death is determined by the complex interactions between the pro-apoptotic and anti-apoptotic members of the Bcl-2 family.

In normal conditions, pro-survival Bcl-2 members sequester the pro-apoptotic Bax-like members by binding to their BH3 domains and preventing their activation. The BH3-only proteins act as damage sensors and diverse cellular insults trigger the apoptotic response by launching particular BH3-only proteins. For example, DNA damage induces p53-mediated transcription of *Puma* and *Noxa*; furthermore, activation of death receptor Fas and TNFR1 leads to cleavage of Bid to its

activated form tBid by caspase-8, providing a cross-talk between the extrinsic and intrinsic apoptotic pathways. Once they are activated by mechanisms such as transcriptional upregulation (Puma, Noxa), post-translational alterations such as phosphorylation (Bad, Bik), dissociation from sequestering proteins (Bim and Bmf from dynein light chain 1 and 2 respectively, Bad from 14-3-3) or proteolysis (Bid), BH3-only proteins are able to interfere with the fine-tuned balance of homo- or hetero-oligomerisation between pro-apoptotic and pro-survival Bcl-2 family members. This is achieved by binding with their target pro-survival Bcl-2 proteins, which relieve their inhibition on Bax/Bak. Interestingly, the affinities of different pairs of BH3-only and Bcl-2-like proteins can vary greatly, for instance Bad and Bmf have higher affinity for Bcl-2, Bcl-xL and Bcl-w, whereas Noxa binds only to Mcl-1 and A1 (Chen et al., 2005).

Alternatively, some BH3-only proteins such as Bid and Bim may also trigger Bax and Bak directly inducing a conformational change which allows oligomerisation and insertion into the outer mitochondrial membrane (Kuwana et al., 2005). Although the mechanism is controversial, Bax and Bak are believed to contribute to the permeabilisation of the outer membrane by forming channels, either alone or by interacting with components of the PT pore, and causing the release of apoptogenic factors such as cytochrome c (Wei et al., 2001).

Recently it was revealed that several members of the Bcl-2 family, including Bcl-2, Bcl-xL, Bax and Bak, are located not only at the mitochondria but also at the ER, and can regulate induction of apoptosis in response to ER stress by affecting multiple processes such as Ca^{2+} homeostasis and the UPR (Hetz, 2007; Szegezdi et al., 2009). Some examples are the activation of the IRE1 arm of the UPR and the regulation of ER membrane permeability in response to ER stress by the pro-apoptotic Bax and Bak through direct binding to IRE1. Bak is also involved in regulating ER swelling and remodelling through interaction with Bcl-xL. Bcl-2 and Bcl-xL on the other hand attenuate pro-apoptotic Ca^{2+} signalling by binding to the IP3R (inositol triphosphate receptor) calcium channel; conversely Bcl-2 phosphorylation by JNK at the ER membrane inhibits such effect. Another level of regulation of Bcl-2 is its transcriptional repression by CHOP, whose

expression is induced after ER stress. The BH3-only protein Bim is also targeted by JNK leading to activation by release from the cytoskeleton where it normally resides and translocation to the ER. *Bim*, as well as the other BH3-only genes *Puma* and *Noxa*, has also been found upregulated in cells treated with ER stressors (Szegezdi et al., 2006).

Collectively all the signals transduced by the Bcl-2 family members in response to prolonged ER stress lead to activation of Bax and Bak and induction of cell death via the mitochondrial pathway (Figure 1.4).

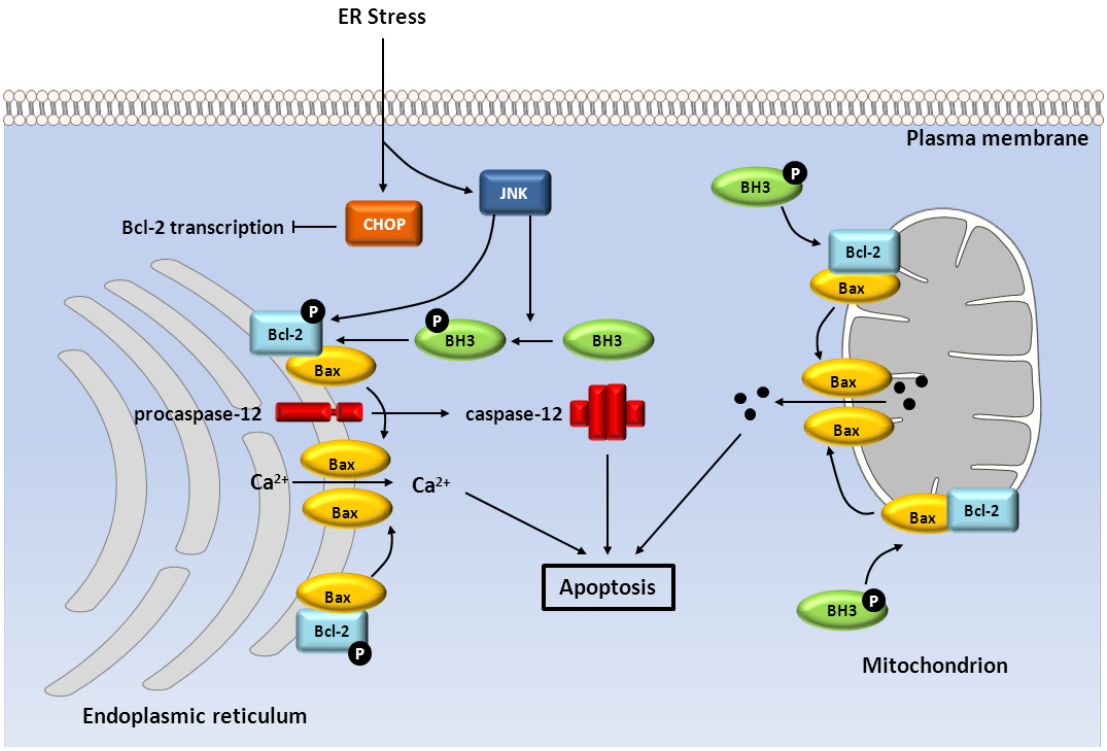

Figure 1.4 Bcl-2 family role in apoptosis at the mitochondria and the ER. In resting conditions, the pro-apoptotic Bax and Bak are kept inactive by interaction with Bcl-2 both on the mitochondrial and endoplasmic reticulum (ER) membranes. In response to death signals, BH3-only proteins are activated (e.g., via phosphorylation) and disrupt the interaction between Bax and Bcl-2. Bax is then able to facilitate the release of proapoptotic factors from the mitochondria. Severe ER stress leads to activation JNK and induction of CHOP. Both JNK and CHOP eliminate the anti-apoptotic effect of Bcl-2; CHOP blocks expression of Bcl-2, whereas JNK phosphorylates it. JNK also phosphorylates BH3-only proteins. Caspase-12 is activated on the ER membrane as well. Collectively, these changes allow activation of Bax and Bak, alteration of Ca^{2+} homeostasis, transmission of the signal from the ER to the mitochondria and execution of death.

More recently Mcl-1 (myeloid cell leukaemia-1), another member of the Bcl-2 family, was shown to be highly involved in the response to ER stress. Mcl-1 was originally identified in differentiating myeloid cells and is essential for early embryonic development (Kozopas et al., 1993; Rinkenberger et al., 2000). In melanoma cells, *Mcl-1* upregulation is a mechanism of resistance to the ER stressors tunicamycin and thapsigargin, and this effect is reversed by the Mcl-1 inhibitor obatoclax (Jiang et al., 2008; Jiang et al., 2009).

Mcl-1 expression is highly regulated at the transcriptional, post-transcriptional and post-translational levels (Figure 1.5). First of all, several pathways have been shown to stimulate *Mcl-1* gene transcription, including MAP kinases, PI3K/AKT and JAK/STAT. Specifically after ER stress *Mcl-1* gene is also upregulated in melanoma cells by the transcription factor Ets-1, which is induced by the IRE1α/XBP-1 branch of the unfolded protein response (Dong et al., 2011); moreover ATF4 transcription factor, an effector belonging to the PERK arm of the UPR and also induced by treatment with the proteasome inhibitor bortezomib, mediates *Mcl-1* upregulation upon proteasome inhibition by directly binding to its promoter and stimulating its transcription in multiple myeloma cells (Hu et al., 2012).

A second level of regulation of Mcl-1 is provided by alternative splicing, which can give rise to a shorter variant (271 amino acids) that lacks the BH1, BH2 and transmembrane domains and induces cell death rather than promoting survival (Michels et al., 2005); furthermore, Mcl-1 mRNA is negatively regulated by miR-29 (Mott et al., 2007).

Mcl-1 is also subject to caspase-3-mediated cleavage on Asp127 and Asp157 residues, with Asp127 being the preferred site of cleavage in cells (Michels et al., 2004). The N-terminus of Mcl-1 is essential for its subcellular localisation and its deletion impairs Mcl-1 pro-survival activity (Germain and Duronio, 2007); the C-terminal 128-350 fragment in fact promotes cell death through direct interaction and activation of Bim and Bax (Herrant et al., 2004; Menoret et al., 2010), so Mcl-1 caspase cleavage both depletes cells of a pro-survival protein and provides a pro-apoptotic one.

Finally, the most important mechanism of regulation of Mcl-1 consists in post-translational modifications (phosphorylation and ubiquitination), which are required for the prompt degradation of this protein in response to stress signals including UV irradiation (Nijhawan et al., 2003). Mcl-1 in fact contains two PEST sequences, rich in proline (P), glutamic acid (E), serine (S), and threonine (T), which are often found in rapidly turned over proteins, and indeed Mcl-1 has a short half-life in cells (typically in the range of one to a few hours) (Craig, 2002).

During oxidative stress Mcl-1 is phosphorylated by JNK at Ser121 and Thr163 and inactivated (Inoshita et al., 2002); Thr163 is also phosphorylated in an ERK-dependent fashion in response to differentiation, resulting in a slowdown of Mcl-1 turnover (Domina et al., 2004), and together with Ser159 by glycogen synthase kinase 3β (GSK-3β), which leads to association with the E3 ligase $SCF^{\beta\text{-}TrCP}$ and therefore to Mcl-1 ubiquitination and degradation (Ding et al., 2007; Maurer et al., 2006). GSK-dependent destruction of Mcl-1 is inhibited in melanoma cells by the p53 induced microRNA-149* (miR-149*) that targets GSK-3α mRNA under ER stress (Jin et al., 2011). $SCF^{\beta\text{-}TrCP}$ is not the only E3 ligase that ubiquitinates Mcl-1 upon GSK-3 phosphorylation: SCF^{Fbw7}, known to target protein such as cJun, Myc and Notch 1 for degradation, also exerts its E3 ligase function on Mcl-1, and in fact there is a close correlation between SCF^{Fbw7} loss and Mcl-1 overexpression in T-cell acute lymphoblastic leukaemia (Inuzuka et al., 2011a; Inuzuka et al., 2011b). It was recently also reported that a further E3 ligase, Mule/ARF-BP1, presents a BH3 domain similar to that of pro-apoptotic Bak that allows it to specifically target Mcl-1 (Warr et al., 2005; Zhong et al., 2005); the extreme N-terminus of Mcl-1 is required for the interaction with Mule and its steady-state ubiquitination and destruction (Warr et al., 2011). Heat shock can trigger interaction with Mule by dissociation of Mcl-1 from its pro-apoptotic BH3-only binding partner Noxa; this is prevented by Hsp70, which reduces the Mcl-1/Mule interaction while enhancing Mcl-1 synthesis (Stankiewicz et al., 2009).

Mcl-1 is also specifically targeted for degradation during mitotic arrest: this is mediated by a site-specific phosphorylation of Mcl-1 at Thr92 by Cdk1/cyclin B1 that allows recognition by the E3 ligase APC/C^{Cdc20} (anaphase-promoting complex/cyclosome and its activator Cdc20), which is

active in mitosis and ubiquitinates targets such as securin and cyclin B1. The presence of a conserved destruction motif (D-box) on Mcl-1 typical of APC/C^{Cdc20} substrates is also required for binding (Harley et al., 2010). Additionally, the E3 ligase SCF^{Fbw7} can ubiquitinate Mcl-1 during mitotic arrest, in this case not in a GSK-3β dependent manner but after phosphorylation of Mcl-1 by JNK, p38 and CKII (casein kinase II) on Ser121/Glu125 and, to a lower affinity, Ser159/Thr163. Mcl-1 therefore affects the response to antitubulin chemotherapeutics (Wertz et al., 2011) and accordingly loss of Mcl-1 coincides with increased cell death in response to the antimitotic kinesin spindle protein (KSP/Eg5) inhibitors in multiple myeloma (Tunquist et al., 2010). A further site of phosphorylation on Mcl-1 during G2/M is Ser64. This modification, stimulated *in vitro* by CDK1, CDK2 and JNK1 kinase, does not have an impact on Mcl-1 stability, but enhances its anti-apoptotic activity by rendering cells resistant to TRAIL-induced apoptosis (Kobayashi et al., 2007).

Contrary to the mentioned E3 ligase complexes, it has been shown that the deubiquitinase USP9X stabilises Mcl-1 and promotes cell viability (Schwickart et al., 2010) and that the binding between Mcl-1 and USP9X can be disrupted by the anticancer drug gemcitabine (Zhang et al., 2011).

The interaction with pro-apoptotic BH3-only members of the Bcl-2 family also influences Mcl-1 stability: for instance, in multiple myeloma cells interaction with Bim confers mutual protection from proteasomal degradation; additionally, binding with Puma is important, although not sufficient, to prevent rapid destruction of Mcl-1 in cancer cell lines (Mei et al., 2005; Wuilleme-Toumi et al., 2007).

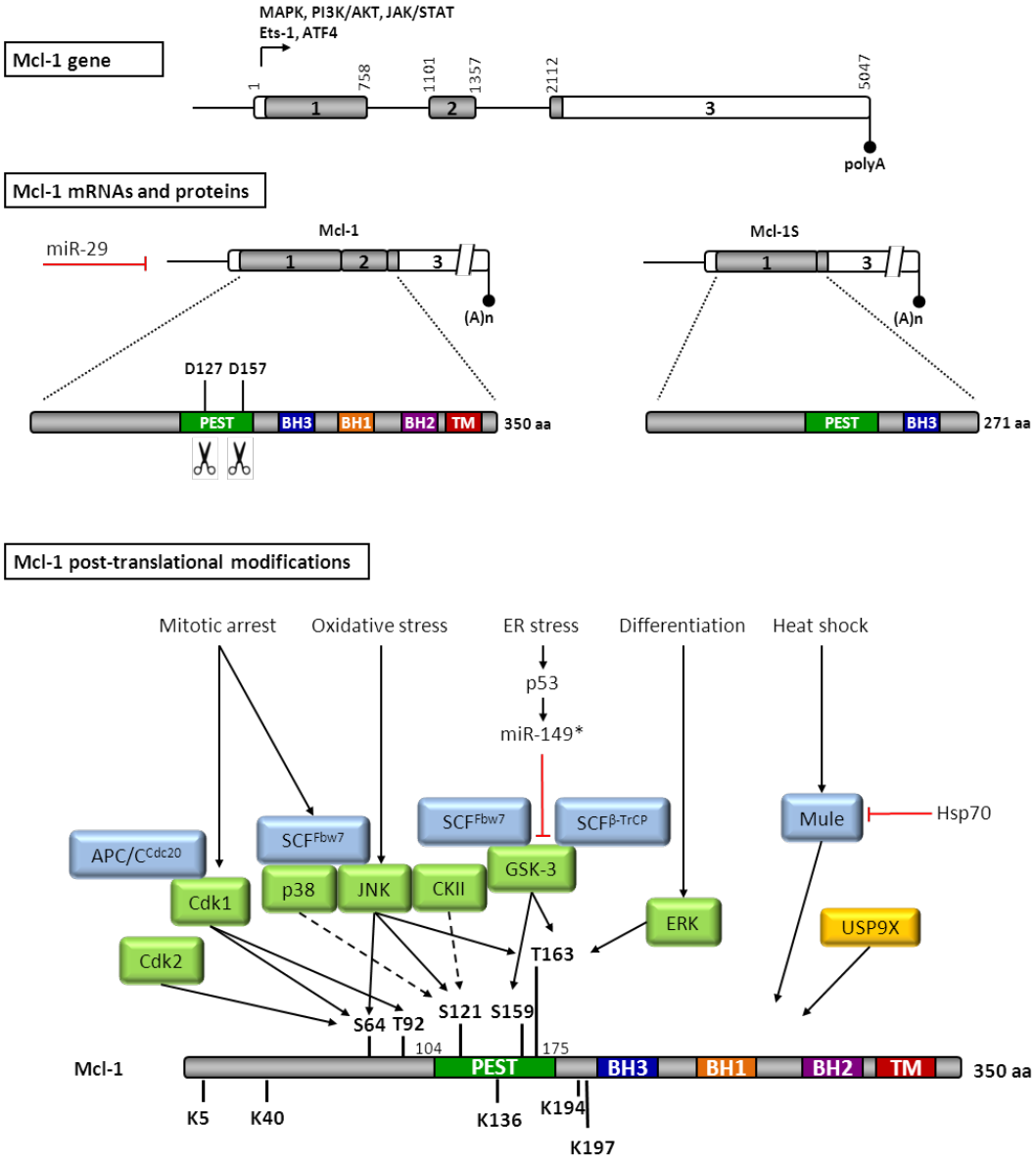

Figure 1.5 Schematic representation of Mcl-1 regulation. The human *Mcl-1* gene (top) comprises three exons (in grey). Its transcription is stimulated by the MAPK, PI3K/AKT and JAK/STAT pathways, as well as by the Ets-1 and ATF4 transcription factors. Alternate splicing gives rise to two distinct Mcl-1 mRNAs (middle) either containing or lacking exon 2 and encoding the Mcl-1 full length and Mcl-1S isoforms, respectively. miR-29 is responsible for Mcl-1 mRNA degradation. The structure and size (in amino acid residues) of the Mcl-1 and Mcl-1S isoforms are shown (bottom). The PEST (aa 104-175), BH (Bcl-2 homology) and TM (transmembrane) domains are indicated, along with the caspase cleavage sites at D127 and D157. These residues are also present in Mcl-1S, but it is not known whether this isoform is similarly cleaved by caspases. In the lower panel post-translational modifications of Mcl-1 are shown. Kinases, E3 ubiquitin ligases and deubiquitinases are labelled in green, light blue and yellow respectively. The protein is phosphorylated on S64 and T92 during mitotic arrest via Cdk1 and Cdk2. Phosphorylation on T92 enables ubiquitination by APC/C^{Cdc20}. Mitotic arrest also induces ubiquitination by SCF^{Fbw7}upon JNK, p38 and CKII-dependent phosphorylation on S121. JNK also phosphorylates S121 and T163 upon oxidative stress and S64 in G2/M. GSK-3 kinase phosphorylates Mcl-1 on S159 and S163 allowing ubiquitination by SCF^{Fbw7} and $SCF^{β\text{-}TrCP}$ in steady state. GSK-3 is inhibited by the p53-induced miR-149* upon ER stress. T163 is also target of ERK-dependent phosphorylation and stabilisation when differentiation is induced. Mule ubiquitinates Mcl-1 in steady state and is inhibited by Hsp70; USP9X is responsible for Mcl-1 deubiquitination. K5, K40, K136, K194 and K197 are published sites of ubiquitination. Dotted arrows are utilised when direct phosphorylation has not been proved.

1.2.5 Ubiquitination: a role in apoptosis and cancer

Recent progress showed that Mcl-1 is only one of many cell death signalling components that are post-translationally modified by ubiquitination and provided strong evidence that ubiquitin-dependent proteasome degradation is a key regulatory mechanism of the apoptotic cascade (Vucic et al., 2011) (Table 1.1).

Enzyme	Substrate(s)	Biological process(es)
E3 ubiquitin ligases		
XIAP	Caspase-3, caspase-7, SMAC	Apoptosis
c-IAP1, c-IAP2	RIP1, TRAF2, NIK, caspase-3, caspase-7, XIAP, SMAC, c-IAP1, c-IAP2	Canonical and non-canonical NF-κB signalling, apoptosis
Mdm2	p53	Cell cycle, apoptosis, senescence
$SCF^{\beta TrCP}$	IκBα, Mcl-1	Canonical NFκB signalling
SCF^{FBW7}	Mcl-1, Myc, Jun	Apoptosis, proliferation
ITCH	FLIP, p63	Apoptosis
SIAH1, SIAH2	HIPK2, PHD1, PHD3	DNA damage, hypoxia
VHL	HIF-1α	Hypoxia
APC/C^{Cdc20}	Mcl-1	Apoptosis upon mitotic arrest
Mule	Mcl-1	Apoptosis
Deubiquitinases		
A20	RIP1, RIP2, TRAF2, TRAF6, UBCH5, UBC13, caspase-8, NEMO, MALT1, others	Downregulates NF-κB activity and promotes apoptosis
CYLD	BCL-3, RIP1	Downregulates NF-κB activity
USP14	Various proteins destined for proteasomal degradation	Attenuates proteasomal function to induce cell death
USP9X	β-catenin, TGFβ, SMADs, Mcl-1, others	Anti-apoptotic
USP7	Mdm2, p53, MdmX, FOXO4, PTEN, claspin, others	Anti-apoptotic

Table 1.1 Ubiquitin-proteasome pathway proteins affecting apoptosis. Adapted from Vucic *et al,* 2011.

Proteasome degradation consists of an ATP-dependent protein hydrolysation by the 26S proteasome, a 2000 kDa proteolytic complex that contains a central 20S core, in which proteins are degraded, and two 19S complexes, which provide substrate specificity and regulation (Baumeister et al., 1998; Coux et al., 1996).

The barrel-shaped 20S proteasome is an abundant particle, comprising four heptameric stacked rings that enclose a central chamber where proteolysis occurs. Its two central rings consist of seven β subunits each, and have a catalytic function, whereas the external rings, composed of seven α subunits, control the passage of substrates and degradation products in and out of the proteasome and serve as docking sites for the regulatory 19S particles. The 19S particles cap the 20S proteasome ends and consist of 19 proteins each. These form a 10-protein base that contains six distinct ATPases and binds directly to the α rings, and a 9-protein lid that includes binding sites for poly-ubiquitin. In fact most substrates of this pathway are first marked for degradation by covalent linkage to multiple molecules of ubiquitin, a 76 amino acids protein that is conjugated through its carboxyl terminus to amino groups of lysine residues. This process requires the coordinated reaction of three enzymes, E1, E2 and E3. Ubiquitin is first activated by ubiquitin-activating enzyme E1, before being transferred to its active site, the amino acid cysteine. This transfer requires ATP, making the process energy-dependent. The ubiquitin molecule is then passed on to the second enzyme of the complex, E2 (ubiquitin-conjugating enzyme), before reaching the final enzyme, E3, the ubiquitin protein ligase, which recognises and binds the target substrate and labels it with the ubiquitin (Figure 1.6). Ubiquitin ligases may exist as single proteins or as multi-subunit complexes, and they may contain one of a number of domains that promotes ubiquitination, including the RING domain or the HECT domain (Deshaies and Joazeiro, 2009). The process is repeated until a short chain is formed, with four or more ubiquitin molecules and can be reverted by the action of deubiquitinating enzymes (Hershko and Ciechanover, 1998; Pickart, 2001). However, there are some conjugation events in which only a single ubiquitin is added by the E3 ligase to a substrate molecule. Mono-ubiquitinated proteins are not targeted to the proteasome for degradation, but may instead be altered in their cellular location or function (Hicke, 2001).

Substrate specificity is mainly defined by the multiple E2 and E3 combinations possible. E2 and E3 belong to large protein families, but while E2 share many well-conserved catalytic domains,

E3 ligases only share a few conserved motifs and are, therefore, very specific in the selection of the proteins to be labelled.

It is also worth mentioning the identification of ubiquitin-independent mechanisms for proteasomal degradation that affects a wide range of proteins, including a number of proto-oncoproteins and tumour suppressors (Jariel-Encontre et al., 2008).

Aside from protein degradation, the proteasome system also plays an important role in the immune response. As part of the continual surveillance by the immune system against autologous cells that are virally infected or have undergone oncogenic transformation, certain peptide fragments of cellular proteins are produced by proteasome cleavage and transported from the cytosol into the endoplasmic reticulum by the transporters associated with antigen processing (TAP). Here these peptides bind to nascent major histocompatibility complex (MHC) class I molecules and are transported to the plasma membrane. If the immune system is not tolerant to a displayed peptide, then cytotoxic $CD8^+$ T lymphocytes will be stimulated and eliminate the offending cell (Kloetzel, 2004).

In the context of tumourigenesis, proteasomal degradation has received much attention as its substrates include oncogenes and tumour suppressors that regulate cell division, cell differentiation, cell death, angiogenesis, invasion etc. Furthermore, the proteasome constitutes a therapeutic target in its own right, as certain tumour cells are more sensitive to its pharmacological inhibitors than normal cells (Drexler, 1997; Lee and Goldberg, 1998; Meriin et al., 1998). This is the case for multiple myeloma, a neoplasm presenting excessive expression of immunoglobulins that is therefore vulnerable to disturbances in the ER-dependent protein folding machinery. Proteasome inhibitors have recently been shown to induce ER stress in cancer cells by causing accumulation of misfolded proteins in the ER and increasing apoptosis (Obeng et al., 2006). The proteasome inhibitor bortezomib has thus recently become front-line therapy for relapsed myeloma (Palumbo and Anderson, 2011).

Proteasome inhibitors also have an effect on MHC-I-dependent antigen presentation as they block the assembly of MHC-I molecules with peptides by preventing the processing of the majority of cell proteins (Rock et al., 1994).

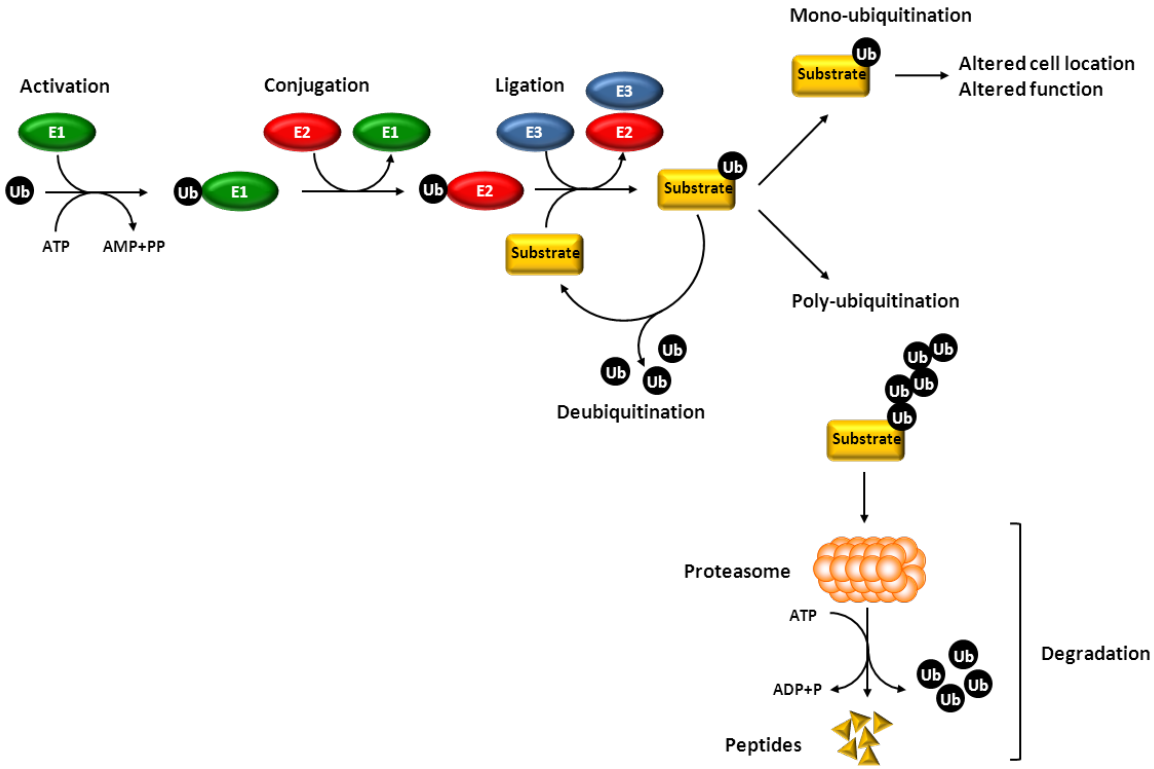

Figure 1.6 The proteasome pathway. The ubiquitination and degradation of substrate proteins is achieved by a series of reactions mediated by the enzymes of the ubiquitin–proteasome system. In the activation reaction, ubiquitin is transferred to an E1 enzyme in an ATP-dependent manner. The activated ubiquitin is subsequently transferred to an E2 enzyme in the conjugating reaction. The E2 enzyme then carries the ubiquitin to the E3 enzyme, which is also known as ubiquitin ligase. The E3 is important not only because it covalently ligates ubiquitin to Lys residues on the substrate protein, but also because it mediates substrate specificity. Deubiquitinating enzymes may reverse substrate protein ubiquitination. The process of ubiquitin ligation may be repeated, which leads to the formation of a poly-ubiquitin chain on the target protein. Ligation of poly-ubiquitin targets substrate proteins for ATP-dependent proteasomal degradation. Conversely, mono-ubiquitination may affect the location and the function of the protein. P, phosphate; PP, diphosphate; Ub, ubiquitin.

1.2.6 SUMOylation: a role in apoptosis and cancer

Another important post-translational modification that is often altered in cancer cells is SUMOylation. The small ubiquitin-like modifiers (SUMOs) are a sub-family of three reversible post-translational modifiers of eukaryotic cellular proteins that share structural similarity with ubiquitin. SUMO-2 and SUMO-3 differ from each other in sequence by only three amino acids and have very similar targets, whereas SUMO-1 shares only ~45% sequence identity with them and has a significantly different substrate proteome.

Like ubiquitin, they are capable of forming a bond to the amino-group of lysine residues via their C-terminal carboxyl group. These lysines are commonly located within a SUMO consensus motif ψKxD/E, where ψ is a hydrophobic amino acid, K the target lysine, x any residue and D/E an acidic residue.

Similarly to ubiquitination, SUMOylation also requires a three-step enzymatic cascade; however, the two systems do not utilise the same enzymes. Before the first conjugation, nascent SUMO needs to be proteolytically processed to reveal a C-terminal di-glycine motif. This is accomplished by SENP SUMO-specific isopeptidases. Mature SUMO is activated by the E1 heterodimer AOS1-UBA2 in an ATP-dependent reaction, which results in a thioester bond between SUMO and UBA2. SUMO is then transferred to the catalytic Cys residue of the E2 conjugating enzyme UBC9. Finally, an isopeptide bond is formed between the C-terminal Gly residue of SUMO and a Lys residue in the substrate. This step is usually aided by a SUMO E3 ligase (Figure 1.7). Typically, only a small fraction of a given protein is SUMOylated and this modification is rapidly reversed by the action of deSUMOylating enzymes.

In contrast to ubiquitin, SUMO-modification is not usually used to tag proteins for degradation, but basically it alters inter- or intramolecular interactions of the modified targets. Among the best studied effects of SUMOylation are nuclear-cytosolic transport, transcriptional regulation and DNA repair (Geiss-Friedlander and Melchior, 2007; Hay, 2005).

SUMO modification is also implicated in apoptosis at various levels: SUMO-1 can associate with Fas receptor and TNF receptor 1, and its overexpression was shown to protect lymphoma cells

from Fas ligand and TNF-induced cell death; furthermore SUMO-1 also binds and modifies the FADD-interacting protein DAXX (Jang et al., 2002; Okura et al., 1996).

Conversely, it has also been reported that SUMO-1 can have pro-apoptotic effects. SUMOylation of PML-RARα fusion protein can lead to apoptosis following arsenic trioxide treatment of acute promyelocytic leukemic cells (Sternsdorf et al., 1999). Furthermore, some studies showed that p53 can be modified by conjugation to SUMO-1 and this leads to an increase in its transactivation ability (Gostissa et al., 1999; Rodriguez et al., 1999). P53 SUMOylation is regulated by Mdm2, an E3 ubiquitin ligase that targets p53 for degradation, and its inhibitor Arf; the latter also promotes Mdm2 SUMO-1 conjugation (Xirodimas et al., 2002). Mdm2 is deSUMOylated by the SUMO-specific protease SUSP4, leading to promotion of Mdm2 self-ubiquitination and p53 stabilisation in response to UV damage (Lee et al., 2006b).

Balancing SUMO equilibrium is therefore extremely important for the cell and in fact genetic studies have shown that SUMO conjugation is required for cell viability (Hayashi et al., 2002; Nacerddine et al., 2005; Seufert et al., 1995).

Alterations to all the different steps of SUMOylation have been detected in tumour cells and are associated with the onset of cancer. Elevated levels of the SUMO E1 enzyme are associated with lower survival rates in patients with hepatocellular carcinoma; UBC9 E2 enzyme is overexpressed in several human tumours, including lung adenocarcinoma, ovarian carcinoma and melanoma, and leads to an increase in cancer cell growth. The SUMO E3 protein PIAS3 (protein inhibitor of activated STAT3) is also up-regulated in a number of different cancer types, while the SUMO protease SENP1 is up-regulated in prostate and thyroid cancer, and this overexpression promotes neoplasia development in the prostate (Hoeller and Dikic, 2009; Sarge and Park-Sarge, 2009).

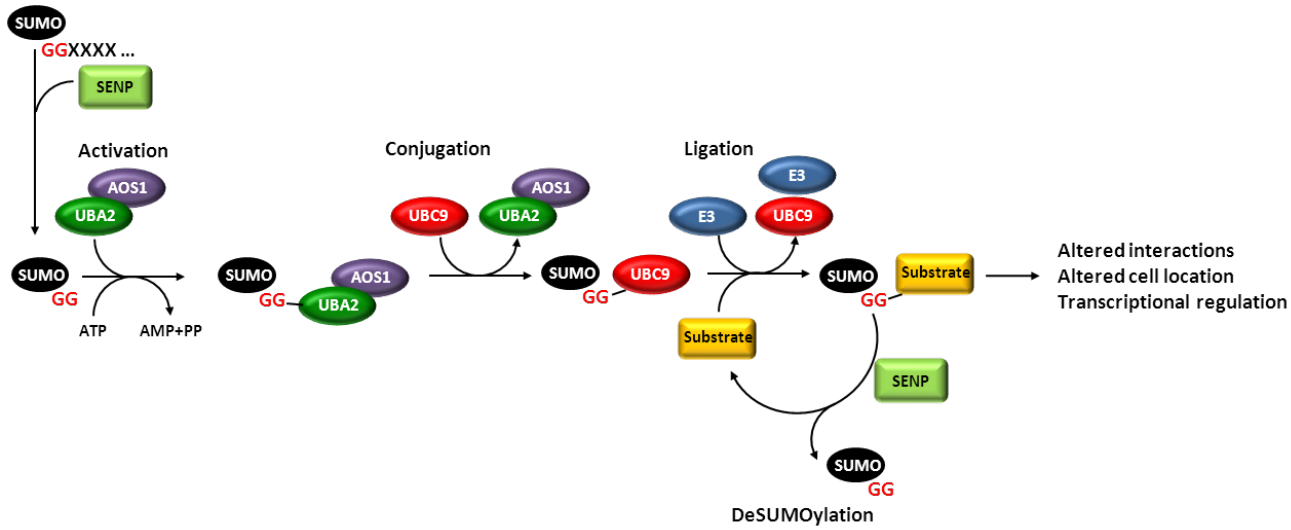

Figure 1.7 The SUMOylation pathway. Before the first conjugation, nascent SUMO is proteolytically cleaved by SENP to reveal its C-terminal Gly-Gly motif. Mature SUMO is activated in an ATP-dependent-fashion by the E1 heterodimer AOS1–UBA2, which results in a thioester bond between the C-terminal Gly residue and UBA2. SUMO is then conjugated to the E2 enzyme UBC9. Finally, a SUMO E3 ligase mediates the ligation of the C-terminal Gly residue of SUMO with the substrate. SUMOylated targets serve as substrates for SENPs, which ensures the reversibility of SUMOylation.

1.3 Tumour antigens

The past few decades of research have proved that cancer is an extremely complex disease, in the sense that each cancer is unique and involves a wide variety of genes and pathways. As a consequence, finding a cure for cancer is a complex challenge and more innovative and specific therapies are needed.

One of the obstacles in treating cancer is the fact that tumour cells appear to be almost identical to normal cells. Conventional chemotherapeutic drugs are unable to differentiate between cancer cells and normal cells, and most of their side-effects result from normal cells being destroyed along with the cancer cells. However the immune system is able to specifically distinguish between normal and cancer cells by recognising cancer antigens displayed on the tumour cell's surface. Hence these antigens represent ideal targets for the development of therapeutic cancer vaccines and thus harness the immune system to control the spread of cancer.

Any protein that is not exposed to the immune system can trigger an immune response. This may include proteins that are normally sequestered from the immune system, proteins that in physiological conditions are produced in extremely small quantities, proteins whose structure is modified due to mutation or proteins that are produced only in certain stages of development (Linley et al., 2011). In addition to polypeptides, other substances like cell surface glycolipids and glycoproteins may also have an abnormal structure in tumour cells and can be targets of the immune system (Reis et al., 2010).

According to their features, tumour antigens have been classified into several different categories.

Over-expressed antigens

This group include those proteins that are normally expressed in cells at lower levels, and aberrantly over-expressed in cancer cells. Some examples are HER-2 in breast carcinoma (Peoples et al., 1995), MUC-1 in lymphomas as well as breast and ovarian cancer (Brossart et al., 1999), and WT1 in several types of leukaemia (Azuma et al., 2002; Ohminami et al., 2000).

Differentiation/lineage-specific antigens

These antigens are molecules expressed by one particular tissue-type, and also by cancer cells derived from that tissue-type. They provide a very interesting target for immunotherapy as their restricted expression lowers the chances of vaccine-related side effects. Many of them have been found in melanoma, such as gp100, Melan-A/MART-1 and tyrosinase, which is required for melanin production (Brichard et al., 1993; Kawakami et al., 1994a; Kawakami et al., 1994b; Wang et al., 1995). Other examples include PSA in prostate cancer (Corman et al., 1998) and mammaglobin-A in breast carcinoma (Jaramillo et al., 2002).

Viral antigens

It is well known that several viruses are able to induce transformation in the infected cells, resulting in tumour formation. These viruses integrate part of their genome into the host, resulting in the expression of viral proteins. E6 and E7 proteins for example are a product of the human papilloma virus (HPV) and are known to inhibit p53 and Rb tumour suppressors respectively. They are expressed in cervical and head and neck cancers (Hung et al., 2008; Lajer and von Buchwald, 2010; Schiffman et al., 2007). The LMP and EBNA proteins of Epstein-Barr virus (EBV) (Thompson and Kurzrock, 2004), Tax protein from human T lymphotrophic virus-1 (HTLV-1) (Grassmann et al., 2005) and HCV-core protein of hepatitis C virus (HCV) (Tsai and Chung, 2010), among many others, also contribute in different way to tumour formation.

Mutated/altered self-antigens

These proteins are the products of mutation in the DNA sequence, such as H-Ras and K-Ras, which are constitutively active Ras mutant forms expressed in 30% of human cancers (Downward, 2003). Alternatively, they can be derived from tumour-specific genomic translocations, such as the fusion proteins BCR-ABL and PML-RARα, found in some types of leukaemia (Druker et al., 2001).

Oncofetal antigens

These proteins are normally produced in the early stages of embryonic development and disappear by the time the immune system is fully developed. Thus self-tolerance does not develop against them. Examples are alphafetoprotein (AFP) in hepatocellular carcinoma and germ cell tumours (Mizejewski, 2002), and carcinoembryonic antigen (CEA), in colorectal, gastric, pancreatic and lung carcinomas (Hammarstrom, 1999; Wang et al., 2008).

Cancer/testis antigens

These proteins are normally expressed only in the germ cells of the testis, in embryonic ovary and in placenta, and are aberrantly expressed in some types of cancer.

1.3.1 The cancer/testis antigens: classification

The first cancer/testis (CT) antigen to be identified was discovered in a melanoma patient, where it was presented as a tumour antigen on the surface of melanoma cells by MHC molecules and recognised by autologous cytotoxic T lymphocytes (Knuth et al., 1989; Van Pel et al., 1995). It is now known that most CT proteins are encoded by genes that are normally only expressed in the germ cells of the testis (Grizzi et al., 2003; Jungbluth et al., 2000b; Tapparel et al., 2003; Xu et al., 2004), although they are occasionally expressed in the ovary (Nelson et al., 2007), trophoblasts (Jungbluth et al., 2007) and some other somatic tissues. However, they have been found to be aberrantly expressed in various tumour types (Hofmann et al., 2008; Scanlan et al., 2004; Simpson et al., 2005), hence the name 'cancer/testis antigens'. Subsequent studies have identified many other CT antigens by several different approaches, such as: T-cell epitope cloning (Boel et al., 1995; Boon et al., 1994; Van den Eynde et al., 1995; van der Bruggen et al., 1991); serological analysis of cDNA expression libraries (SEREX) (Chen et al., 1997b); differential gene expression analysis (Lucas et al., 1998; Rimoldi et al., 1999); and bioinformatics methods (Lucas et al., 2000; Scanlan et al., 2002a). To date, more than 100 gene families have been identified, some of which contain multiple members and splicing variants that have been recently classified in a database (Almeida et al., 2009; Scanlan et al., 2004). These high levels of multigenicity suggest that the CT antigens family are likely to have formed by gene retrotransposition, duplication and subsequent divergence (Chomez et al., 2001). Among these CT antigen families, 19 have been found to elicit humoral and cellular immune responses in cancer patients and, for this reason, they are considered to be good candidates for the formulation of cancer vaccines.

CT antigens are divided between those encoded by the X chromosome (CT-X) and those that are not (non-X CT). Non-X CT antigen genes are distributed throughout the genome and are normally expressed in spermatocytes (Grizzi et al., 2003; Tapparel et al., 2003; Xu et al., 2004). In contrast, CT-X genes are highly expressed in the spermatogonia (mitotically proliferating germ cells) (Jungbluth et al., 2000b), and it has been estimated that 10% of the genes on the X-chromosome belong to the CT-X family (Ross et al., 2005). They have been shown to diverge faster and

undergo stronger diversifying selection when compared to non-X CTs and other control genes located both on the X chromosome and on autosomes (Stevenson et al., 2007a). CT-X genes have also been found to be expressed in 30-40% of tumour types (Old, 2001).

A more recent classification of CT antigens suggested the subdivision of these genes into three groups: testis-restricted CTs, corresponding to the classically described CT genes only expressed in testis and cancer; testis/brain restricted CTs, which are also expressed in brain tissue; and testis-selective CTs, which show additional expression in somatic tissues. CT-X genes were found to be significantly more testis-restricted than non-X CT (Hofmann et al., 2008).

The most important families of CT-X antigens are listed in Table 1.2.

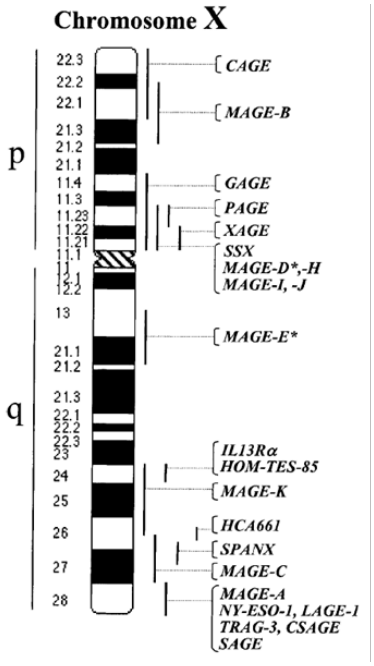

CT antigen family	CT identifier	Number of genes in the family	Chromosome location
MAGE-A	CT1	12	Xq28
MAGE-B	CT3	6	Xp21-p22
MAGE-C1	CT7	2	Xq26, Xq27.2
MAGE-C2	CT10	1	Xq27
NY-ESO-1	CT6	3	Xq28
GAGE	CT4	18	Xp11.4-p11.2
XAGE	CT12	11	Xp11.22-p11.21
PAGE	CT16	7	Xp11.23-p11.21
SSX	CT5	10	Xp11.23-p11.22
SPANX	CT11	12	Xp11.22, Xq27.3-q27.1
CSAGE/TRAG-3	CT24	3	Xq28

Table 1.2 CT-X antigen most studied families. *Antigens without specific CT expression profile. Adapted from Zendman *et al*, 2003.

1.3.1.1 The MAGE family

The *MAGE* (Melanoma Antigen Genes) family is one of the broadest and most studied of the CT gene families, and is composed of more than 50 genes divided into subfamilies (*MAGE-A to –L*). The predominant feature in *MAGE* genes is a large central region termed the MAGE homology domain (MHD) (Barker and Salehi, 2002; Chomez et al., 2001; Xiao and Chen, 2004). This region is conserved in many multicellular organisms, including *Drosophila* and *Aspergillus*, but is apparently lacking in *C. elegans* and in unicellular organisms such as yeast and protozoa.

Human MHDs are 165–171 amino acids in length, and based on alignment can be divided into five regions, in which domains 1, 3 and 5 are very similar while the linking domains 2 and 4 are less well conserved. Structural predictions suggest that the MHD contains at least four potential α-helical domains and five regions of β-sheet structure; furthermore the structure of the MHD of MAGE-A4 has been recently resolved by X-ray crystallography (PDB entry 2wa0). Despite its intra- and interspecies conservation, the MHD shows no significant homology to other proteins that would provide clues to its function and its cellular role remains uncertain.

Most of *MAGE* genes consist of little more than a single MHD, flanked by a small amount of poorly conserved N- and C-terminal sequence. The first cluster of *MAGE* genes (*MAGE-A*) was described at Xq28 (De Plaen et al., 1994), and two more clusters were then identified at Xp21-p22 (*MAGE-B*, (Muscatelli et al., 1995)) and Xq26-27 (*MAGE-C*, (Lucas et al., 1998)). These three subfamilies form the type I *MAGE* genes. Besides from mapping on the X chromosome, type I *MAGEs* present the open reading frame (ORF) encoded in the last exon. *MAGE-C1* has more extended N- and C-termini than the others, but these are unremarkable apart from the presence of several tandem repeat sequences in the N-terminal region. In mouse two groups of type I *MAGE* have been identified and named *mMage-a* and *–b* as their sequences and iso-electric points were closest to those of the human *MAGE-A* and *MAGE-B*. They were found expressed only in male germ cells and, for some of them, in tumour cells (Chomez et al., 2001). *MAGE-C* orthologues have not been identified in mouse.

Type II *MAGE* family members cannot be defined as CT antigens as they are more ubiquitously expressed in normal tissues and not overexpressed in cancer. Their genes are encoded on several different chromosomes. *MAGE-D to –L* belong to this second group: *Necdin*, *MAGE-F1* and *MAGE-G1* resembles more the type I *MAGEs*, whereas *MAGE-D1* to *-D4*, *MAGE-E1* and *MAGE-L2* code for larger proteins presenting a second domain loosely conserved, named as the MHD2 domain, with no homology to other proteins. In *MAGE-D1*, this is separated from the MHD domain by an interspersed repeat domain (IRD) consisting of 25 tandem repeats of the hexapeptide WQXPXX (Figure 1.8). Differently from Type I *MAGEs*, type II ORFs are encoded on multiple exons, and some of them present several splicing variants.

In mouse, *mMage-D* genes have been characterised to be highly homologous to their human counterparts (up to 99% amino acid identity for *MAGE-D2*) (Chomez et al., 2001).

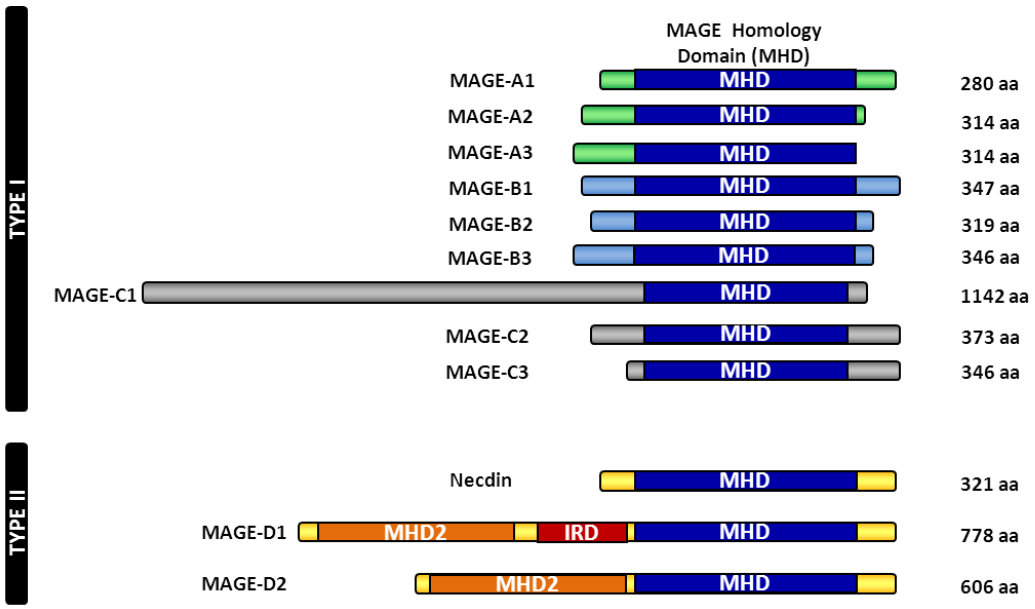

Figure 1.8 Schematic representation of some MAGE family members. MHD: MAGE homology domain; IRD: interspersed repeat domain.

1.3.1.2 The NY-ESO-1 family

Besides the MAGE family, NY-ESO-1 is one of the most immunogenic CT antigens. Also known as CTAG1 or CT6, it was first discovered by SEREX in oesophageal squamous cell carcinoma (Chen et al., 1997a; Chen et al., 1997b).

NY-ESO-1 is a 180 amino acid long 18 kDa protein with a glycine-rich N-terminal region and an extremely hydrophobic C-terminus. It belongs to a family of at least three genes, *NY-ESO-1*, *LAGE-1* and *ESO3*, which map in tandem on chromosome Xq28.

LAGE-1 presents high homology to *NY-ESO-1* (84% identity). Both genes are encoded on three exons and have the capacity to generate shorter products from alternative reading frames, including a smaller 109 amino acids product named CAMEL (Aarnoudse et al., 1999). *LAGE-1* also presents two splicing variants, *LAGE-1a* and *LAGE-1b* encoding polypeptides of 210 and 180 residues, respectively (Lethe et al., 1998).

Conversely, *ESO3* presents less than 50% sequence homology with the other two members of the family and it is ubiquitously expressed in normal tissues, therefore it cannot be classified as a CT antigen (Alpen et al., 2002).

The only predicted domain for NY-ESO-1 is a Pcc-1 domain in its C-terminus (amino acids 89 to 164), that is homologous to a yeast transcription factor involved in cell cycle progression and polarised growth (Kisseleva-Romanova et al., 2006).

NY-ESO-1 is known to interact with MAGE-C1 (Cho et al., 2006). However, its cellular function is unknown and a biological characterisation of this protein is yet to be reported.

1.3.1.3 The GAGE/PAGE/XAGE family

This superfamily of X chromosome coded GAGE-like proteins includes in total more than 30 genes coding for relatively small proteins (79-146 amino acids) for which no orthologues have been found so far. *GAGE* was first identified as an antigen in a human melanoma cell line (Van den Eynde et al., 1995). During the search for *GAGE*-like genes, *PAGE-1* was identified in a prostate cancer cell lines, and subsequently the *PAGE* family was enlarged to 7 members

(Brinkmann et al., 1999; Brinkmann et al., 1998). The *XAGE* family also presents homologies with *GAGE* and *PAGE* genes, and was identified in Ewing's sarcoma, melanoma and lung carcinoma (Zendman et al., 2002b).

Recently, PAGE-4 have been demonstrated to be a highly (100%) intrinsically disordered protein (IDP), meaning it lacks stable 3D structure under physiological conditions *in vitro* (Hellman et al., 2011; Zeng et al., 2011). IDPs have been shown to play important roles in transcriptional regulation and signalling (Uversky and Dunker, 2010). A subsequent study showed that many CT antigens are IDPs and can potentially bind DNA (Rajagopalan et al., 2011).

1.3.1.4 The SSX, SPANX, and CSAGE/TRAG-3 families

The antigen HOM-MEL-40 has been firstly identified in melanoma and subsequently found to be derived from the *SSX2* gene, that had been previously described fused to the *SYT* gene in the t(X,18) chromosomal translocation in sarcoma (Tureci et al., 1996). The SSX family was then expanded to 10 proteins of 188 amino acids encoded by six exons. Several orthologues have been annotated, restricted to mammalian genomes (Smith and McNeel, 2010).

The 12 *SPANX* genes code for small (around 100 amino acids), nuclear putative proteins exclusively expressed in testis and some tumour types. The first one, *CTp11*, was in fact first characterised in a melanoma cell line (Zendman et al., 2003). Their function is currently unknown.

CSAGE and *TRAG3* are homologue genes firstly discovered in chondrosarcoma (Lin et al., 2002) and ovarian cancer (Duan et al., 1999), respectively, and are encoded on the X chromosome.

The number of non-familial CT antigens is also constantly increasing, and these includes synaptonemal complex protein 1 (SCP-1), known to play a role in the pairing of chromosomes in meiosis and overexpressed in renal cell carcinoma (Meuwissen et al., 1992); BRDT, belonging to the RING3 family of transcriptional regulators (Jones et al., 1997); the protease TSP50 (Shan et

al., 2002); the proacrosin binding partner OY-TES-1 (Ono et al., 2001), and many others (see http://www.cta.lncc.br).

1.3.2 CT antigen expression

1.3.2.1 CT genes in normal tissues

According to RT-PCR analysis, CT antigen expression in normal tissues is largely limited to testis, foetal ovary and foetal placenta. Testis is the only tissues expressing all of the antigens, whereas only few CT mRNAs are present in placenta, including *MAGE-A3*, *-A4*, *-A8* and *–A11*. Very low expression levels of *NY-ESO-1* have also been found in adult ovary, uterus and breast, as well as pancreas and liver, but no protein was detectable in these tissues (Scanlan et al., 2002b). In addition to mRNA analysis, immunohistochemistry (IHC) has been used to study the expression of CT antigens both in normal and malignant tissues (Figure 1.9). The MAGE-A proteins presents high homology, therefore it proved difficult to produce antibodies that recognise only a specific member of the family. The monoclonal antibody 57B was utilised to determine the expression patterns of *MAGE-A* in the testis; MAGE-A were only detected in spermatogonia and spermatocytes, but not in any other normal tissue. The staining was strongly nuclear, with some milder cytoplasmic signal. Spermatids were negative for 57B (Jungbluth et al., 2000a). Similar results were obtained with another MAGE-A monoclonal antibody, namely M454 (Jungbluth et al., 2000b). *MAGE-C1* expression was also analysed, using the monoclonal antibody CT7.33, that gave the same pattern of expression of MAGE-A in germ cells. However, MAGE-C1 subcellular localisation was equally nuclear and cytoplasmic (Jungbluth et al., 2002).

NY-ESO-1 staining, also both cytoplasmic and nuclear, is positive in the spermatogonia and primary spermatocytes (but not in post-meiotic spermatogenic cells), the oogonia of the foetal ovary, and the trophoblast (both cytotrophoblast and syncytiotrophoblast) of the placenta (monoclonal antibody ES121) (Jungbluth et al., 2001; Jungbluth et al., 2007).

SSX was found to be expressed exclusively in the nuclei of spermatogonia and primary spermatocytes. Intriguingly, IHC staining for SSX was observed only in a sub-population of spermatogonia; its expression was heterogeneous. Normal thyroid, previously found to be positive for SSX2 mRNA, was negative upon IHC staining. This demonstrates that the mRNA data do not always correspond to actual CT protein expression (dos Santos et al., 2000; Scanlan et al., 2002b).

Not all CT antigens show strictly pre-meiotic expression. For example, SPANX proteins are exclusively expressed in haploid spermatids and spermatozoa, both X- and Y-bearing (Hendriksen, 1999).

In all the studies mentioned, no expression was found in other testis-associated cells, such as Sertoli cells and Leydig cells.

The expression of some CTs was assessed at the protein level also during human gonadal development. *MAGE-A1* and *NY-ESO-1* peak at the beginning of the second trimester, both in testis and ovary. This corresponds to a period of high proliferation of oogonia and gonocytes; a subsequent reduction was observed as the cells started differentiating and entered cell cycle arrest. In oocytes, *MAGE-A1* expression terminates around birth, while *NY-ESO-1* is still expressed at the neonatal stage. Differently from these two antigens, *GAGE* is expressed throughout gonadal development until adulthood (Gjerstorff et al., 2007).

Another study showed that *MAGE-A* are also expressed during differentiation of human embryonic stem cells (hESC) to embryoid bodies, as well as in neurons of the early developing central nervous system and peripheral nerves. *GAGE* on the other end is expressed in the early ectoderm and peripheral adrenal cortex (Gjerstorff et al., 2008).

Interestingly, several CT genes and their products, including *SSX*, *NY-ESO-1*, and *MAGE-D1*, were found expressed in undifferentiated mesenchymal stem cells and down-regulated after osteocyte and adipocyte differentiation (Cronwright et al., 2005). More recently, it was published that antigens belonging to the *MAGE*, *GAGE*, *NY-ESO-1* and *SSX* families were expressed at the mRNA level in putative melanoma stem cells; *MAGE-A* was also detected at the protein level (Sigalotti et al., 2008).

1.3.2.2 CT genes in cancer

The frequency of an individual CT is variable in different tumour types. Based on *in silico* analyses, cancer types can be divided into high expressers, such as melanoma, hepatocarcinoma, non-small-cell lung cancer and bladder cancer; moderate CT gene expressers, like breast and prostate cancer; and low expressers, for example renal and colon cancer, as well as most hematopoietic malignancies (Scanlan et al., 2004). An exception to the latter is multiple myeloma, which has been shown to express several CT antigens, in particular MAGE-C1 (Tinguely et al., 2008). Table 1.3 summarises the expression frequencies (%) of several CT antigens in various cancers. In general, *MAGE-A1*, *MAGE-A3*, *MAGE-A4*, *NY-ESO-1*, *SSX2* and *PRAME* (Preferentially Expressed Antigen of Melanoma) are the most frequently expressed CT genes in tumour samples.

CT Antigen	Frequency (%) of Expression in Tumour Type																
	Blad	Brn	Brst	Col	Eso	Gas	H/N	Liver	Leu/Lym	NSCLC	Mel	MM	Ov	Pancr	Pros	Renal	Sarc
MAGE-A1	57	25	18	2	53	29	28	58	0	70	48	26	20	28	15	0	14
MAGE-A2	-	18	-	-	-	-	-	35	-	28	60	-	21	-	-	-	82
MAGE-A3	50	11	-	-	32	-	51	42	32	35	64	52	22	-	-	-	-
MAGE-A4	-	11	-	-	90	-	60	15	61	19	16	24	16	-	-	-	-
MAGE-A6	-	14	-	-	-	-	-	38	-	25	82	47	-	-	-	-	-
MAGE-A11	-	-	-	-	-	-	-	38	-	76	-	-	-	-	-	-	-
MAGE-A12	51	45	-	-	-	-	-	38	-	36	74	15	-	-	-	-	46
MAGE-B1	0	0	17	0	-	0	0	48	0	14	22	-	-	-	0	0	9
MAGE-B2	-	-	-	-	-	-	-	60	-	52	22	37	-	-	-	-	-
MAGE-C1	44	9	30	10	-	-	36	48	0	33	33	66	-	-	-	-	60
MAGE-C2	-	12	-	-	-	-	10	47	0	30	33	50	-	-	-	-	-
NY-ESO-1	40	7	-	0	41	0	17	25	-	18	33	22	33	0	25	9	55
LAGE-1	27	2	-	-	39	-	19	26	-	34	38	49	21	-	-	-	27
GAGE-1	12	-	9	0	-	-	19	38	1	19	28	-	31	-	10	0	25
XAGE-1	-	-	-	-	-	-	-	-	-	40	24	-	-	-	-	-	70
PAGE-5	-	-	5	11	-	-	-	-	-	39	22	-	0	-	-	44	-
SSX-2	44	6	7	12	-	-	35	9	36	16	35	-	-	-	40	5	50
SPANXC	9	-	25	22	0	-	-	-	-	33	70	-	-	-	-	-	-
CSAGE/TRAG3	-	-	-	-	55	10	-	18	-	41	-	-	-	-	-	-	79
BORIS	-	-	71	-	-	-	17	-	-	36	27	-	-	-	-	-	-
BRDT	-	-	-	-	-	-	-	29	-	38	0	-	-	-	-	-	-
NFX2	-	-	-	-	-	-	-	-	-	15	5	-	-	-	-	-	-
PASD1	-	70	45	40	-	45	28	-	25	30	42	87	-	-	30	-	-
PRAME	18	44	40	4	-	50	48	-	36	62	92	32	-	-	10	41	61
SCP1	-	24	-	-	-	-	-	28	23	7	14	-	0	48	-	-	-
TSP50	-	-	28	-	-	-	-	-	-	-	22	-	-	-	-	-	-

Table 1.3 Published mRNA expression frequencies of some CT genes in various cancers. Abbreviations: Blad, bladder; Brn, brain; Brst, breast; Col, colon; Eso, esophageal; Gas, gastric; H/N, head and neck, Leu/Lymph, leukaemia/lymphoma; NSCLC, non-small cell lung cancer; Mel, melanoma; MM, multiple myeloma; Ov, ovarian; Pancr, pancreatic; Pros, prostate; Sarc, sarcoma. Adapted from Scanlan *et al.*, 2004 and http://www.cta.lncc.br.

An interesting feature of CT expression in cancer is the tendency for it to be clustered, i.e. CT genes are often co-expressed or none of them is expressed. For example, an analysis of melanoma

and breast cancer specimens showed no CT expression in 26% and 47% of samples respectively, vs. expression of three or more CT antigens in 65% and 40% of CT-positive samples, respectively. Similar results were obtained in a study carried out in lung cancer (Sahin et al., 1998; Sugita et al., 2002).

Immunohistochemical analysis has revealed that CT antigens are rarely homogeneously expressed in tumours. They are frequently found in only a relatively small proportion of a tumour's cells, and this phenomenon is yet to be fully understood (Aubry et al., 2001; Chitale et al., 2005; Dhodapkar et al., 2003; Jungbluth et al., 2000b; Li et al., 2005). Figure 1.9 shows that the heterogeneous expression pattern can differ for different CT antigens. For example, NY-ESO-1 is mostly cytoplasmic, and is often found in focal clusters, with the exception of synovial sarcoma, where it shows mostly diffuse homogeneous staining (Figure 1.9E and F). Instead, MAGE-C1 staining shows single positive cells dispersed throughout the tumour (Figure 1.9D). Analysis of the phenotypic and functional differences between these cells and those in the tumour that do not express CT antigens could clarify the role of these proteins in malignancy.

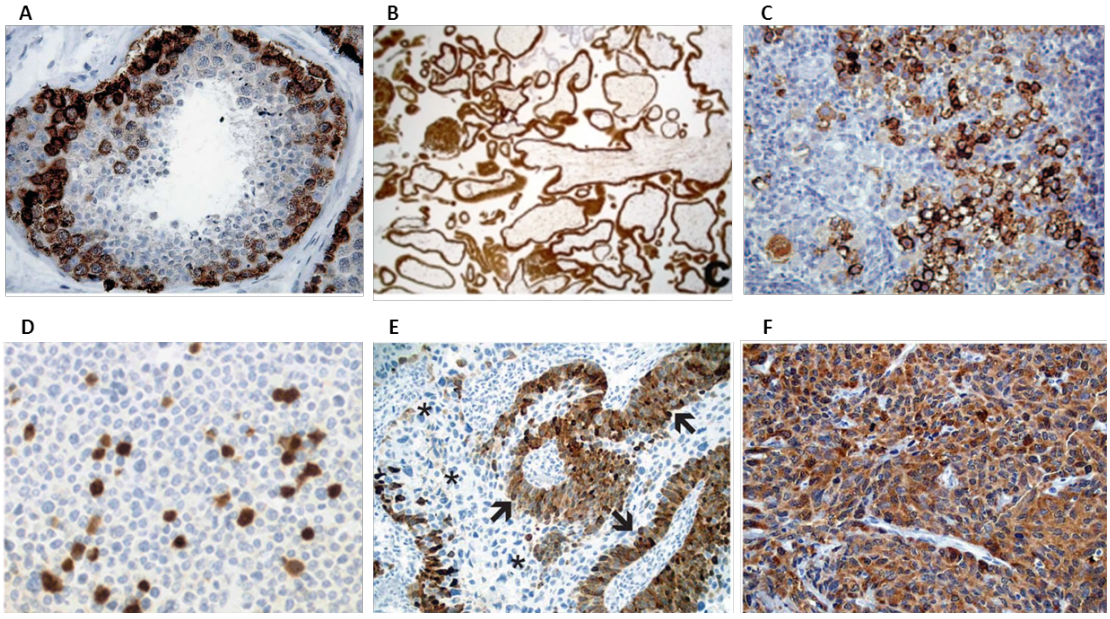

Figure 1.9 CT antigen expression in normal tissues and tumours. A. ES121 (NY-ESO-1) in testis. B. 57B (MAGE-A) in 8 week placenta. C. CT7.33 (MAGE-C1) in foetal ovary. D. CT7.33 (MAGE-C1) in plasma cell myeloma, heterogeneous scattered staining. E. E978 (NY-ESO-1) in urothelial carcinoma, heterogeneous staining with immunopositive foci (arrows) and negative tumour cells (asterisk). F. E978 (NY-ESO-1) in synovial sarcoma, homogeneous staining. Adapted from Scanlan *et al.* 2002, Jungbluth *et al.* 2007, Simpson *et al.* 2005, Tinguely *et al.* 2008, Jungbluth *et al.* 2000, Gnjatic *et al.* 2006.

Interestingly, a higher frequency of *MAGE* mRNA expression was found in metastatic vs. primary melanoma (Brasseur et al., 1995; Velazquez et al., 2007) and in invasive vs. superficial bladder cancer (Patard et al., 1995). In the latter, *NY-ESO-1* expression could be correlated with high grade (Kurashige et al., 2001). A correlation with disease progression was also observed in prostate cancer (Suyama et al., 2010), where MAGE-C2 is a predictor of recurrence (von Boehmer et al., 2011) and SSX proteins were expressed only in the metastatic lesions (Smith et al., 2011). Another melanoma study showed that the expression of *MAGE-C1* and *MAGE-C2* is a predictor of lymph node metastasis (Curioni-Fontecedro et al., 2011). In breast cancer, CT expression correlated with hormone-receptor negative and high-grade breast cancers (Chen et al., 2011; Grigoriadis et al., 2009). In multiple myeloma, the frequency of CT expression at the mRNA level correlates with increased stage (van Baren et al., 1999), elevated plasma cell proliferation (Jungbluth et al., 2005), early relapse and reduced survival (Atanackovic et al., 2009). Intriguingly, plasma cell myelomas showing MAGE-C1 cytoplasmic subcellular localisation had a better prognosis than myelomas with combined nuclear-cytoplasmic or nuclear expression only (Tinguely et al., 2008).

All these evidence show that CTs could be used as effective biomarkers for the staging of cancer.

1.3.3 CT antigen regulation

As mentioned above, CT antigen gene expression is restricted to cancers, gametes and trophoblast cells, but is not detected in normal cells. This suggests that there should be a common mechanism of regulation shared by these cell types. Epigenetic modifications have been linked to CT expression, firstly with regard to DNA methylation on the cytosine of CpG dinucleotides. Such dinucleotides are often clustered in regions larger than 200bp called CpG islands, presenting a C+G content over 50%. These regions, accounting for 1% of the genome, are often associated with the 5' regulatory sequences of genes. When CpG islands are methylated, methyl-binding proteins can bind these regions and subsequently recruit histone deacetlyases (HDAC), which in turn deacetylate the histones. This leads to a tighter packing of the DNA, which cannot be accessed by transcription factors, resulting in gene silencing (Bestor, 1998). Methylation of CpG islands is a regulatory mechanism shared by imprinted genes, X-chromosome inactivated genes, tissue specific genes and germ-line specific genes.

CT promoters contain CpG islands that are normally methylated, and become aberrantly demethylated in cancer. This has been demonstrated for several of them, starting from *MAGE-A1*, whose promoter contains multiple cis-regulatory sequences, including some Ets and Sp1 transcription factor binding sites: in cancer cells, the CpG islands in the proximity of these sites are demethylated, hence the transcription factor can bind and activate transcription (De Smet et al., 1995). In agreement with this, the DNA methyl-transferase inhibitor 5-aza-2-deoxycytidine (5-Aza-CdR) can induce expression of *MAGEs* (De Smet et al., 1996; De Smet et al., 1999; Sigalotti et al., 2002b; Weber et al., 1994) , *NY-ESO-1* (Sigalotti et al., 2002a), *LAGE-1* (Lethe et al., 1998), *SSX2* (Sigalotti et al., 2002a), *CAGE* (Cho et al., 2002) and *GAGE* (Sigalotti et al., 2002a). This effect has been shown to be clonally inherited throughout cellular replication in melanoma (Fratta et al., 2010).

In cancer, alterations of DNA methylation have been described. The specific hypermethylation and silencing of tumour suppressor promoters is believed to be a primary event in tumourigenesis (Robertson and Wolffe, 2000). Global hypomethylation has also been observed, which can cause

chromosome instability, loss of imprinting and aberrant transcription (Esteller and Herman, 2002). The latter is likely to be the cause of CT expression in several tumours. Indeed, a study indicated that in tumours hypomethylation of the *MAGE* gene promoter is associated with global hypomethylation, while it is not associated with tumour suppressor gene hypermethylation (Kaneda et al., 2004). Similar results were obtained for *NY-ESO-1* in ovarian cancer (Woloszynska-Read et al., 2008).

However, several studies showed that treatment with 5-Aza-CdR is not sufficient to trigger CT genes expression (Karpf et al., 2004; Suyama et al., 2002; Zendman et al., 2002a). Also, DNA is hypomethylated for instance in colon cancer (Goelz et al., 1985), but this typology of tumour rarely expresses CT antigens. As mentioned above, the acetylation status of histones affects transcription as well, and trichostatin A, an HDAC inhibitor, can act synergistically with 5-Aza-CdR to induce the expression of *MAGE-A1*, *-A2*, *-A3*, and *-A12* as well as *NY-ESO-1* (Oi et al., 2009; Wischnewski et al., 2006). More recently, it has been demonstrated that inhibition of histone methyltransferase and histone demethylases enhances CT expression, indicating that not only DNA methylation but also histone methylation has a role in regulating their transcription (Rao et al., 2011).

Some transcription factors regulating CT expression have also been identified. BORIS (brother of the regulator of imprinted sites) is a CT antigen and a testis-specific mammalian paralogue of the transcription regulator CTCF, containing an 11 zinc finger domain that binds DNA (Loukinov et al., 2002). CTCF works forming methylation-dependent insulators that regulate genomic imprinting and X chromosome inactivation (Ohlsson et al., 2001). *BORIS* and *CTCF* expression is inversely correlated during male germ cell development, and in particular demethylation is linked with upregulation of *BORIS* and downregulation of *CTCF*. BORIS has proved to be a very interesting protein, as it is the first CT antigen described to affect other CT antigens' expression at the transcriptional level. BORIS has been reported to induce demethylation and derepression of *MAGE-A1* and *NY-ESO-1* (Hong et al., 2005; Vatolin et al., 2005); subsequent studies showed that it can directly bind the promoters of *MAGE-A2*, *-A3* and *-A4* (Bhan et al., 2011) and *TSP50*

(Kosaka-Suzuki et al., 2011) to induce their expression. *TSP50* is also controlled by p53 tumour suppressor, which represses its expression by direct binding to its promoter (Xu et al., 2007), and by Sp1, which when phosphorylated by ERK in response to bFGF mediates *TSP50* downregulation (Wang et al., 2010).

A recent report demonstrated that γ-radiation promotes the expression of several CT antigens both in cancer cell lines and in fresh tumour biopsies, thereby increasing the immunological recognition of the tumour by $CD8^+$ T cells (Sharma et al., 2011).

Furthermore, two studies suggested that microRNAs may also play a role in the regulation of CT antigens. They showed that *MAGE-A* genes are regulated by the microRNA 34a, which directly targets their 3′ untranslated regions and decreases MAGE-A protein levels in medulloblastoma cell lines (Weeraratne et al., 2011), and that *PRAME* is similarly regulated by microRNA-211 in melanoma (Sakurai et al., 2011).

To summarise, epigenetic reprogramming via alterations in DNA methylation and chromatin re-structuring is so far the main trigger of the aberrant expression of CT antigens in malignancies (Figure 1.10). However, global demethylation cannot account for the heterogeneous expression pattern often observed in tumours. It has therefore been proposed that the aberrant expression of CT antigens could be associated to the induction or activation of a gametogenic program in cancer, through a so far unknown mechanism. This is supported by the fact that, a part from epigenetic remodelling, tumourigenesis shares with gametogenesis several other feature, such as cellular immortality, migratory behaviour, immune evasion, and ectopic production of gonadotropins (Old, 2001).

Although the regulation of CT antigens expression at the mRNA level has been partially elucidated, nothing is known about their protein turnover and post-translational regulation. This could give important clues about their function and tools to manipulate their expression in order to increase their antigen presentation and therefore their immunogenicity.

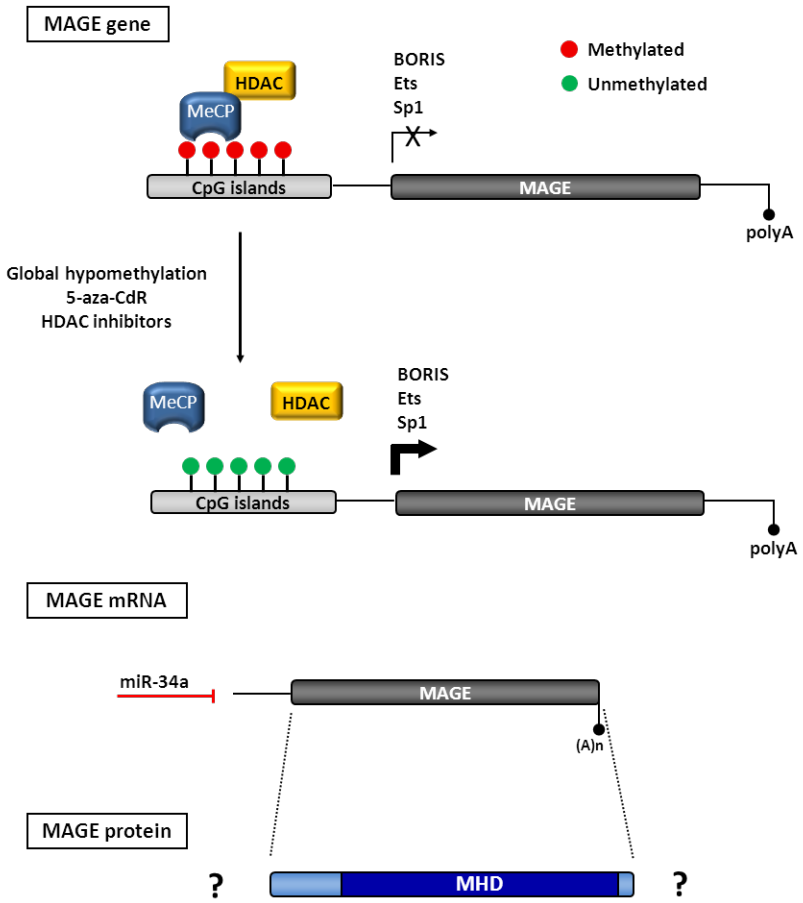

Figure 1.10 Regulation of MAGE antigens. MAGE genes, as all CT antigens, normally present methylated CpG islands on their promoters which allow binding of methylCpG binding proteins (MeCP), recruitment of histone deacetylases (HDAC) and inhibition of transcription. Cancer-associated global hypomethylation, as well as treatment with 5-Aza-CdR or HDAC inhibitors, lead to CpG island demethylation, binding of transcription factors such as BORIS, Ets and Sp1, and gene expression. miR-34a is responsible for MAGE mRNA degradation. Nothing is known about MAGE protein regulation.

1.3.4 CT antigens in cancer immunotherapy

Cancer immunotherapy is based on the concept of immune surveillance: in the same way that it recognises and destroys infectious agents or damaged cells, the immune system is capable of detecting and eliminating cancer cells. Cancer develops when the immune system fails to recognise cancer cells, or the immune response directed against it is suppressed or outpaced (Schuster et al., 2006). Immunotherapy aims to initiate, strengthen and sustain the tumour-specific immune response, and it has significantly developed in the last decades, mainly with the formulation of monoclonal antibodies and cancer vaccines.

Monoclonal antibodies directed against tumour antigens boost the patient's immune response to attack the tumour cells and prevent tumour growth by altering signal transduction within the cell, for example by blocking specific cell receptors. Clinical trials of monoclonal antibody therapy are in progress for many types of cancer. Examples of such therapy are the drugs trastuzumab (Herceptin®), directed against the overexpressed HER-2 receptor in the treatment of breast cancer, and bevacizumab (Avastin®), which targets the VEGF-A protein involved in signalling for the formation of new blood vessels and is used in colorectal, lung and breast cancers. Monoclonal antibodies can also be conjugated with radioactive particles to specifically direct radiotherapy to the cancer cells, minimising side effects. An example is Iodine (^{131}I) tositumomab, effective in patients with relapsed follicular lymphoma.

Vaccine therapy can be subdivided into two groups: prophylactic cancer vaccines and therapeutic cancer vaccines. The former are administered before the occurrence of tumours to individuals that are at high risk for developing cancer or have been diagnosed with pre-malignant lesions in target tissues (Finn and Forni, 2002). The FDA has so far approved two prophylactic cancer vaccines: one against human papilloma virus, which causes cervical cancer (Plummer and Franceschi, 2002; Schultz, 2003) and one against hepatitis B virus, which can cause liver carcinoma (Huang and Lin, 2000; Viviani et al., 1999). Very recently, initial evidence has emerged of a prophylactic therapy against breast carcinoma that targets *α-lactalbumin*, a breast-specific gene that is expressed in the majority of human breast carcinomas and in mammary epithelial cells only

during lactation. This vaccine granted protection from tumour formation in mouse models, therefore it represents a promising approach for breast cancer prevention in women in their post-child-bearing years (Jaini et al., 2010).

However, most cancer vaccines are therapeutic, in that they are intended to treat existing cancer rather than to prevent it. Vaccination can be undertaken after surgery to generate a specific immune response capable of clearing any residual cancer, thus preventing relapse. However, there exist significant challenges for their development, such as choice of the tumour antigen, choice of the adjuvant, delivery system and usage of modulators of cancer immunosuppression (Finn, 2003). Moreover, the tumour can acquire the ability to escape the immune system, for example via the production of cytokines like IL-10 or TGF-β; also, recent findings showed that regulatory T cells, whose function is to maintain T-cell tolerance to self-antigens, can suppress immunity directed against the tumour (Zou, 2006).

Several different vaccination strategies have emerged, resulting in clinical trials (Ribas et al., 2003; Rosenberg et al., 2004). For example, the use of DNA vaccines has been investigated, whereby plasmids encoding the target antigen are administered with the aim of increasing recognition of tumour targets or stimulating immunity. Likewise, dendritic cells (DC) have been used to vaccinate against tumours. Dendritic cells are specialised antigen-presenting cells that can be generated *ex vivo* from peripheral blood monocytes or bone marrow/circulating hematopoietic stem cells cultured in the presence of cytokine cocktails. They can then be pulsed with tumour antigens and safely re-administered in the patient, where their immunogenicity leads to the induction of antigen-specific immune responses (Ballestrero et al., 2008; Nencioni and Brossart, 2004).

To date, tumour vaccination has had limited success in a therapeutic setting and only a minority of patients have exhibited actual tumour regression. Comparatively, adoptive T cell therapy (ACT) has shown more striking results in clinical trials. ACT exploits the evidence that some lymphocytes have trafficked into the tumour micro-environment; these can be isolated and expanded *in vitro* with cytokines, including IL-2, allowing the generation of antigen-specific T

cells. The aim is to subsequently re-infuse these cells into the patient, where they will infiltrate the tumour lesion and react to it. ACT therapy has been employed for the treatment of late-stage melanoma patients in several clinical trials with highly significant results: extremely large lesions showed complete regression, and patient response rate was dramatically increased (Rosenberg and Dudley, 2009; Rosenberg et al., 2008). It was further demonstrated that some of these lymphocytes recognised specific antigens prevalent in melanoma (Panelli et al., 2000; Seiter et al., 2002). Although ACT has been successful for melanoma, bladder carcinoma and lung carcinoma, retrieving T cells has proved problematic in many other tumour types (Heidecker et al., 2000; Weynants et al., 1999).

The CT antigens represent an ideal target for cancer vaccines: first of all their restricted expression pattern in normal tissues allows a selective action against tumour cells without targeting other tissues. Testis cells do not express antigen presenting MHC class I molecules, moreover the blood-testis barrier prevents the immune system from contacting with CT gene products. As a consequence immune recognition of these proteins occurs spontaneously only in cancer patients. The exceptions to this are a humoral response to MAGE-B1 observed in systemic lupus erythematosus (McCurdy et al., 1998) and to SPA17 in vasectomised men (Lea et al., 1997).

A second reason for which CT antigens are good target for cancer immunotherapy is the fact that they are expressed in a great variety of tumours, and this widens the applicability of the vaccination. CT antigens such as NY-ESO-1, MAGE-A1, MAGE-A3 and SSX2 are able to elicit strong spontaneous immunogenicity, inducing both the cellular and the humoral branches of the immune response. The MAGE proteins and NY-ESO-1 in particular have been a focus of investigation for the formulation of therapeutic vaccines.

1.3.4.1 MAGE-based cancer vaccines

Significant effort has gone into developing cancer vaccines towards MAGE-A. These approaches have included immunotherapy using MAGE-A peptides and recombinant proteins combined with immune-stimulatory molecules to enhance the immune response to the tumour antigen.

Several early clinical trials involved MAGE peptide vaccination, mostly in metastatic melanoma patients. In a MAGE-A3 trial, seven of 25 patients showed significant tumour regression; however, even in these patients CTL responses were rarely detected. In a following study a monoclonal CTL response could be detected in a single patient after MAGE-A3 peptide vaccination (Coulie et al., 2001; Marchand et al., 1999). Furthermore, Graff-Dubois *et al.* demonstrated that a peptide composed by two epitopes, the first shared by MAGE-A2, -A3, -A4, -A6, -A10, -A12 and the second derived from MAGE-A1, was able to induce cytolytic T lymphocytes that recognise each of these MAGE proteins and therefore targeted MAGE-A expressing tumour cells in a very large variety of cancers (Graff-Dubois et al., 2002).

Though initially some successful responses have been reported, other studies could not show consistent benefit in MAGE peptide vaccination. A more efficient immunotherapy was achieved by inducing or augmenting MAGE expression by epigenetic therapies such as DNA demethylating agents and histone deacetylase inhibitors (Cruz et al., 2011; Goodyear et al., 2010; Serrano et al., 2001).

A number of clinical trials have involved MAGE recombinant proteins rather than peptides, because they have the potential to activate a broad array of T-cell responses. Two large phase III clinical studies utilising MAGE-A3 adjuvant immunotherapy have been launched recently: the DERMA trial in melanoma, based on a randomised phase II study in patients with metastatic melanoma, and the MAGRIT trial in non-small cell lung cancer, launched after promising results obtained in a phase II study in 182 patients with resected NSCLC (Sang et al., 2011; Tyagi and Mirakhur, 2009). The aim of these studies is to investigate the efficacy in preventing cancer relapse and the side effects of MAGE-A3 immunotherapy administered after tumour resection in MAGE-A3-positive stage IB, II and IIIA patients.

1.3.4.2 NY-ESO-1-based cancer vaccines

NY-ESO-1 is the most immunogenic CT antigen known to date. In contrast to other antigens, it is common to observe simultaneous antibody and T-cell responses to NY-ESO-1, which is able to elicit a strong integrated $CD4^+$ and $CD8^+$ T cell immune response (Jager et al., 1998; Jager et al., 2000b; Jager et al., 1999). Systematic review of the protein showed an epitope hot spot for T-cell response in the central portion of the NY-ESO-1 protein, covering approximately amino acids 80-110 (Chen et al., 2004; Davis et al., 2004; Gnjatic et al., 2000; Jackson et al., 2004).

Serum antibodies to this protein have been detected in melanoma, lung cancer, ovarian cancer, bladder cancer, breast cancer and oesophageal cancer to mention some. Immunological response may vary by individual, by cancer type and by the grade of differentiation. For example, in patients with lung cancer, antibodies to NY-ESO-1 are observed more frequently in non-small cell lung cancer than in small cell carcinoma, and more frequently in undifferentiated tumours as compared with more differentiated adenocarcinoma or squamous cell carcinoma (Tureci et al., 2006). The clinical effect of detectable antibodies remains unclear. NY-ESO-1 is an intracellular antigen therefore circulating antibodies cannot mediate direct anti-tumour effects, although their presence indicates that the immune system is responding against the antigen.

Multiple, small parallel coordinated clinical trials around NY-ESO-1 have been performed or are underway (Chen et al., 2004; Davis et al., 2004; Jager et al., 2000a). The extent of these trials is now over 30 around the world and they utilise different approaches, such as peptides, protein, viral vectors and dendritic cells, in conjunction with several adjuvants and in different cancer types.

Although it was demonstrated that vaccination can efficiently induce an antibody, $CD8^+$ and $CD4^+$ T-cell response to NY-ESO-1, the clinical effects observed so far are controversial: a study reported in 2008 has shown that a monoclonal antibody raised against CTLA-4, a modulator of immunosuppression, can enhance NY-ESO-1-specific T-cell response and therefore improve the clinical outcome of NY-ESO-1 vaccine in metastatic melanoma (Yuan et al., 2008). Furthermore, a recently developed vaccine consisting of full-length recombinant NY-ESO-1 protein formulated

with ISCOMATRIX adjuvant generated strong humoral and T-cell-mediated immune responses and reduced the risk of relapse in patients with fully resected melanoma. However, no favourable clinical response was noted in advanced melanoma patients in response to NY-ESO-1 ISCOMATRIX vaccine because of regulatory T-cell-mediated attenuation (Davis et al., 2004; Nicholaou et al., 2009). Conversely, vaccination with a synthetic peptide based on NY-ESO-1 was able to induce anti-NY-ESO-1 humoral and T-cell mediated response in a small group of patients with confirmed metastatic and stages III/IV melanoma, NSCLC, breast cancer, ovarian cancer and sarcoma, and positively correlated with survival (Karbach et al., 2010). Nonetheless, in a subsequent clinical study in oesophageal and prostate cancer patients, vaccination with NY-ESO-1 protein did not alter the tumour size (Kawada et al., 2012).

In conclusion it appears that, despite some promising outcomes, current NY-ESO-1 vaccines have a lot of room for improvement, both in antigen and in adjuvant formulations.

1.3.5 Biological functions of CT antigens

Most studies of CT antigens to date have focused on their immunological implications: based on their immunogenicity in cancer patients and restricted expression in somatic cells, CT antigens are potentially ideal targets for cancer vaccines.

Nevertheless, relatively little is known about the biological function of CT genes, and a central question in CT research remains whether CT gene expression contributes to tumourigenesis or is a consequence of it. In addressing this issue, it is important to consider whether our existing knowledge about CT antigen biology can be related to processes that are deregulated in cancer.

1.3.5.1 Function of MAGE proteins

Several functional studies seem to indicate that the type I MAGE proteins can act as oncogenes. For example, *MAGE* expression has been associated with drug resistance: exogenous expression of MAGE-A1 lowers cell sensitivity to Tumour Necrosis Factor (TNF) in cervical cancer cells (Park et al., 2002), whereas MAGE-A2 and MAGE-A6 confer insensitivity to anti-growth signals induced by paclitaxel and doxorubicin in human tumour cell lines (Bertram et al., 1998; Duan et al., 2003; Glynn et al., 2004). Moreover in gastrointestinal stromal tumour the expression of *MAGE* and *NY-ESO-1* is associated with tumour progression under imatinib treatment, as well as tumour recurrence (Perez et al., 2011).

The expression of some *MAGE* genes confers resistance to apoptosis. For instance, multiple MAGE proteins promote cell viability *in vitro* and *in vivo* in mast cells (Yang et al., 2007a). Another well-studied mechanism is the inhibition of p53 tumour suppressor by several members of the MAGE family. MAGE-A2 is able to down-regulate p53 transactivating function by binding to it and recruiting histone deacetylases to p53-responsive promoters (Monte et al., 2006) and by blocking p53 interaction with the chromatin of target genes (Marcar et al., 2010). MAGE-A2 interaction with p53 also affects cellular senescence by interfering with p53 acetylation at the PML-nuclear bodies and by reducing PML post-translational modification (Peche et al., 2011). In addition, MAGE-A3 and MAGE-C2 have been shown to interact with KAP-1, a transcriptional

co-repressor that regulates p53 function and is also an E3 ubiquitin ligase, thus promoting cell survival (Yang et al., 2007b). Based on these data, three novel compounds were identified that interfere with MAGE/KAP binding and could potentially be developed as chemo-therapeutic drugs (Bhatia et al., 2011), although potential side effects should be taken into considerations since MAGE-A3 and MAGE-C2 also regulate KAP-1 repression on genome loci that are target of a Krueppel-associated box (KRAB) domain zinc finger transcription factors, such as *ID1* and *Ki67* (Xiao and Chen, 2004).

Recently, a very interesting study shed a new light on the MAGE protein function: Doyle et al demonstrated that several MAGE members bind E3 RING ubiquitin ligases through the MHD, and enhance their ubiquitin ligase activity. An example is the complex formed by MAGE-C2 and KAP-1, which targets p53 for proteasome-dependent degradation and therefore represents a novel mechanism of p53 regulation by MAGE (Doyle et al., 2010; Espantman and O'Shea, 2010).

Although hematologic malignancies are considered low CT expressers, recent findings demonstrated that multiple myeloma represents an exception. The MAGE proteins can affect apoptosis in this tumour type: *MAGE-A3* and *MAGE-C1* knock-down leads to induction of cell death in MM cell lines, and improved response to the cytotoxic agent melphalan and the proteasome inhibitor bortezomib, both conventional therapies for MM; moreover these two genes are important for the survival of clonogenic myeloma precursors (Atanackovic et al., 2010). Further investigations showed that silencing of *MAGE-A* in MM results in a p53-dependent activation of pro-apoptotic Bax expression and in a reduction of survivin (Nardiello et al., 2011).

MAGE-A3 has also been shown to affect cell death by binding to murine procaspase-12 and inhibiting its cleavage and activation in response to insults targeting the endoplasmic reticulum (Morishima et al., 2002), but the relevance of these findings in human is uncertain as no human homologue of caspase-12 has been described so far (Lamkanfi et al., 2004).

Recent evidence has also shown that MAGE-A3 mediates fibronectin-controlled cancer progression and metastasis (Liu et al., 2008). Forced expression of MAGE-A3 resulted in

p21$^{Cip1/Waf1}$ down-regulation, accelerated cell cycle progression, increased cell migration rate and invasion *in vitro*, and promoted the formation of lung metastases *in vivo* in a mouse model.

Some MAGE protens are known to regulate the activity of transcription factors other than p53. MAGE-A1 interacts with the transcriptional regulator SKI-interacting protein (SKIP), repressing the transcription of its target gene *Notch1* (Laduron et al., 2004), whereas MAGE-A11 can activate a hypoxic response after binding with the hypoxia-inducible factor (HIF) prolyl hydroxylase 2 (PHD2) in a novel, tumour-associated HIF regulatory mechanism (Aprelikova et al., 2009). MAGE-A11 can also interact with the androgen receptor (AR), leading to an increase in the activity of this receptor. MAGE-A11 is phosphorylated and ubiquitinated upon epidermal growth factor (EGF) signalling, and this leads to an increase in the androgen-dependent transcriptional activity. A role of MAGE-A11 in prostate cancer has, therefore, been suggested (Bai et al., 2005; Bai and Wilson, 2008; Karpf et al., 2009). Further studies showed that the interaction occurring between the AR N-terminus and a highly conserved MAGE-A11 motif in the MAGE homology domain is modulated by MAP kinase phosphorylation of MAGE-A11 at Ser-174 (Askew et al., 2009). MAGE-A11 also links the N-terminus domain of AR to p300 acetyltransferase to promote AR transcriptional activity (Askew et al., 2010).

Although many studies have reported potentially oncogenic functions of type I MAGE antigens, other evidence has shown that at least one of them, MAGE-A4, can act as a tumour suppressor gene. This protein in fact binds gankyrin and suppresses its oncogenic activity (Nagao et al., 2003): gankyrin, frequently overexpressed in hepatocellular carcinoma, destabilises Rb tumour suppressor inhibiting cell cycle arrest and apoptosis. The binding of MAGE-A4 partially inhibits anchorage-independent growth *in vitro* and tumour formation *in vivo*. In addition, a cleaved C-terminal form of MAGE-A4 binds with the transcription factor MIZ-1 and leads to the induction of apoptosis by increasing the level of p53 protein (Sakurai et al., 2004), and its ability to promote apoptosis has been demonstrated in non-small cell lung cancer (Peikert et al., 2006). Accordingly, *MAGE-A4* expression is associated to a significantly longer survival in a breast cancer

retrospective study (Bandic et al., 2006). However, studies showed that MAGE-A4 presence is and unfavourable prognostic factor for survival in advanced stages of non-small cell lung cancer (Yoshida et al., 2006) and is significantly correlated with invasive phenotype and high tumour grade in transitional cell bladder carcinoma (Kocher et al., 2002).

Another clue about the possibility that some of the MAGE proteins can act as oncosuppressors was given by a recent study from Caballero *et al.* reporting that *MAGE* genes are frequently mutated in human melanoma and these mutations are not concentrated on particular hot spots, suggesting them to be inactivating mutations, which are commonly observed for tumour suppressor genes (Caballero et al., 2010).

The type II MAGE proteins cannot be considered cancer/testis antigens, being expressed in several somatic tissues other than testis. Nevertheless, they present the MAGE homology domain and therefore clues about their functions could help clarifying the role of other cancer-expressed MAGE genes.

One of the better characterised members of the type II MAGE family is Necdin. This protein was originally identified in embryonal carcinoma cells undergoing neural differentiation, and later described to be expressed in the central nervous system where it is localised to the nuclei of postmitotic neurons (Maruyama et al., 1991). This led to the hypothesis that Necdin could play a role in cell cycle exit or stabilisation. Indeed, Necdin interacts through its MHD with cell cycle related proteins, such as SV40 large antigen, adenoviral E1A, and E2F-1 (Kuwako et al., 2004; Taniura et al., 1998). The latter normally promotes cell cycle progression from G1 to S phase, and following binding with Necdin it goes through conformational changes that result in an inhibition of cell growth. Necdin can also bind to the tumour suppressor p53 and inhibit p53-dependent apoptosis, while enhancing cell cycle arrest. This suggests that Necdin could promote survival (Hayashi et al., 1995; Taniura et al., 1999). Recently it has been demonstrated that in post mitotic neurons Necdin can suppress p53-dependent apoptosis also by facilitating the interaction of p53 with the Sirtuin1 deacetylaseand promoting p53 deacetylation (Hasegawa and Yoshikawa, 2008).

Necdin in turn is regulated by p53, as its promoter contains a p53 binding site and the gene is a transcriptional target of p53 in hematopoietic stem cells, where Necdin acts as a rheostat controlling quiescence (Kubota et al., 2009; Liu et al., 2009).

Necdin also interacts with and reduces the stability of HIF-1α (hypoxia-inducible factor 1α), a fundamental transcription factor that mediates cellular and systemic homeostatic responses to hypoxia. Necdin impairs the transactivation of HIF-1α-induced genes, such as VEGF, resulting in an anti-angiogenic effect observed both *in vitro* and *in vivo* (Moon et al., 2005). Aside from interacting with transcription factors, Necdin can also directly repress transcription by binding with DNA on promoters containing tandem guanosine clusters (Matsumoto et al., 2001).

Downregulation of Necdin has been observed in urothelial carcinoma and melanoma (Chapman et al., 2008; Hoek et al., 2004). More recently, it has been demonstrated that Necdin is negatively regulated at the transcriptional level by STAT3 in human melanoma, prostate and breast cancer cell lines (Haviland et al., 2011).

Necdin is a maternally imprinted gene (Jay et al., 1997) and promotes differentiation of neurons (Kuwajima et al., 2006) and myoblasts (Brunelli et al., 2004; Pessina et al., 2011) while inhibiting adipogenesis (Bush and Wevrick, 2012; Fujiwara et al., 2012; Tseng et al., 2005). Interestingly, the human *Necdin* gene is located on chromosome 15 in an area associated with Prader-Willi Syndrome (Nakada et al., 1998), a neurological disorder characterised by respiratory failure, myasthenia, obesity, developmental delay and mental retardation. It is a classic genomic imprinting disorder due to inactivation of genes normally expressed only from the paternal allele (Jiang et al., 1998). Mouse knockouts of the *Necdin* orthologue show similar symptoms to Prader-Willi syndrome, with variable penetrance dependent upon the mouse background, suggesting that Necdin might be involved in this pathology and play a role in development (Aebischer et al., 2011; Gerard et al., 1999; Muscatelli et al., 2000).

MAGE-D1 (also named NRAGE or Dlxin) is another type II MAGE that plays an important role in regulating apoptosis and transcription. It interacts with p75NTR, a neurotrophin receptor

capable of mediating cell death. The MAGE-D1/p75NTR complex augments neurotrophin-mediated apoptosis through a JNK-dependent mitochondrial pathway (Salehi et al., 2000; Salehi et al., 2002). Furthermore, *MAGE-D1* knockout mice show resistance to developmental apoptosis in sympathetic neurons, a phenotype also displayed by *p75NTR* knockout mice; in addition they also present defects in motoneuron apoptosis (Bertrand et al., 2008).

MAGE-D1can also induce apoptosis by binding UNC5H1 axon guidance receptors (Williams et al., 2003), by activating p38 and the bone morphogenetic protein (BMP) pathway in neural progenitors (Kendall et al., 2005), by forming a complex with BRCA2 tumour suppressor (Tian et al., 2005) and by interacting through the interspersed repeat domain with the apoptosis inhibitor XIAP and accelerating its degradation, which in turn activates caspase-mediated cell death (Jordan et al., 2001).

Via the same domain, MAGE-D1 also interacts with some members of the Dlx/Msx homeodomain proteins, a family of transcriptional regulators which play important roles in the development of craniofacial, limb and nervous system; Dlx generally act as transcription activators whereas Msx act as transcription inhibitors. Msx1 and Msx2 have a role in controlling the cell cycle, and the latter can promote cell death. The interaction of MAGE-D1with Dlx5 is required for Dlx5-dependent transcription (Masuda et al., 2001). Moreover, MAGE-D1 can form a ternary complex with Msx and Necdin and promote myogenic differentiation (Kuwajima et al., 2004).

As a whole, and contrarily to most type I MAGE proteins, MAGE-D1 acts as an apoptosis inducer.

Human Magphinin (MAGE-D4) protein also belongs to the MAGE-D subfamily. It is an alternative splicing product of *Trophinin*, a cell adhesion molecule involved in human embryo implantation. It is expressed in both male and female germ cells, with a different subcellular localisation at various stages of the cell cycle, and its ectopic expression in NIH 3T3 inhibits cell

cycle progression; therefore it is suggested as regulating cell proliferation during gametogenesis (Aoyama et al., 2008; Saburi et al., 2001).

The function of type I and type II MAGE genes is summarised in Table 1.4.

TYPE I MAGE	Interacting protein	Function
MAGE-A1	SKIP	Transcriptional repression
MAGE-A2	p53	Down-regulation of p53 transactivation function
MAGE-A3	KAP-1	Down-regulation of p53 transactivation function
		Repression of KRAB targets
	caspase-12	Inhibition of cleavage in response to ER stress
	-	Promotion of survival in MM
	-	Increase in migration, invasion and metastasis
MAGE-A4	Gankyrin	Suppression of the oncogenic activity of gankyrin
	MIZ-1	Increase in p53 levels
MAGE-A11	Androgen Receptor (AR), p300	Increase in AR activity
	PHD2	Activation of the hypoxic response
MAGE-C1	-	Promotion of survival in MM
MAGE-C2	KAP-1	Down-regulation of p53 transactivation function
		Ubiquitination of p53
TYPE II MAGE	**Interacting protein**	**Function**
Necdin	SV40 LT	Not described
	Adenovirus E1A	Not described
	E2F-1	Inhibition of cell growth
	p53	Inhibition of apoptosis, increase in cell cycle arrest
	Sirtuin1	Promotion of p53 deacetylation
	HIF-1α	Inhibition of angiogenesis
MAGE-D1	p75NTR	Increase in neurotrophin-mediated apoptosis
	UNC5H1	Induction of apoptosis
	XIAP	Activation of p38, induction of apoptosis in neural progenitors
		Degradation of XIAP, induction of apoptosis
	Dlx/Msx	Transcriptional regulation
	BRCA2	Suppression of cell proliferation
MAGE-D4	-	Inhibition of cell cycle progression

Table 1.4 Function of MAGE proteins in relation to their binding partners.

1.3.5.2 Function of SSX proteins

Aside from the MAGE proteins, one of the best characterised families of CT antigens is the SSX family.

SSX1, *SSX2* and *SSX4* are involved in the t(X;18) translocation characteristic of synovial sarcomas, which gives rise to a fusion protein bearing transforming activity (Storlazzi et al., 2003; Yang et al., 2002). Immunofluorescence experiments carried out to investigate the localisation of

SSX1 and SSX2 showed a diffuse, nuclear staining, whereas the fusion proteins resulting from the chromosome translocation, SS18-SSX1 and SS18-SSX2, localise at nuclear bodies (dos Santos et al., 1997; dos Santos et al., 2000). Subsequent studies showed that they co-localise with members of the Polycomb group complex, known to have an important role in chromatin remodelling during cell cycle progression and differentiation (Simon and Kingston, 2009; Soulez et al., 1999). Nevertheless, no direct binding between Polycomb proteins and fusion proteins was observed.

SSX proteins present a KRAB-like domain and a C-terminal domain named SSX repression domain (SSXRD), both associated with transcriptional repression (Smith and McNeel, 2010). Downregulation of SSX proteins in a melanoma cell line resulted in decreased cell migration associated with reduced expression of matrix metalloproteinase 2, suggesting a potential role of SSX in cancer metastases formation (Cronwright et al., 2005).

1.3.5.3 Function of other CT antigens

Similarly to the MAGE proteins, several other CT antigens have been shown to promote tumourigenesis by affecting cell cycle and apoptosis or inducing drug resistance. For instance, GAGE7C, one of the numerous members of the GAGE family, can inhibit apoptosis induced by interferon-γ (IFN-γ) or Fas, and confers resistance to the therapeutic agent taxol and to ionising radiation (γ-radiation) in human tumour-derived cell lines (Cilensek et al., 2002). Further investigations showed that the taxol resistance is mediated by GAGE7C interaction with interferon regulatory factor 1 (IRF1) and nucleophosmin NPM/B23 (Kular et al., 2009).

CAGE, identified by SEREX in gastric cancer expression libraries, is induced at the G1 phase of the cell cycle preceding the induction of cyclin B. It has several tumour-promoting functions: firstly it was proved to increase growth rate, cell adhesion and motility of L929 fibroblasts through activation of focal adhesion kinase (FAK); secondly, it stimulates cell proliferation by up-regulating *cyclin D1* and *cyclin E* through AP-1 and E2F transcription factors; and thirdly, it down-regulates *p53* tumour suppressor expression via HDAC2 interaction, conferring resistance to chemotherapeutic drugs (Cho et al., 2002; Kim et al., 2010; Por et al., 2010; Shim et al., 2006).

TSP50 is a protease aberrantly expressed in breast cancer and is capable of promoting cell proliferation through the activation of the nuclear factor κB (NF-κB) signalling pathway by inducing IκB (inhibitor of NF-κB) α degradation (Shan et al., 2002; Song et al., 2011).

PLU-1 is a transcriptional co-repressor that regulates gene expression through interaction with the developmental transcription factors BF-1 (brain factor-1) and PAX9 (paired box gene 9) (Tan et al., 2003). It is most highly expressed in pre-meiotic spermatogonia and during pachytene and diplotene in the first meiotic prophase (Madsen et al., 2003). Recent reports showed that Plu-1 is a histone H3K4 demethylase enzyme that regulates proliferation of breast cancer cells through repression of tumour suppressor genes, including BRCA1 (Yamane et al., 2007). It is also a marker of a subpopulation of slow-cycling melanoma cells that are required for continuous tumour growth (Roesch et al., 2010).

The Piwi-like2 (*Piwil2*) gene is a testis specific member of the highly conserved Piwi gene family, which comprises nucleic acid-binding proteins known for their essential role in the self-renewal pathway of stem cells, gametogenesis and RNA interference (RNAi) (Cox et al., 1998; Deng and Lin, 2002; Kuramochi-Miyagawa et al., 2004). In human cancer cells Piwil2 acts as an oncogene by promoting the expression of *STAT3* and *Bcl-xL*, an antiapoptotic member of the Bcl-2 gene family; this results in inhibition of apoptosis and promotion of proliferation via STAT3/Bcl-xL signalling pathways (Lee et al., 2006a). Piwil2 also represses the tumour suppressor *p53* expression by binding to STAT3. The interaction increases STAT3 phosphorylation by the c-Src kinase and translocation to the nucleus, where it binds to *p53* promoter and inhibits its transcription (Lu et al., 2012). Finally, Piwil2 is able to modulate chromatin epigenetic modifications and relaxation of chromatin to facilitate DNA repair, enhancing therefore cisplatin resistance (Wang et al., 2011; Yin et al., 2011).

Recently, the CT antigen PRAME has been focus of several functional studies. PRAME has been identified as a dominant ligand-dependent repressor of retinoic acid receptor (RAR) signalling. PRAME protein is present at RAR target promoters, where it recruits Polycomb proteins and inhibits RA-induced differentiation, growth arrest and apoptosis in solid tumour cell lines (Epping

et al., 2005). Accordingly, it has been shown to correlate with worse prognosis in several solid carcinomas, such as melanoma, neuroblastoma and pre-menopausal breast cancer among others (Ikeda et al., 1997; Oberthuer et al., 2004; van 't Veer et al., 2002). More recent data showed that PRAME inhibits myeloid differentiation also in normal haematopoietic cells and leukaemic progenitor cells (Oehler et al., 2009). Despite this, its expression correlates with favourable prognosis, higher rates of overall and disease-free survival and lower relapse rate in childhood acute myelogenous leukaemia carrying the *BCR/ABL* t(9;22) (Ph+) and *AML1/ETO* t(8;21) translocations (Steinbach et al., 2002a; Steinbach et al., 2002b; van Baren et al., 1998). Consistent with this, PRAME promotes apoptosis in a caspase-independent fashion in *in vitro* studies in leukaemic cells and decreases tumourigenicity in *in vivo* models (Tajeddine et al., 2005). It is therefore possible that PRAME has different effects in solid tumours compared with some hematologic malignancies. This does not apply to all types of leukaemia though, as it has been also shown that in chronic myeloid leukaemia BCR-ABL-mediated upregulation of *PRAME* is responsible for inhibiting TRAIL apoptotic function (De Carvalho et al., 2011; Watari et al., 2000).

A novel function of PRAME has recently been elucidated: it has been identified as a subunit of a Cullin2-based E3 ubiquitin ligase specifically enriched at transcriptionally active promoters that are also bound by nuclear transcription factor Y (NFY), a transcription factor implicated in early embryonic development, in the maintenance of ES cells as well as in the inhibition of differentiation (Bhattacharya et al., 2003; Grskovic et al., 2007; Gurtner et al., 2008). This suggests a role of the PRAME ubiquitin ligase complex in NFY-dependent transcription (Costessi et al., 2011).

The function of some other CT antigens has been described in the germ cells but not in cancer cells so far: this is the case of TAF7L, NXF2 and BRDT.

TAF7L is a germ cell-specific paralogue of the TFIID (Transcription Factor II D) subunit TAF7. It is expressed through most of the male germ cell differentiation, but its intracellular localisation

changes from cytoplasmic in spermatogonia and early spermatocytes to nuclear in late pachytene spermatocytes and haploid round spermatids, in which phases TAF7L replaces TAF7 as a TFIID subunit (Pointud et al., 2003). Mice lacking *TAF7L* present sperm abnormalities, such as reduced amount of sperm in the epididymides, changes in morphology and reduced motility (Cheng et al., 2007).

NXF2 belongs to a family of nuclear RNA export factors (NXF) involved in mRNA transport from nucleus to cytoplasm in eukaryotes. It is expressed not only in the testis but also in the neurons of the brain, and in lung carcinoma, bladder carcinoma and sarcoma. NXF2 was found to interact with the fragile X mental retardation protein (FMRP) in the brain and testis of mice. This complex destabilises post-transcriptionally the mRNA of another member of the family, NXF1, in mouse neuronal cells (Lai et al., 2006; Zhang et al., 2007). NXF2 also interacts with cytoplasmic motor proteins, suggesting that it plays an important role not only in mRNA nuclear export but also in cytoplasmic mRNA localisation (Takano et al., 2007). Finally *NXF2* null mutant mice develop fertility defects at the meiosis stage (Pan et al., 2009).

BRDT (Bromodomain, testis-specific) contains two bromodomains, through which it binds hyperacetylated histone H4 and induces chromatin reorganisation in mammalian spermiogenesis. It also presents a RING finger domain, typical of proteins playing a key role in the ubiquitination pathway, and a PEST sequence, present in proteins that have a short intracellular half-life (Dhar et al., 2012; Moriniere et al., 2009; Pivot-Pajot et al., 2003; Scanlan et al., 2000; Shang et al., 2007).

Other CT antigens whose role in gametogenesis has been partially or thoroughly clarified are SCP-1 (synaptonemal complex protein 1), which is involved in chromosome pairing in meiosis (Tureci et al., 1998); SPO11, a meiosis-specific endonuclease (Romanienko and Camerini-Otero, 1999); OY-TES-1, important for acrosin packaging in the acrosome of sperm heads (Ono et al., 2001); BORIS, involved in the cancellation of imprinting during the final round of mitosis in spermatogenesis (Loukinov et al., 2002); ADAM2, a metalloprotease involved in egg/sperm membrane interaction (Gupta et al., 1996; Primakoff and Myles, 2000; Scanlan et al., 2002a; Vidaeus et al., 1997); SLCO6A1, a gonad-specific anion transport protein identified as a CT

antigen in lung cancer and medulloblastoma (Lee et al., 2004; Oba-Shinjo et al., 2008); the sperm-associated antigen 9 (SPAG9), a member of c-JunNH2-terminal kinase-interacting protein family involved in the interactions during the sperm-egg fusion and in the signalling pathway of mitogen-activated protein kinase (Jagadish et al., 2006; Jagadish et al., 2005); and testis specific protein 1 (TPX1), a cysteine-rich secretory protein that is important for the attachment of spermatogenic cells to the surrounding Sertoli cells (Busso et al., 2005).

Despite the efforts to elucidate CT antigen biological role, the majority of gene families have not been fully characterised. For some of these only the subcellular localisation has been described. For example, exogenous overexpressed XAGE-1b, a 470 bp transcript of the *XAGE-1* gene, localises in nuclear foci identified as SC35 pre-mRNA splicing factor containing bodies (Zendman et al., 2002a). HOM-TES-85, a CT protein with structural similarities to the N-myc oncoprotein, localises at loci of transcriptional activity and splicing, but for this protein and XAGE-1b no further functional studies have been performed to date (Tureci et al., 2002). Similarly, proteins of the SPANX family are associated with the nuclear envelope of human spermatids and spermatozoa, but the biological meaning of this localisation has not yet been determined (Westbrook et al., 2004).

Some other CT antigens present homologies with well-known proteins that could give a clue about their function: CT17 presents similarities with phosphatidylserine-specific phospholipase A1, an enzyme that play a role in sperm acrosomal exocytosis (Roldan, 1998); HAGE presents helicase-like features (Martelange et al., 2000); PASD1, first identified in lymphoma by SEREX, contains a PAS (Per ARNT Sim) domain, a putative leucine zipper and a nuclear localisation signal, suggesting it may act as a transcription factor (Cooper et al., 2006; Liggins et al., 2004; Sahota et al., 2006). PAS domains have important roles as sensory modules for oxygen tension, redox potential or light. The domain functions through protein-protein interactions or through binding cofactors in response to stimuli. Proteins that contain a PAS domain include Hypoxia-inducible factors (HIF) (Taylor and Zhulin, 1999).

The function of CT antigens other than the MAGE proteins is summarised in Table 1.5.

CT-X	Interacting protein	Function
CAGE	HDAC2	Downregulation of p53
	-	Increase in FAK-dependent cell growth, adhesion and motility
	-	Stimulation of cell proliferation via upregulation of cyclin D1 and cyclin E
GAGE7C	IRF1, NPM/B23	Inhibition of IFN-γ and Fas induced apoptosis
NXF2	-	mRNA export to the cytoplasm
SSX	-	Increase in cell migration
	-	Transcriptional repression
TAF7L	-	Transcription factor subunit in spermatocytes and spermatids
Non-X CT	**Interacting protein**	**Function**
ADAM2	-	Egg-sperm membrane interaction
BORIS	-	Cancellation of imprinting in late spermatogenesis
	-	Induction of MAGE-A1, -A2, -A3, -A4 and NY-ESO-1 expression
BRDT	-	Transcriptional regulation
OY-TES-1	-	Acrosin packaging in sperm head
Piwil2	STAT3	Downregulation of p53
	-	Upregulation of STAT3 and Bcl-xL
	-	Modulation of chromatin remodelling
PLU-1	BF-1, PAX9	Transcriptional repression
	-	Downregulation of BRCA1 via histone demethylation
PRAME	RAR	Inhibition of RA-induced cell death and differentiation in solid tumour cells
	-	Inhibition of myeloid differentiation
	-	Promotion of apoptosis in some leukaemia cells
	-	Inhibition of TRAIL-dependent apoptosis in CML
	Cullin2-based E3 ligase	Subunit of the E3 ligase, role in NFY-dependent transcription
SCP-1	-	Structural components of synaptonemal complexes, chromosome pairing in meiosis
SLCO6A1	-	Gonad-specific anion transporter
SPAG9	-	Egg-sperm fusion
SPO11	-	Meiosis-specific endonuclease
TPX1	-	Attachment of spermatogenic cells to Sertoli cells
TSP-50	IκBα	Promotion of cell proliferation through NF-κB

Table 1.5 Function of CT antigens other than the MAGE family. The CT genes have been divided in CT-X, encoded on the X chromosome, and non-X CT, encoded on different chromosomes.

In summary, the CT antigens display a wide variety of functions that differ among the families and within members of the same family. This suggests that the high number of CT genes identified so far is probably not a product of redundancy but implies a high degree of functional specialisation.

In the contest of tumourigenesis, it is not possible to assert that CT antigens can be considered to be oncogenes based on the knowledge gained so far. Although mutations have been found in some of the CT genes in human cancers (Sjoblom et al., 2006), it has not yet been established whether or not these mutations influence malignant transformation and further investigation is needed to clarify the significance of numerous uncharacterised CT proteins.

1.4 Aim of study

The aim of this study was to investigate the expression, the regulation and the biological role of three CT genes in cancer cells: NY-ESO-1, whose cellular function is totally unknown, its binding partner MAGE-C1, and MAGE-C2, a protein that is closely related to MAGE-C1.

Firstly, the expression pattern of these CT antigens was analysed in a panel of cancer cell lines including melanoma, NSCLC and multiple myeloma cell lines, all of which have been previously described to frequently express multiple CT antigens. This approach allowed us to establish similarities between established cell lines and tumour samples in terms of frequency of expression, pattern homogeneity and subcellular localisation, and therefore provided an *in vitro* model for following studies.

Secondly, the regulation of CT antigens at the protein level was examined, focusing on the processing and degradation of CT products, and in particular on the proteasome pathway. This level of regulation of CT proteins is particularly interesting, as it has potential consequences not only in terms of their function but also on antigen presentation. In this context, we examined the effects of proteasome inhibition on the three CT antigens and we tried to understand the influence that MAGE-C1 and NY-ESO-1 binding partners have on each other's localisation and function by employing both endogenous and exogenous approaches. Preliminary data on ubiquitin-like modifications of MAGE-C1 were also presented.

Finally, to improve our understanding of MAGE-C1 and NY-ESO-1, their role in the cell response to different death-inducing stressors was investigated via transient siRNA-mediated depletion, before analysing their ability to specifically affect proteins whose role is fundamental in apoptosis, including p53 and the Bcl-2 family. In particular, a characterisation of MAGE-C1 binding with Mcl-1 pro-survival protein was carried out and preliminary observations regarding the effect of MAGE-C1 on Mcl-1 protein stability were reported.

Chapter II: Materials and Methods

2.1 Materials

2.1.1 Reagents

5x Agarose Sample Buffer

50% (w/v)	Sucrose
100 mM	EDTA, pH 8.0
0.1% (w/v)	Bromophenol blue
0.1% (w/v)	Xylene cyanol FF

Agarose gel for DNA electrophoresis

Agarose powder (GibcoBRL, UK) was weighed and dissolved in 1X TAE buffer at an appropriate concentration. The mixture was heated in a microwave oven to dissolve the agarose and the solution allowed cooling to 40˚C. Ethidium bromide was added to a final concentration of 20 µg/ml. The agarose solution was poured into a casting tray with the required comb and was left to solidify at room temperature.

Ammonium Persulphate (APS)

10% (w/v) stock solution was prepared in water, and stored at –20 ˚C in aliquots.

Ampicillin Stock solution

1 g of the antibiotic was dissolved in 10 ml sterile distilled water making a 100 mg/ml stock solution. This was filter sterilised and stored at –20 ˚C as aliquots.

Blocking Solution

5% (w/v) fat-free milk (Marvel, UK) was prepared in phosphate buffered saline (1X TBS-T).

Cell culture Media

RPMI 1640 and Dulbecco's Modified Eagle's Medium (DMEM) were from GIBCO and stored at 4˚C.

Cell culture Media supplements

Foetal calf serum (FCS) was purchased from PAA Laboratories and tested for its ability to support growth of various cell lines. It was heated inactivated for 30 minutes at 55 ˚C and stored at -20 ˚C in 50 ml aliquots.

L-Glutamine was purchased from Gibco-BRL at a 200 mM concentration stored at -20 ˚C and used at a final concentration of 2 mM.

Penicillin / Streptomycin were purchased from Gibco-BRL at 1000,000 unit/ml stored at -20 ˚C and used at a final concentration of 200 units/ml.

COmpleteTM protein inhibitor cocktail

1 x COmplete^{TM} protein inhibitor (Boehringer Mannheim, UK) tablet was dissolved in 2.0 ml of sterilised distilled water as a 20x stock solution that is stable at -20 ˚C for 12 weeks.

DAPI staining solution

A stock solution of 10 mg/ml was made by dissolving 4'-6-diamidino-2-phenylindole dihydrochloride hydrate (DAPI; Sigma, MO, USA) in water and then adding 10 x PBS to make a 1 µg/ml working solution in 1 x PBS.

DNA Marker

100bp and 1kb DNA ladders were purchased from New England Biolabs and were used as a size standard for agarose gel electrophoresis.

Doxorubicin

The solution was purchased from Pharmacia (UK) at a concentration of 0.5 mg/ml. It was used at a final concentration of 1 μM.

EDTA Solution

A 0.5 M C10H14N2O8Na2.2H2O (EDTA) stock solution was made up by dissolving 18.6 g of EDTA in 70 ml distilled water. The pH was adjusted to pH 8.0 with NaOH and the volume made up to 100 ml with distilled water.

Ethidium Bromide

A 10 mg/ml stock solution was prepared by dissolving 0.2 g ethidium bromide in 20 ml of distilled water the stored at 4 ˚C in the dark.

Freezing Medium

90% (v/v) Foetal Calf Serum (FCS)

10% (v/v) DMSO

Stored at 4°C.

Iodoacetamide

Iodoacetamide was purchased from Sigma-Aldrich and dissolved in water at a stock concentration of 0.5 M. Iodoacetamide was added to lysis buffers when required at a final concentration of 5 mM.

IP (immunoprecipitation) lysis buffer

150 mM	NaCl
2 mM	EDTA
50 mM	Tris, pH 7.4
1% (v/v)	NP40

Stored at RT. COmplete™ protein inhibitor cocktail and iodoacetamide were freshly added before use.

Kanamycin stock solution

Kanamycin was dissolved at 50 mg/ml in distilled water, filter sterilised and stored at -20°C in aliquots.

Lipotransfection reagents

Lipotransfections were performed with Fugene 6 (Roche) or Lipofectamine®2000 (Invitrogen), following the manufacturer's recommendations or as otherwise stated.

Luria Broth (LB)-agar plates

LB-agar powder (Sigma) was dissolved as recommended by the manufacturer's instruction and autoclaved. The solution was then cooled to 55°C before addition of 100 µg/ml ampicillin or 50 µg/ml kanamycin. 20 ml of LB-agar was then poured into 10cm dishes, allowed to set and plates were stored at 4°C.

LB medium

LB powder (Sigma) was dissolved as recommended by the manufacturer's instruction, autoclaved and stored at RT.

Mowiol

6 ml Glycerol
2.4 g Mowiol 4-88 (Calbiochem)
12 ml Tris-HCL 200 mM (pH 8.5)

The solution was made up to 50 ml final volume, heated to 60°C overnight to dissolve all components, filtered through a 0.45 μm filter and stored in aliquots at -20°C.

NETN buffer

50 mM	Tris pH 8.0
150 mM	NaCl
1 mM	EDTA
1% (v/v)	NP40

Stored at RT. COmplete™ protein inhibitor cocktail and iodoacetamide were added before use.

Nocodazole

Nocodazole was purchased from Sigma Aldrich and dissolved in DMSO at a stock concentration of 10 mM to be used at a final concentration of 10 μM.

Nutlin-3

Nutlin-3 was purchased from Sigma Aldrich and dissolved in DMSO at a stock concentration of 10 mM to be used at a final concentration of 10 μM.

Para-formaldehyde Fixing Solution

A 4 % (w/v) of para-formaldehyde was dissolved in warm PBS in the fume hood, aliquoted and stored at -20 ˚C. The aliquot in use was kept at 4 ˚C.

Phosphate Buffered Saline (PBS)

12.5 mM	NaCl
1 mM	Sodium dihydrogen phosphate, NaH2PO4
1.6 mM	Disodium dihydrogen phosphate, Na_2HPO_4

10X PBS was purchased from GIBCO, diluted to 1X concentration in distilled water and autoclaved.

PNGase F enzyme

The PNGase F enzyme was purchased from New England Biolabs (P0704).

Ponceau S Staining Solution (10 X)

Ponceau S (sodium salt) was purchased from Sigma-Aldrich.

Primers used in PCR and qRT-PCR

For *NY-ESO-1* K124A point mutation the following primers from Operon were utilised:

FOR 5'-GCCAGGGGTGCTTCTGGCGGAGTTCACTGTGTCC-3'

REV 5'-GGACACAGTGAACTCCGCCAGAAGCACCCCTGGC-3'

For *Mcl-1* qRT-PCR the Hs_MCL1_1_SG QuantiTect Primer Assay from Qiagen was utilised and *GAPDH* was used as internal control

GAPDH FOR 5'-TGTCAGCAATGCATCCTGCA-3'

GAPDH REV 5'-TGTATGCAGGGATGATGTTC-3'

Propidium Iodide Solution

A stock solution of 1 mg/ml (20X) Propidium iodide was purchased from Sigma. The PI solution was made up as follows in 1X PBS:

50 µg/ml	RNaseA (Boeringer Mannheim)
50 µg/ml	Propidium iodide

Proteasome inhibitors

MG132 was purchased from Calbiochem and dissolved in DMSO at a stock concentration of 20 mM. A final concentration of 20 μM was used or as otherwise stated.

Epoxomicin was purchased from Enzo Life Sciences and dissolved in DMSO at a stock concentration of 1mM to be used at a final concentration of 1 μM.

Protein G Sepharose

Stored in 20% ethanol at 4˚C (Pharmacia Biotech). Protein G Sepharose beads were washed 3 times with cold PBS and resuspended in one volume of PBS before use.

Protein molecular weight markers

The prestained protein markers broadrange (#P7708S) were purchased from New England Biolabs and were used as a size standard for SDS-polyacrylamide gel electrophoresis.

Qiagen Solution-1-Resuspension solution for plasmid preparations

50 mM	Tris-HCl pH 8.0
10 mM	EDTA pH 8.0
100 μg/ml	RNase A (stored at 4 ˚C after addition of RNase)

Qiagen Solution-2-Lysis solution for plasmid preparations

200 mM	NaOH
1% (w/v)	SDS

Qiagen Solution-3-Neutralising solution for plasmid preparations

3 M	CH_3COOH, pH 5.5

Qiagen Elution Buffer

1.25 M	NaCl
50 mM	Tris pH8.5
15%	Isopropanol

Qiagen Equilibration Buffer

750 mM	NaCl
50 mM	MOPS pH 7.0
15 %	Isopropanol
0.15%	Triton® X-100

Qiagen Wash Buffer

1 M	NaCl
50 mM	MOPS pH 7.0
15%	Isopropanol

RIPA (radioimmunoprecipitation) Lysis Buffer

150 mM	NaCl
1% (v/v)	NP40
0.1% (w/v)	SDS
50 mM	Tris base

Stored at RT. COmplete™ protein inhibitor cocktail and iodoacetamide were added before use.

Ribonuclease A (RNase A)

50 mg of ribonuclease A (Sigma) was dissolved in 1 ml of 10 mM Tris-HCl pH7.5 and 15 mM NaCl to make a 10 mg/ml stock solution which was stored in single-use aliquots at –20 ˚C. (Boiling to remove DNase was not recommended by the manufacturer).

SDS Solution

A 10% (w/v) solution of sodium dodecyl sulphate (SDS) was purchased from Severn Biotech LTD and stored at room temperature.

2X SDS-PAGE loading dye

100 mM	Tris-HCl (pH 6.8)
4% (w/v)	SDS
20% (v/v)	Glycerol
0.2% (w/v)	Bromophenol Blue

Before use, 5% (v/v) β-Mercaptoethanol was added fresh to the 2X SDS-PAGE loading dye.

5X SDS-PAGE loading dye

250 mM	Tris-HCl
10% (w/v)	SDS
50% (v/v)	Glycerol
0.5% (w/v)	Bromophenol blue

Before use, 12.5% (v/v) β-Mercaptoethanol was added fresh to the 5X SDS-PAGE loading dye.

10x SDS-PAGE Running Buffer

720 g	Glycine
150 g	Tris
50 g	SDS

Made up to 5 litres with distilled water.

10x SDS-PAGE Transfer Buffer

725 g	Glycine
145 g	Tris

Made up to 5 litres with distilled water. The buffer was then used with 20% ethanol as 1X solution.

siRNA oligonucleotides

For MAGE-C1:

siMAGEC1 5'-GUGGAGAGGAGAGAGGGAGUCCUCCCA-3'

siMAGEC1#8 5'-UUACAAAGACAUAGGAGUCAUCAGGGU-3'

For NY-ESO-1:

siNYESO1 5'-GGACACAGUGAACUCCUUCAGAAGCAC-3'

DS NC1 oligonucleotide was used as a negative control. All oligonucleotides were purchased from IDT- Integrated DNA Technologies.

Stripping Buffer

62.5 mM	15.5 ml of 1 M Tris-HCl, pH 6.7
100 mM	1.75 ml of β-mercaptoethanol
2%	5 g SDS

Made up to 250 ml in distilled water.

50x TAE (Tris-Acetate-EDTA) buffer

242 g	Tris base
57.1 ml	Glacial acetic acid
100 ml	0.5 M EDTA, pH 8.0

Made up to 1 litre with distilled water and adjusted to pH 8.5. Used at 1X concentration.

TE Buffer

10 mM	1.0 ml of 1 M Tris-HCl pH 8.0 (sterile)
1 mM	0.2 ml of 0.5 M EDTA, pH8.0 (sterile)

Make up to 100 ml of sterile distilled water.

Thapsigargin

Thapsigargin was purchased from Sigma Aldrich and dissolved in DMSO at a stock concentration of 1 mM to be used at a final concentration of 1 μM.

Tris Stock solutions

Tris base was dissolved in water to provide 0.5 M, 1 M and 1.5 M solutions which were pH adjusted with concentrated HCl.

10x Tris Buffered Saline Tween (TBS-T)

121 g	Tris base
36.53 g	NaCl
250 ml	Tween-20 (Sigma)

Adjust pH to 7.6 with about 60 ml 33% HCl in a total volume of 5 litres. Used at 1x concentration.

Triton® X-100

A 20% (v/v) stock solution in PBS was made and stored at room temperature

Tunicamycin

Tunicamycin was purchased from Calbiochem and dissolved in DMSO at a stock concentration of 10mg/ml, to be used at a final concentration of 10μg/ml.

Urea buffer

8 M	urea
1 M	thiourea
0.5% (w/v)	CHAPS (3-[(3-Cholamidopropyl)dimethylammonio]-1-propanesulfonate)
50 mM	DTT (Dithiothreitol)
24 mM	spermine

USP2 enzyme

The purified USP2 enzyme was kindly provided by Dr. John Christianson's lab (LICR Oxford).

Water

Nanopure water (Type I) generated from the MilliQ water system was used for all procedures.

2.1.2 Antibodies

Primary Antibodies

Antigen	Name	Source	Species	WB/IF working concentration
Bcl-2	C2	Santa Cruz	mouse	1:1000/ -
β-Tubulin	TUB2.1	Abcam	mouse	1:2000/ -
KU80	Ab-2	Neomarker	mouse	1:1000/ -
MAGE-C1	CT7.33	Ludwig/ NY branch	mouse	1:1000/1:200
MAGE-C2	CT10#5	Ludwig/ NY branch	mouse	1:1000/1:100
Mcl-1	22	Santa Cruz	mouse	1:1000/ -
Mcl-1	S-19	Santa Cruz	rabbit	1:1000/ -
Mcl-1	HPA008455	Sigma (Prestige Antibodies)	rabbit	- /1:50
MHC Class I	HC10	Gift from Dr. Paul Lehner's lab	mouse	1:1000/ -
Mouse IgG	Mouse IgG	Sigma	mouse	Used for IP
Mouse IgG	Mouse IgG	Sigma	rabbit	Used for IP
Myc-tag	9E10	Ludwig/ Czech Republic	mouse	1:1000/ -
NY-ESO-1	E978	Ludwig/ NY branch	mouse	1:1000/ -
NY-ESO-1	NY41	Ludwig/ NY branch	rabbit	1:1000/1:100
PARP	46D11	Cell Signaling	rabbit	1:1000/ -
p53	DO-1	Santa Cruz	mouse	1:1000/ -
PCNA	PC10	Ludwig/ Czech Republic	mouse	1:2000/ -
Pericentrin	ab28144	Abcam	mouse	- /1:200
Pericentrin	ab4448	Abcam	rabbit	- /1:200
SUMO-1	38-1900	Invitrogen	rabbit	1:500/ -
Ubiquitin	FK2	Enzo Life Sciences	mouse	1:1000/ -
V5	46-0705	Invitrogen	mouse	1:2000/1:100

Secondary Antibodies

Antigen	Name	Source	Species	WB/IF working concentration
Mouse-IgG	Mouse secondary Ab	Dako	rabbit-HRP	1:2000/ -
Rabbit-IgG	Rabbit secondary Ab	Dako	goat-HRP	1:2000/ -
Alexa Fluor® 488 goat anti-mouse IgG (H+L)	A11070	Molecular Probes	goat	- /1:400
Alexa Fluor® 488 goat anti-rabbit IgG (H+L)	A11017	Molecular Probes	goat	- /1:400
Alexa Fluor® 546 goat anti-mouse IgG (H+L)	A11071	Molecular Probes	goat	- /1:400
Alexa Fluor® 546 goat anti-rabbit IgG (H+L)	A11018	Molecular Probes	goat	- /1:400
Alexa Fluor® 647 goat anti-rabbit IgG (H+L)	A21244	Molecular Probes	goat	- /1:400

Abbreviations – horse-radish peroxidase (HRP), immunofluorescence (IF), western blot (WB).

2.1.3 Plasmids

Plasmid Name	Relevant Information	Source / Reference:
pcDNA3.1/V5-His-TOPO	Empty vector containing CMV and T7 promoter sites	Invitrogen
pcDNA3.1/V5-His-TOPO MAGE-C1 1-138	Amino acids 1 to 138 of MAGE-C1 were cloned into pcDNA3.1/V5-His-TOPO	Ludwig Institute for Cancer Research – NY Branch
pcDNA3.1/V5-His-TOPO MAGE-C1 600-901	Amino acids 600 to 901 of MAGE-C1 were cloned into pcDNA3.1/V5-His-TOPO	Ludwig Institute for Cancer Research – NY Branch
pcDNA3.1/V5-His-TOPO MAGE-C1 902-1029	Amino acids 902 to 1029 of MAGE-C1 were cloned into pcDNA3.1/V5-His-TOPO	Ludwig Institute for Cancer Research – NY Branch
pcDNA3.1/V5-His-TOPO MAGE-C1 1030-1142	Amino acids 1030 to 1142 of MAGE-C1 were cloned into pcDNA3.1/V5-His-TOPO	Ludwig Institute for Cancer Research – NY Branch
pcDNA3.1/V5-His-TOPO NY-ESO-1	Full length NY-ESO-1 was cloned into pcDNA3.1/V5-His-TOPO	Ludwig Institute for Cancer Research – NY Branch
pcDNA3.1/V5-His-TOPO NY-ESO-1 1-90	Amino acids 1 to 90 of NY-ESO-1 were cloned into pcDNA3.1/V5-His-TOPO	Ludwig Institute for Cancer Research – NY Branch
pcDNA3.1/V5-His-TOPO NY-ESO-1 91-180	Amino acids 91 to 180 of NY-ESO-1 were cloned into pcDNA3.1/V5-His-TOPO	Ludwig Institute for Cancer Research – NY Branch
pcDNA3.1/V5-His-TOPO NY-ESO-1 50-150	Amino acids 50 to 150 of NY-ESO-1 were cloned into pcDNA3.1/V5-His-TOPO	Ludwig Institute for Cancer Research – NY Branch
pcDNA3.1/V5-His-TOPO MAGE-C1 MHD	Amino acids 900 to 1116 of MAGE-C1 were cloned into pcDNA3.1/V5-His-TOPO	Ludwig Institute for Cancer Research – NY Branch
pIC113	Empty vector containing EGFP tag, based on pEGFP-C1 (Clontech)	Ludwig Institute for Cancer Research - La Jolla
pIC113 NY-ESO-1	Full length NY-ESO-1 cloned in pIC113	Ludwig Institute for Cancer Research – NY Branch
pIC113 NY-ESO-1 K124A	NY-ESO-1 containing Lys to Ala mutation at codon 124 cloned in pIC113	Anna Pagotto
pcDNA3.1/Myc Mcl-1	Full length Mcl-1 was cloned into pcDNA3.1/Myc	Graham Packham Lab

pcDNA3.1/Myc Mcl-1 1-127	Amino acids 1 to 127 of Mcl-1 were cloned into pcDNA3.1/Myc	Graham Packham Lab
pcDNA3.1/Myc Mcl-1 128-350	Amino acids 128 to 350 of Mcl-1 were cloned into pcDNA3.1/Myc	Graham Packham Lab

All plasmids constructed by our laboratory were sequenced to confirm their identity. All cDNA encode human wild-type proteins unless otherwise stated.

2.1.4 Cell lines

Name	Tissue Type/Origin
H1299	Human lung carcinoma; p53-null; from American Type Culture Collection (ATCC)
H29	Human small cell lung cancer – from Dr. Michael Seckl
H146	Human small cell lung cancer – from Dr. Michael Seckl
H209	Human small cell lung cancer – from Dr. Michael Seckl
H524	Human small cell lung cancer – from Dr. Michael Seckl
H889	Human small cell lung cancer – from Dr. Michael Seckl
H2171	Human small cell lung cancer – from Dr. Michael Seckl
HC33	Human small cell lung cancer – from Dr. Michael Seckl
NIH3T3	Mouse fibroblast - from American Type Culture Collection (ATCC)
RPMI8226	Multiple Myeloma – from Ludwig Institute for Cancer Research NY Branch
SK007	Multiple Myeloma – from Ludwig Institute for Cancer Research NY Branch
SK-MEL-2	Human melanoma – from Memorial Sloan-Kettering Institute
SK-MEL-7	Human melanoma – from Memorial Sloan-Kettering Institute

SK-MEL-14	Human melanoma – from Memorial Sloan-Kettering Institute
SK-MEL-17	Human melanoma – from Memorial Sloan-Kettering Institute
SK-MEL-19	Human melanoma – from Memorial Sloan-Kettering Institute
SK-MEL-21	Human melanoma – from Memorial Sloan-Kettering Institute
SK-MEL-23	Human melanoma – from Memorial Sloan-Kettering Institute
SK-MEL-26	Human melanoma – from Memorial Sloan-Kettering Institute
SK-MEL-37	Human melanoma – from Memorial Sloan-Kettering Institute
U266	Multiple Myeloma – from Ludwig Institute for Cancer Research NY Branch
U2OS	Human osteosarcoma - from American Type Culture Collection (ATCC)
WM115	Human melanoma – from Wistar Institute
WM278	Human melanoma – from Wistar Institute

2.2 Methods

2.2.1 Tissue culture

Maintaining cell lines

All the cell lines are cultured in the Complete Medium (DMEM or RPMI 1640) supplemented L-Glutamine, penicillin/streptomycin and 10% (v/v) of foetal calf serum in the flasks or dishes (Greiner) maintained in the Heraecus incubator at 37 ˚C in the presence of 10% CO_2. Medium was changed every 3-5 days depending on the cell lines. On reaching confluence, the cells were washed once with 1X PBS and incubated with 2-4 ml pre-warmed Trypsin-EDTA (Gibco, BRL) at 37 ˚C until the cells detached from the flasks or dishes. Trypsin was inhibited by addition of an appropriate volume of fresh growth medium and this culture was then seeded on to fresh flasks or dishes at the desired density.

Freezing / thawing of cells

Cells were grown to about 80% confluency and collected by trypsinisation (as described above). The cell pellet was resuspended in the appropriate amount of freezing medium and aliquoted in cryovials (Corning). The vials were then labelled and cooled at the rate of 1 ˚C per minute in a Nalgen Cryo 1 ˚C freezing container or in a tissue-insulated polystyrene box when placed in a -80˚C freezer (New Brunswick Scientific) for at least 24 hr before being transferred to liquid nitrogen tank for long term storage.

To thaw cells from liquid nitrogen stock, vials were placed in the 37 ˚C water bath for 2 minutes and then transferred to a 6cm or 10cm dish with the appropriate pre-warmed fresh growth medium and kept in the 37 °C incubator overnight for recovering.

Hypoxic conditions

Hypoxic conditions were achieved in an AnaeroJar from Oxoid – Thermo Scientific.

2.2.2 DNA techniques

Bacterial strains and culture

Chemically competent *Escherichia coli* strains OneShot® TOP10 (Invitrogen), XL10-Gold® Ultracompetent (Stratagene) and alpha-select™ silver efficiency (Bioline) were used as a host for plasmid DNA. Bacteria were cultured in Luria Broth media containing the appropriate antibiotic (100 µg/ml ampicillin or 50 µg/ml kanamycin) at 37°C shaking at 350 RPM.

Transformation

The competent cells were thawed on ice. The desired plasmid DNA (100 ng) was added to the vial of competent cells, and this was incubated on ice for 30 minutes. The bacteria were subjected to heat shock for 60 seconds at 42 ˚C in a water bath, and then incubated on ice for another 5 minutes. 250 µl of SOC medium (Invitrogen) was added to the cells and allowed to shake at 37°C for 1h before plating on agar plates, containing the appropriate antibiotic. Plates were incubated at 37°C overnight and colonies selected the next day.

Small scale preparation of plasmid DNA (QIAprep® Spin Miniprep Kit, QIAGEN)

A single bacterial colony was picked up and inoculated in 5 ml of LB medium, containing the appropriate antibiotic, in a sterile test tube. The tube was shaken at 37°C for at least 12h. Cells were collected by centrifugation for 5min at 6,000g and pellet dissolved in 250µl Qiagen Solution 1. 250 µl of Qiagen Solution 2 was then added and tubes were inverted 5 times for gentle mixing. 350 µl of Qiagen Solution 3 was added and tubes were inverted another 5 times. The lysates were then centrifuged for 10min at 20,000g in a tabletop centrifuge and the supernatant was transferred

to a Qiagen Spin column. The spin column was washed once with Qiagen PE buffer containing ethanol and flow-through was discarded. Plasmid DNA was eluted from the column with 50-100 µl of ultrapure distilled water. The concentration was determined using Nanodrop spectrophotometer (Thermo Scientific)

Large scale preparation of plasmid DNA (QIAfilter® Plasmid Maxi Kit, QIAGEN)

A single bacterial colony was picked up and inoculated in 5ml of LB medium, containing the appropriate antibiotic, in a sterile test tube and shaken for at least 12h at 37°C. 200ml of LB medium was then inoculated with 200-400 µl of the bacterial suspension and shaken for a further 16h at 37°C. The plasmid DNA preparation was carried out according to the QIAfilter® Plasmid Maxi Kit manufacturer's protocol.

Agarose gel electrophoresis

Agarose (Helena) was dissolved in 1X TAE buffer (at the desired percentage), boiled until completely dissolved and allowed to cool. Ethidium bromide (purchased as a 10 mg/ml solution) was added to a final concentration of 20 µg/ml. Gels were run in Hoefer running tanks at 90V. Bands were visualised in a UV-imaging system (UVP Bio Imaging Systems, Labworks gel analysis software).

DNA samples were mixed with 6X DNA loading buffer to a final concentration of 1X and run alongside the appropriate-sized DNA ladder (Hyperladder I, Bioline).

Site-directed mutagenesis

Site-directed mutation was performed by PCR mutagenesis using the Stratagene QuikChange® XL site-directed Mutagenesis Kit according to the manufacturer's recommendations.

PCR Mix:

100 ng	Template DNA
5 µl	10X Buffer
1.5 µl	10µM forward primer
1.5 µl	10µM backward primer
3 µl	Quicksolution®
1 µl	dNTPs (10µM)
1 µl	PfuTurbo polymerase

Added up to 50 µl with ultrapure distilled water. The primers utilised are listed in Reagents.

Thermocycle program:

50"	90°C	
50"	90°C	
50"	65°C	18 cycles
10'	68°C	
7'	68°C	
∞	4°C	

The mix was then incubated with 1 µl DpnI (10U/µl) for 1h at 37°C and 5 µl was taken from this to transform 50-100 µl XL10-Gold® Ultracompetent cells. Colonies were picked, grown on small scale (typically 5 ml LB) and plasmids purified using the QIAprep® Spin Mini Kit. The resulting plasmids were sequenced to check for appropriate mutation.

2.2.3 RNA manipulation

RNA extraction and reverse transcription

RNA was extracted from cells or tissues according to the Qiagen RNeasy mini kit protocol, including a treatment with DNase I (Qiagen) to eliminate possible genomic DNA contamination. Up to 5 µg of total RNA were used to generate cDNA with the SuperScript® First Stand Synthesis System (Invitrogen) following the manufacturer's protocol.

Real-time quantitative PCR (qRT-PCR)

Real-time quantitative PCR was performed on the 7500 real time PCR system (Applied Biosystem) using the QuantiTect SYBR Green PCR kit (Qiagen). Each reaction was performed in triplicate using 1 µl of cDNA in a final volume of 25 µl. The primers utilised are listed in Reagents. The following thermal cycle was used for all the samples: 10 min-95°C; 40 cycles of 30s-95°C, 40s-primer specific annealing temperatures, 40s-72°C. For each experiment, the threshold was set to cross a point at which real-time PCR amplification was linear. The expression level of each target gene was analysed based on ΔΔCt method, with GAPDH as internal control.

2.2.4 Protein manipulation

Sample preparation

Cells grown in monolayers were washed two times with 1X PBS and lysed in RIPA buffer or NETN buffer or IP buffer (150-250 µl per 10 cm dish). The cells were scraped with a sterile disposable cell scraper (Greiner) and transferred to an eppendorf tube and centrifuged at 14,000 rpm, 4˚C for 15 minutes (eppendorf 5417R). The supernatant was collected (soluble fraction). The remaining pellet was then dissolved in Urea buffer for 20min at RT. After a 20min spin at 20,000g, the supernatant was collected (insoluble fraction). Alternatively, the cells were collected and lysed in Urea buffer immediately to prepare a 'total lysate'.

Protein concentration determination

The protein concentrations of cell extracts were determined using BioRad (Bradford) protein assay reagent system. 1 µl of cell lysate was mixed with 200 µl of 1x BioRad assay reagent and then measured at 595 nm in the spectrophotometer ((Anthus Labtech instrument, using Magellan software). All samples were measured in duplicates and the absorbance was compared against the standard curve made at the same time from known concentrations of bovine serum albumin (BSA; Sigma, UK) in the same solutions using the same method.

Preparation of SDS-PAGE gels

All plates were washed with water and detergent, dried and assembled in the casting trays (Biorad). The acrylamide content of the gels varied between 6%-15% depending on the size of the protein of interest. The acrylamide gels were overlaid with 70% isopropanol solution and left to polymerise. After polymerisation, the isopropanol was removed and a 4% stacking gel was set with the appropriate number and size wells.

	Resolving Gels					**Stacking**
	6%	**8%**	**10%**	**12%**	**15%**	
Acryl/Bis	2 ml	2.7 ml	3.3 ml	4.0 ml	5.0 ml	1.3 ml
1.5 M Tris-HCl pH 8.8	2.5 ml	2.5 ml	2.5 ml	2.5 ml	2.5 ml	--
1.0 M Tris-HCl pH 6.8	--	--	--	--	--	2.5 ml
10% SDS	100 µl	100 µl	100 µl	100 µl	100 µl	100 µl
10% APS	100 µl	100 µl	100 µl	100 µl	100 µl	50 µl
TEMED	10 µl	8 µl	5 µl	5 µl	5 µl	10 µl
Distilled Water	5.3 ml	4.6 ml	4.0 ml	3.3 ml	2.3 ml	6.1 ml
Total volume	**10 ml**	**10 ml**	**10 ml**	**10 ml**	**10 ml**	**10 ml**

All resolving and stacking gels were prepared using 30% acrylamide/bis-acrylamide (Acryl/Bis) 29:1 (NBL, UK or BioRad, UK). Values given are per 10 ml of gel required. Abbreviations: Ammonium Persulphate (APS); N,N,N',N',-tetramethy-ethylenediamine (TEMED), Tris (Tris(hydroxymethyl) aminomethane), sodium dodecyl sulphate (SDS).

SDS-polyacrylamide gel electrophoresis (PAGE)

Known concentrations of protein were mixed with appropriate volumes of 2x or 5x SDS-PAGE loading dye and boiled for 5 min. Equal amounts of proteins were loaded in respective wells cast in the stacking gel. The gels were run at 130 V for 1.5 h in 1x SDS PAGE running buffer using a Biorad system. Prestained protein markers were purchased from New England Biolabs and used as a size standard.

Immunoblotting

After the samples were separated through the gel, the gel was transferred to a wet transfer unit and the proteins blotted onto nitro-cellulose membrane (Whatman) for 1h at a constant voltage of 55

V or 20V overnight in a Hoefer Transphor Electrophoresis unit. The membrane was then stained with Ponceau S solution (purchased as a 0.1% (w/v) solution in 5% acetic acid) to determine the success of the transfer of proteins and equal loading of the lanes. The membranes were then washed in water and incubated in 5% fat-free milk (Marvel, UK) in 1X TBS-Tween at room temperature for 40-60 minutes. Primary antibody was added at the recommended concentrations, diluted in TBS-Tween plus 5% milk, for 3h at RT or overnight at 4ºC. After three 15min washes in 1X TBS-Tween, the secondary HRP-labeled antibody was added for 1h at RT (1:2000). Membranes were washed another three times for 15min in TBS-Tween. The results were visualised by enhanced chemoluminescent detection (ECL) using X-ray films (Amersham Biosciences). If probing with another primary antibody was required, the gels were either immediately reprobed or incubated with stripping buffer for 30 min at 55°C and reblocked in 5% milk, before incubation with the new primary antibody.

Immunoprecipitation (with cell lysates)

Cells grown in monolayers were washed three times with 1X PBS and lysed in IP lysis buffer with protease inhibitors (150-250 µl per 10 cm dish). The cells were scraped with a sterile disposable cell scraper (Greiner), transferred to an eppendorf tube and left in ice for 20 minutes, to be then centrifuged at 14,000 rpm, 4˚C for 20 minutes (eppendorf 5417R). The resulting lysate was removed to a fresh eppendorf tube and the cell debris discarded. The protein concentration was determined using the BioRad assay system. 500-2000 µg of cell lysate was precleared with 40 µl of 70% packed protein G beads (equilibrated in PBS buffer) for 30-60 minutes at 4˚C on an eppendorf rotating wheel. The lysate was spun at 14000rpm for 15 seconds and the supernatant was removed and replaced into a fresh tube with blocked protein G sepharose beads (blocked overnight in DMEM, containing 5% FBS) and 1 µg of purified antibody or 1-5 µl ascites/mg lysate and rotated for 4h to overnight at 4ºC. Non-specific mouse, goat or rabbit IgG was used as a control. The beads were then washed three times in ice-cold IP buffer and after addition of SDS-

PAGE loading dye, boiled and analysed by SDS-polyacrylamide gel electrophoresis and western blotting.

Immunofluorescent staining

Cells were grown in 24 well plates on coverslips (VWR), ideally to 70-80% confluency. After appropriate treatment, the cells were washed twice with PBS and fixed in 4% paraformaldehyde for 20min at RT. Permeabilisation was performed using 0.1% Triton (diluted in PBS) for 4min on ice. Cells were then blocked with 0.2% fish skin gelatine (FSG) diluted in PBS for 20min at RT. The appropriate primary antibody was diluted 1:50 - 1:200 in 0.2% FSG and incubated with the cells for 60min at RT. After three washes of 10 minutes each with PBS, the secondary fluorescent labelled antibody (Alexa Fluor®), diluted 1:400 in 0.2% FSG, was added for another 20min at RT. This was followed by another three washes with PBS. Where necessary, TO-PRO® (Molecular Probes) or DAPI (Sigma) was added to the second wash as a nuclear counterstain. The coverslips were then mounted onto poly-lysine microscope slides using a mowiol-glycerol based solution containing 2.5% DABCO anti-fading agent. After drying, the slides were analysed by confocal microscopy (Zeiss), using LSM image viewer software.

Deubiquitination assay

Cell lysates were collected and lysed in RIPA buffer supplemented with COmplete^{TM} protein inhibitor cocktail, followed by incubation with USP2 at room temperature for 30 minutes. The cell lysate was then analysed via SDS-PAGE and immunoblotting.

Deglycosylation assay

Cell lysates were collected and lysed in RIPA buffer supplemented with COmplete^{TM} protein inhibitor cocktail, followed by incubation with PNGase F according to the manufacturer's protocol. The cell lysate was then analysed via SDS-PAGE and immunoblotting.

2.2.5 Cell based assays

Cell cycle analysis

Cells were harvested following treatment with trypsin, washed in PBS and fixed in 90% ethanol overnight at 4ºC. The following day, cells were washed in PBS and resuspended in PBS containing 50 µg/ml propidium iodide (purchased as a 1 mg/ml solution dissolved in water from Sigma) and 50 µg/ml RNase A for 1h and subsequently analysed on BD FACSCanto™ Flow Cytometer (BD Biosciences)

Cell transfection

FuGENE® 6 (Roche) or Lipofectamine 2000 (Invitrogen) were used as lipid carriers according to the manufacturers' protocols. The DNA plasmids utilised are listed in paragraph 2.1.3.

Lipofectamine 2000 (Invitrogen):

Cells were grown at 80-90% confluency in antibiotic-free medium. For a 6 cm dish, 3 µg of each DNA plasmid were diluted in 0.5 ml DMEM without FBS and antibiotics forming a first mix, and 20 µl of Lipofectamine were diluted in 0.5 ml DMEM without FBS and antibiotics forming a second mix; after a 5 minute incubation, the Lipofectamine/DMEM mix was added drop-wise to the DNA/DMEM mix, and the resulting transfection mix was incubated for 20 minutes. This was then added drop-wise to a 6 cm dish already containing 4 ml of antibiotic-free medium and the cells were incubated for 4~6 h at 37°C in a CO_2 incubator. The medium was then replaced with fresh, complete medium and cells were harvested 48 h after transfection.

FuGENE® 6 (Roche):

All transfections were performed utilising a 3:1 ratio of FuGENE® 6 (µl) to total DNA (µg). Cells were grown at 60-70% confluency in complete medium. For a 6 cm dish, FuGENE® 6 was diluted in 200 µl DMEM without FBS and antibiotics; after a 5 minute incubation, 3 µg of each DNA plasmid were added to the transfection mix, which was incubated for further 20 minutes

before being added drop-wise to a 6 cm dish already containing 4.8 ml of complete medium. Cells were harvested 48 h after transfection.

Heat shock

Cells were grown to sub-confluency and the medium removed and retained in a tissue culture hood. The monolayer of cells was exposed to heat shock for 30 minutes in a water-bath set at 44ºC. The medium was then replaced on the cells and the dishes were placed back in a 37˚C incubator with 10% carbon dioxide. The cells were harvested after the appropriate time points.

RNA interference

RNA interference of MAGE-C1 and NY-ESO-1 were performed using Lipofectamine 2000 (Invitrogen) according to the manufacturer's protocol. The siRNA oligonucleotides, utilised at a 40 nM final concentration, are listed in paragraph 2.1.1.

Briefly, cells were grown at 30-40% confluency in antibiotic-free medium. For a 6 cm dish, 200 pmol of each siRNA oligonucleotide were diluted in 0.5 ml DMEM without FBS and antibiotics forming a first mix, and 10 µl of Lipofectamine were diluted in 0.5 ml DMEM without FBS and antibiotics forming a second mix; after a 5 minute incubation, the Lipofectamine/DMEM mix was added drop-wise to the siRNA/DMEM mix, and the resulting transfection mix was incubated for 20 minutes. This was then added drop-wise to a 6 cm dish already containing 4 ml of antibiotic-free medium and the cells were incubated for 4~6 h at 37°C in a CO_2 incubator. The medium was then replaced with fresh, complete medium and cells were harvested 72 h after transfection.

Ultraviolet light treatment (UV)

Cells were grown to sub-confluency and the medium removed and retained in a tissue culture hood. The monolayer of cells was exposed to 50 J/ M^2 (high dose) of ultraviolet light using a spectrolinker XL-1500 UV crosslinker (Spectronics Corporation). The medium was replaced on

the cells and the dishes were placed back in a 37˚C incubator with 10% carbon dioxide. The cells were harvested after the appropriate time points.

2.2.6 Data analysis

Computer images

All autoradiographs were scanned using the Epson perfection 1660 Photo scanner and the Adobe Photoshop 7.0 software. Images were manipulated only as a whole for size, brightness and contrast. No signal was modified in relation to the whole image. ImageJ® software was used to quantify gel bands from western blots.

Statistics

Differences were considered significant at a value of $p \leq 0.05$. The T-test was used to calculate the statistical significance between two measurements.

Chapter III: NY-ESO-1, MAGE-C1 and MAGE-C2 are heterogeneously expressed in human cancer cell lines

3.1 Introduction

Cancer/testis antigens are expressed in many types of cancer. In most cases, their expression is not homogenous (Aubry et al., 2001; Chitale et al., 2005; Dhodapkar et al., 2003; Jungbluth et al., 2000b; Li et al., 2005), and they are only expressed in particular subpopulations of cells within the tumour. The reasons for this heterogeneous expression are currently unknown. An *in vitro* experimental system is therefore needed to study this peculiar expression pattern and, thus, gain a better understanding of the biological functions of these proteins. To achieve this, cancer cell lines were screened for CT gene expression, to evaluate whether the heterogeneous expression pattern observed in tumours could be reproduced in an established cell line. Three CT antigens were included in this screening: NY-ESO-1, MAGE-C1, and MAGE-C2.

NY-ESO-1 is one of the most immunogenic CT antigens identified to date. Over 30 clinical trials around the world, involving over 300 patients, have investigated or are investigating this protein's potential as a cancer vaccine. However, its precise biological function is not yet known, and further investigation of the biology of this protein could substantially help the formulation of more efficient cancer immunotherapies. One of the main reasons that so little is known about NY-ESO-1 is the absence of evolutionary homologs, thus preventing the immediate use of animal models such as knockout mice. The closest relative of NY-ESO-1 in mice, *ESO-3*, is not a CT antigen since it presents universal expression in normal tissues (Alpen et al., 2002).

In addition to its expression in the testis, NY-ESO-1 is also found in normal ovary, the placenta and many types of malignancy (Gnjatic et al., 2006). Immunohistochemical analysis of the testis has revealed that NY-ESO-1 is only found in early spermatogonia, where its expression is predominantly cytoplasmic, and is gradually lost with sperm cell differentiation. Non-gametogenic cells of the testis, including Sertoli cells, do not express NY-ESO-1 and neither do other somatic cells. The presence of NY-ESO-1 has also been found at the protein level in testicular foetal germ cells, as early as week 18 (Satie et al., 2002), as well as in germ cells of the foetal ovary (Nelson et al., 2007). Approximately one-third to one-fourth of all melanomas, lung, oesophageal, liver, prostate, ovarian, bladder cancers and multiple myeloma express NY-ESO-1. Its expression is rare, however, in other cancer types such as colorectal, pancreatic and renal tumours, or lymphoma (Jungbluth et al., 2001; Juretic et al., 2003). The co-expression pattern of NY-ESO-1 with other CT antigens has been established (Bolli et al., 2005; Vaughan et al., 2004). Moreover, NY-ESO-1 has been demonstrated to bind to MAGE-C1 (Cho et al., 2006), but the biological importance of this binding remains unknown.

MAGE-C1 was identified by SEREX and representational difference analysis (RDA). The *MAGE-C1* mRNA expression pattern follows that of other CT antigens, with expression in a variety of malignant neoplasms, and only in testis in normal adult tissues. As with other CT antigens, certain tumours such as colonic carcinomas and renal cell carcinomas rarely express MAGE-C1 antigen. Synovial sarcomas, which exhibit a high expression of NY-ESO-1, reveal little MAGE-C1 reactivity suggesting that the regulation and function of these two proteins could be partially independent from their binding. Other tumours, such as carcinomas of the urinary bladder, lung, liver and mammary gland, as well as multiple myeloma and malignant melanoma, exhibit a higher incidence of expression (Jungbluth et al., 2002).

Recently, a MAGE-C1-related family member called MAGE-C2 was identified (Lucas et al., 2000; Riener et al., 2009; Zhuang et al., 2006). *MAGE-C2* maps to chromosome X, in close proximity to the *MAGE-C1* and *MAGE-A* genes. Its protein localisation is restricted to the nucleus of neoplastic cells, and this contrasts with NY-ESO-1, MAGE-C1 and most of the MAGE-A

antigens, which are predominantly present in the cytoplasm. Interestingly, although MAGE-C2 shares significant similarity to MAGE-C1 at the molecular level, no binding with NY-ESO-1 has been observed. This difference between the two members of the same subfamily may be particularly useful in determining their differential roles in cancer cells. MAGE-C2 is highly expressed in hepatic carcinoma, lung carcinoma, melanoma and multiple myeloma.

Eleven melanoma cell lines, seven small cell lung cancer (SCLC) lines and three multiple myeloma (MM) cell lines were screened for the expression of NY-ESO-1, MAGE-C1 and MAGE-C2. Melanoma cell lines were chosen because melanoma is the cancer type with the highest level of CT antigen expression. Although melanoma is one of the rarest types of skin cancer, it accounts for 75% of all deaths associated with skin cancer and is one of the most aggressive tumour types, being highly invasive and metastatic. In its early stages melanoma can be cured by surgical resection, but once it has progressed to the metastatic stage it is extremely difficult to treat and does not respond to current therapies. NY-ESO-1 is more frequently expressed in metastatic than in primary malignant melanomas, and its expression is associated with thicker primary lesions and a higher frequency of metastatic disease, indicative of poor prognosis (Velazquez et al., 2007).

Similarly, lung cancers frequently express CT antigens, although most of the studies on CT genes in this tumour type have been carried out in non-small cell lung cancer (NSCLC) samples and cell lines (Scanlan et al., 2004). Results demonstrate that NY-ESO-1 expression is frequently present in primary NSCLC, especially advanced cases with lymph node metastasis (Konishi et al., 2004); moreover, its expression is significantly associated with prognostic factors that are related to a poor outcome in this type of malignancy (Grah et al., 2008). SCLC accounts for 15% of all lung tumour cases, and was chosen for screening because it shares some important features with melanoma: it has a neural origin and is a particularly invasive type of cancer; it metastasises mostly to the brain, liver and bone. Although initially sensitive to chemotherapy, SCLC ultimately

carries with it a worse prognosis. The choice of SCLC also permits the identification of possible differences in the expression pattern of CT antigens with NSCLC.

Multiple myeloma arises from aberrant proliferation of plasma cells and is the second most common hematologic malignancy. Clinical remissions of MM are commonly achieved, mainly by autologous stem cell transplantation as well as by the administration of recently introduced drugs such as bortezomib. However, the median survival has still not improved beyond 4-5 years, due to frequent relapse (Kumar et al., 2008). Myeloma is also susceptible to a graft versus myeloma effect mediated by donor T-cells following allogeneic stem cell transplantation (Bruno et al., 2007). Unfortunately, this is associated with graft versus host disease and infections related to immunosuppression. Accordingly, alternative therapies that target remaining myeloma cells more specifically and effectively are needed.

It is known that MM express multiple CT antigens (Sahota et al., 2006; Tinguely et al., 2008), therefore they represent potential targets for immunotherapy in this tumour type. Furthermore, CT gene expression in MM has been associated with poor prognosis, suggesting that they could play an active role in the progression of neoplasia (Andrade et al., 2008; Atanackovic et al., 2009; Jungbluth et al., 2005; van Baren et al., 1999).

3.2 Results

3.2.1 NY-ESO-1, MAGE-C1 and MAGE-C2 expression patterns vary in different human melanoma cell lines

To evaluate both the expression levels and expression patterns of NY-ESO-1, MAGE-C1 and MAGE-C2, western blot analysis and immunofluorescence were performed, respectively.

Three previously described antibodies were utilized for the screening: NY-41 rabbit polyclonal raised against NY-ESO-1, CT7.33 mouse monoclonal raised against MAGE-C1 and CT10#5 raised against MAGE-C2 (Cho et al., 2006; Jungbluth et al., 2002; Zhuang et al., 2006). All three antibodies were tested for specificity performing RNAi experiments for the different CT antigens in multiple cell lines. CT10#5 also recognised a non-specific upper band (~53kDa) which was not affected by the siRNA transfection (data not shown).

Eleven melanoma cell lines were tested to start with: SK-MEL-2, SK-MEL-7, SK-MEL-14, SK-MEL-17, SK-MEL-19, SK-MEL-21, SK-MEL-23, SK-MEL-26, SK-MEL-37, WM115 and WM278. Most of the SK-MEL cell lines are derived from metastatic sites, whereas WM cells are derived from primary tumours. These cell lines make up a panel that covers different typologies of melanoma cells. For example, SK-MEL-19 cells have a proliferative signature, whereas WM278 cells have an invasive one.

Western blot experiments, carried out loading a high amount of protein lysate for each cell line (100 μg) to ensure the detectability of the proteins, revealed that CT antigens were expressed at high levels in all of the cell lines studied, excluding SK-MEL-7 (10 cell lines out of 11) (Figure 3.1A), an observation that is consistent with the high percentage of positivity in melanoma samples reported in the literature (Scanlan et al., 2004). Moreover, co-expression of two or more CT antigens was observed in 9 out of 11 cell lines (SK-MEL-2, SK-MEL-14, SK-MEL-17, SK-MEL-19, SK-MEL-21, SK-MEL-23, SK-MEL-26, SK-MEL-37 and WM115), and these data are in agreement with previous reports that these proteins are known to be frequently expressed in

clusters in tumour samples (Coral et al., 2002; Wischnewski et al., 2007). Both NY-ESO-1 and MAGE-C1expression were found in these 9 cell lines. This is particularly interesting as NY-ESO-1 and MAGE-C1 are known to bind to each other. A very weak NY-ESO-1 positivity was also detected in SK-MEL-7 and WM278, possibly ascribable to non-specific signal considering that a high amount of loaded protein lysate. The MAGE-C1 immunoblot appeared fuzzy and presented more than one band (the expected molecular weight is 125 kDa). As the mouse monoclonal antibody used for this experiment has been characterised as highly specific, this result could be due to post-translational modification or processing of the protein. MAGE-C2 was expressed in 6 out of 11 cell lines (SK-MEL-2, SK-MEL-14, SK-MEL-17, SK-MEL-23, SK-MEL-37, WM278). Moreover, a weak MAGE-C2 positivity was also detected in SK-MEL-21, SK-MEL-26 and WM115. Among these 11 melanoma cell lines, 5 showed co-expression of all of the three CT antigens studied at high levels (SK-MEL-2, SK-MEL-14, SK-MEL-17, SK-MEL-23 and SK-MEL-37), whereas 4 of the cell lines expressed only NY-ESO-1 and MAGE-C1 (SK-MEL-19, -21, -26 and WM115). WM278 expressed MAGE-C2, but not MAGE-C1 and only very low levels of NY-ESO-1. Finally, SK-MEL-7 showed extremely low or null expression of the three CT antigens.

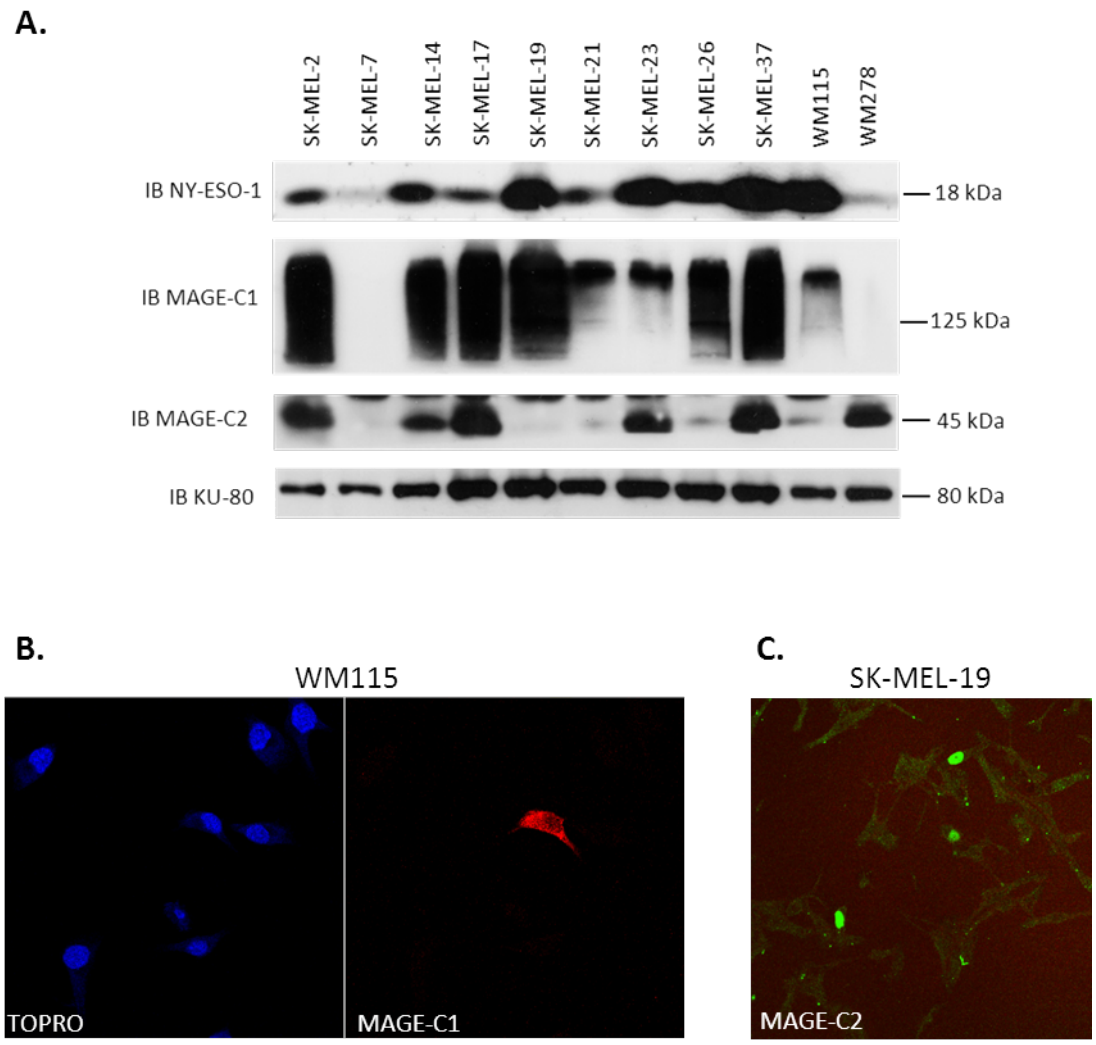

Figure 3.1 Analysis of CT antigen expression in melanoma cell lines. Eleven melanoma cell lines were tested for CT antigen expression: SK-MEL-2, -7, -14, -17, -19, -21, -23, -26, -37, WM115 and WM278. A. Western blot analysis was performed using antibodies raised against NY-ESO-1 (rabbit polyclonal NY-41), MAGE-C1 (mouse monoclonal CT7.33 antibody), MAGE-C2 (mouse monoclonal CT10#5) and KU-80 (as a loading control). B. Staining of endogenous MAGE-C1 performed in WM115 cells using CT7.33 antibody. TOPRO was used for nuclei staining. C. Staining of endogenous MAGE-C2 performed in SK-MEL-19 cells using CT10#5 antibody.

Interestingly, immunofluorescence staining showed that the expression pattern of these proteins differed between the different cell lines. For each of the three antigens investigated, the staining pattern was defined as "homogeneous" when the signal was detected in all of the cells, or "heterogeneous" when only a subpopulation of cells was positive; when none of the cells showed positivity, the antigen was classified as "not expressed". The adopted classification was solely based on the detectability of the proteins in immunofluorescence and did not take into consideration variations in the subcellular localisation or in the expression levels of the CT antigens.

The data obtained from the melanoma cell line screening are summarised in Table 3.1.

MELANOMA CELL LINES			
	NY-ESO-1	MAGE-C1	MAGE-C2
SK-MEL 2	Homogeneous	Homogeneous	Homogeneous
SK-MEL 7	Not expressed	Not expressed	Not expressed
SK-MEL 14	Heterogeneous	Heterogeneous	Heterogeneous
SK-MEL 17	Homogeneous	Homogeneous	Homogeneous
SK-MEL 19	Heterogeneous	Heterogeneous	Heterogeneous
SK-MEL 21	Homogeneous	Not expressed	Not expressed
SK-MEL 23	Heterogeneous	Not expressed	Heterogeneous
SK-MEL 26	Homogeneous	Heterogeneous	Not expressed
SK-MEL 37	Homogeneous	Homogeneous	Homogeneous
WM115	Heterogeneous	Heterogeneous	Not expressed
WM278	Not expressed	Not expressed	Homogeneous

Table 3.1 Summary of melanoma staining screening.

NY-ESO-1 was found to localise predominantly in the cytoplasm. It was homogeneously expressed in five of the analysed cell lines (SK-MEL-2, SK-MEL-17, SK-MEL-21, SK-MEL-26

and SK-MEL37); heterogeneously expressed in four (SK-MEL-14, SK-MEL-19, SK-MEL23, WM115); and not expressed in the remaining two (SK-MEL-7 and WM278). These results are in agreement with the results obtained from the western blot.

MAGE-C1 immunofluorescence staining revealed that this protein, like NY-ESO-1, is also predominantly cytoplasmic. It was homogeneously expressed in SK-MEL-2, SK-MEL-17 and SK-MEL-37 cells; heterogeneously expressed in SK-MEL-14, SK-MEL-19, SK-MEL-26, and WM115; and not detectable in SK-MEL-7, SK-MEL-21, SK-MEL-23 and WM278. The fact that SK-MEL-21 and SK-MEL-23 staining was negative, in contrast with the result from the western blot, is probably due to a very low expression level of MAGE-C1 in comparison with the other cell lines. WM115 cells showed similar expression levels in the western blot and, correspondingly, the number of positive cells observed in the immunofluorescence heterogeneous staining was particularly low (Figure 3.1B).

Finally, MAGE-C2 staining showed that is has a nuclear localisation. The protein was homogeneously expressed in SK-MEL-2, SK-MEL-17, SK-MEL-37 and WM278 cells; heterogeneously expressed in SK-MEL-14, SK-MEL19 and SK-MEL-23; and not expressed in SK-MEL-7, SK-MEL-21, SK-MEL-26 and WM115. As before, the discrepancy between the western blot and the staining observed in SK-MEL-19 cells is explained by a low number of MAGE-C2 positive cells (Figure 3.1C). Considering the heterogeneity observed for MAGE-C2, it is highly unlikely that the CT10#5 antibody recognised in the staining the 53 kDa non-specific band detected in western blot, as this was present at similar levels in all the analysed cells lines (Figure 3.1A).

The staining of three representative cell lines is shown in Figure 3.2. SK-MEL-37 cells (Figure 3.2A) express all of the proteins analysed at a very high level. It is important to note that, although all of the cells express NY-ESO-1 and MAGE-C1 and for this reason the staining has been defined as homogeneous, the intracellular localisation of these two proteins in this cell line varies: some cells show a very low signal in the nucleus, whereas it is stronger in others. This observation suggests that NY-ESO-1 and MAGE-C1 may shuttle between the cytoplasm and the nucleus and,

therefore, may have a function in both of these cellular compartments. Moreover, it is notable that for each of the three proteins analysed, the staining observed is weak in some cells (white arrows) and stronger in others (yellow arrows). A possible explanation is that CT genes may have particular functions in specific phases of the cell cycle, and that their expression may therefore be finely regulated. This hypothesis is supported by the heterogeneous staining observed in some cell lines, such as SK-MEL-14 (Figure 3.2B). In these cases, the variability observed in CT gene expression levels is even more striking, and cells expressing high (yellow arrows), intermediate (white arrows) and null levels (red arrows) of CT antigens can be distinguished. This cell line resembles the heterogeneous pattern observed for CT antigens in several types of cancer, and is therefore a good candidate with which to clarify the phenotypic differences between CT-expressing and non-expressing cells.

Finally, SK-MEL7 staining is negative for the three antigens (Figure 3.2C), in agreement with the western blot. This cell line therefore represents a good negative control for the specificity and sensitivity of the antibodies used. As further negative controls, each primary antibody alone (without secondary antibodies) and each secondary antibody alone (without primary antibodies) were tested in staining. To ensure the comparability between the different experiments, all the picture were taken utilising the same microscope settings.

This screening of melanoma cell lines has therefore enabled the identification of an *in vitro* model that mirrors the heterogeneity of CT genes in tumours. In particular, SK-MEL-37 and SK-MEL-14 cells appear to be a useful tool for studying the biological significance of these proteins.

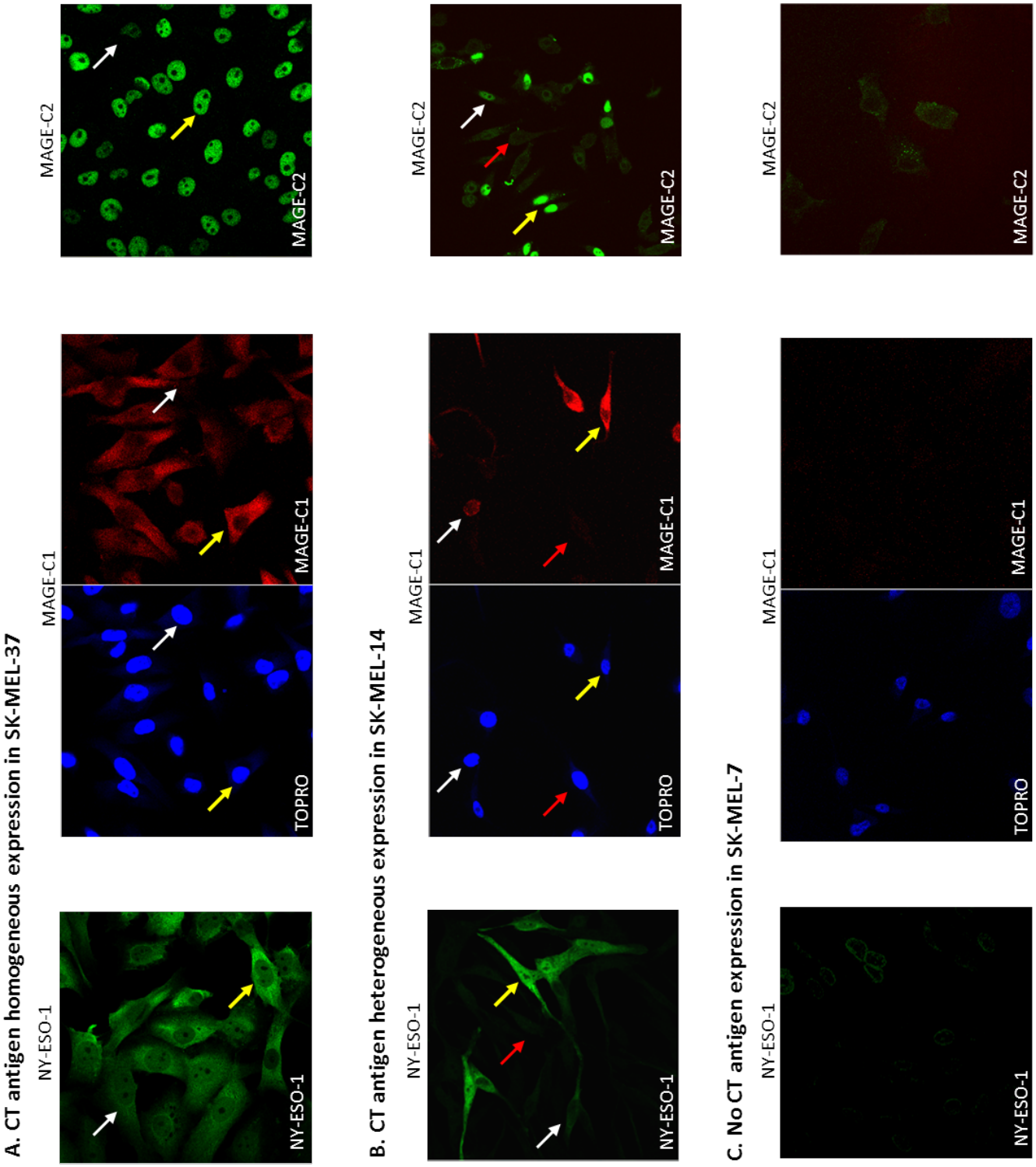

Figure 3.2 Immunofluorescence staining of endogenous CT antigens in human melanoma cell lines. Melanoma cell lines were tested for NY-ESO-1, MAGE-C1 and MAGE-C2 expression by immunofluorescence. Cells were fixed with paraformaldehyde and immunostained with NY-41 rabbit polyclonal, CT7.33 mouse monoclonal and CT10#5 mouse monoclonal antibodies, and then with secondary FITC- or TRITC-labelled antibodies. TOPRO was used for nuclei staining. The yellow, white and red arrows indicate cells expressing high level, intermediate level or no CT antigens respectively. A. Staining of endogenous NY-ESO-1, MAGE-C1 and MAGE-C2 showing a homogeneous pattern in SK-MEL-37 cells. B. Staining of endogenous NY-ESO-1, MAGE-C1 and MAGE-C2 showing a heterogeneous pattern in SK-MEL-14 cells. C. Negative staining for NY-ESO-1, MAGE-C1 and MAGE-C2 in SK-MEL-7 cells.

3.2.2 NY-ESO-1 and MAGE-C1 are not always co-expressed in the same cells

Since NY-ESO-1 and MAGE-C1 were co-expressed in the majority of the cell lines analysed, and are known to bind to each other, a double staining for these proteins was performed in SK-MEL-14 (Figure 3.3), a cell line that was found to express both genes heterogeneously. The double staining showed that although some cells co-express the two genes (red arrow), others highly express only one of them (yellow and white arrows). These two CT antigens are, therefore, not necessarily co-expressed at high levels in the same cells, suggesting that they could be differentially regulated and that their function could be, at least in part, independent from their binding.

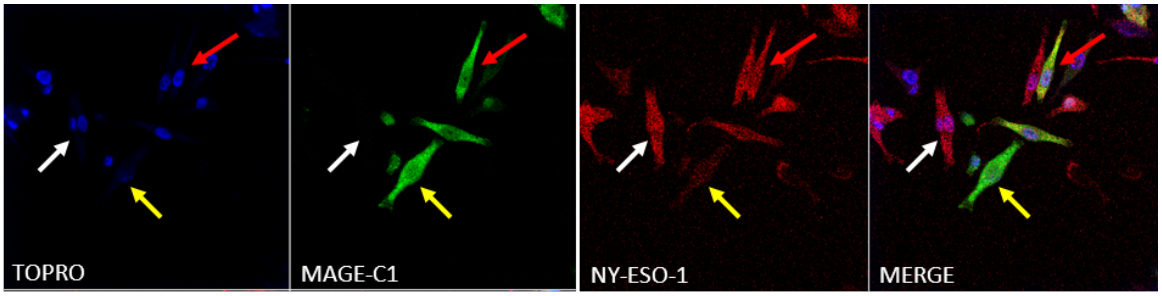

Figure 3.3 Immunofluorescence double staining of endogenous MAGE-C1 and NY-ESO-1 in SK-MEL-14. Cells were fixed with paraformaldehyde and immunostained with CT7.33 and NY-41, and then with secondary FITC- and TRITC-labelled antibodies, respectively. TOPRO was used for nuclei staining. The red, yellow and white arrows indicate cells co-expressing the two antigens, expressing relatively high levels of MAGE-C1 only and expressing relatively high levels of NY-ESO-1 only, respectively.

3.2.3 NY-ESO-1, MAGE-C1 and MAGE-C2 expression patterns vary in different human SCLC cell lines

Seven small cell lung cancer (SCLC) cell lines were used for this second set of screening experiments: HC33, H69, H146, H209, H524, H889 and H2171. As with the melanoma cell lines studied, the SCLC cell lines possess different features: for example, H69 and H146 are derived from the pleural fluid of patients, whereas H209 cells have been isolated from a metastasis to the bone marrow.

Western blot analysis and immunofluorescence staining were performed as described for the melanoma cell lines. Western blot analysis revealed that CT antigen expression occurred in 5 out

of 7 cell lines: HC33, H209, H2171, H146, and H889. In contrast, H69 and H524 showed no positivity (Figure 3.4). NY-ESO-1 was demonstrated to be expressed in 3 of the 7 cell lines (HC33, H209 and H146), whilst MAGE-C1 was positive in 4 cell lines (H209, H2171, H146 and H889). Finally, MAGE-C2 was found to be expressed in only one cell line, H146.

Co-expression of CT genes was observed in 2 cell lines: H209 and H146. The latter was the only SCLC cell line found to express all three CT proteins studied, whereas H209 cells were positive for NY-ESO-1 and MAGE-C1. 3 cell lines expressed only one of the proteins: HC33 cells were positive for NY-ESO-1, whereas H2171 and H889 were positive for MAGE-C1.

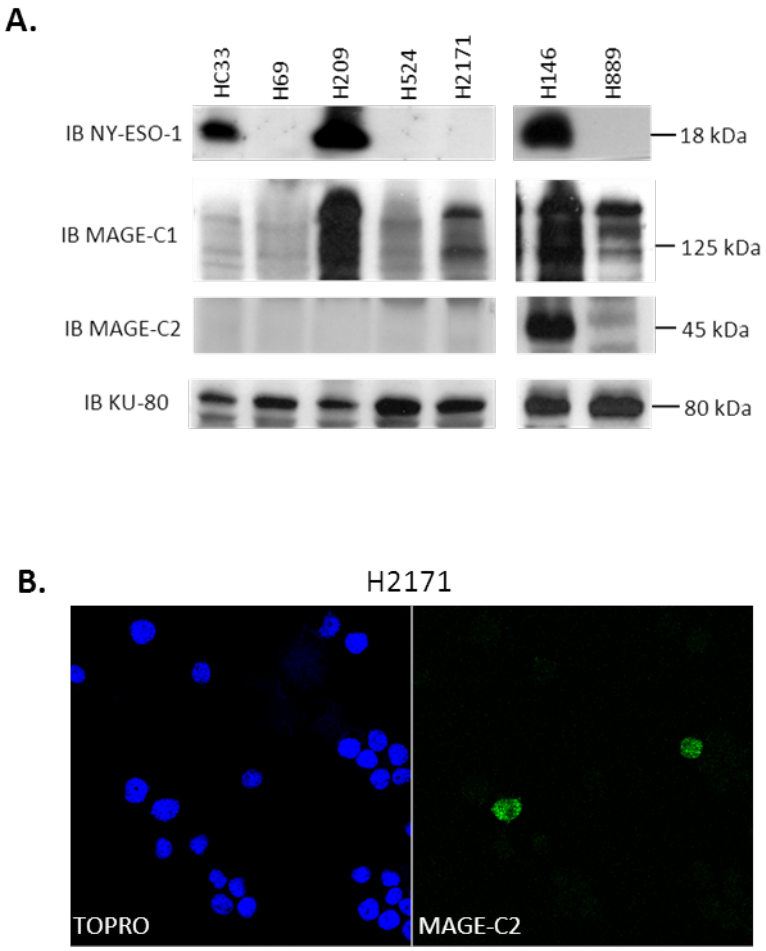

Figure 3.4 Analysis of CT antigen expression in SCLC cell lines. Seven SCLC cell lines were tested for CT antigen expression: HC33, H69, H209, H524, H2171, H146 and H889. A. Western blot analysis was performed using antibodies raised against NY-ESO-1 (rabbit polyclonal NY-41), MAGE-C1 (mouse monoclonal CT7.33 antibody), MAGE-C2 (mouse monoclonal CT10#5) and KU-80 (as a loading control). B. Staining of endogenous MAGE-C2 in the H2171 cell line. Cells were fixed with paraformaldehyde and immunostained with CT10#5 mouse monoclonal antibodies, and then with secondary FITC-labelled antibody. TOPRO was used for nuclei staining.

Immunofluorescence experiments were then performed on these SCLC cell lines and, interestingly, diverse patterns of expression similar to those detected for the melanoma cell lines studies were observed.

The results obtained from this second screening are summarised in Table 3.2.

SCLC CELL LINES			
	NY-ESO-1	MAGE-C1	MAGE-C2
HC33	Heterogeneous	Not expressed	Not expressed
H69	Not expressed	Not expressed	Not expressed
H146	Heterogeneous	Heterogeneous	Heterogeneous
H209	Homogeneous	Heterogeneous	Not expressed
H524	Not expressed	Not expressed	Not expressed
H889	Not expressed	Heterogeneous	Not expressed
H2171	Not expressed	Heterogeneous	Heterogeneous

Table 3.2 Summary of SCLC staining screening.

NY-ESO-1 staining appeared to be homogeneous in one of the SCLC cell lines (H209), heterogeneous in two (HC33 and H146), and negative in the remaining 4 cell lines (H69, H524, H889 and H2171). MAGE-C1 was found to be heterogeneously expressed in 4 of the cell lines (H146, H209, H889, H2171), whereas no expression was detected in the other 3 (HC33, H69 and H524); no homogeneously positive pattern was observed. Finally, MAGE-C2 was heterogeneously expressed in H146 and H2171, and was not expressed in the remaining five cell lines (HC33, H69, H209, H524 and H889).

These data are in agreement with the western blot analysis, apart from the H2171 cell line, which seemed not to express MAGE-C2. The apparent discrepancy between the immunoblot and immunofluorescence staining may be explained by the fact that the percentage of MAGE-C2 positive cells in the H2171 staining was very low (Figure 3.4B).

Similarly to the melanoma cell lines study, representative SCLC cell lines for each staining pattern are shown in Figure 3.5. It is noticeable that, as with the melanoma cell lines, the intensity of the staining in CT positive cells is variable, with cells expressing high levels (yellow arrows), intermediate levels (white arrows) and no protein (red arrows) (Figure 3.5B). This observation, together with the fact that almost all of the SCLC cell lines expressing CT genes showed a heterogeneous expression pattern, seems to strengthen the hypothesis of a link between CT gene expression and the cell cycle.

To summarise, this second screening study demonstrated that SCLC cell lines indeed express CT antigens, with a pattern that mimics the one observed in *in vivo* tumours. Moreover, it has enabled the identification of one of the SCLC cell lines, H146, as expressing all of the CT antigens under investigation in this study. The H146 cell line showed heterogeneous expression for all the proteins of concern, therefore, it appears to be a good model for studying both their cellular function and possible connections between their effects in cancer cells.

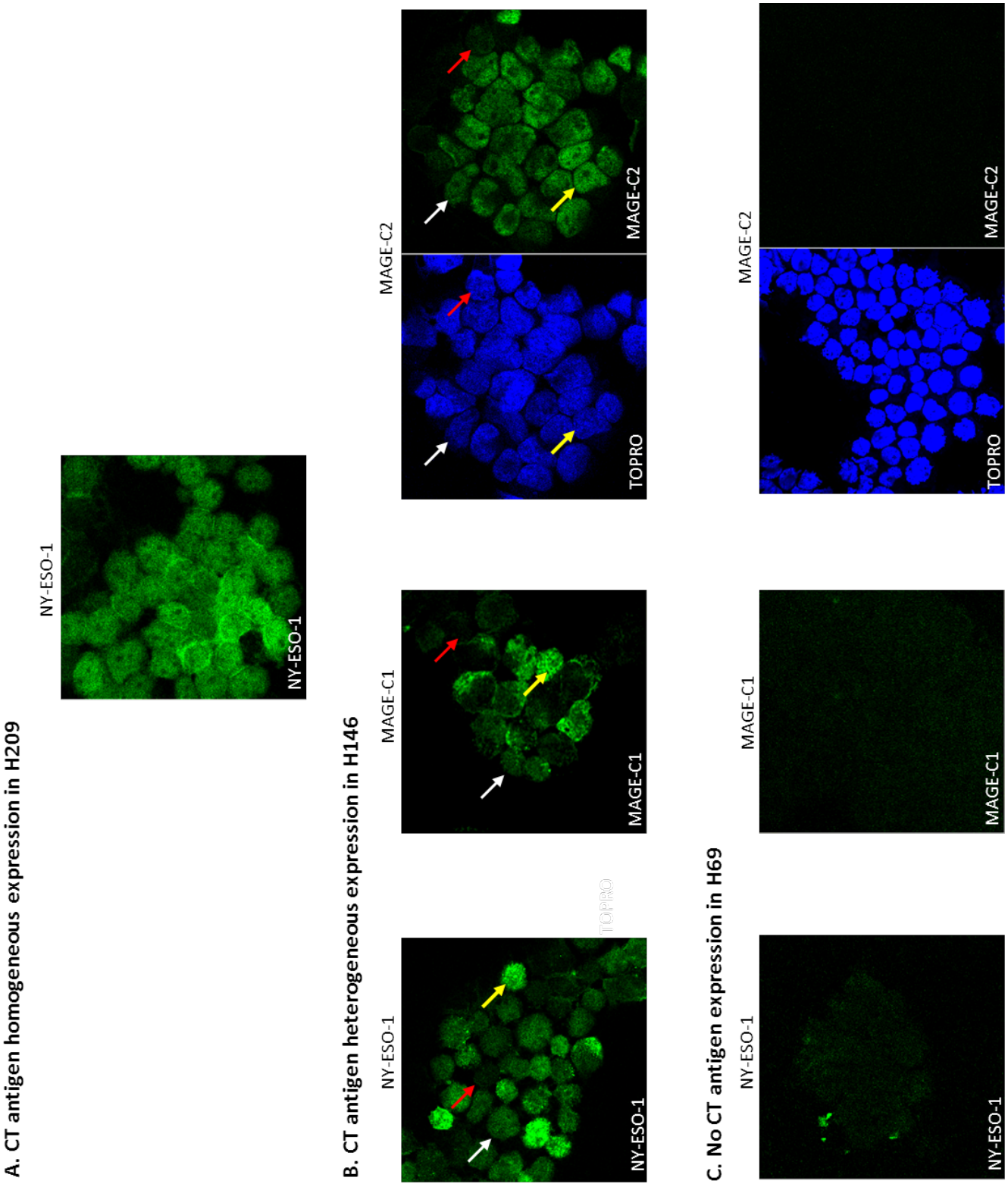

Figure 3.5 Immunofluorescence staining of endogenous CT antigens in human SCLC cell lines. SCLC cell lines were tested for NY-ESO-1, MAGE-C1 and MAGE-C2 expression by immunofluorescence. Cells were fixed with paraformaldehyde and immunostained with NY-41 rabbit polyclonal, CT7.33 mouse monoclonal and CT10#5 mouse monoclonal antibodies, and then with a secondary FITC-labelled antibody. TOPRO was used for nuclei staining. A. Staining of endogenous NY-ESO-1 showing a homogenous pattern in H209. B. Staining of endogenous NY-ESO-1, MAGE-C1 and MAGE-C2 showing a heterogeneous pattern in H146. C. Negative staining for NY-ESO-1, MAGE-C1 and MAGE-C2 in H69.

3.2.4 NY-ESO-1, MAGE-C1 and MAGE-C2 expression patterns vary in different human MM cell lines

In order to complete our panel of cell lines we screened three multiple myeloma (MM) cell lines for the expression of NY-ESO-1, MAGE-C1 and MAGE-C2.

Western blot analysis revealed that NY-ESO-1 and MAGE-C1 were co-expressed in two out of the three cell lines, namely U266 and SK007. The former also expressed MAGE-C2 whereas the latter did not, which is particularly interesting considering that SK007 cell line is derived from U266 by selecting for resistance to 8-azaguanine; such selection therefore also leads to loss of MAGE-C2 expression. Conversely, the third cell line, RPMI8226, did not express any of the CT antigens of interest (Figure 3.6A).

Immunofluorescence staining showed that NY-ESO-1 is both nuclear and cytoplasmic in SK007 and U266; moreover, it is homogeneously expressed in all cells. The weak staining observed in RMPI8226 cells, which according to the immunoblot do not express NY-ESO-1, is possibly due to cross-reaction with the NY-ESO-1 homologue LAGE-1. This protein presents a molecular weight of 21 kDa and no such band was detected by the NY41 antibody in previous experiments (Figure 3.1A and Figure 3.4A), suggesting that the antibody should not recognise LAGE-1 in western blot. The very high correspondence observed earlier between western blot and immunofluorescence expression data seems to indicate that the strong staining obtained utilising the NY41 antibody generally corresponds to NY-ESO-1, although a co-expression of LAGE-1 cannot be excluded. The specificity of NY41 was also proved in several melanoma cell lines in which RNAi experiments for NY-ESO-1 were performed (including SK-MEL14, SK-MEL23 and SK-MEL37, data not shown).

MAGE-C1 was also homogeneously expressed in SK007 and U266, but its staining varied in terms of localisation: whereas it was exclusively cytoplasmic in SK007, it appeared both nuclear and cytoplasmic in U266; more in detail, in this cell line some cells displayed a prevalently nuclear signal (red arrows) whereas some others presented a stronger cytoplasmic signal (yellow arrows). These results are particularly interesting considering that a more nuclear staining of

MAGE-C1 in tumour samples has been associated with poor prognosis in MM (Tinguely et al., 2008).

Finally, MAGE-C2 was heterogeneously expressed in the nucleus of U266 cells. Furthermore, staining could be detected in some sparse RPMI8226 cells; the fact that the western blot is negative for MAGE-C2 is probably due, similarly to SK-MEL-19 and H2171, to the extremely low number of cells expressing this CT antigen (Figure 3.6B).

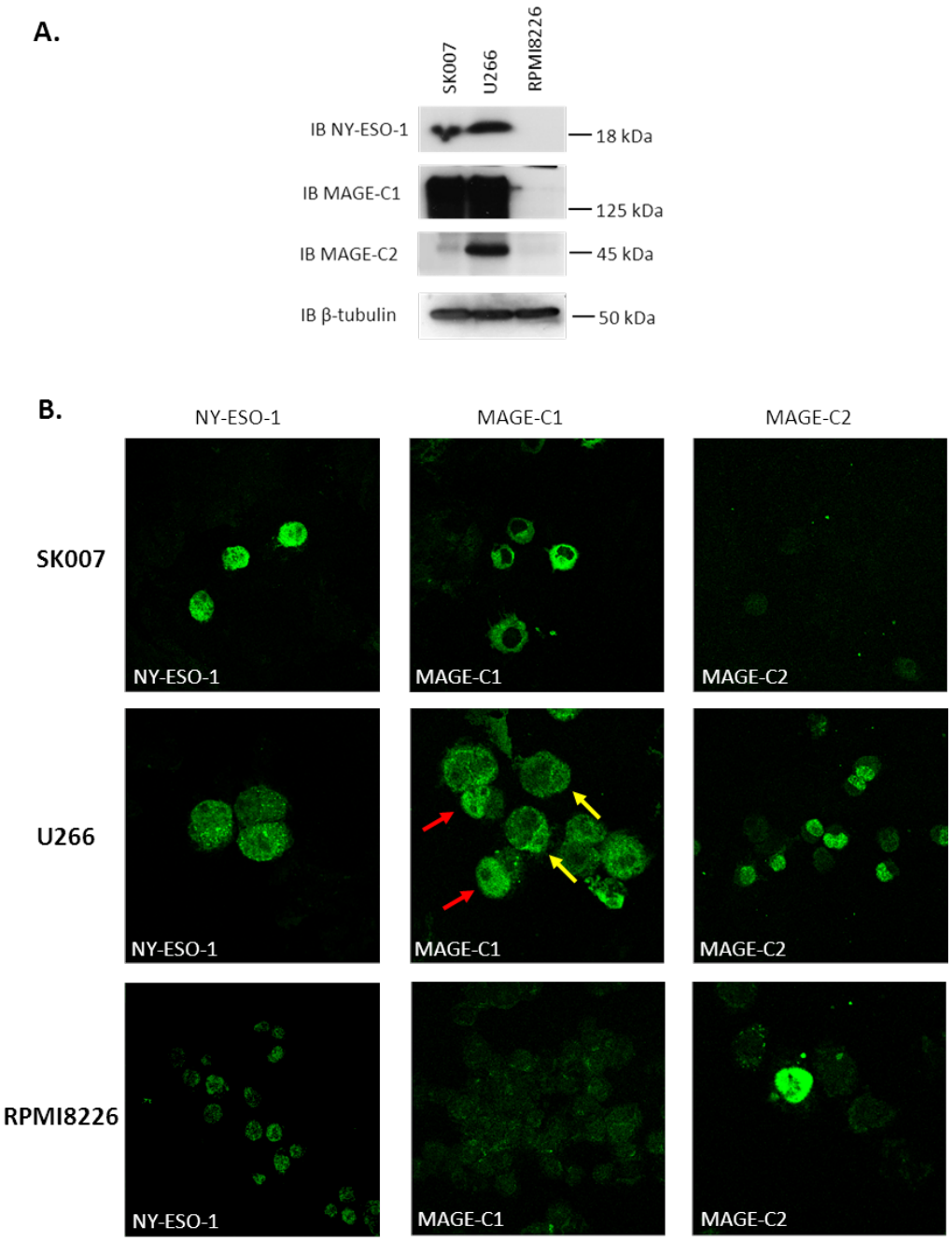

Figure 3.6 Analysis of CT antigen expression in MM cell lines. Three MM cell lines were tested for CT antigen expression: SK007, U266 and RPMI8226. A. Western blot analysis was performed using antibodies raised against NY-ESO-1 (mouse monoclonal E978), MAGE-C1 (mouse monoclonal CT7.33 antibody), MAGE-C2 (mouse monoclonal CT10#5) and β-tubulin (as a loading control). B. Staining of endogenous CT antigens in human MM cell lines. Cells were fixed with paraformaldehyde and immunostained with NY-41 rabbit polyclonal, CT7.33 mouse monoclonal and CT10#5 mouse monoclonal antibodies, and then with a secondary FITC-labelled antibody. The yellow and red arrows indicate cells expressing predominantly cytoplasmic or predominantly nuclear MAGE-C1 respectively.

The results obtained in MM cell lines are summarised in Table 3.3.

MULTIPLE MYELOMA CELL LINES			
	NY-ESO-1	MAGE-C1	MAGE-C2
SK007	Homogeneous	Homogeneous	Not expressed
U266	Homogeneous	Homogeneous	Heterogeneous
RPMI8226	Homogeneous	Not expressed	Heterogeneous

Table 3.3 Summary of MM staining screening.

3.3 Summary and discussion

CT antigens frequently show a heterogeneous pattern in tumour samples (Aubry et al., 2001; Chitale et al., 2005; Dhodapkar et al., 2003; Jungbluth et al., 2000b; Li et al., 2005). This suggests that the subpopulation of cells expressing these proteins must somehow be different from the negative cells. As a consequence, a comparative study of these two subpopulations of cells could help to determine the biological role of these tumour antigens. In order to verify whether this heterogeneity could be observed also in *in vitro* conditions, screening of different cancer cell lines was performed. Western blot analyses and immunofluorescence experiments were carried out to determine the expression levels and the expression patterns of three CT antigens: NY-ESO-1, MAGE-C1 and MAGE-C2.

The results obtained demonstrated that these genes are expressed in the majority of the 11 melanoma, 7 SCLC and 3 MM cell lines studied. Moreover, in many cell lines co-expression of two or more CT genes was observed, and this result resembles the frequent co-expression reported in tumour samples (Sahin et al., 1998; Sugita et al., 2002). Interestingly, all three proteins showed heterogeneous expression in many of the cell lines analysed. This screening experiment has therefore enabled the identification of an experimental system for studying CT antigen function and regulation in melanoma, small cell lung cancer and multiple myeloma.

Different expression patterns were found in the cell lines: some homogeneously expressed all of the CT genes studied (SK-MEL-2, SK-MEL17 and SK-MEL-37) whereas others heterogeneously express all of them (SK-MEL-14, SK-MEL-19, H146). In contrast, some cell lines expressed no CT antigens (SK-MEL-7, H69 and H524). Several cell lines co-expressed two of the three genes and a correlation in the expression of the binding partners NY-ESO-1 and MAGE-C1 could be observed. Some of the SCLC cell lines also expressed either NY-ESO-1 or MAGE-C1, suggesting that their regulation is at least partially different and that the two proteins could also have independent roles. This hypothesis is supported by the fact that when a heterogeneous co-expression pattern was found, the cell subpopulations positive for the two different CT antigens

did not totally overlap. MAGE-C2 expression appeared less correlated with the other CT genes and, in general, less frequent (11 out of 21 cell lines, versus 15 expressing MAGE-C1 and 14 expressing NY-ESO-1).

Among the cell lines studied, SK-MEL-14 and H146 express NY-ESO-1, MAGE-C1 and MAGE-C2 with a heterogeneous pattern. Notably, variations in the staining intensity of positive cells were noticed, suggesting that the regulation of CT protein levels could be a dynamic process correlated for example with the cell cycle or with the differentiation status of the cell. This observation can also be extended to SK-MEL-37 cells, although the extent of the variation is less striking, probably because the basal levels of CT proteins is higher than in SK-MEL-14. In SK-MEL-37 a differential intracellular localisation was also observed for NY-ESO-1 and MAGE-C1. Although these proteins are mostly cytoplasmic, some nuclear staining was detected and the intensity of this staining varied in different cells, suggesting that the proteins may shuttle between the cytoplasm and the nucleus. This diversity was even more striking for MAGE-C1 in U266 MM cell line, which presented some cells with a markedly nuclear location and some others where MAGE-C1 was almost exclusively cytoplasmic.

These observations encourage the use of SK-MEL-14, SK-MEL-37, H146 and U266 as *in vitro* models for studying CT regulation and function.

Chapter IV: NY-ESO-1 affects the stability of MAGE-C1 MAGE homology domain

4.1 Introduction

Most studies published to date have focused on the transcriptional regulation of CT genes. They have demonstrated that CT antigen promoters are methylated on CpG islands. This mechanism is supposed to silence their expression in normal somatic cells (Coral et al., 2002; De Smet et al., 1996; De Smet et al., 1999; Gure et al., 2002; Weber et al., 1994; Wischnewski et al., 2007), whereas DNA demethylation could be one of the causes for their aberrant expression in cancer. Moreover, histone acetylation has been shown to influence the transcription of these genes (Oi et al., 2009; Wischnewski et al., 2006). In contrast, the post-translational regulation of the CT antigens has not yet been clarified, and represents a particularly interesting field of investigation since these proteins are often heterogeneously expressed in tumour samples and, in the light of the results outlined above, in cancer cell lines.

Understanding CT proteins turnover and degradation could not only give us new insights about their function, but also provide tools to modulate their expression in cancer cells and their processing for antigen presentation.

Eukaryotic cells contain two major systems for protein degradation. The first to be discovered was the lysosomal apparatus, a membrane-enclosed vacuole containing multiple acid proteases (cathepsins) and other hydrolases. This structure is involved primarily in the non-specific degradation of membrane associated proteins, extracellular proteins taken up by endocytosis and

macromolecules from autophagy. The protein breakdown by the lysosome-endosome pathway is also the source of antigenic peptides that are presented to $CD4^+$ T cells on MHC class II molecules (Bainton, 1981; Dice, 1987; Gronostajski et al., 1985).

However, the bulk of cytosolic and nuclear proteins in mammalian cells are hydrolysed in an ATP-dependent pathway by the 26S proteasome upon ubiquitination (Baumeister et al., 1998; Coux et al., 1996). This pathway is also responsible for the production from intracellular proteins of peptides presented to cytotoxic T lymphocytes by MHC class I molecules. These include viral antigens and tumour antigens like the CT antigens (Rock et al., 1994).

This chapter aims to investigate the role of the proteasome degradation pathway in CT antigen post-translational regulation utilising proteasome inhibitors. Furthermore, we will assess whether the binding between the two CT proteins MAGE-C1 and NY-ESO-1 is affected when the proteasome pathway is blocked, and we will examine the effect of NY-ESO-1 on MAGE-C1 protein stability. Finally, we will examine whether ubiquitin-like modifications also play a role in the regulation of MAGE-C1 in particular.

4.2 Results

4.2.1 Proteasome inhibitor MG132 induces insoluble MAGE-C1, which accumulates at the centrosome.

To determine whether the proteasome pathway could be involved in the post-translational regulation of CT antigens, the SK-MEL-37 melanoma cell line, previously shown to express MAGE-C1, MAGE-C2 and NY-ESO-1 proteins (Figure 3.1), was treated for 4 hours with 40 μM MG132, a selective proteasome inhibitor. DMSO was used as a negative control since it was utilised to dissolve MG132.

SK-MEL-37 cell line appeared to be a good model to start our investigation for several reasons: first of all, it allowed studying the effect of proteasome inhibitors on the three antigens simultaneously; furthermore, the high expression levels and the morphology of the cells permitted a more detailed characterisation of their subcellular localisation by immunofluorescence, if compared to other, smaller-looking cells co-expressing the antigens, such as SK-MEL-14; finally, this melanoma cell line was chosen over SCLC or MM cell lines as it is more prone to manipulations, such as DNA and siRNA transfections, that were to be performed in following experiments.

Cells were collected separating the soluble fraction, which included the components of the cytoplasm and the nucleoplasm, from the insoluble fraction, which consists of all of the cellular components that cannot be solubilised by RIPA lysis buffer (i.e. the cytoskeleton and nuclear matrix). Interestingly, western blot analysis showed an increase in MAGE-C1 protein level in the insoluble fraction upon MG132 treatment (Figure 4.1A). A similar trend was also observed for the loading control β-tubulin though; therefore quantification was performed utilising the ImageJ programme. This showed a 2.13 fold increase in MAGE-C1 in the MG132 treated sample over the control, after normalisation for β-tubulin.

A slight increase in the soluble fraction could also be observed, as was a shift in the protein migration, both in the soluble and insoluble fraction, potentially due to post-translational modification of MAGE-C1.

Immunofluorescence staining was then performed to investigate the subcellular localisation of MAGE-C1 upon MG132 treatment. Intriguingly, treatment with the proteasome inhibitor caused a change in the subcellular localisation of MAGE-C1: whereas the protein was mostly cytoplasmic in DMSO treated cells, an accumulation at the centrosome was noticed upon treatment. The centrosomal localisation was confirmed by performing a double staining experiment with pericentrin, a protein that is exclusively found in this structure (Figure 4.1B). A further observation was a decrease in the nuclear staining of MAGE-C1 upon MG132 treatment, suggesting that inhibition of the proteasome could trigger MAGE-C1 shuttling from the nucleus to the cytoplasm or inhibit the opposite translocation.

Although proteasome activity can be found throughout the cytosol, proteasomes are concentrated at the mammalian centrosome, an observation that has led to the description of the centrosome as a proteolytic centre (Wigley et al., 1999). Moreover, treatment of cells with inhibitors of proteasome activity has been proved to promote redistribution of the proteasome and associated regulatory proteins to the centrosome (Fabunmi et al., 2000) and it has been reported that poly-ubiquitinated, aggregation-prone misfolded proteins are transported on microtubules to the centrosome (Ardley et al., 2003; Bence et al., 2001; Johnston et al., 1998).

Considering these findings, we can speculate that MAGE-C1 protein is normally processed and possibly degraded by the proteasome and that, if such process is inhibited, it forms insoluble aggregates that accumulate at the centrosome.

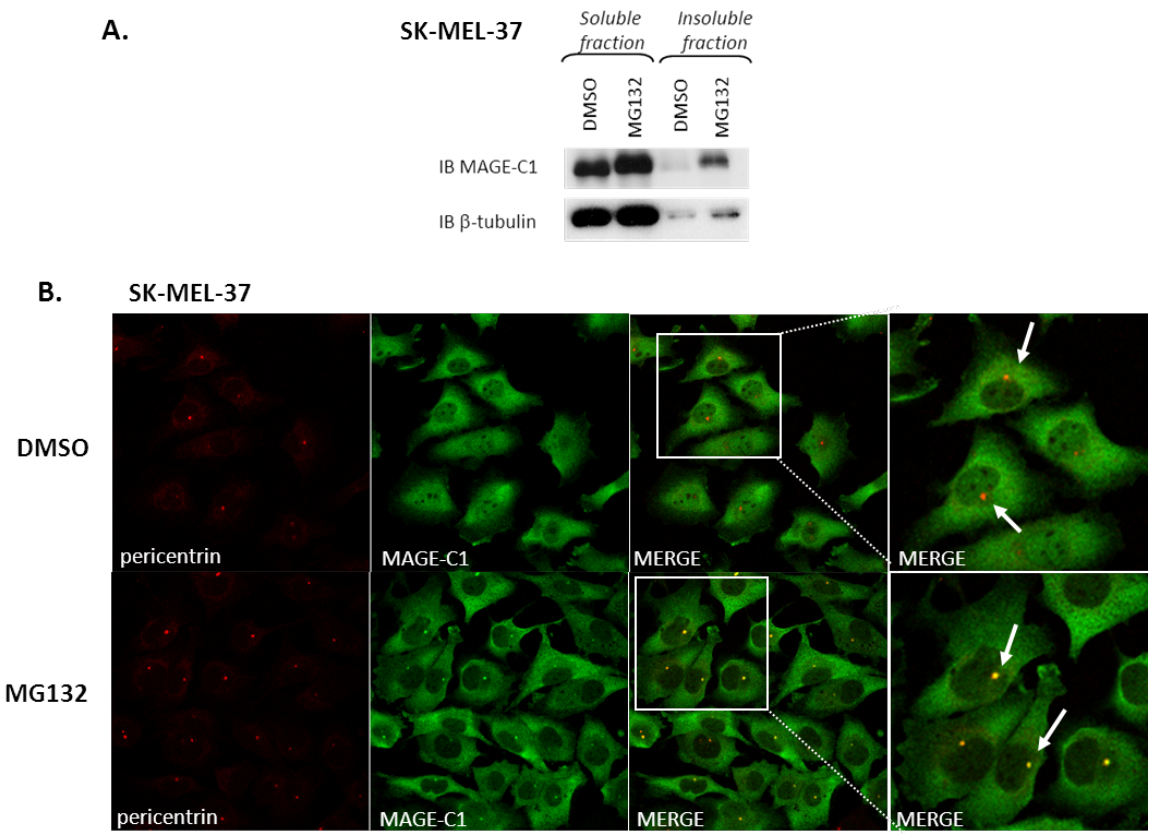

Figure 4.1 Proteasome inhibitor MG132 induces insoluble MAGE-C1, which accumulates at the centrosome. SK-MEL-37 melanoma cells were treated with MG132 40μM or DMSO (negative control) for 4h. A. Western blot analysis of endogenous MAGE-C1. After treatment, SK-MEL-37 cells were lysed and soluble and insoluble fractions analysed by SDS-PAGE, and immunoblotted for MAGE-C1 using mouse monoclonal CT7.33 antibody or mouse monoclonal β-tubulin antibody (as a loading control). B. Immunofluorescence double staining of endogenous MAGE-C1 and pericentrin. Cells were fixed with paraformaldehyde and immunostained with CT7.33 mouse monoclonal antibody and pericentrin rabbit polyclonal antibody, and then with secondary FITC- and TRITC-labelled antibodies, respectively. The white arrows indicate the centrosome.

4.2.2 MAGE-C1 and NY-ESO-1 co-localise at the centrosome after MG132 treatment

Since MAGE-C1 has been shown to bind NY-ESO-1 (Cho et al., 2006), it seemed particularly interesting to investigate whether treatment with the proteasome inhibitor could also affect the localisation of NY-ESO-1. SK-MEL-37 melanoma and H146 SCLC cell lines, which express endogenous NY-ESO-1 (Figures 3.1 and 3.4), were treated with 40 μM MG132 for 4 hours. Cells were then analysed by immunoblot or immunostained for NY-ESO-1.

Western blot analysis showed that, as for MAGE-C1, there is an increase of NY-ESO-1 protein in the insoluble fraction upon treatment (Figure 4.2A).

Double staining of NY-ESO-1 and the centrosome marker pericentrin demonstrated that, like MAGE-C1, NY-ESO-1 accumulates at the centrosome after treatment in both cell lines (Figure 4.2B). Moreover, it was possible to detect centrosomal NY-ESO-1 in some untreated H146 cells, indicating that this protein probably shuttles between the centrosome and the cytoplasm under normal conditions and that its localisation becomes more evident if its cellular level increases.

Finally, a double staining for MAGE-C1 and NY-ESO-1 was carried out and confirmed the co-localisation of the two proteins at the centrosome (Figure 4.2C).

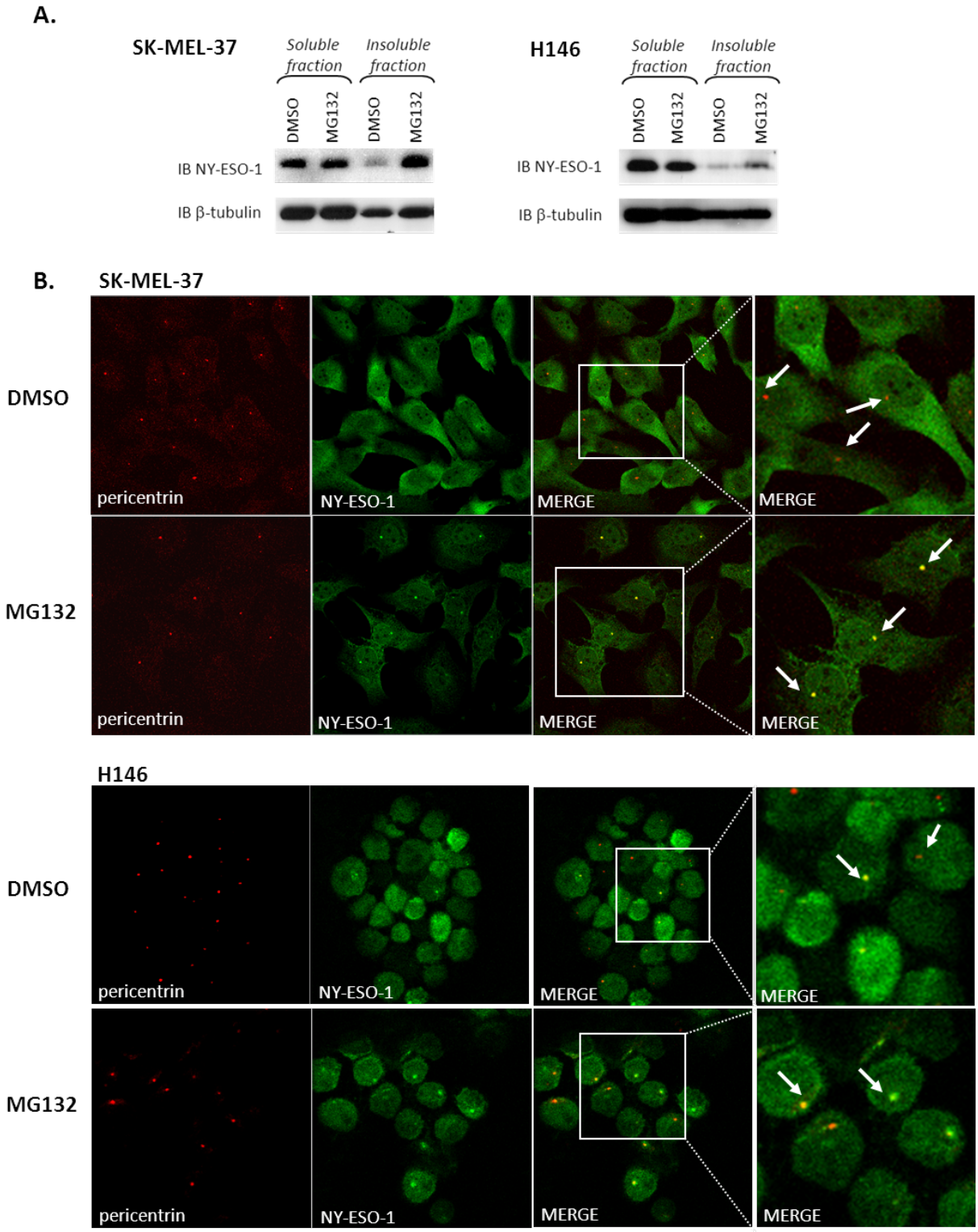
A.
SK-MEL-37
Soluble fraction
Insoluble fraction
DMSO
MG132
DMSO
MG132
IB NY-ESO-1
IB β-tubulin
H146
Soluble fraction
Insoluble fraction
DMSO
MG132
DMSO
MG132
IB NY-ESO-1
IB β-tubulin
B.
SK-MEL-37
DMSO
MG132
pericentrin
NY-ESO-1
MERGE
MERGE
H146
DMSO
MG132
pericentrin
NY-ESO-1
MERGE
MERGE

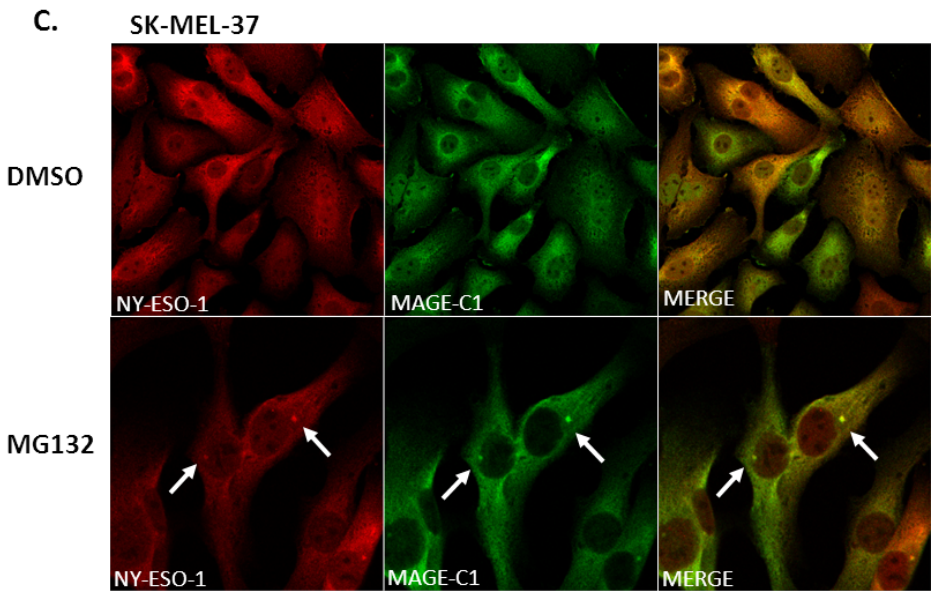

Figure 4.2 MAGE-C1 and NY-ESO-1 co-localise at the centrosome after MG132 treatment. SK-MEL-37 melanoma cells and H146 SCLC cells were treated with MG132 40μM or DMSO (negative control) for 4h. A. Western blot analysis of endogenous NY-ESO-1. Cells were lysed after treatment, and soluble and insoluble fractions analysed by SDS-PAGE and immunoblotted for NY-ESO-1 using rabbit polyclonal NY-41 antibody or mouse monoclonal β-tubulin antibody (as a loading control). B. Immunofluorescence double staining of endogenous NY-ESO-1 and pericentrin. Cells were fixed with paraformaldehyde and immunostained with NY-41 rabbit polyclonal antibody and pericentrin mouse monoclonal antibody, and then with secondary FITC- and TRITC-labelled antibodies, respectively. The white arrows indicate the centrosome. C. Immunofluorescence double staining of endogenous MAGE-C1 and NY-ESO-1. Cells were fixed with paraformaldehyde and immunostained with CT7.33 mouse monoclonal antibody and NY-41 rabbit polyclonal antibody, and then with secondary FITC- and TRITC-labelled antibodies, respectively. The white arrows indicate the centrosome.

4.2.3 Proteasome inhibitor MG132 induces insoluble MAGE-C2

MAGE-C2 is the MAGE protein with highest homology to MAGE-C1, therefore we tested whether it was also affected by MG132 treatment.

Again, western blot and immunofluorescence analyses were performed after treatment to assess MAGE-C2 expression levels and localisation. The staining observed for this protein did not highlight any differences between DMSO and MG132 treated cells (Figure 4.3B). However, western blot analysis did show that MAGE-C2 protein levels were influenced by this treatment as a slight increase in MAGE-C2 protein level was observed in the insoluble fraction (Figure 4.3A). The MAGE-C2 band is indicated by an arrow in the figure, as a non-specific upper band was also present in the soluble fraction. Since MAGE-C2 is exclusively nuclear, this finding could be explained by the association of MAGE-C2 to proteins pertaining to the insoluble fraction in the nuclear matrix or with the formation of aggresomes in the nucleus, although of small entity as they were not detected in the staining.

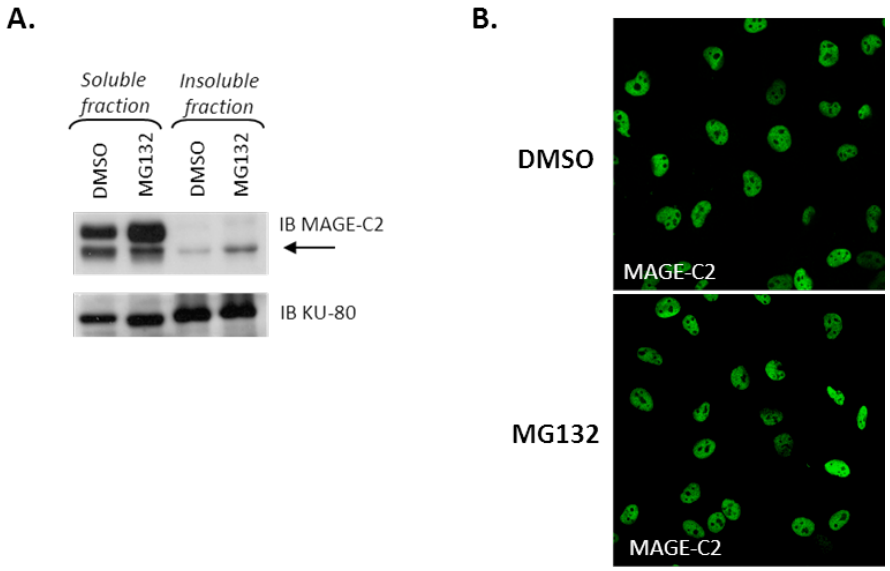

Figure 4.3 Proteasome inhibitor MG132 induces insoluble MAGE-C2. SK-MEL-37 melanoma cells were treated with MG132 40µM or DMSO (negative control) for 4h. A. Western blot analysis of endogenous MAGE-C2. After treatment cells were lysed and soluble and insoluble fractions analysed by SDS-PAGE and immunoblotted for MAGE-C2 using mouse monoclonal CT10#5 antibody or mouse monoclonal KU-80 antibody (as a loading control). The arrow indicates the MAGE-C2 band. B. Immunofluorescence staining of endogenous MAGE-C2. Cells were fixed with paraformaldehyde and immunostained with CT10#5 mouse monoclonal antibody and then with secondary FITC-labelled antibody.

4.2.4 MAGE-C1 and NY-ESO-1 centrosome localisation is specifically induced by proteasome inhibitors.

Although MG132 potently inhibits the proteasome, it also impairs other intracellular, non-proteasomal proteolytic activities such as calpain and lysosomal proteases (cathepsins) (Lee and Goldberg, 1998; Tawa et al., 1997).

To prove that the centrosomal localisation observed for MAGE-C1 and NY-ESO-1 was truly due to proteasome inhibition, SK-MEL-37 cells were also treated with epoxomicin, a different proteasome inhibitor which does not affect non-proteasomal proteases (Meng et al., 1999). Also in this case, the treatment induced centrosome localisation for both proteins (Figure 4.4A).

In addition, to rule out a dose-dependent effect in the MG132 treatment, lower doses of drug (20μM and 1μM) were utilised for the 4 hours treatment: accumulation of MAGE-C1 and NY-ESO-1 at the centrosome could be observed with all drug concentrations (Figure 4.4B).

These results corroborated our findings that the accumulation of MAGE-C1 and NY-ESO-1 at the centrosome is specifically induced by inhibition of the proteasome.

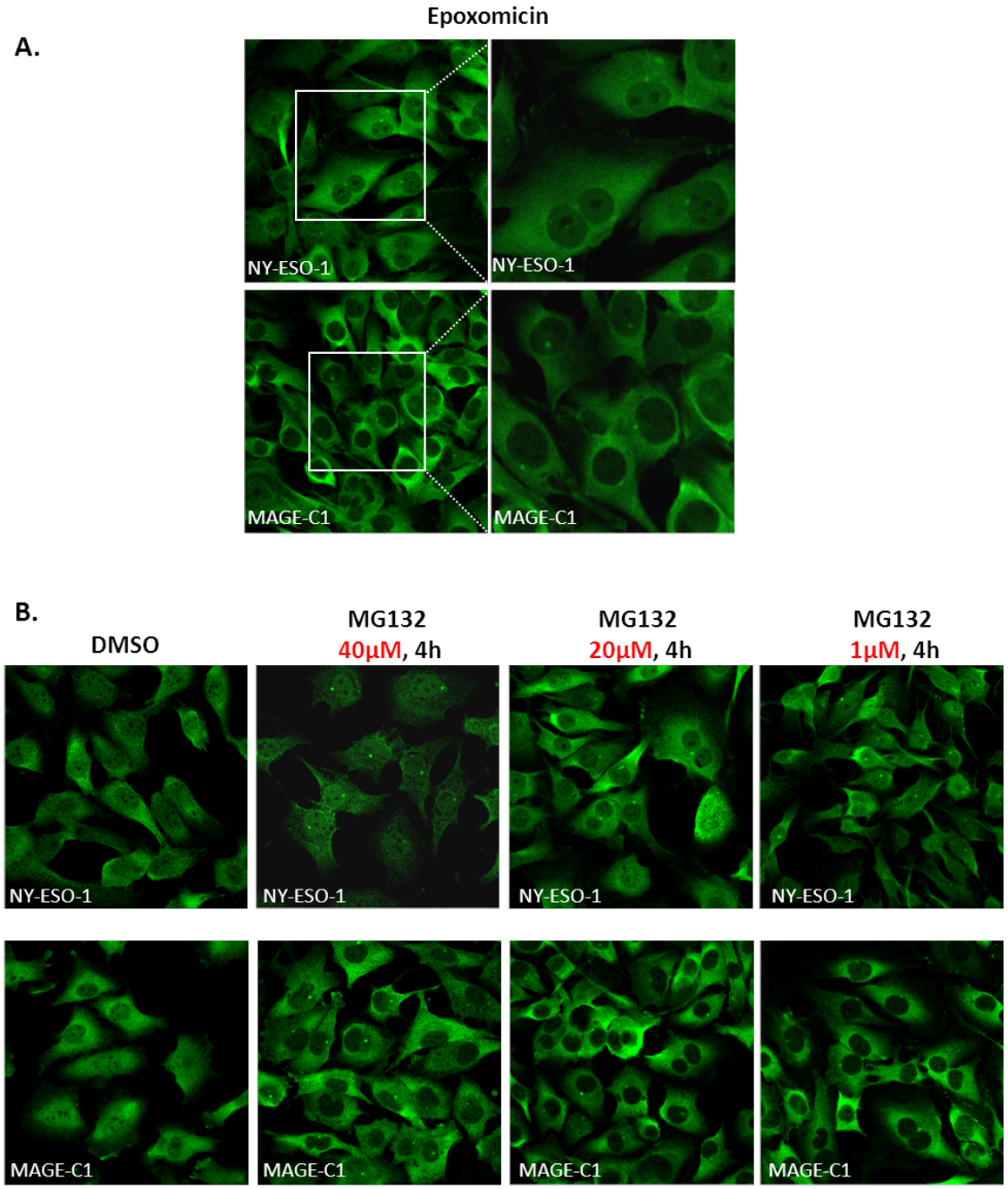

Figure 4.4 MAGE-C1 and NY-ESO-1 centrosomal localisation is specifically induced by proteasome inhibitors. A. Immunofluorescence staining of endogenous MAGE-C1 and NY-ESO-1. SK-MEL-37 cells were treated with epoxomicin 1µM or DMSO (negative control) for 4h, fixed with paraformaldehyde and immunostained with NY-41 rabbit polyclonal antibody and CT7.33 mouse monoclonal antibody, and then with secondary FITC-labelled antibody. B. Immunofluorescence staining of endogenous MAGE-C1 and NY-ESO-1. SK-MEL-37 cells were treated with MG132 40µM, 20µM and 1µM or DMSO (negative control) for 4h, fixed with paraformaldehyde and immunostained with NY-41 rabbit polyclonal antibody and CT7.33 mouse monoclonal antibody, and then with secondary FITC-labelled antibody.

4.2.5 MAGE-C1 and NY-ESO-1 localise at the centrosome independently from each other

Since MAGE-C1 and NY-ESO1 are frequently co-expressed in cancer cells and they form a complex, we tested whether their co-expression and, as a consequence, their binding was necessary for their stabilisation in the insoluble fraction and accumulation at the centrosome upon inhibition of the proteasome pathway.

HC33 SCLC cells (expressing NY-ESO-1 but not MAGE-C1) and U2OS osteosarcoma cells (expressing MAGE-C1 but not NY-ESO-1, Figure 5.1) were treated with MG132 followed by western blot and immunofluorescence. In both cell lines the CT antigens accumulated at the centrosome (Figure 4.5B) and were stabilised in the insoluble fraction (Figure 4.5A), despite the lack of their respective binding partner.

RNAi for one or the other of the two genes was also performed in SK-MEL-37; peripheral areas characterised by low transfection efficiency were chosen from the immunofluorescence in order to visualise both transfected and non-transfected cells at the same time. The staining showed that in cells depleted of one CT antigen, the other still accumulated at the centrosome upon MG132 treatment (Figure 4.5C).

Finally, to further demonstrate that the centrosomal localisation of NY-ESO-1 is a general feature of the protein, a vector coding for an EGFP-NY-ESO-1 fusion protein was transfected into NIH 3T3 mouse fibroblast cells, which does not express NY-ESO-1 as this CT antigen is present only in primates; cells transfected with EGFP-NY-ESO-1 were then analysed by immunofluorescence. Interestingly, NY-ESO-1 showed a centrosomal localisation in transfected cells without MG132 treatment, and this could be explained by the fact that this peculiar localisation could be a condition normally found in cells, that becomes more evident if the amount of NY-ESO-1 protein increases (i.e. following transfection). Transfected cells were co-stained for NY-ESO-1 to confirm the specificity of the EGFP fusion protein and transfection efficiency was tested by western blot analysis (Figure 4.5D).

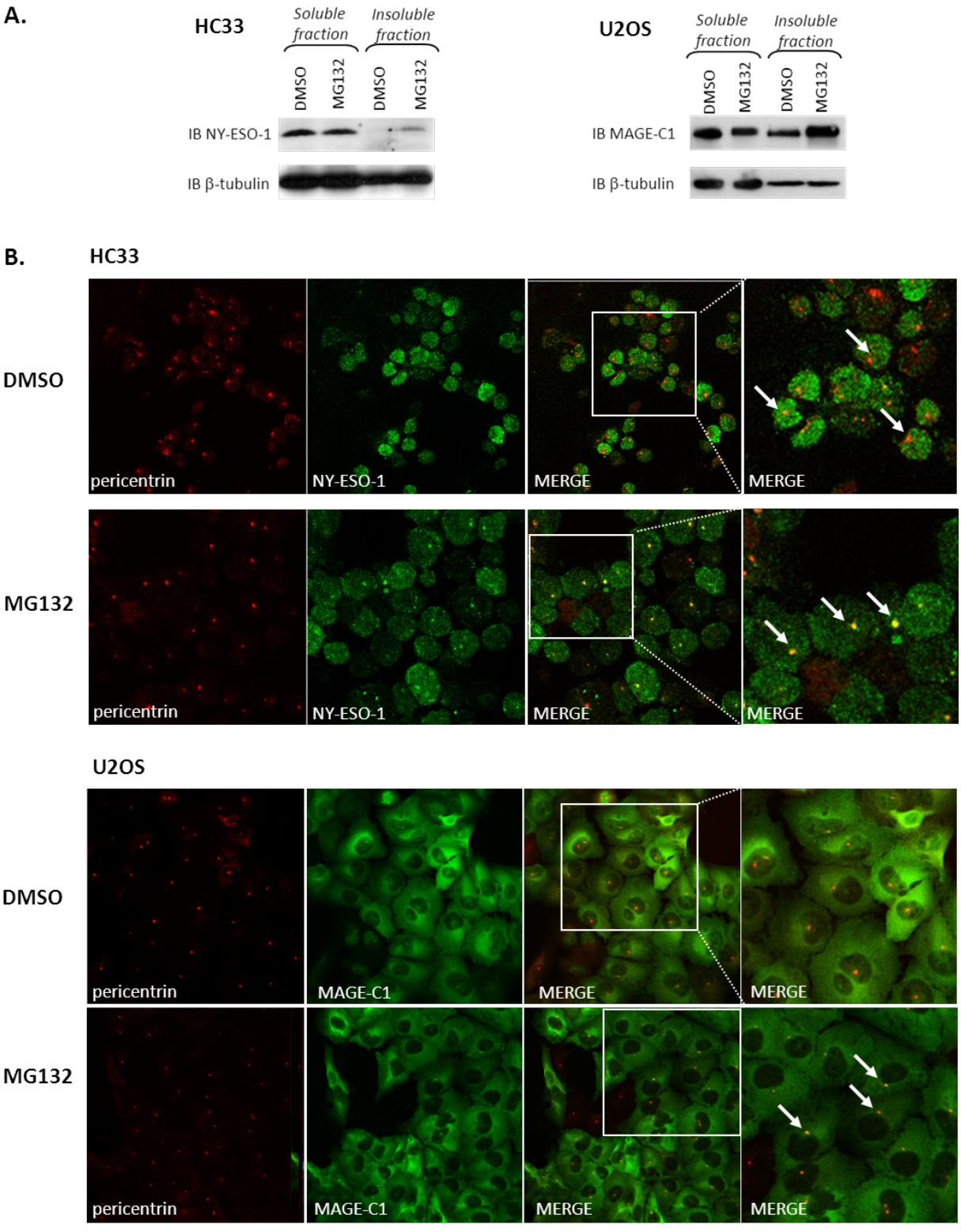
A.
HC33
Soluble fraction
Insoluble fraction
DMSO
MG132
DMSO
MG132
IB NY-ESO-1
IB β-tubulin
U2OS
Soluble fraction
Insoluble fraction
DMSO
MG132
DMSO
MG132
IB MAGE-C1
IB β-tubulin
B.
HC33
DMSO
pericentrin
NY-ESO-1
MERGE
MERGE
MG132
pericentrin
NY-ESO-1
MERGE
MERGE
U2OS
DMSO
pericentrin
MAGE-C1
MERGE
MERGE
MG132
pericentrin
MAGE-C1
MERGE
MERGE

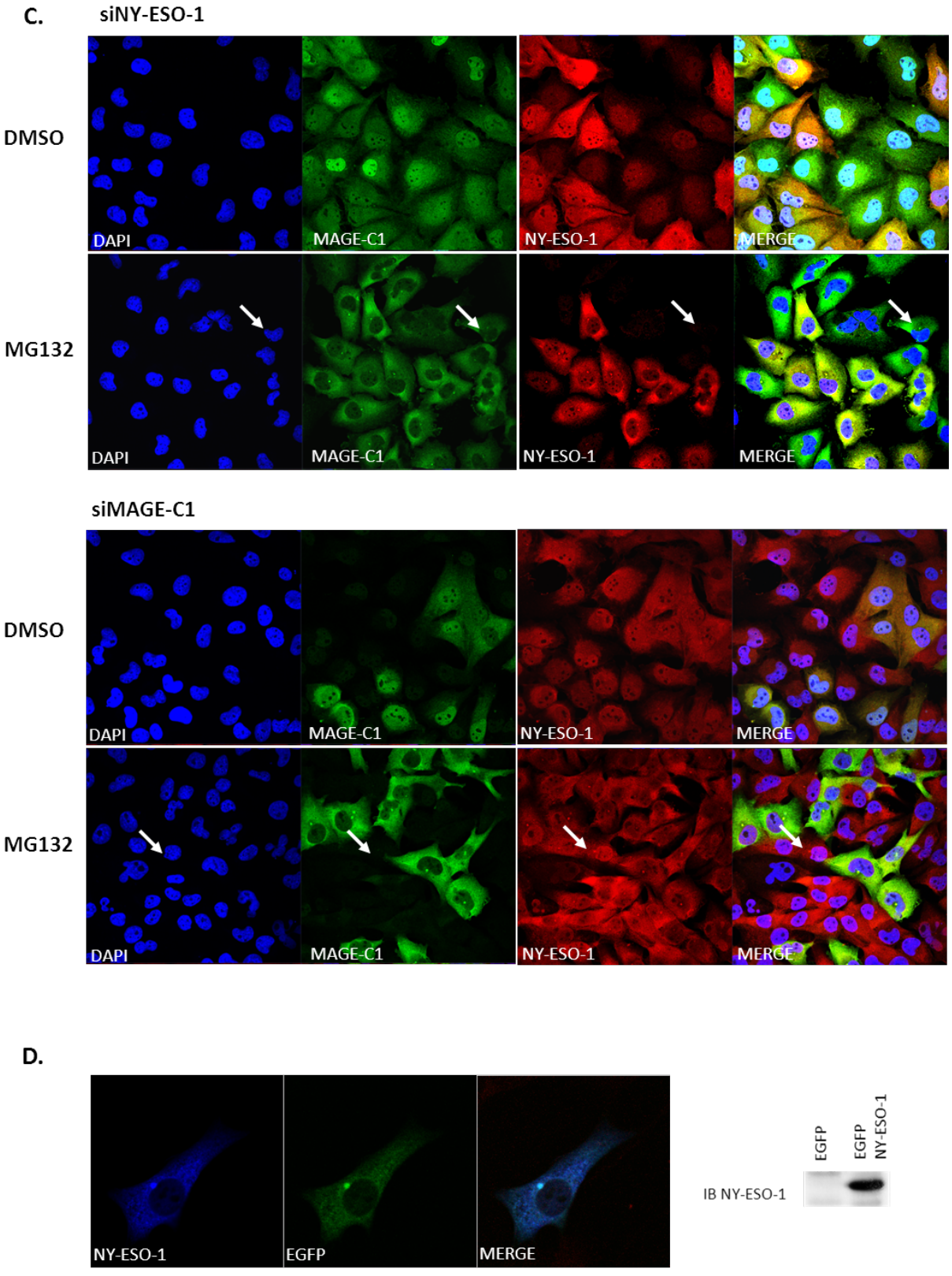
C.
siNY-ESO-1
DMSO
MG132
DAPI
MAGE-C1
NY-ESO-1
MERGE
siMAGE-C1
DMSO
MG132
DAPI
MAGE-C1
NY-ESO-1
MERGE
D.
NY-ESO-1
EGFP
MERGE
EGFP
EGFP
NY-ESO-1
IB NY-ESO-1

Figure 4.5 MAGE-C1 and NY-ESO-1 localise at the centrosome independently from each other. A.HC33 SCLC cells and U2OS osteosarcoma cells were treated with MG132 40μM or DMSO (negative control) for 4h. After treatment cells were lysed and soluble and insoluble fractions analysed by SDS-PAGE and immunoblotted with NY-41 rabbit polyclonal antibody for NY-ESO-1, with CT7.33 mouse monoclonal antibody for MAGE-C1 or with mouse monoclonal β-tubulin antibody (as a loading control). B. *Top panel*: immunofluorescence double staining of endogenous NY-ESO-1 and pericentrin in HC33 cells. Cells were treated with MG132 40μM or DMSO (negative control) for 4h, then fixed with paraformaldehyde and immunostained with NY-41 rabbit polyclonal antibody and pericentrin mouse monoclonal antibody, and then with secondary FITC- and TRITC-labelled antibodies, respectively. *Lower panel*: immunofluorescence double staining of endogenous MAGE-C1 and pericentrin in U2OS. Cells were treated with MG132 40μM or DMSO (negative control) for 4h, then fixed with paraformaldehyde and immunostained with CT7.33 mouse monoclonal antibody and pericentrin rabbit polyclonal antibody, and then with secondary FITC- and TRITC-labelled antibodies, respectively. The white arrows indicate the centrosome. C. Immunofluorescence double staining of endogenous NY-ESO-1 and MAGE-C1 in SK-MEL-37 cells. Cells were transfected with a NY-ESO-1 or a MAGE-C1 specific siRNA oligonucleotide according to the lipofectamine2000 protocol. 72h after transfection cells were treated with MG132 40μM or DMSO (negative control) for 4h, fixed with paraformaldehyde and immunostained with CT7.33 mouse monoclonal antibody and NY-41 rabbit polyclonal antibody, and then with secondary FITC- and TRITC-labelled antibodies, respectively. DAPI was used for nuclei staining. D. NIH-3T3 mouse fibroblast cells were transfected with pIC113-EFGP vector or pIC113-EGFP-NY-ESO-1 vector according to the lipofectamine2000 protocol. *Left panel*: cells were fixed with paraformaldehyde and immunostained with NY-41 rabbit polyclonal antibody, and then with secondary cy5-labelled antibody. *Right panel*: Cells were lysed, and the soluble fraction analysed by SDS-PAGE and immunoblotted for NY-ESO-1 using rabbit polyclonal NY-41 antibody.

4.2.6 The MAGE homology domain of MAGE-C1 is stabilised by MG132 treatment

We proceeded our investigation by identifying the region of MAGE-C1 which is responsible for the MG132 sensitivity. For this purpose several V5/His- tagged deletion mutants of MAGE-C1 were utilised, encompassing the regions 1-138 (MAGE-$C1_{1-138}$), 600-901 (MAGE-$C1_{600-901}$), 902-1029 (MAGE-$C1_{902-1029}$) and 1030-1142 (MAGE-$C1_{1030-1142}$) (Figure 4.6A). The deletion mutants did not cover the entire length of the protein as it proved very difficult to correctly amplify the portion between amino acids 139 and 600, due to the high GC content and the high number of repeats in this region.

The constructs were transfected into the MAGE-C1-negative H1299 (Figure 5.1) and NIH 3T3 cell lines. While MAGE-$C1_{1-138}$ and MAGE-$C1_{600-901}$ were transfected with good efficiency and gave a single band in western blot, transfection of the C-terminal fragments MAGE-$C1_{902-1029}$ and MAGE-$C1_{1030-1142}$ presented low efficiency, especially for the former. Notably, both constructs had a multi-band pattern in western blot, possibly due to processing or degradation; moreover deletion mutant MAGE-$C1_{1030-1142}$ was mostly insoluble.

Interestingly, in both cell lines we observed that MG132 treatment-induced stabilisation of the two fragments covering the MAGE homology Domain (MHD), i.e. MAGE-$C1_{902-1029}$ and MAGE-$C1_{1030-1142}$. Whereas MAGE-$C1_{902-1029}$ was stabilised both in the soluble and in the insoluble fraction, MAGE-$C1_{1030-1142}$ levels increased only in the soluble fraction.

These data indicate that the low expression level of the two C-terminal deletion in untreated cells is due to high protein instability and therefore that the MHD, a domain extremely conserved in the MAGE family, is a target of proteasome-dependent processing.

MAGE-$C1_{600-901}$ was only slightly stabilised by the treatment, whereas the N-terminus fragment MAGE-$C1_{1-138}$ was not affected (Figure 4.6B).

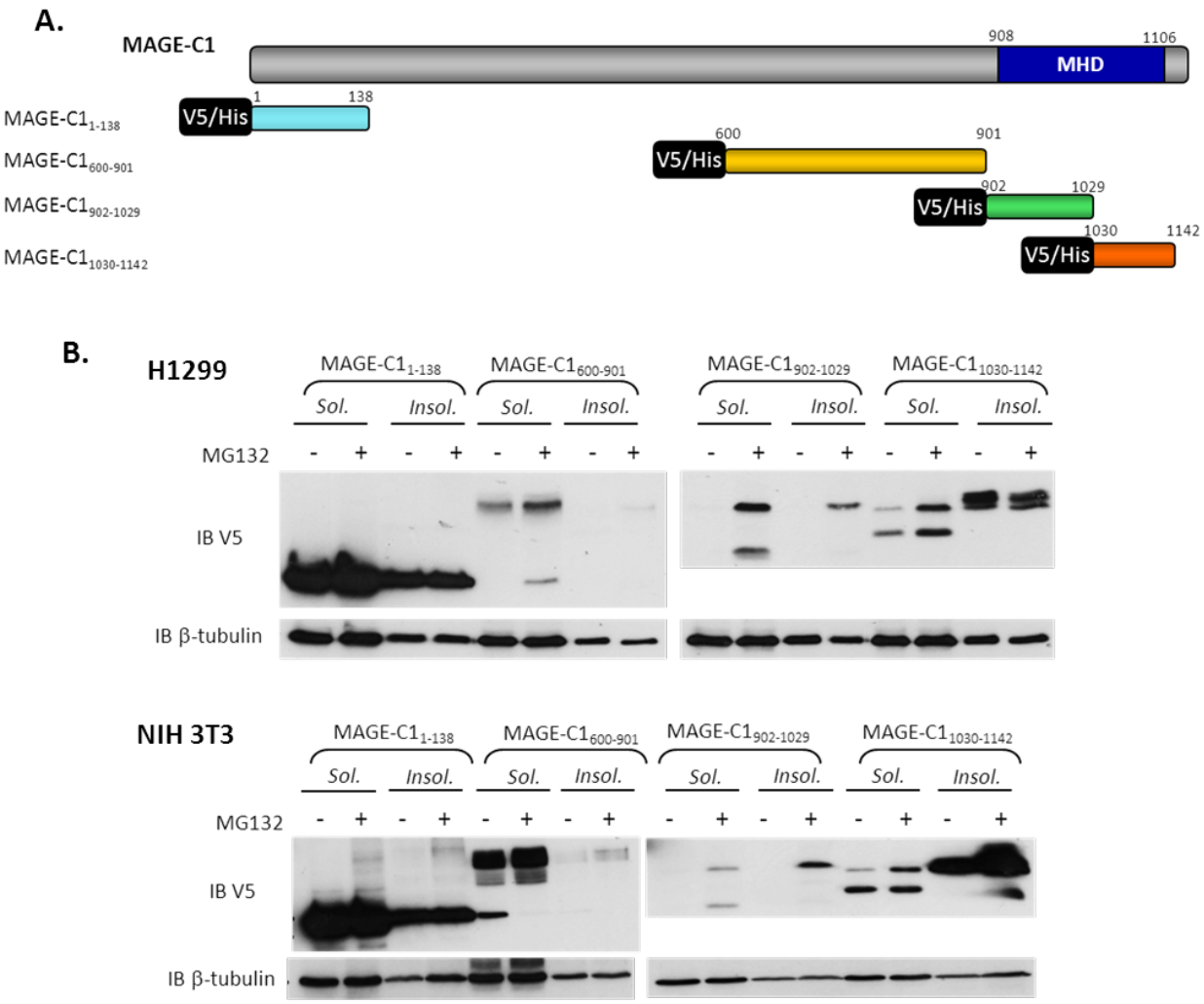

Figure 4.6 The MAGE homology domain of MAGE-C1 is stabilised by MG132 treatment. A. Schematic representation of MAGE-C1 deletion mutants MAGE-C1$_{1-138}$, MAGE-C1$_{600-901}$, MAGE-C1$_{902-1029}$ and MAGE-C1$_{1030-1142}$. All the fragments were subcloned in a pcDNA3.1/V5-His-TOPO plasmid. B. H1299 NSCLC cells and NIH 3T3 mouse fibroblasts were transfected with MAGE-C1$_{1-138}$, MAGE-C1$_{600-901}$, MAGE-C1$_{902-1029}$ and MAGE-C1$_{1030-1142}$ vectors according to the Fugene6 protocol and treated with MG132 40μM or DMSO (negative control) for 4h. After treatment cells were lysed and soluble and insoluble fractions analysed by SDS-PAGE and immunoblotted with V5 mouse monoclonal antibody or with mouse monoclonal β-tubulin antibody (as a loading control).

We also analysed the subcellular localisation of the MAGE-C1 deletion mutants via immunofluorescence (Figure 4.7). NIH 3T3 cells were transfected with the four constructs and either treated with MG132 or with DMSO as a negative control. Staining performed with the anti-V5 antibody showed that, whereas MAGE-C1$_{1-138}$ and MAGE-C1$_{600-901}$ are mostly nuclear with some cytoplasmic staining, the two fragments covering the MHD (MAGE-C1$_{902-1029}$ and MAGE-C1$_{1030-1142}$) are prevalently cytoplasmic. This agrees with the staining previously observed for

endogenous MAGE-C1, which is both cytoplasmic and nuclear, and suggests that this protein might shuttle between the two compartments in response to specific signals.

Treatment with MG132 did not significantly alter the localisation of any MAGE-C1 deletion mutant in NIH 3T3 cells.

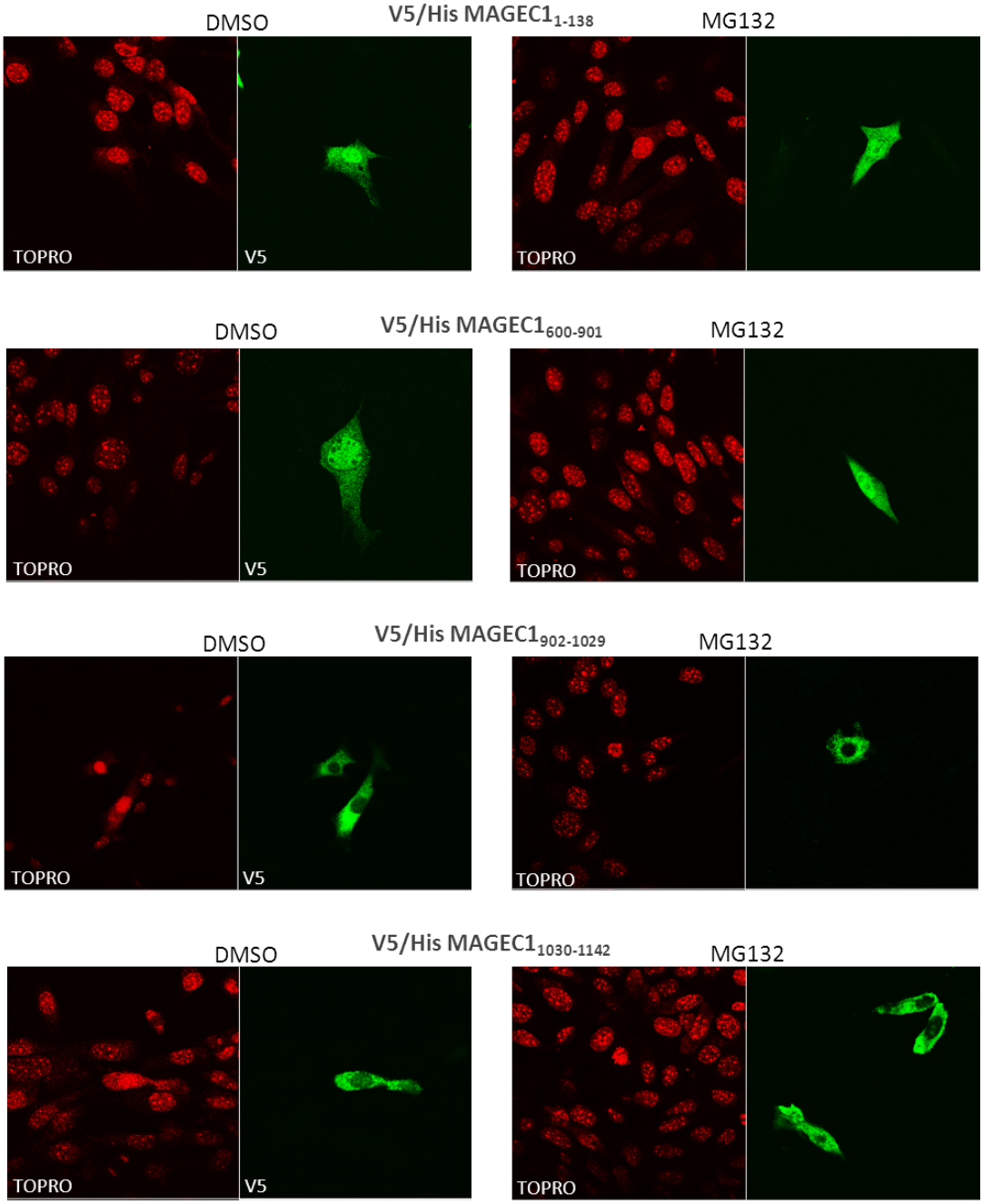

Figure 4.7 Subcellular localisation of MAGE-C1 deletion mutants. Immunofluorescence staining of exogenous MAGE-C1 deletion mutants MAGE-C1$_{1-138}$, MAGE-C1$_{600-901}$, MAGE-C1$_{902-1029}$ and MAGE-C1$_{1030-1142}$. NIH 3T3 mouse fibroblasts were transfected according to the Fugene6 protocol and treated with MG132 40µM or DMSO (negative control) for 4h. Cells were fixed with paraformaldehyde and immunostained with V5 mouse monoclonal antibody and then with secondary FITC-labelled antibody. TOPRO was used for nuclei staining.

4.2.7 NY-ESO-1 deletion mutants 91-180 and 50-150 are stabilised and localise at the centrosome upon MG132 treatment.

In order to understand which part of NY-ESO-1 is responsible for the increased levels in the insoluble fraction and the centrosomal localisation, NY-ESO-1 full-length (F.L.) and three deletion mutants were utilised, i.e. NY-ESO-$1_{1\text{-}90}$, NY-ESO-$1_{91\text{-}180}$ and NY-ESO-$1_{50\text{-}150}$, all of which were V5/His tagged (Figure 4.8A).

Similarly to what was done for MAGE-C1, these four NY-ESO-1 constructs were transfected in NIH 3T3 cells, which were then treated with MG132 for 4 hours and collected separating the soluble and insoluble fractions. Expression levels and subcellular localisation were analysed by immunoblot (Figure 4.8B) and immunofluorescence (Figure 4.9).

The western blot showed that NY-ESO-$1_{F.L.}$, NY-ESO-$1_{91\text{-}180}$ and NY-ESO-$1_{50\text{-}150}$ are stabilised after MG132 treatment, both in the soluble and in the insoluble fraction, while NY-ESO-$1_{1\text{-}90}$ was only slightly affected. The stabilisation of NY-ESO-$1_{F.L.}$ after treatment is consistent with the endogenous data shown before (Figure 4.2).

NY-ESO-$1_{91\text{-}180}$ expression was particularly low, again suggesting protein instability seen the increase upon MG132 treatment. Furthermore a shift in the migration of NY-ESO-$1_{91\text{-}180}$ and NY-ESO-$1_{50\text{-}150}$ could be noticed in the insoluble fraction upon treatment, possibly due to post-translational modification such as ubiquitination, followed by aggregation.

As a whole, the portion of NY-ESO-1 included between amino acid 91 and amino acid 150 appears to be crucial for stabilisation.

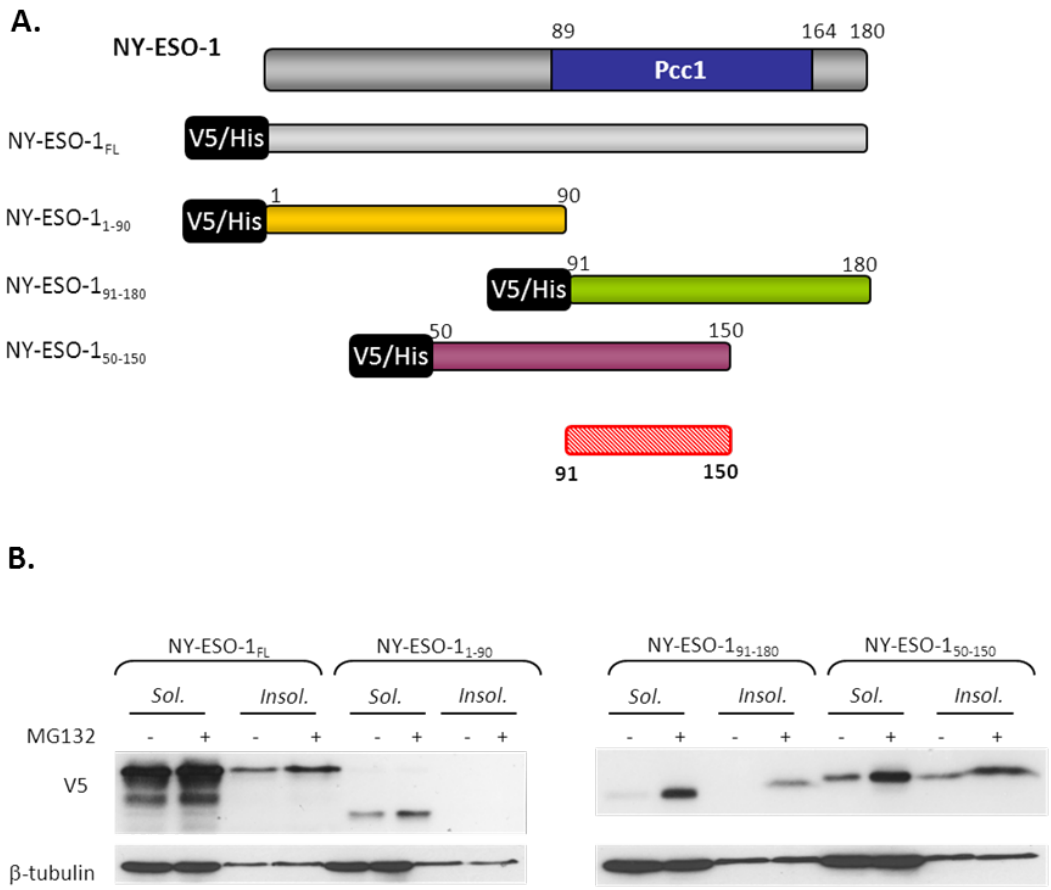

Figure 4.8 NY-ESO-1 deletion mutants 91-180 and 50-150 are stabilised after MG132 treatment. A. Schematic representation of NY-ESO-1full length construct and deletion mutants NY-ESO-$1_{1\text{-}90}$, NY-ESO-$1_{91\text{-}180}$ and NY-ESO-$1_{50\text{-}150}$. All the fragments were subcloned in a pcDNA3.1/V5-His-TOPO plasmid. The region of sensitivity to MG132 treatment (aa 91-150) is labelled in red. B. NIH 3T3 mouse fibroblasts were transfected with NY-ESO-$1_{F.L.}$, NY-ESO-$1_{1\text{-}90}$, NY-ESO-$1_{91\text{-}180}$ and NY-ESO-$1_{50\text{-}150}$ vectors according to the Fugene6 protocol and treated with MG132 40μM or DMSO (negative control) for 4h. After treatment cells were lysed and soluble and insoluble fractions analysed by SDS-PAGE and immunoblotted with V5 mouse monoclonal antibody or with mouse monoclonal β-tubulin antibody (as a loading control).

Immunofluorescence was also carried out in NIH 3T3 cells transfected with the constructs and either treated with MG132 or with DMSO as a negative control. Staining performed with the anti-V5 antibody showed that whereas NY-ESO-$1_{91\text{-}180}$ and NY-ESO-$1_{50\text{-}150}$ show both cytoplasmic and nuclear staining, NY-ESO-$1_{1\text{-}90}$ is more markedly nuclear. Treatment with MG132 did not affect the localisation of any NY-ESO-1 deletion mutant (Figure 4.9).

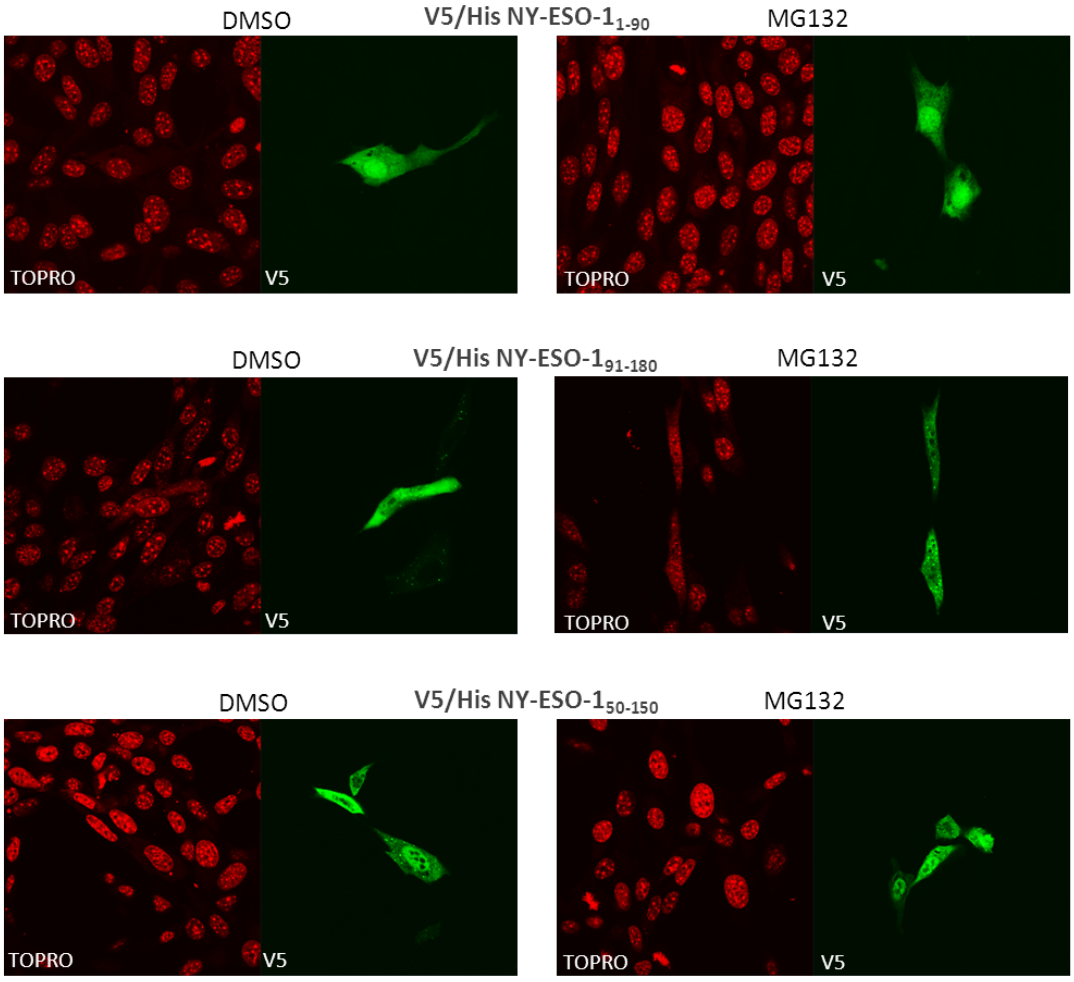

Figure 4.9 Subcellular localisation of NY-ESO-1 deletion mutants in NIH3T3 cells. Immunofluorescence staining of exogenous NY-ESO-1 deletion mutants NY-ESO-1$_{1-90}$, NY-ESO-1$_{91-180}$ and NY-ESO-1$_{50-150}$. NIH 3T3 mouse fibroblasts were transfected according to the Fugene6 protocol and treated with MG132 40µM or DMSO (negative control) for 4h. Cells were fixed with paraformaldehyde and immunostained with V5 mouse monoclonal antibody and then with secondary FITC-labelled antibody. TOPRO was used for nuclei staining.

Similar immunofluorescence experiments were also carried out in SK-MEL-37 cells. In this cell line NY-ESO-1$_{1-90}$ presented an almost exclusively nuclear staining, whereas NY-ESO-1$_{91-180}$ and NY-ESO-1$_{50-150}$ also showed some cytoplasmic localisation. NY-ESO-1$_{91-180}$ was difficult to detect in untreated cells, again probably due to high instability of the protein as it was more promptly found in MG132 treated cells. While NY-ESO-1$_{1-90}$ localisation did not change upon MG132 treatment, for NY-ESO-1$_{91-180}$ and NY-ESO-1$_{50-150}$ accumulation at the centrosome could

be observed and was confirmed by co-immunostaining with the centrosomal marker pericentrin (Figure 4.10). These two constructs are the same that are stabilised upon MG132 therefore these results link once again NY-ESO-1 stabilisation with its centrosomal localisation at least in SK-MEL-37.

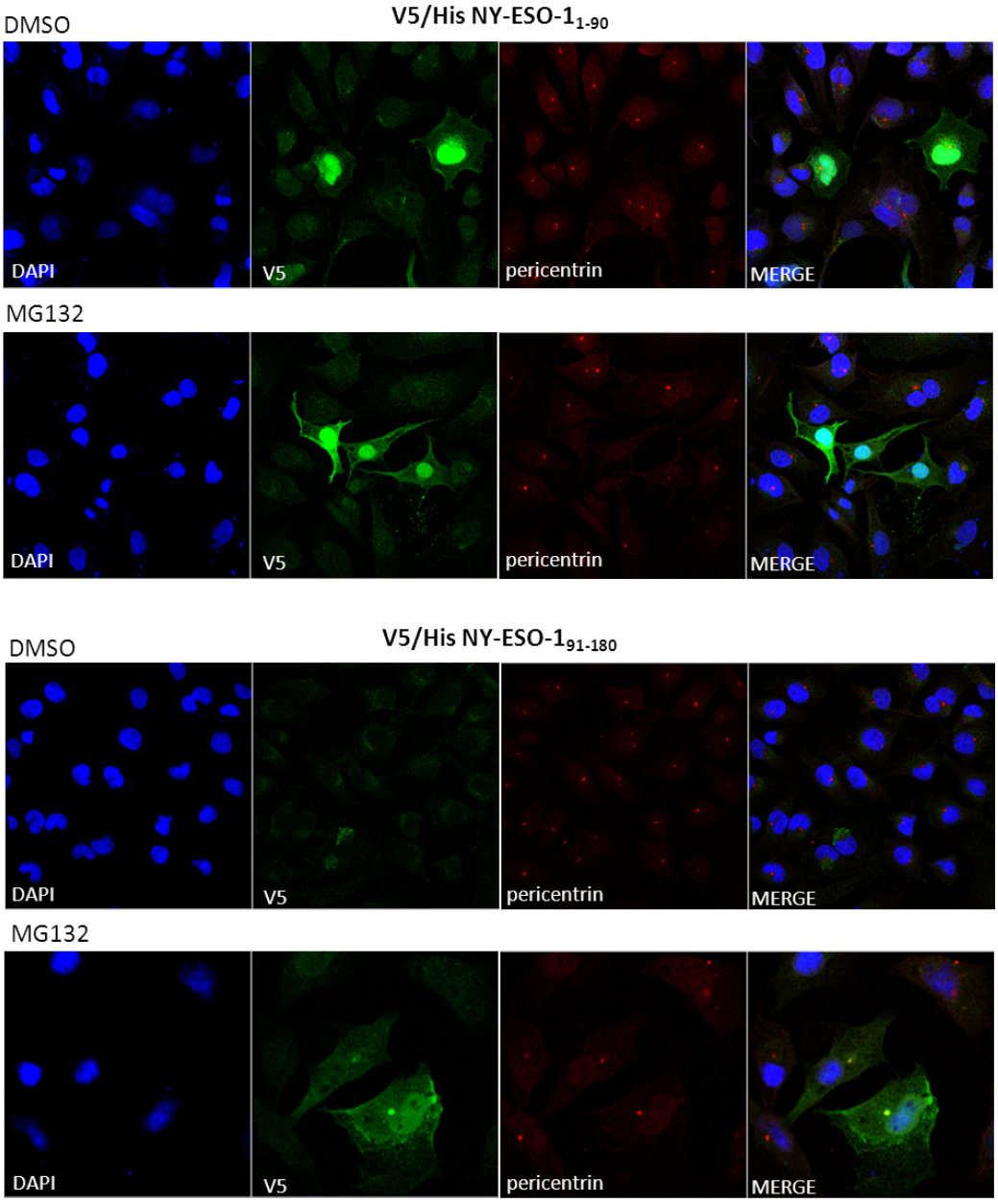

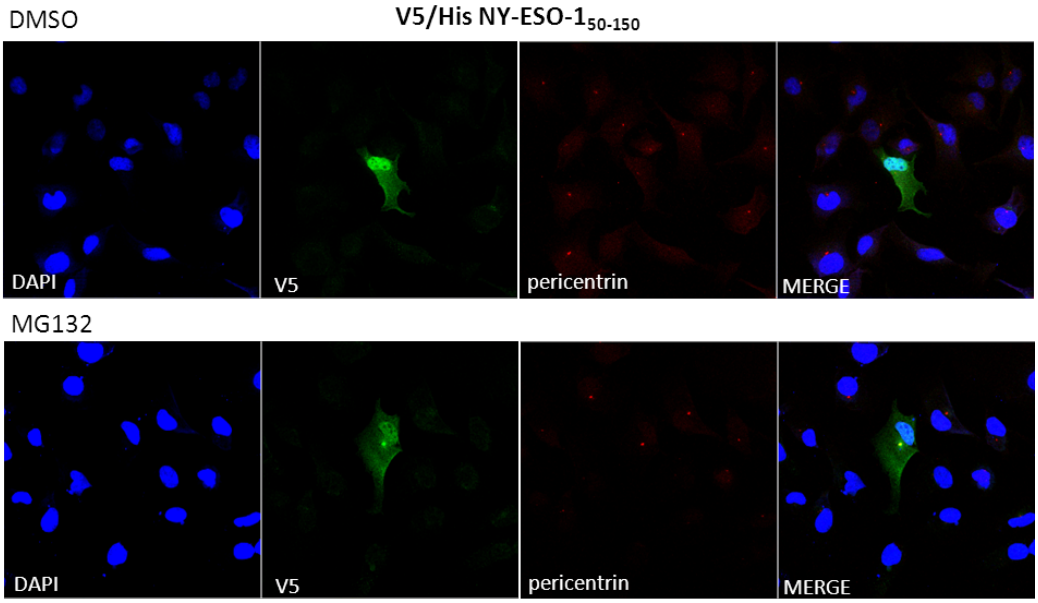

Figure 4.10 Subcellular localisation of NY-ESO-1 deletion mutants in SK-MEL-37 cells. Immunofluorescence staining of exogenous NY-ESO-1 deletion mutants NY-ESO-1$_{1-90}$, NY-ESO-1$_{91-180}$ and NY-ESO-1$_{50-150}$. SK-MEL-37 melanoma cells were transfected according to the Fugene6 protocol and treated with MG132 40µM or DMSO (negative control) for 4h. Cells were fixed with paraformaldehyde and double stained with V5 mouse monoclonal and pericentrin rabbit polyclonal antibodies, and then with secondary FITC- and TRITC-labelled antibodies, respectively. DAPI was used for nuclei staining.

4.2.8 Lysine 124 is not essential for NY-ESO-1 localisation at the centrosome.

We identified the region between amino acids 91 and 150 of NY-ESO-1 to be essential for centrosomal localisation upon MG132 treatment in SK-MEL-37 (Figure 4.10). This portion of the CT antigen includes the only lysine present in the protein, K124 (Figure 4.11A). Lysines can be modified by several post-translational modifications, including ubiquitination. We decided to mutate this residue to an alanine (A), a residue that is not post-translationally modified.

Site-directed mutagenesis performed on a wild-type EGFP-NY-ESO-1 produced the EGFP-NY-ESO-1 K124A mutant construct, which was transfected in NIH 3T3 cells.

Immunofluorescence staining showed that EGFP-NY-ESO-1 K124A could still localise at the centrosome of NIH 3T3 despite the amino acid mutation (Figure 4.11B), meaning that either this residue is not involved in the centrosome accumulation of NY-ESO-1 or that it has to be un-modified for it to take place.

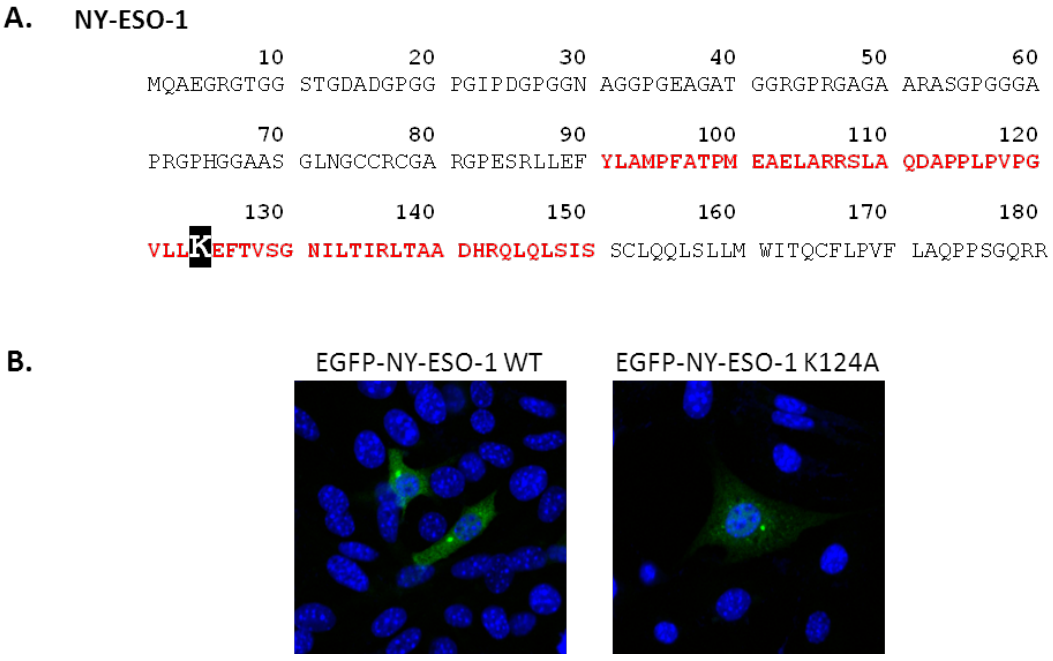

Figure 4.11 Lysine 124 is not essential for NY-ESO-1 localisation at the centrosome. A. NY-ESO-1 protein sequence. The region of sensitivity to MG132 treatment (aa 91-150) is labelled in red and K124 is labelled in black. B. NIH-3T3 mouse fibroblast cells were transfected with pIC113-EGFP-NY-ESO-1 or pIC113-EGFP-NY-ESO-1 K124A vectors according to the lipofectamine2000 protocol and then fixed with paraformaldehyde. DAPI was used for nuclei staining.

4.2.9 NY-ESO-1 enhances the stabilisation of MAGE-C1 MHD upon MG132 treatment.

In order to investigate whether MG132 treatment could influence not only the localisation of these proteins, but also their binding, immunoprecipitation experiments were performed on SK-MEL-37 cells. Cells were treated with 40 μM MG132 for 4 h, and endogenous MAGE-C1 or NY-ESO-1 were subsequently immunoprecipitated (Figure 4.12A). Immunoprecipitation was carried out on the soluble fraction, as the buffer utilised for the insoluble fraction extraction disrupts interactions. An increase in the amount of the co-immunoprecipitated protein (NY-ESO-1 and MAGE-C1, respectively) could be observed upon treatment in both experiments. It is important to point out that the amount of protein in the input does not change after treatment; therefore this observation cannot be attributed to an increase in the protein levels of MAGE-C1 and NY-ESO-1. This suggests that inhibition of the proteasome positively influences the binding between these two proteins.

The biological function of the MAGE-C1/NY-ESO-1 complex has not been investigated. Since the binding between these proteins is strengthened by MG132 treatment, we asked whether their interaction could influence their stability.

To address this point, each previously described MAGE-C1 deletion mutant (Figure 4.6A) was co-transfected with an EGFP-tagged NY-ESO-1 plasmid in NIH 3T3 cells. Transfection of empty pcDNA3.1, the plasmid in which these deletion mutants were inserted upon their cloning, was used as a negative control. The cells were treated with MG132 and the soluble and insoluble cell fractions were collected.

Immunoblot showed that only the two C-terminal MAGE-C1 constructs were affected by the co-transfection with EGFP-NY-ESO-1, and in particular MAGE-$C1_{902\text{-}1029}$ was stabilised in the absence of the treatment, both in the soluble and in the insoluble fractions, whereas MAGE-$C1_{1030\text{-}1142}$ stability decreased in both fractions (Figure 4.12B).

In summary, NY-ESO-1 is able to influence the stability of the two deletion mutants mapping to the MHD. This is particularly interesting as the MHD is the region of binding between the two proteins (Cho et al. 2006).

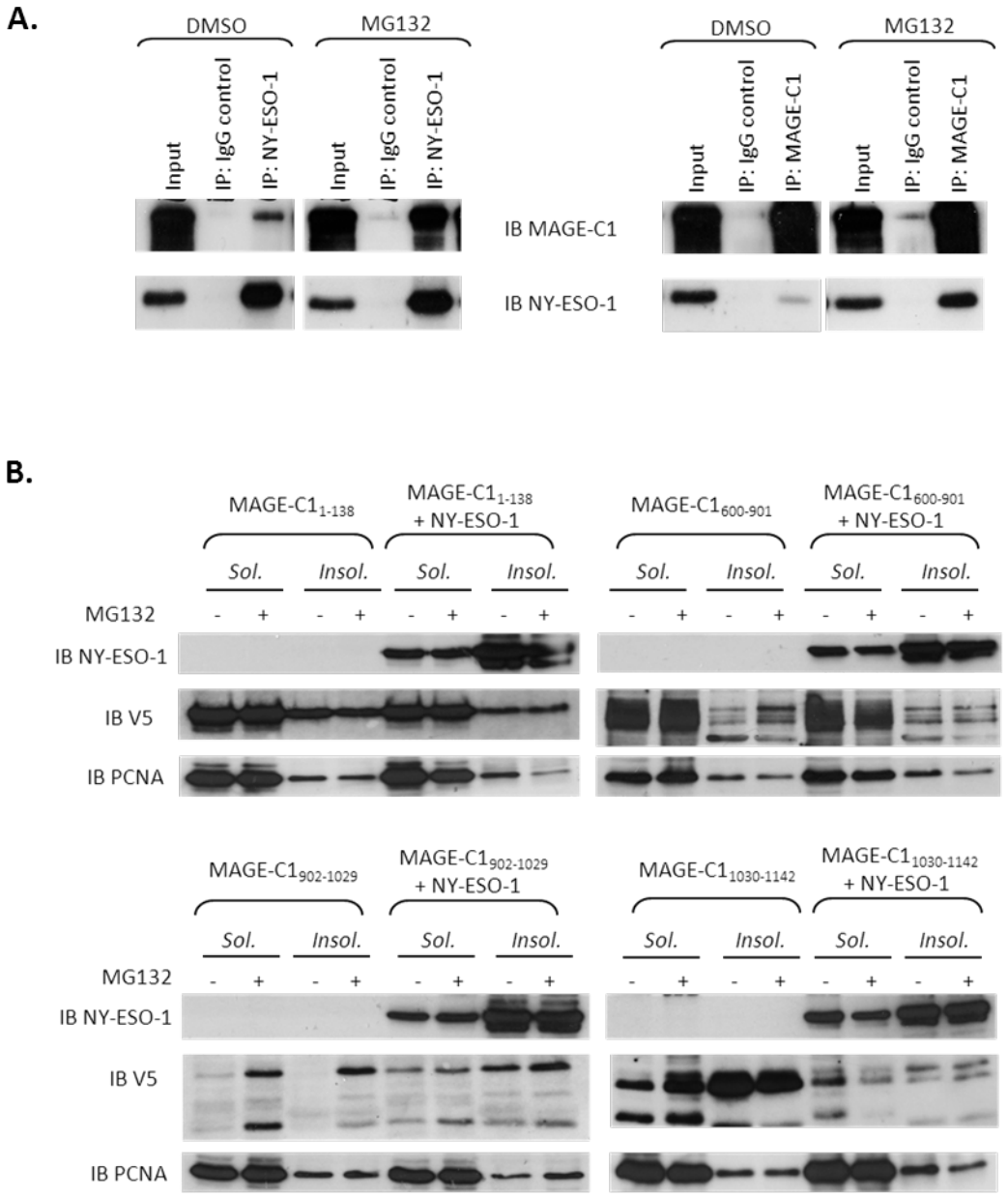

Figure 4.12 NY-ESO-1 modulates the stability of MAGE-C1 C-terminus. A. *Left panel*: NY-ESO-1 was immunoprecipitated with NY-41 rabbit polyclonal antibody in cell lysate from the SK-MEL-37 melanoma cell line after treatment with 40 µM MG132 or DMSO (negative control) for 4h. The protein complexes were then analysed by SDS-PAGE and immunoblotted for MAGE-C1 (CT7.33 antibody) or NY-ESO-1 (NY-41 antibody). *Right panel:* MAGE-C1 was immunoprecipitated with CT7.33 mouse monoclonal antibody in cell lysate from SK-MEL-37 melanoma cell line after treatment with 40 µM MG132 or DMSO (negative control) for 4h. The protein complexes were then analysed by SDS-PAGE and immunoblotted for MAGE-C1 (CT7.33 antibody) or NY-ESO-1 (NY-41 antibody). B. NIH 3T3 mouse fibroblasts were co-transfected with MAGE-C1$_{1\text{-}138}$, MAGE-C1$_{600\text{-}901}$, MAGE-C1$_{902\text{-}1029}$ or MAGE-C1$_{1030\text{-}1142}$ vectors and pIC113-EGFP-NY-ESO-1 according to the Fugene6 protocol and treated with MG132 40µM or DMSO (negative control) for 4h. After treatment cells were lysed and soluble and insoluble fractions analysed by SDS-PAGE and immunoblotted with V5 mouse monoclonal antibody, with E978 mouse monoclonal against NY-ESO-1 or with PCNA mouse monoclonal antibody (as a loading control).

The fact that NY-ESO-1 exerted opposite effects on MAGE-C1$_{902\text{-}1029}$ and MAGE-C1$_{1030\text{-}1142}$ appeared controversial and is possibly attributable to the fact that the MAGE domain was split into two halves. This issue prompted us to obtain a V5/His construct covering the whole MAGE domain, MAGE-C1$_{MHD}$ (Figure 4.13A).

First, we tested whether this deletion mutant was also stabilised by MG132 by transfecting H1299 cells and analysing them by western blot after treatment. Like MAGE-C1$_{902\text{-}1029}$ and MAGE-C1$_{1030\text{-}1142}$, MAGE-C1$_{MHD}$ levels increased upon proteasome inhibition in both cellular subfractions; moreover, it showed a multiband pattern as observed with the other two C-terminal constructs (Figure 4.13B). These results indicated that the MHD of MAGE-C1 is processed by the proteasome pathway.

Immunofluorescence staining of transfected H1299 showed that MAGE-C1$_{MHD}$ is mostly cytoplasmic, with some nuclear staining, and that MG132 treatment does not affect its subcellular localisation (Figure 4.13B).

Finally, we co-transfected MAGE-C1$_{MHD}$ and EGFP-NY-ESO-1 plasmids in H1299 cells as above with the other deletion mutants, in order to assess the effect of NY-ESO-1 on the MHD. Western blot showed that upon co-transfection with NY-ESO-1 and MG132 treatment, MAGE-C1$_{MHD}$ stabilisation in the insoluble fraction was more marked (Figure 4.13C).

These data indicate that NY-ESO-1 favours the accumulation of stabilised MHD in the insoluble fraction, possibly corresponding to aggregated protein.

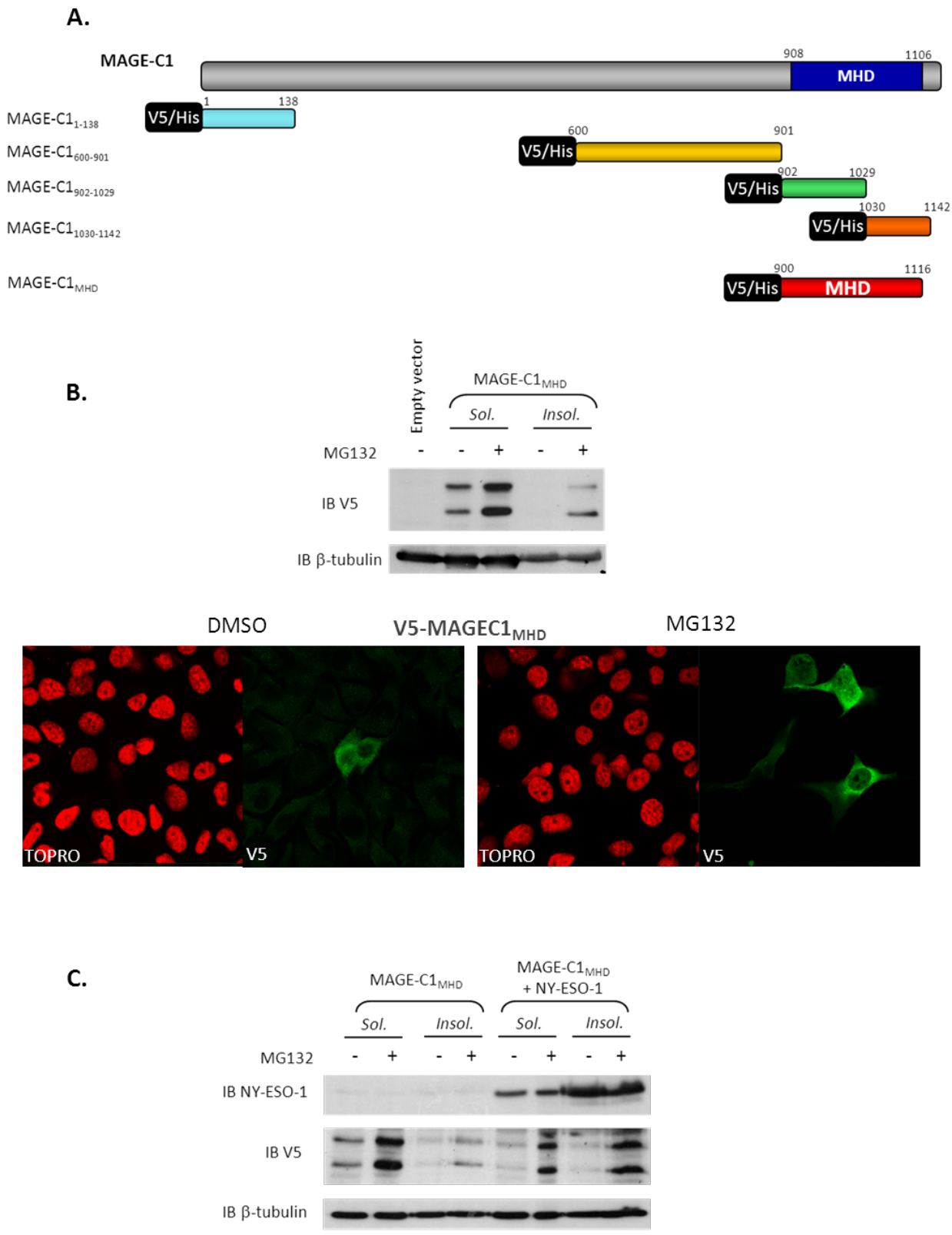
A.
MAGE-C1
908
1106
MHD
1
138
MAGE-C1 1-138
V5/His
600
901
MAGE-C1 600-901
V5/His
902
1029
MAGE-C1 902-1029
V5/His
1030
1142
MAGE-C1 1030-1142
V5/His
900
1116
MAGE-C1 MHD
V5/His
MHD
B.
Empty vector
MAGE-C1 MHD
Sol.
Insol.
MG132
- - + - +
IB V5
IB β-tubulin
DMSO
V5-MAGEC1 MHD
MG132
TOPRO
V5
TOPRO
V5
C.
MAGE-C1 MHD
MAGE-C1 MHD + NY-ESO-1
Sol.
Insol.
Sol.
Insol.
MG132
- + - + - + - +
IB NY-ESO-1
IB V5
IB β-tubulin

Figure 4.13 NY-ESO-1 enhances the stabilisation of MAGE-C1 MHD upon MG132 treatment. A. Schematic representation of MAGE-C1 deletion mutant MAGE-$C1_{1\text{-}138,}$ MAGE-$C1_{600\text{-}901}$, MAGE-$C1_{902\text{-}1029}$, MAGE-$C1_{1030\text{-}1142}$ and MAGE-$C1_{MHD}$. All the fragments were subcloned in a pcDNA3.1/V5-His-TOPO plasmid. B. H1299 NSCLC cells were transfected with MAGE-$C1_{MHD}$ vector or empty pcDNA3.1 vector according to the Fugene6 protocol and treated with MG132 40μM or DMSO (negative control) for 4h. *Top panel*: after treatment cells were lysed and soluble and insoluble fractions analysed by SDS-PAGE and immunoblotted with V5 mouse monoclonal antibody or with mouse monoclonal β-tubulin antibody (as a loading control). *Lower panel*: cells were fixed with paraformaldehyde and immunostained with V5 mouse monoclonal antibody and then with secondary FITC-labelled antibody. TOPRO was used for nuclei staining. C. H1299 NSCLC cells were co-transfected with MAGE-$C1_{MHD}$ vector and pIC113-EGFP-NY-ESO-1 according to the Fugene6 protocol and treated with MG132 40μM or DMSO (negative control) for 4h. After treatment cells were lysed and soluble and insoluble fractions analysed by SDS-PAGE and immunoblotted with V5 mouse monoclonal antibody, with E978 mouse monoclonal against NY-ESO-1 and with mouse monoclonal β-tubulin antibody.

4.2.10 MAGE-C1 is SUMOylated.

So far, we have shown that MAGE-C1 is sensitive to proteasome inhibitors, indicating that it is a target of the proteasome system, and that the MHD is responsible for such effect. Moreover, a shift was detected in the gel migration pattern of endogenous and transfected full length MAGE-C1 upon MG132 treatment, which could be due to post-translational modifications (Figure 4.14A).

Given the extent of such shift, we were able to exclude modifications involving addition of small chemical groups, such as phosphorylation and acetylation. Since proteasome-dependent degradation is strictly linked with protein ubiquitination, we tested whether MAGE-C1 was ubiquitinated.

U2OS cells were treated with DMSO, MG132 or with the drug tunicamycin as a further negative control; the lysates were collected and then incubated with the USP2 purified enzyme (ubiquitin-specific peptidase 2), a protease that de-ubiquitinate a wide range of targets including Mdm2 and cyclin D1 (Shan et al., 2009; Stevenson et al., 2007b). Enzymatic treatment did not cause any reduction in MAGE-C1 shift upon MG132 treatment as shown by western blot analysis, meaning that the protein cannot be de-ubiquitinated by USP2 and therefore, given the vast amount of targets of this enzyme, it is unlikely to be ubiquitinated upon MG132 treatment.

To also rule out a post-translational glycosylation of MAGE-C1 following proteasome inhibition, U2OS cells were incubated with PNGase F, one of the most widely used enzymes for the removal from glycoproteins of N-linked glycans, which are extremely important for proper protein folding in eukaryotic cells. Again, no alteration of the MG132-induced MAGE-C1 shift was observed, which indicated that MAGE-C1 is not N-glycosilated either.

Western blot against ubiquitin and MHC Class I (normally glycosylated) were used as positive controls for USP2 and PNGase F efficiency respectively (Figure 4.14B).

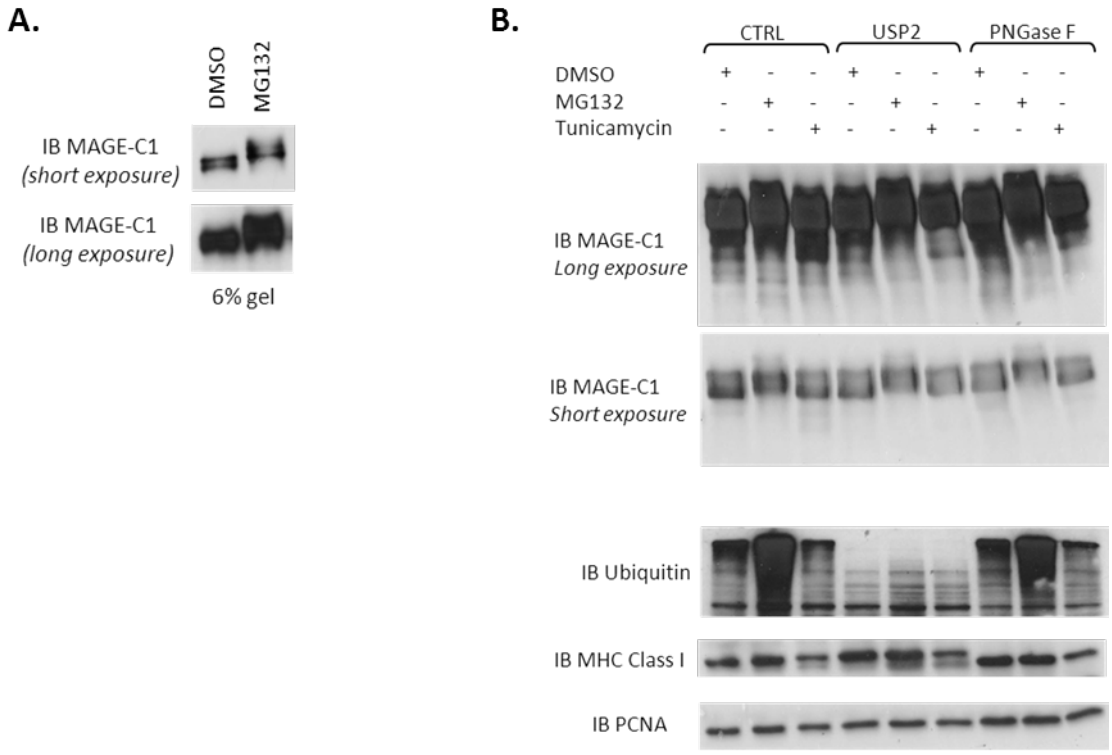

Figure 4.14 MAGE-C1 is not ubiquitinated or glycosylated upon MG132 treatment. A. Western blot analysis of endogenous MAGE-C1 in U2OS cells treated with MG132 40µM or DMSO (negative control) for 4h. After the treatment, cells were lysed with urea buffer, analysed by SDS-PAGE (6%gel), and immunoblotted for MAGE-C1 using mouse monoclonal CT7.33 antibody. B. U2OS cells were treated with MG132 40µM for 4h, tunicamycin 10µg/ml for 24h or DMSO (negative control). After the treatment, cells were lysed with RIPA buffer and incubated with USP2 or PNGase F purified enzymes according to the manufacturer protocol. Cell lysates were then analysed by SDS-PAGE, and immunoblotted for MAGE-C1 using mouse monoclonal CT7.33 antibody in a 6% gel, or with mouse monoclonal anti-ubiquitin, mouse monoclonal HC-10 anti-MHC Class I and PCNA mouse monoclonal antibody (as a loading control) in a 12%gel.

Having excluded ubiquitination and glycosylation, we tested whether MAGE-C1 was SUMOylated upon treatment with proteasome inhibitors. U2OS cells were treated with MG132 and MAGE-C1 was immunoprecipitated. Immunoblot analysis was then performed, probing for MAGE-C1 to control the efficiency of the immunoprecipitation.

Interestingly, western blot analysis showed that MAGE-C1 is conjugated with SUMO-1 (Figure 4.15A). SUMOylation of MAGE-C1 though occurred in the untreated sample as well; therefore, the protein shift observed after MG132 treatment cannot be attributed to this modification.

Intriguingly, unpublished data from collaborators show that the nuclear pool of MAGE-C1 presents an upper band which is not present in the cytoplasmic fraction (Figure 4.15B). As SUMOylation is known to be important for protein localisation, we can hypothesis that the pool of MAGE-C1 residing in the nucleus is SUMO-1- modified.

We utilised two different programs to predict SUMOylation sites on MAGE-C1; the first program, SUMOsp 2.0 (Ren et al., 2009), predicted a site at K931 whereas the second program, SUMOplot™ (http://www.abgent.com/sumoplot/), predicted a site at K926 (Figure 4.15C). Both sites are part of high probability motifs and map in MAGE-C1 MHD.

Interestingly, a multiple alignment of several members of the MAGE family revealed that K926 is significantly conserved in the MAGE proteins, with the exception of the MAGE-A subfamily. Furthermore, K931 is highly conserved in the type I MAGE subfamily, which includes the CT-X MAGE-A, MAGE-B and MAGE-C families (Figure 4.15D). Hence we can hypothesise that other MAGE protein could be regulated at the post-translational level by SUMO-modification on their MAGE homology domain.

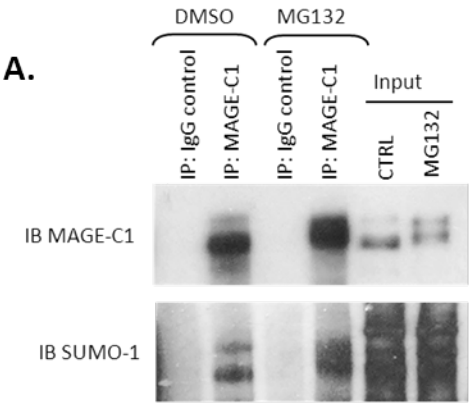

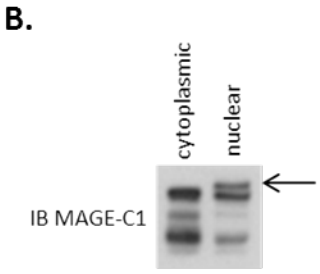

C.

SUMOsp 2.0

File Tools Help

Predicted Sites

Position	Peptide	Score	Cutoff	Type
931	PITKAEM	3.544	3.33	TypeII: Non-consensus

SUMOplot™ Analysis Program

No.	Pos.	Group	Score
1	K926	LLKYQ VKQP ITKAE	0.82

Motifs with high probability
Motifs with low probability
Overlapping Motifs

D.

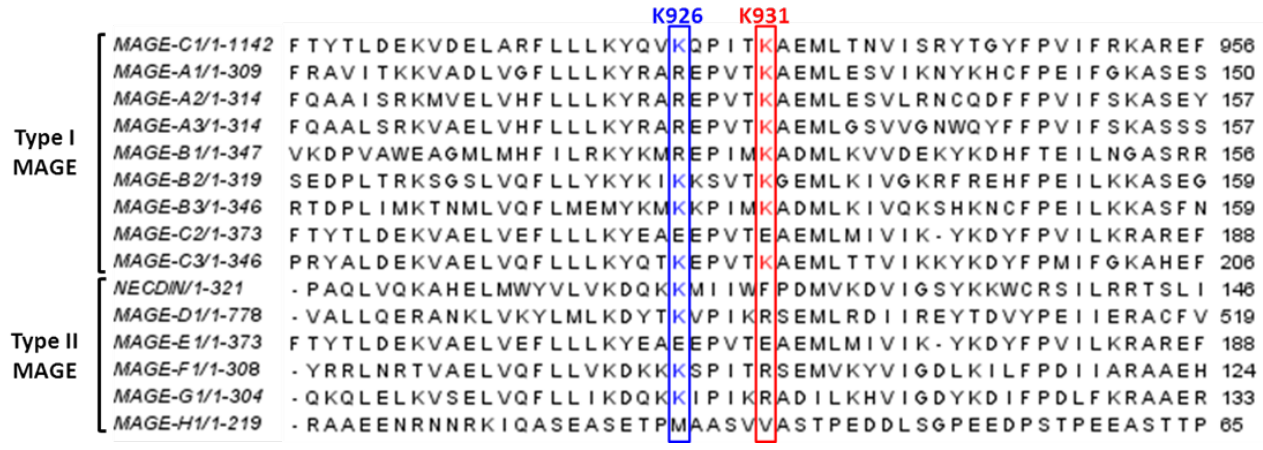

Figure 4.15 MAGE-C1 is SUMO-1-conjugated. A. MAGE-C1 was immunoprecipitated with CT7.33 mouse monoclonal antibody in cell lysate from U2OS cell line after treatment with 40 μM MG132 or DMSO (negative control) for 4h. The protein complexes were then analysed by SDS-PAGE and immunoblotted for MAGE-C1 (CT7.33 antibody) or SUMO-1. B. *From Dr. Otavia Caballero.* Western blot analysis of endogenous MAGE-C1 (CT7.33 antibody) in SK-MEL-37 cells following separation of the nuclear and cytoplasmic fractions according to the manufacturer's protocol. C. Prediction of putative SUMOylation sites on MAGE-C1 protein utilising SUMOsp 2.0 (top) or SUMOplot™ (bottom). D. Multiple alignment of part of the MHD of several MAGE family members obtained utilising ClustalW. Type I and type II MAGE are indicated.

4.3 Summary and discussion

In this chapter the role of the proteasome degradation system in the regulation of CT antigens was analysed.

We started out by examining the effect of proteasome inhibitors on endogenous MAGE-C1, MAGE-C2 and NY-ESO-1 proteins in several cancer cell lines. Interestingly, all three proteins were stabilised in the insoluble fraction of the cell lysate, and for MAGE-C1 a shift in the protein migration was observed, suggesting post-translational modification; furthermore, MAGE-C1 and NY-ESO-1 accumulated at the centrosome upon treatment.

The centrosome is an organelle that serves as the main microtubule organising center (MTOC), as well as a regulator of cell-cycle progression. It is also important for asymmetric cell division in stem cells, and aberrant numbers of centrosomes in cells have been associated with cancer (Badano et al., 2005).

A further crucial role of the centrosome is the organisation and subcellular localisation of proteasomes. It has been shown that multiple members of the ubiquitin-proteasome degradation pathway localise at the centrosome and that these proteasomal complexes are active in this site (Anton et al., 1999; Fabunmi et al., 2000; Wigley et al., 1999).

The formation of pericentriolar protein aggregates had already been observed for heat shock protein 70 (Hsp70) in mammalian cells stressed by heat shock or viral infection. Furthermore, insoluble juxtanuclear inclusions reacting with antibodies against proteasomes and ubiquitin were detected in HeLa and other cells after treatment with a potent proteasome inhibitor, PSI. These structures, named aggresomes, were often found close to a centrosome and their formation was blocked by disruption of microtubules (Johnston et al., 1998; Wojcik, 1997a, b).

We can therefore hypothesise that MAGE-C1 and NY-ESO-1 form insoluble aggregates in the proximity of the centrosome when their subcellular levels increase, i.e. after proteasome inhibition or transfection. Such aggregates are likely to be destined for proteasome degradation or processing at the centrosome. Another possibility is that these CT antigens have an actual function

at the centrosome, as it has been shown for example for Parkin, an E3 ligase that accumulates at the centrosome together with one of its substrates upon treatment with the proteasome inhibitor lactacystin (Zhao et al., 2003). Several MAGE proteins are able to bind E3 ligases, including MAGE-C2 protein, which is highly homologous to MAGE-C1. The latter could therefore also be a co-factor of E3 enzymes (Doyle et al., 2010). Furthermore, recent findings showed that proteasome inhibition also impinges on the turnover of centrosomal proteins, affecting microtubule nucleation and organisation (Didier et al., 2008; Ehrhardt and Sluder, 2005). MAGE-C1 and NY-ESO-1 could be involved in such process as well. To this end it is worth reporting that in multiple myeloma, a tumour type that often express MAGE-C1 and NY-ESO-1, centrosome amplification occurs in about a third of cases and is associated with overexpression of CT genes of the MAGE family (Chng and Fonseca, 2009).

As MAGE-C1 and NY-ESO-1 form a complex, we checked whether their centrosomal location was dependent on their co-expression. In cancer cell lines presenting one or the other CT gene, the expressed protein could still accumulate at the centrosome upon MG132 treatment, despite the absence of the binding partner. Similarly, in SK-MEL-37 cells, which co-express the two, depletion of one or the other antigen by RNAi did not impair the ability of its interactor to accumulate at the centrosome upon MG132 treatment. Therefore MAGE-C1 and NY-ESO-1 are independently capable of localising at the centrosome.

Then we mapped on MAGE-C1 and NY-ESO-1 the regions of sensitivity to proteasome inhibition taking advantage of some deletion mutants. Interestingly, MAGE-C1 MAGE homology domain (MHD) was stabilised by MG132 treatment. This domain is conserved within the family and it does not present any region of similarity with known domains. Its function has not been characterised, although for some MAGEs it is a site for protein-protein interaction. This is the case of MAGE-C1, which binds to NY-ESO-1 through the MHD (Cho et al., 2006). These results are particularly interesting considering that two MAGE-C1 epitopes have been identified to date that are presented by MHC-I molecules on multiple myeloma cells and are able to induce a $CD8^+$

T-cell response, and both of these peptide are part of the MHD (amino acids 959-968 and 1083-1091) (Anderson et al., 2011).

NY-ESO-1 region of sensitivity to MG132 treatment is included between amino acids 91-150. Accordingly, only the deletion mutants including this portion of the protein localised at the centrosome upon MG132 treatment in SK-MEL-37 cells.

Similarly to what was observed for MAGE-C1, this region of NY-ESO-1 is part of a 'hot spot', identified roughly between amino acids 80-110, which is important for the cellular immune response against NY-ESO-1 in cancer (Gnjatic et al., 2006; Nicholaou et al., 2006). Moreover it contains the only lysine residue of NY-ESO-1 (K124), an amino acid that can be conjugated with ubiquitin in proteins that are target of the proteasome degradation pathway. Therefore we tested whether mutation of this residue could affect NY-ESO-1 accumulation at the centrosome, but no effect of such substitution was observed.

Since MAGE-C1 and NY-ESO-1 binding is increased upon by MG132 treatment, we asked whether the biological function of this complex, so far unknown, could be linked to proteasome degradation. Intriguingly, co-transfection of a full length NY-ESO-1 plasmid with the different MAGE-C1 deletion mutants revealed that co-expression with NY-ESO-1 impinges on MAGE-C1 C-terminus stabilisation by MG132. Specifically, NY-ESO-1 increased the rate of accumulation of the MHD in the insoluble fraction, suggesting enhanced stabilisation of this domain and formation of protein aggregates.

In the last part of the chapter we investigated the shift observed for MAGE-C1 upon MG132 treatment. To clarify whether this modification could be ubiquitination, cells expressing MAGE-C1 were incubated with a de-ubiquitinating enzyme (USP2). This did not change the migration pattern of MAGE-C1, suggesting that this protein is not ubiquitinated. Alternatively, it is possible that MAGE-C1 cannot be de-ubiquitinated by USP2, although this enzyme has an extremely wide number and variety of targets.

Utilising a glycosidase (PNGase F) we also ruled out the possibility that such shift was due to glycosylation. Instead, immunoprecipitation experiments of endogenous MAGE-C1 in cells treated with MG132 revealed that MAGE-C1 is SUMO-1-conjugated.

Although this modification does not account for the MG132-dependent change in MAGE-C1 migration pattern, as SUMOylation could be detected also in untreated condition, it represents a novel feature of MAGE-C1 that could also be shared by the other MAGE protein, since the two putative SUMOylation sites identified by SUMO prediction programs both reside in the MHD and are conserved.

To summarise, we demonstrated that MAGE-C1 and NY-ESO-1 represent targets of proteasome degradation, and that NY-ESO-1 is able to stabilise the insoluble MAGE-C1 MAGE homology domain. This is the first report of a functional role of the MAGE-C1/NY-ESO-1 interaction. Furthermore, we were able to show that MAGE-C1 protein is also post-translationally modified by SUMOylation.

Chapter V: MAGE-C1 inhibits apoptosis and affects Mcl-1 stability in response to endoplasmic reticulum stress

5.1 Introduction

MAGE-C1 and NY-ESO-1 are often co-expressed in cancer cell lines, as outlined in Chapter III, and in tumour samples, such as multiple myeloma and non-small cell lung cancer samples (Andrade et al., 2008; Cho et al., 2006).

While NY-ESO-1 biological function is totally unknown, few pieces of data indicate that MAGE-C1 plays a role in multiple myeloma: immunohistochemistry analysis on tumour samples revealed that a cytoplasmic localisation of MAGE-C1 is associated with a better prognosis than in myelomas with combined nuclear-cytoplasmic or nuclear expression only (Tinguely et al., 2008). This suggests that MAGE-C1 subcellular localisation could be critical for its function. Furthermore, it has been shown that MAGE-C1 and MAGE-A3 can promote the survival of multiple myeloma cells and that silencing of these cancer/testis genes further improves the response of myeloma cells to conventional therapies (Atanackovic et al., 2010); the molecular mechanism behind this effect has not been elucidated.

In order to investigate more in depth MAGE-C1 and NY-ESO-1 possible involvement in tumourigenesis, we decided to test their role in cell survival to several types of stress in cell lines other than multiple myeloma, which would extend our knowledge to other tumour types.

We chose a range of different cellular stresses in order to analyse various pathways that are important for transformation and tumour progression.

Heat shock and endoplasmic reticulum (ER) stress were the first types of stress we considered. The heat shock response (HSR) was originally discovered as a response to thermal stress, but is also triggered by a variety of stress conditions that result in accumulation of misfolded or aggregated proteins, cell cycle arrest and stagnation of growth and proliferation. The HSR is mediated by Hsf (Heat shock factor) transcription factors which binds to heat shock elements (HSE) in the promoters of a wide range of target genes: heat shock proteins (Hsp), which are molecular chaperones deployed to prevent protein misfolding and to assist in their refolding to the native state; components of the proteolytic system; RNA- and DNA-modifying enzymes, which are necessary to repair nucleic acid damage; metabolic enzymes; regulatory proteins such as transcription factors or kinases; structural proteins of the cytoskeleton; and finally transport, detoxifying, and membrane-modulating proteins (Richter et al., 2010).

Heat shock and other stressful conditions that induce the heat shock response can also lead to apoptosis or necrosis, determined by the intensity and duration of the stress.

Elevated expression of members of the Hsp family has been reported in several types of malignancies, including breast and lung tumours. Because Hsp proteins plays a critical role in folding, maturation, and stability of several important signalling proteins, their inhibition by small molecules leads to degradation of these proteins and inactivation of the corresponding signalling pathways. As a consequence, inhibitors of Hsp proteins, such as geldanamycin for Hsp90, have been studied for their anticancer activities (Neckers, 2002).

In a similar way to heat shock, endoplasmic reticulum (ER) stress causes disruption of protein folding and post-translational modification capacity, affecting secreted proteins and membrane proteins. This organelle in fact is a main site for protein folding, as well as lipid biosynthesis and calcium storage in cells. ER stress can occur as a result of a wide variety of stress stimuli, including expression of mutant proteins that cannot be properly folded, depletion of energy supply, changes to the redox environment and Ca^{2+} depletion (Boyce and Yuan, 2006), resulting in activation of the unfolded protein response (UPR). However, if stress persists, apoptosis can be triggered (Rao et al., 2004).

In cancer aberrant activation of the UPR has been reported and many response genes and ER chaperones, including GRP78, show increased expression. This is possibly due to the poor vascularisation of the tumour leading to low oxygen supply, nutrient deprivation and pH changes (Moenner et al., 2007). As a consequence it has been argued that activation of the UPR might contribute to the survival and growth of cancer cells, therefore down-regulation of this response using specific inhibitors provides new perspectives for cancer therapy (Healy et al., 2009).

Aside from heat shock and ER stress, we also utilised two different sources of genotoxic stress: UV irradiation and doxorubicin treatment. UV irradiation leads to the production of pyrimidine dimers and 6-4 photoadducts on DNA. This triggers classic DNA damage response pathways orchestrated by the tumour suppressor p53: cells undergo growth arrest mediated by $p21^{waf1}$ to allow time to repair the damage to their genome; in the event of irreparable damage cells undergo apoptosis (Smith et al., 2000; Smith and Fornace, 1997). Importantly, the *p53* gene is itself a frequent target of UV-induced mutations, therefore it has been suggested that UV not only is an initiator of tumourigenesis by causing DNA alterations, but also promotes tumourigenesis by selecting for survival cells carrying mutant *p53* genes (Ziegler et al., 1994).

The chemotherapeutic drug doxorubicin also stimulates the p53 pathway by intercalating to DNA and inhibiting the progression of the enzyme topoisomerase II and therefore the process of replication; furthermore it induces ROS generation in various tumour cells. Various mutations of *p53* and attenuation of p53 activation by doxorubicin were reported as important mechanisms of drug resistance in tumour cells (Anthoney et al., 1996; McCurrach et al., 1997).

A further type of stress we considered in our analysis was hypoxia: reduction of the normal oxygen level often occurs in rapidly growing tumours due to inadequate blood supply; to counteract this unfavourable environment cancer cells undergo genetic changes that allow them to survive and that ultimately contribute to tumour progression. These include the induction of genes involved in anaerobic metabolism, angiogenesis, cell growth, invasion and metastasis. As a consequence hypoxia is associated with resistance to therapy and poor outcome, indicating that

mediators of the hypoxic response, such as the key transcription factor Hypoxia-inducible factor-1α (HIF-1α), might be important therapeutic targets (Harris, 2002).

5.2 Results

5.2.1 MAGE-C1, but not NY-ESO-1, inhibits cell death in response to specific types of cellular stress.

In order to understand the biological significance of MAGE-C1 and NY-ESO-1, we first examined their role in regulating cell fate.

Cell lines expressing only one or the other protein were utilised because they gave the possibility to study their function independently from the expression of the other member of the complex, and subsequently to assess whether this was affected by exogenous expression of the other CT protein. U2OS osteosarcoma and H1299 NSCLC cells were chosen for this purpose, as western blot analysis revealed that the former express only MAGE-C1 but not NY-ESO-1, whereas the latter showed expression of NY-ESO-1 but not MAGE-C1 (Figure 5.1A). SK-MEL-37 melanoma cells were utilised as a positive control, as they present high levels of both proteins.

Immunofluorescence staining showed that MAGE-C1 subcellular localisation in U2OS cells is mostly cytoplasmic, with some nuclear staining. Moreover, heterogeneity was detected, similar to what was observed with melanoma, SCLC and MM cell lines (see Chapter III), with cells showing strong staining as opposed to cells with weaker or no staining. The staining of NY-ESO-1 in H1299 cells was instead homogeneous and both nuclear and cytoplasmic (Figure 5.1B).

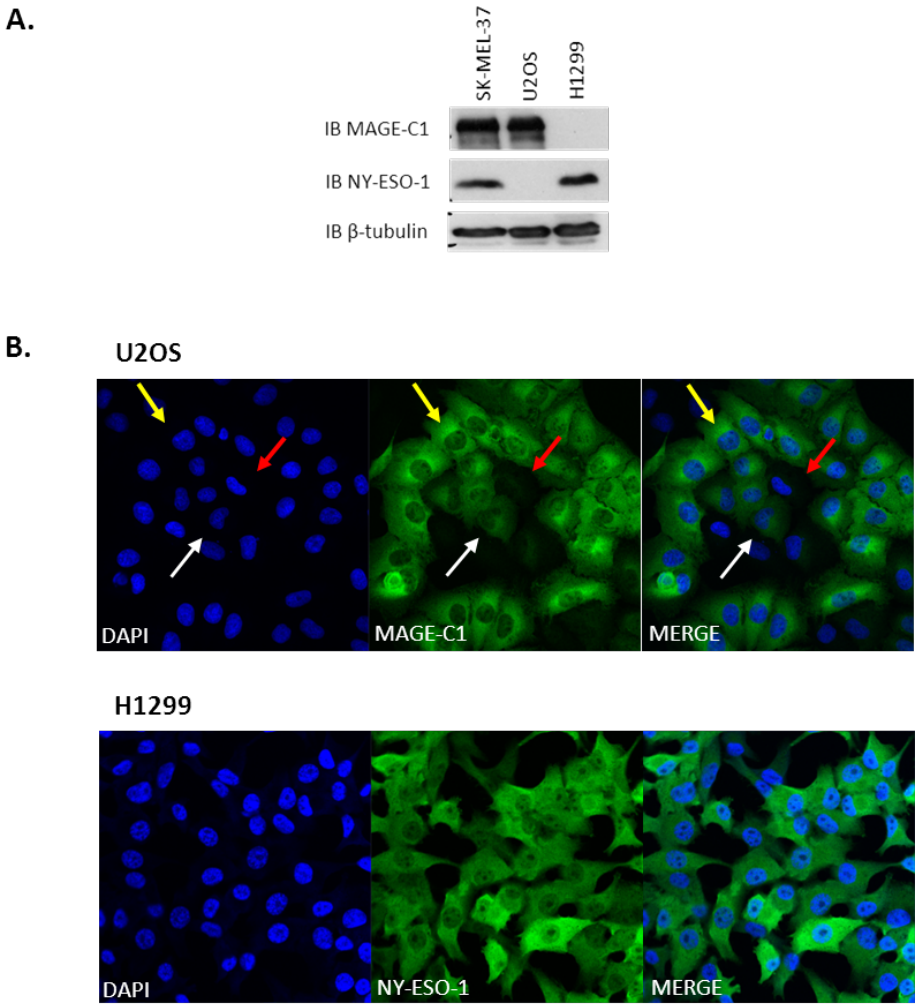

Figure 5.1 Characterisation of MAGE-C1 and NY-ESO-1 expression in U2OS and H1299 cancer cell lines. A. Western blot analysis of endogenous MAGE-C1and NY-ESO-1 in U2OS and H1299 cell lines. Cells were lysed in urea buffer, analysed by SDS-PAGE, and immunoblotted for MAGE-C1 using mouse monoclonal CT7.33 antibody, for NY-ESO-1 using mouse monoclonal E978 antibody or with β-tubulin mouse monoclonal antibody (as a loading control). B. Immunofluorescence staining of endogenous MAGE-C1 and NY-ESO-1 in U2OS and H1299 cells respectively. Cells were fixed with paraformaldehyde and immunostained with CT7.33 mouse monoclonal antibody or NY-41 rabbit polyclonal antibody, and then with secondary FITC-labelled antibody. DAPI was used for nuclei staining. The yellow, white and red arrows indicate cells expressing high level, intermediate level or no MAGE-C1 respectively.

The effects of MAGE-C1 depletion were analysed in U2OS cells using RNAi (Figure 5.2). Cells were transfected with a negative control siRNA (siCTRL) or with a MAGE-C1 specific siRNA (siMAGEC1) and 72 hours after transfection they were either left untreated or given different types of stress to induce cell death. The treatments included: heat shock at 44ºC for 30 minutes, in which case cells were collected either immediately after heat shock (heat shock 0h) or 20 hours

after the shock (heat shock 20h) in order to assess both immediate and more belated cell death; tunicamycin and thapsigargin, two drugs that induce endoplasmic reticulum stress by preventing glycosylation of newly synthesised glycoproteins and by inhibiting the sarcoplasmic/endoplasmic reticulum Ca^{2+}-dependent ATPase (SERCA) respectively; high doses of UV irradiation; hypoxic conditions; doxorubicin treatment.

Cells were harvested for western blot analysis to confirm the efficacy of the silencing in the different conditions (Figure 5.2A) or stained with Propidium Iodide (PI) to examine the various phases of the cell cycle via flow cytometry. The SubG1 phase, which corresponds to fragmented DNA and therefore is an indicator of cell death, was quantified in the different conditions and compared (Figure 5.2B, upper panel). MAGE-C1 siRNA induced a significant increase (p value<0.05) in the SubG1 subpopulation in untreated cells and after heat shock, ER stress and UV irradiation. Western blot for total PARP performed in untreated conditions and after tunicamycin and thapsigargin treatment showed an increase in PARP cleavage, confirming the induction of apoptosis upon MAGE-C1 knockdown (Figure 5.2B, lower panel). On the other hand in hypoxic conditions and after doxorubicin treatment the increase in SubG1 upon MAGE-C1 RNAi was not significant, although a trend could be observed.

A different siRNA oligonucleotide targeting MAGE-C1 (siMAGEC1 #8) was also utilised to test the consistency of the results obtained. Again, U2OS cells were transfected with this siRNA and the siCTRL and subsequently treated with tunicamycin. Both in untreated and treated conditions a statistically significant increase in apoptosis was observed (Figure 5.2C).

To rule out the possibility of off-target effects of the siRNA raised against MAGE-C1, it was transfected in H1299 cells, which do not express this gene. In this cell line the knockdown did not have any apoptotic effect, both in untreated cells and after heat shock, which was chosen as it gives the highest amount of cell death in Figure 5.2B. This result confirmed the specificity of our findings (Figure 5.2D).

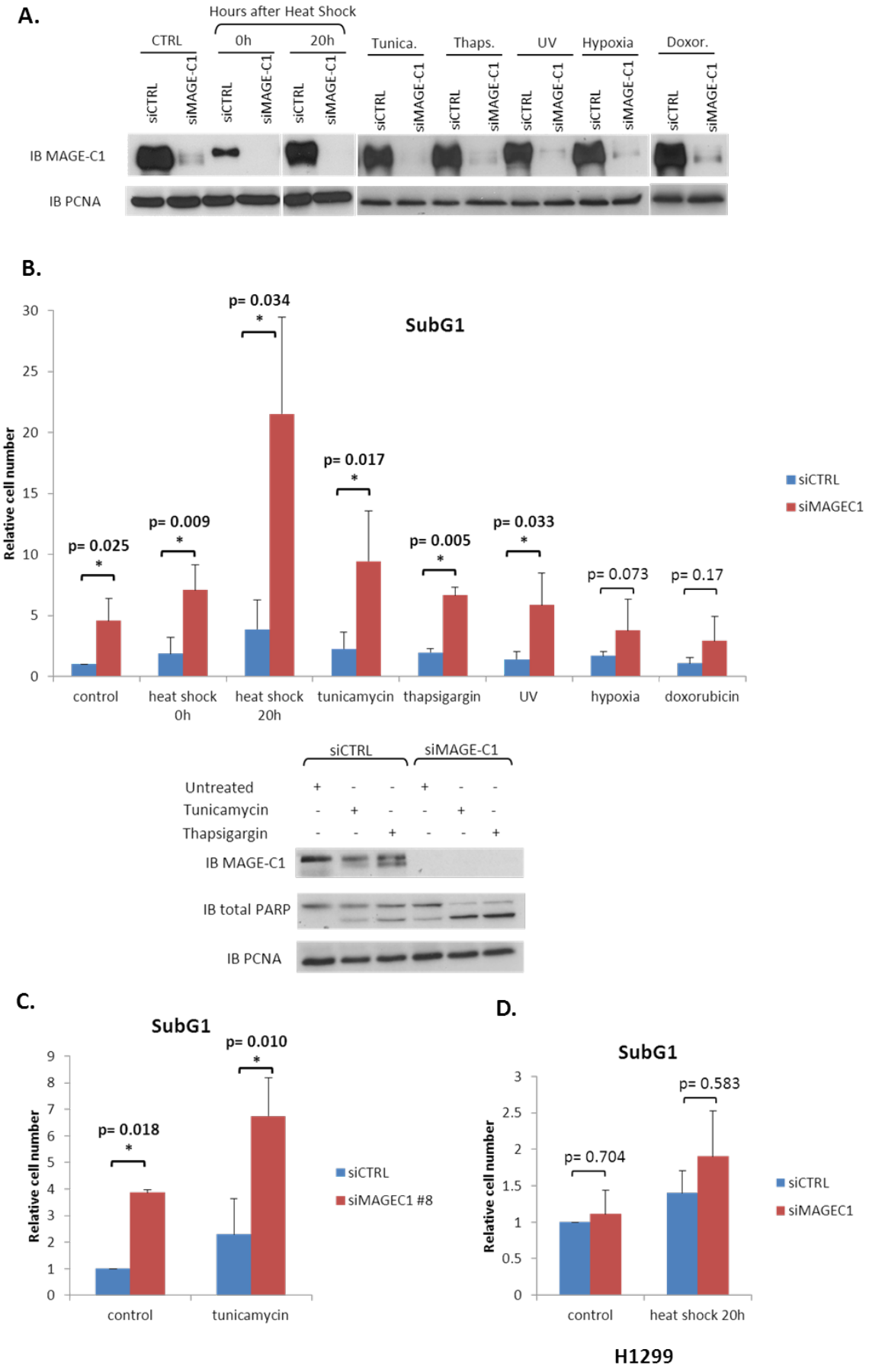
A.
Hours after Heat Shock
CTRL
0h
20h
Tunica.
Thaps.
UV
Hypoxia
Doxor.
siCTRL
siMAGE-C1
IB MAGE-C1
IB PCNA
B.
SubG1
Relative cell number
p= 0.025
p= 0.009
p= 0.034
p= 0.017
p= 0.005
p= 0.033
p= 0.073
p= 0.17
control
heat shock 0h
heat shock 20h
tunicamycin
thapsigargin
UV
hypoxia
doxorubicin
siCTRL
siMAGEC1
Untreated
Tunicamycin
Thapsigargin
IB MAGE-C1
IB total PARP
IB PCNA
C.
SubG1
Relative cell number
p= 0.018
p= 0.010
control
tunicamycin
siCTRL
siMAGEC1 #8
D.
SubG1
Relative cell number
p= 0.704
p= 0.583
control
heat shock 20h
siCTRL
siMAGEC1
H1299

Figure 5.2 MAGE-C1 RNAi induces cell death in response to specific types of stress. U2OS cells were transfected with a MAGE-C1 specific siRNA (siMAGEC1) or a scrambled siRNA (siCTRL) according to the lipofectamine2000 protocol. 72h after transfection cells were exposed to: heat shock at 44ºC for 30' (cells were collected immediately after heat shock -0h- or 20h after heat shock), 10µg/ml tunicamycin for 24h, 1µM thapsigargin for 24h, 50 J/m^2 UV, hypoxia O/N, and 1µM doxorubicin for 24h. A. Cells were lysed in RIPA buffer, analysed by SDS-PAGE, and immunoblotted for MAGE-C1 using mouse monoclonal CT7.33 antibody or with PCNA mouse monoclonal antibody (as a loading control). B. Cells were fixed, stained with PI and analysed by flow cytometry. The SubG1 subpopulation was quantified for each sample, normalised on the untreated siCTRL-transfected sample and represented in a graph. The experiment was repeated at least three times and p values<0.05 were considered significant (*). *Lower panel*: Cells treated with tunicamycin or thapsigargin were lysed in urea buffer, analysed by SDS-PAGE, and immunoblotted for MAGE-C1 using mouse monoclonal CT7.33 antibody, with total PARP rabbit polyclonal antibody or with PCNA mouse monoclonal antibody (as a loading control). C. Cells transfected with a different MAGE-C1 specific siRNA (siMAGEC1 #8) or a scrambled siRNA (siCTRL) and treated with tunicamycin were fixed, stained with PI and analysed by flow cytometry. The SubG1 subpopulation was quantified for each sample, normalised on the untreated siCTRL-transfected sample and represented in a graph. D. H1299 cells exposed to heat shock were fixed after 20h, stained with PI and analysed by flow cytometry. The SubG1 subpopulation was quantified for each sample, normalised on the untreated siCTRL-transfected sample and represented in a graph.

The other phases of the cell cycle (G0/G1, S and G2/M) were also examined after MAGE-C1 knockdown in U2OS cells. Cells were treated as in Figure 5.2, harvested and stained with PI followed by flow cytometry analysis. The different phases were plotted altogether in Figure 5.3A and separately in Figure 5.3B. No significant changes in G0/G1, S and G2/M were detected in MAGE-C1 siRNA-transfected cells following any type of stress analysed. A general small decrease in all phases of the cell cycle in MAGE-C1 siRNA-transfected cells can be attributed to the increase in SubG1. Doxorubicin-induced G2/M arrest has been described previously (Bartek and Lukas, 2007; Smits and Medema, 2001).

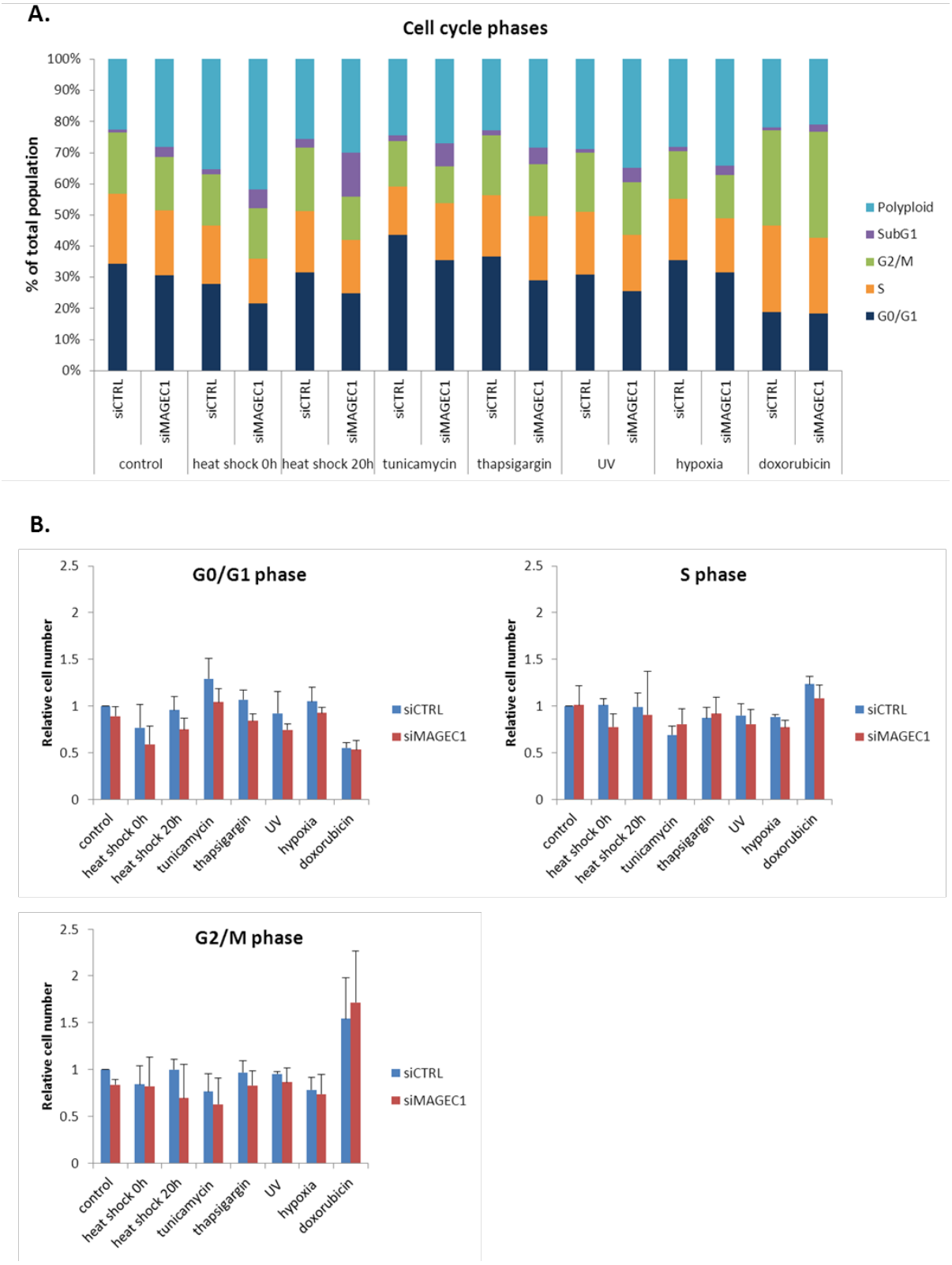

Figure 5.3 MAGE-C1 RNAi does not affect the cell cycle. U2OS cells were transfected with a MAGE-C1 specific siRNA (siMAGEC1) or a scrambled siRNA (siCTRL) according to the lipofectamine2000 protocol, and treated like in Figure 5.2. The different phases of the cell cycle (G0/G1, S and G2/M) were quantified. A. Graphic representation of the proportion of cells in different phases of the cell cycle as a percentage of the entire population (10,000 cells). B. Each cell cycle phase was plotted separately after normalisation on the untreated siCTRL-transfected sample.

In order to investigate whether NY-ESO-1 also had an effect on cell viability, H1299 were transfected with NY-ESO-1 siRNA and either heat shocked or left without treatment. Again, heat shock was chosen as it had the strongest effect in terms of cell death in the previous experiments. After heat shock no significant difference in the amount of SubG1 phase could be detected between control siRNA and NY-ESO-1 siRNA transfected cells (Figure 5.4A) or in any of the other cell cycle phases (Figure 5.4B and 5.4C).

From these data we can conclude that, whereas NY-ESO-1 does not affect cell survival, MAGE-C1 acts as an inhibitor of cell death in response to specific types of stress, such as ER stress, heat shock and UV irradiation, and accordingly might be involved in the molecular pathways connected with them.

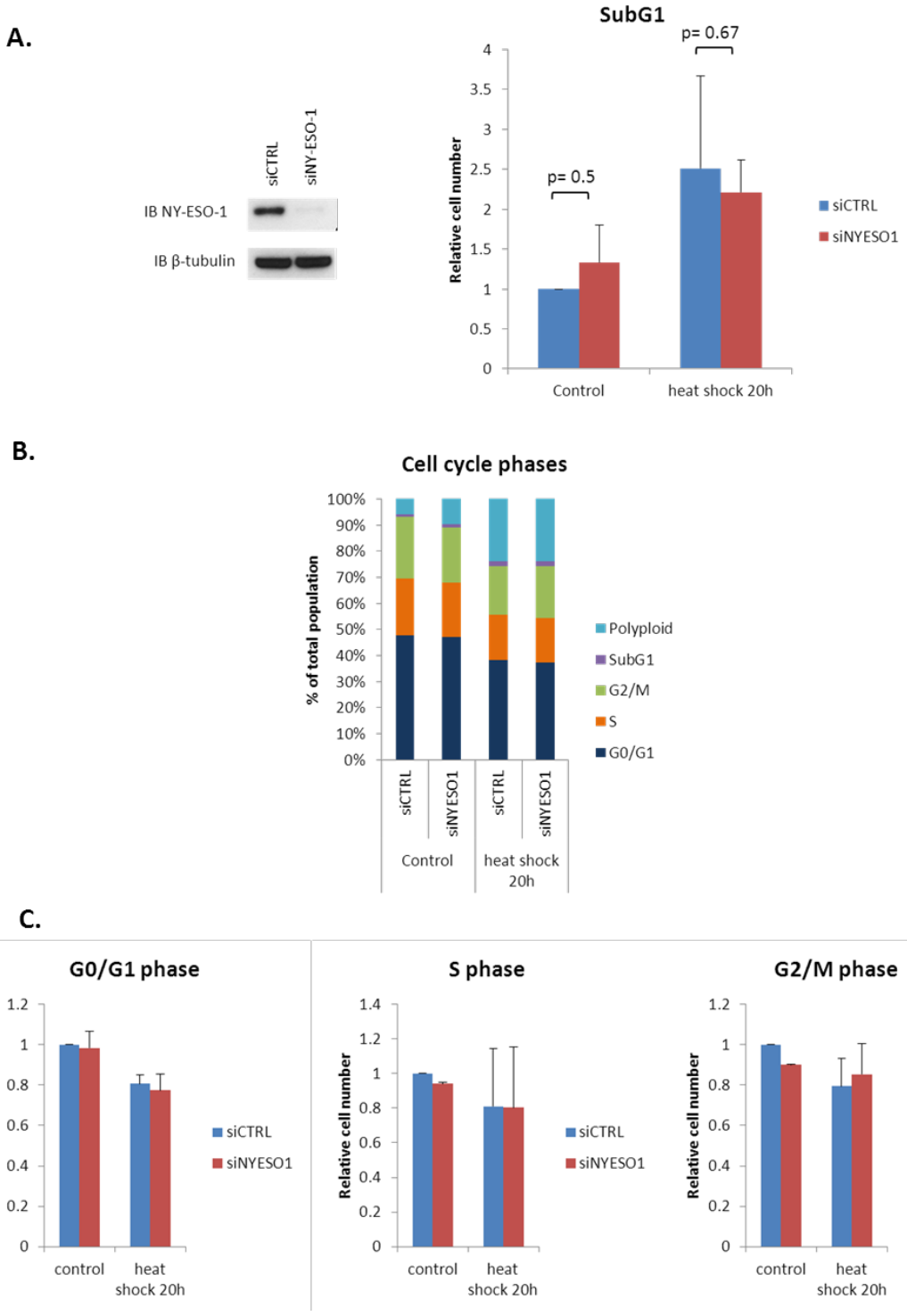

Figure 5.4 NY-ESO-1 RNAi does not affect apoptosis or the cell cycle. H1299 cells were transfected with a NY-ESO-1 specific siRNA (siNYESO1) or a scrambled siRNA (siCTRL). 72h after transfection cells were exposed to heat shock at 44ºC for 30' and collected after 20h. A. *Left:* Cells were lysed in RIPA buffer, analysed by SDS-PAGE, and immunoblotted for NY-ESO-1 using mouse monoclonal E978 antibody or with β-tubulin mouse monoclonal antibody (as a loading control). *Right*: cells were fixed, stained with PI and analysed by flow cytometry. The SubG1 subpopulation was quantified for each sample, normalised on the untreated siCTRL-transfected sample and represented in a graph. B. The different phases of the cell cycle (G0/G1, S and G2/M) were quantified. Graphic representation of the proportion of cells in different phases of the cell cycle as a percentage of the entire population (10,000 cells). C. Each cell cycle phase was plotted separately after normalisation on the untreated siCTRL-transfected sample.

5.2.2 MAGE-C1 does not affect p53 protein levels.

As we observed an increase in apoptosis when we depleted MAGE-C1, we proceeded investigating which pathway was mediating this effect.

The p53 tumour suppressor protein plays a crucial role in regulating both the intrinsic and the extrinsic apoptotic pathways (Figure 1.1) and several members of the MAGE family have been shown to inhibit p53 function: MAGE-C2, highly homologous to MAGE-C1, and MAGE-A3 have been shown to interact with KAP-1, a co-repressor of p53 expression and function, to promote cell survival (Yang et al., 2007b); KAP-1 is also an E3 RING ubiquitin ligase, and the MAGE-C2-KAP-1 complex is able to target p53 for proteasome-dependent degradation (Doyle et al., 2010; Espantman and O'Shea, 2010). Another member of the family, MAGE-A2, forms a complex with the histone deacetylase HDAC3 and recruits it to p53-responsive promoters, inhibiting transcription (Monte et al., 2006) ; it is also able to inhibit p53 interaction with chromatin (Marcar et al., 2010) and to affect p53 acetylation at the level of PML-nuclear bodies, resulting in an impairment of senescence (Peche et al., 2011).

To test a possible involvement of p53 in MAGE-C1 pro-survival effect, MAGE-C1 RNAi experiments were performed in U2OS cells, both in untreated conditions and after heat shock and tunicamycin treatment (Figure 5.5A). Cells were also treated with Nutlin-3, a compound that stabilises p53 protein by inhibiting its binding with the E3 ubiquitin ligase Mdm2. This allowed to test whether any observed difference was Mdm-2-dependent.

Western blot analysis did not show any change in p53 levels. The same experiment was executed in SK-MEL-37 cells, which express high levels of MAGE-C1 (Figure 3.1) and harbour a conformational mutant form of p53 (R175H), which is more stable than the wild-type p53, hence the high level in untreated condition (Asher et al., 2003). In a similar way to what was observed with wild-type p53 in U2OS cells, mutant p53 was not affected by depletion of MAGE-C1, both in untreated conditions and after heat shock or tunicamycin treatment (Figure 5.5B), suggesting that the p53 pathway is not primarily involved in MAGE-C1 RNAi-induced apoptosis; this

supports the fact that doxorubicin treatment, which acts primarily through the p53 pathway, does not cause a significant increase in SubG1 in cells depleted for MAGE-C1.

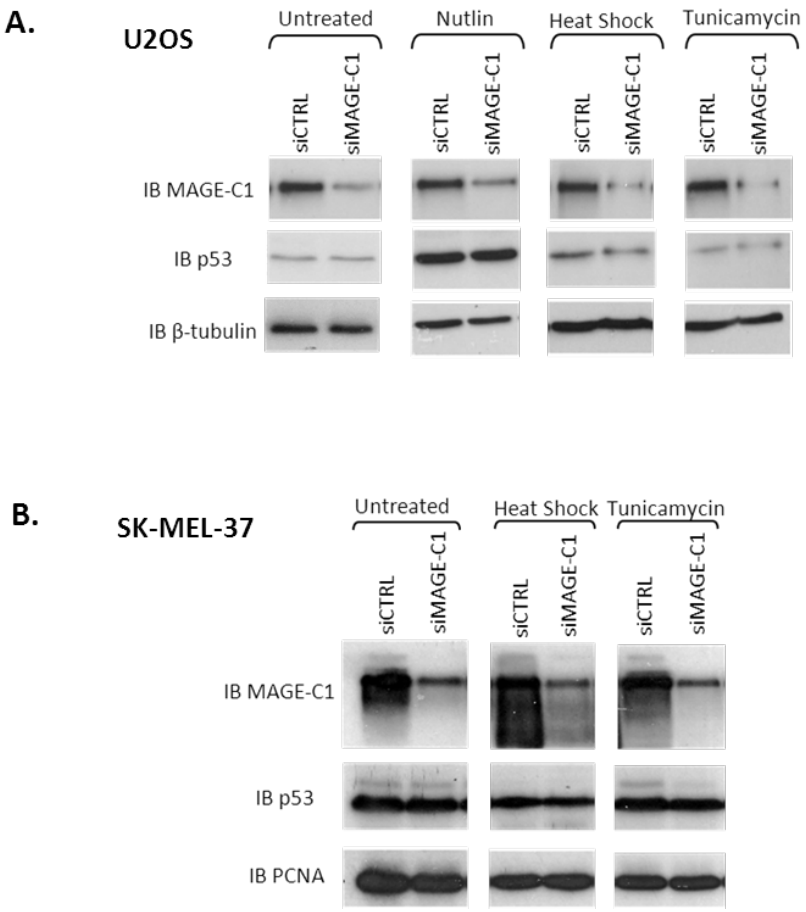

Figure 5.5 MAGE-C1 RNAi does not affect p53 protein levels. U2OS cells were transfected with a MAGE-C1 specific siRNA (siMAGEC1) or a scrambled siRNA (siCTRL) according to the lipofectamine2000 protocol. 72h after transfection cells were exposed to 10μM Nutlin-3 for 24h, heat shock at 44ºC for 30' (cells were collected 20h after heat shock) or 10μg/ml tunicamycin for 24h. Cells were then lysed in urea buffer, analysed by SDS-PAGE, and immunoblotted for MAGE-C1 using mouse monoclonal CT7.33 antibody, for p53 using DO-1 mouse monoclonal antibody or with β-tubulin mouse monoclonal antibody (as a loading control). B. SK-MEL-37 cells were transfected with a MAGE-C1 specific siRNA (siMAGEC1) or a scrambled siRNA (siCTRL) according to the lipofectamine2000 protocol. 72h after transfection cells were exposed to heat shock at 44ºC for 30' (cells were collected 20h after heat shock) or 10μg/ml tunicamycin for 24h. Cells were then lysed in urea buffer, analysed by SDS-PAGE, and immunoblotted for MAGE-C1 using mouse monoclonal CT7.33 antibody, for p53 using DO-1 mouse monoclonal antibody or with PCNA mouse monoclonal antibody (as a loading control).

5.2.3 MAGE-C1 affects Mcl-1 protein levels in response to tunicamycin treatment.

The Bcl-2 family of proteins is also highly involved in the control of apoptosis through the intrinsic pathway (Figure 1.1). In addition to their role at the mitochondria, different Bcl-2 related proteins are located to the endoplasmic reticulum (ER) membrane and recent findings highlighted their role in ER stress-induced cell death: in normal conditions, the pro-apoptotic members Bax and Bak are inactive due to their binding with the pro-survival member Bcl-2 both on the mitochondrial and ER membranes; in response to ER stress, JNK is activated and subsequently phosphorylates and inactivates Bcl-2. Moreover Bcl-2 expression is repressed by the ER stress-induced transcription factor CHOP. This allows activation of Bax and Bak and execution of cell death (Szegezdi et al., 2006). Furthermore, it was demonstrated that another pro-survival member of the Bcl-2 family, Mcl-1, is essential for the survival of melanoma cells to ER stress induced by tunicamycin and thapsigargin (Jiang et al., 2008); consistently, the BH3 mimetic obatoclax, by antagonising Mcl-1, is able to overcome resistance of melanoma cells to apoptosis induced by ER stress (Jiang et al., 2009).

Since Bcl-2 and Mcl-1 have an important role in ER stress-induced apoptosis and considering the apoptotic effect induced by ER stressors after MAGE-C1 knockdown, we decided to test the expression of these two genes in U2OS cells depleted for MAGE-C1 and treated with tunicamycin. Interestingly, a significant decrease in Mcl-1 protein levels was detected in tunicamycin treated cells upon MAGE-C1 RNAi (Figure 5.6A), while no significant difference was observed for Bcl-2 (Figure 5.6B). It is therefore possible that MAGE-C1 loss increases apoptosis in response to ER stress in a Mcl-1-dependent fashion.

To test whether this decrease was due to a transcriptional inhibition or was post-translational, *Mcl-1* specific qRT-PCR was performed on lysates from U2OS after MAGE-C1 knockdown and tunicamycin treatment (Figure 5.6C). No significant difference in *Mcl-1* mRNA levels was observed between control siRNA and MAGE-C1 siRNA, leading to the conclusion that MAGE-C1 does not affect the mRNA expression of the *Mcl-1* gene.

Finally, immunofluorescence co-staining of MAGE-C1 and Mcl-1 was performed in U2OS cells upon MAGE-C1 siRNA transfection and tunicamycin treatment. In untreated conditions Mcl-1 localised mostly at the mitochondria, as previously described, both in siCTRL and siMAGE-C1 transfected cells; after tunicamycin treatment, Mcl-1 staining appeared weaker and diffuse, suggesting re-localisation and possibly degradation of the protein; this was particularly evident in MAGE-C1 siRNA transfected cells, where Mcl-1 staining was almost totally lost (Figure 5.6D). The discrepancy between western blot and staining in terms of protein amount can be attributed to the use of different primary antibodies.

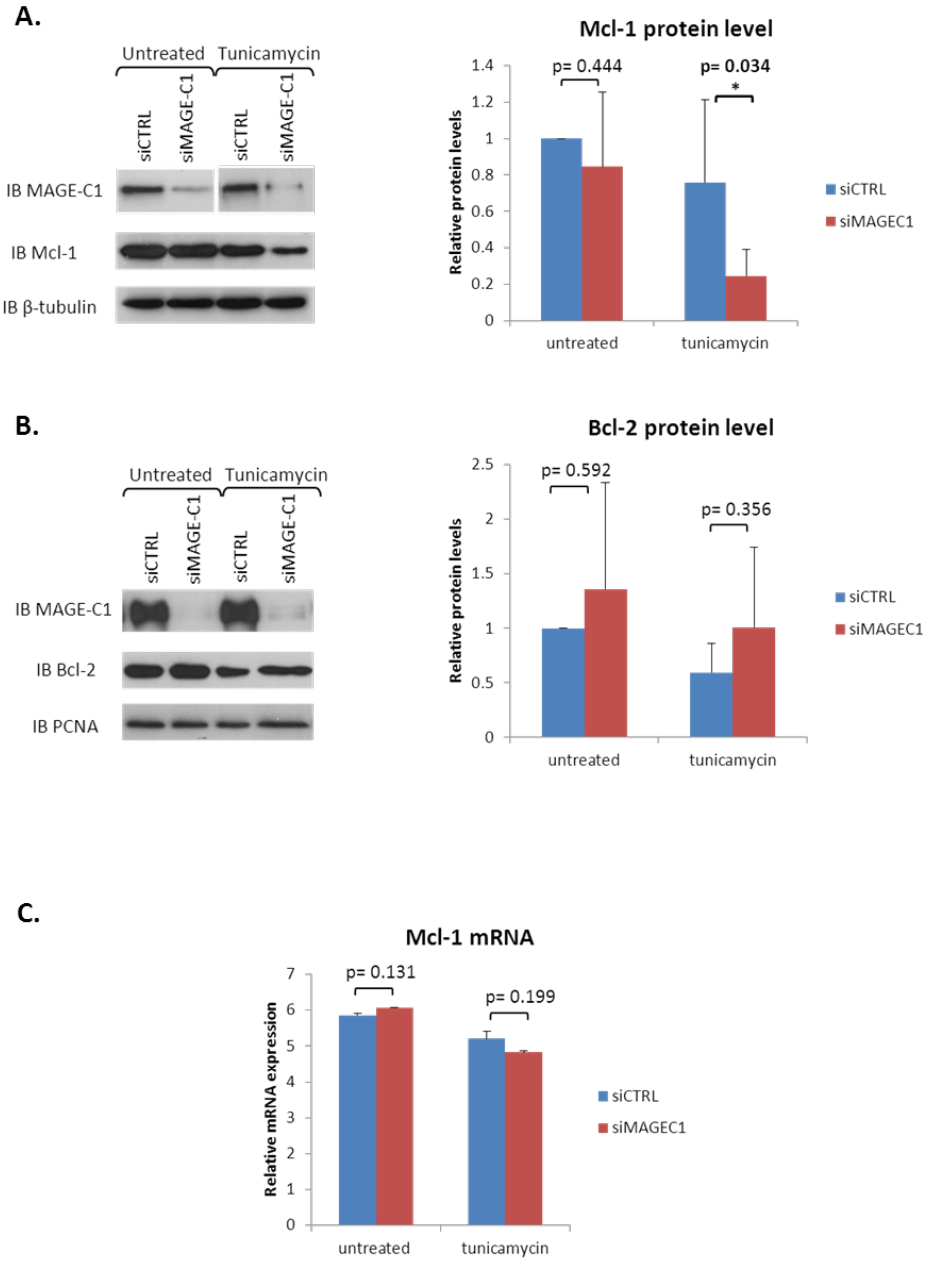

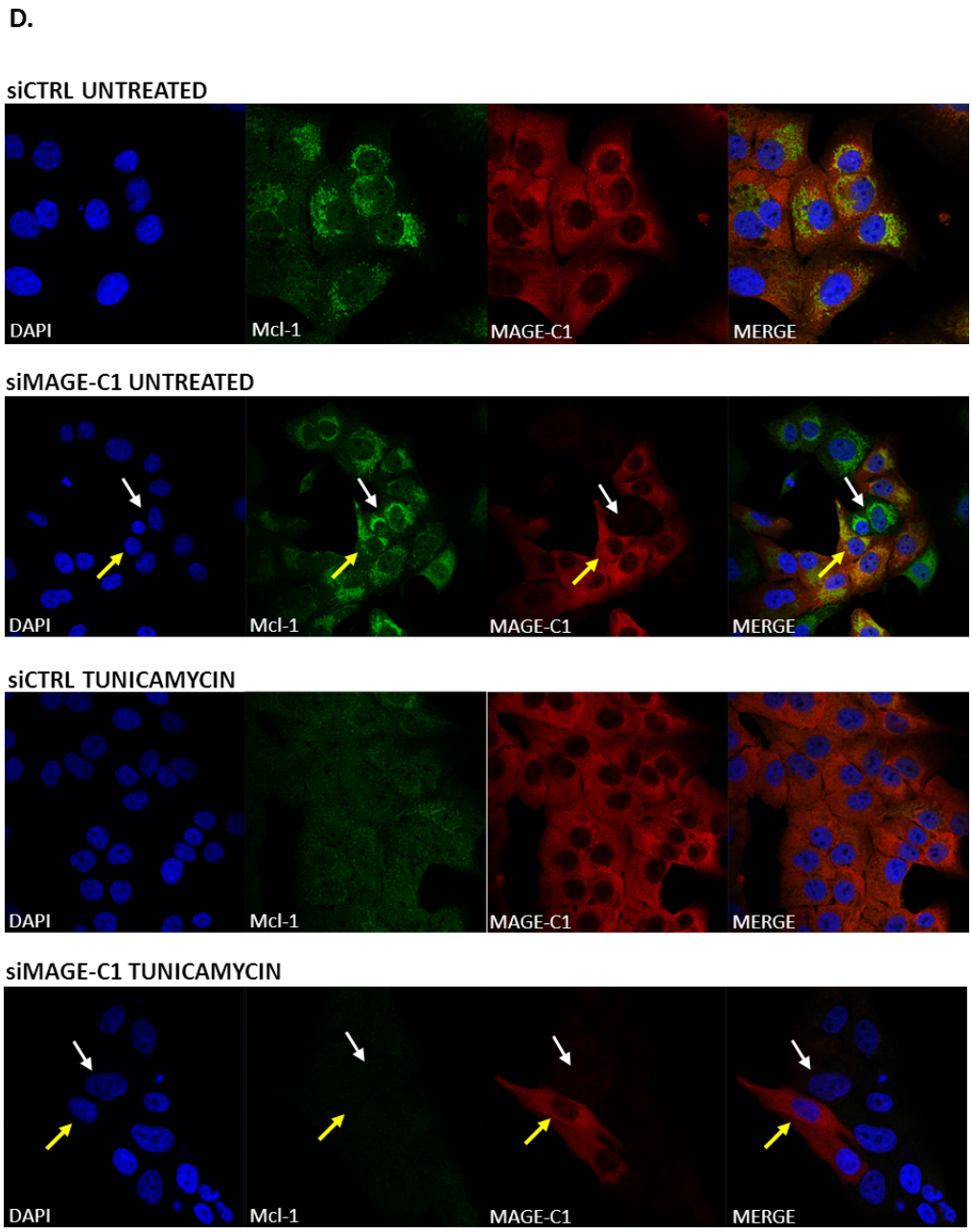

Figure 5.6 MAGE-C1 RNAi affects Mcl-1 protein levels upon tunicamycin treatment. U2OS cells were transfected with a MAGE-C1 specific siRNA (siMAGEC1) or a scrambled siRNA (siCTRL) according to the lipofectamine2000 protocol. 72h after transfection cells were exposed to 10µg/ml tunicamycin for 24h. A. Cells were lysed in urea buffer, analysed by SDS-PAGE, and immunoblotted for MAGE-C1 using mouse monoclonal CT7.33 antibody, with Mcl-1 rabbit polyclonal antibody or with β-tubulin mouse monoclonal antibody (as a loading control) in A, or with mouse monoclonal CT7.33 antibody, Bcl-2 mouse monoclonal antibody or with PCNA mouse monoclonal antibody (as a loading control) in B. The signal was quantified using ImageJ, normalised first by the loading control and then by the untreated siCTRL-transfected sample and represented in a graph. The experiments were repeated at least three times and p values<0.05 were considered significant (*). C. Cells were harvested and mRNA levels of Mcl-1 were analysed by RT-qPCR based on ΔΔCt method using GAPDH as an internal control. D. Immunofluorescence double staining of endogenous Mcl-1 and MAGE-C1. Cells were fixed with paraformaldehyde and immunostained with Mcl-1 rabbit polyclonal antibody (Sigma) and CT7.33 mouse monoclonal antibody, and then with secondary FITC- and TRITC-labelled antibodies, respectively. DAPI was used for nuclei staining. The yellow and white arrows indicate cells expressing or depleted for MAGE-C1 respectively.

5.2.4 MAGE-C1 regulates Mcl-1 accumulation upon proteasome inhibition during ER stress.

Mcl-1 protein is distinct from other Bcl-2 family members in its extremely unstable nature, which allows cells to switch quickly to either survival or apoptotic mode in response to various stresses. Rapid proteasomal degradation is an important mechanism to control its levels: Mcl-1 contains a PEST region, which is associated with proteins that have a short intracellular half-life; ERK-dependent phosphorylation of the PEST region (Thr163) stabilises Mcl-1 protein (Domina et al., 2004); on the contrary, Mcl-1 phosphorylation on Ser159 by GSK-3 leads to increased degradation (Ding et al., 2007) (Figure 1.4).

Having ruled out a role of MAGE-C1 in controlling *Mcl-1* gene transcription, we proceeded examining the effect of MAGE-C1 on Mcl-1 protein by testing Mcl-1 accumulation upon treatment with a proteasome inhibitor, MG132. MAGE-C1 expression was knocked down by RNAi in U2OS cells that were then treated with tunicamycin as above; MG132 was added during the last four hours of tunicamycin treatment to induce Mcl-1 stabilisation.

Western blot analysis revealed that, as previously observed, Mcl-1 levels decrease after tunicamycin treatment and MAGE-C1 RNAi. Differently from Figure 5.6A, a decrease of smaller entity in Mcl-1 protein was also detected in the control siRNA after treatment; this is attributable to the variability in the amount of apoptosis induced by tunicamycin, which is reflected in Mcl-1 levels, as indicated by the error bars in Figure 5.2B and Figure 5.6A.

Upon MG132 treatment Mcl-1 was stabilised as expected, but the extent of such stabilisation was consistently lower in siMAGEC1 transfected cells (Figure 5.7). This leads to the conclusion that in the absence of MAGE-C1 Mcl-1 stability after ER stress induction is compromised.

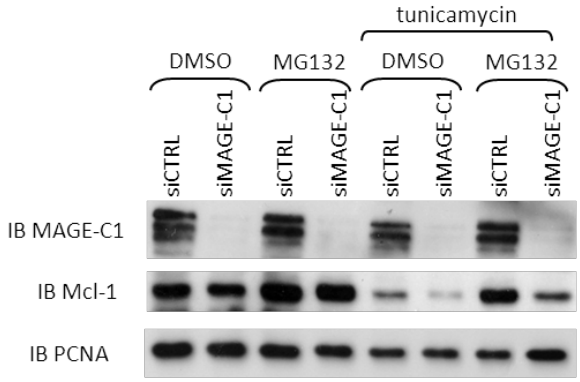

Figure 5.7 MAGE-C1 RNAi affects Mcl-1 stabilisation in ER stress conditions. U2OS cells were transfected with a MAGE-C1 specific siRNA (siMAGEC1) or a scrambled siRNA (siCTRL) according to the lipofectamine2000 protocol. 72h after transfection cells were exposed to 10µg/ml tunicamycin for 24h, and in the last 4 hours of treatment 40µM MG132 or DMSO (negative control) were added. Cells were lysed in urea buffer, analysed by SDS-PAGE, and immunoblotted for MAGE-C1 using mouse monoclonal CT7.33 antibody, with Mcl-1 rabbit polyclonal antibody or with PCNA mouse monoclonal antibody (as a loading control).

5.2.5 MAGE-C1 binds Mcl-1.

As MAGE-C1 affects Mcl-1 in a post-translational fashion, we proceeded to examine the binding between these two proteins with immunoprecipitation experiments. Since we saw an effect of MAGE-C1 depletion on Mcl-1 stabilisation by MG132, cells were also treated with this proteasome inhibitor. MAGE-C1 protein was then immunoprecipitated in U2OS and SK-MEL-37 cells and the binding with Mcl-1 was tested. Interaction was detected in both cell lines, and was particularly evident upon MG132 treatment (Figure 5.8A and B). Moreover, in both cell lines the co-immunoprecipitated Mcl-1 run at a slightly higher molecular weight than in the input, both in untreated and MG132 treated cells, suggesting that the subset of Mcl-1 that binds to MAGE-C1 could be post-translationally modified and possibly phosphorylated considering the extent of the shift; this would explain the considerable amount of protein that had to be immunoprecipitated to detect the binding, especially in untreated conditions.

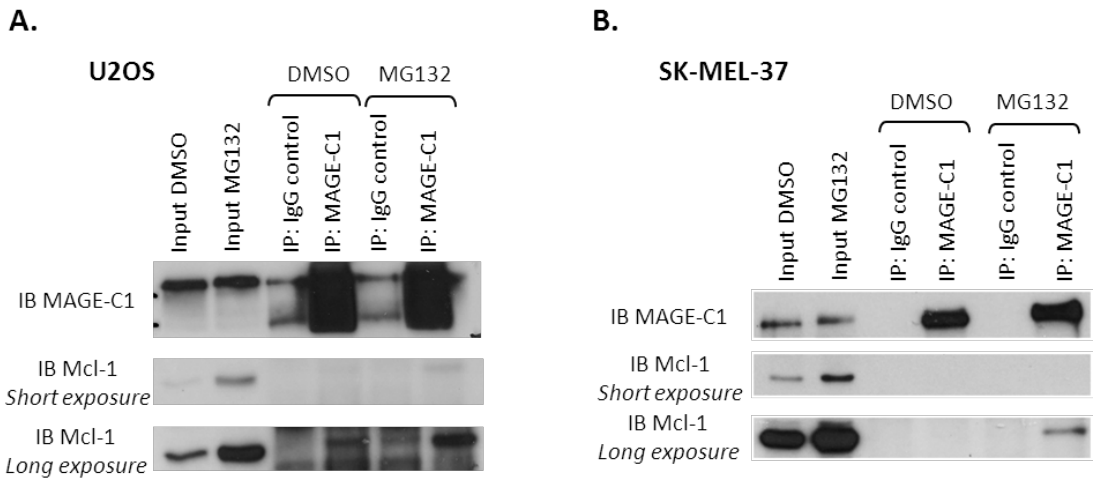

Figure 5.8 MAGE-C1 binds Mcl-1. MAGE-C1 was immunoprecipitated with CT7.33 mouse monoclonal antibody in cell lysate from U2OS (A) or SK-MEL-37 (B) cell lines after treatment with 40 μM MG132 or DMSO (negative control) for 4h. The protein complexes were then analysed by SDS-PAGE and immunoblotted for MAGE-C1 (CT7.33 antibody) or Mcl-1 (rabbit polyclonal antibody).

5.2.6 MAGE-C1 binding to Mcl-1 is independent of NY-ESO-1.

Since MAGE-C1 and NY-ESO-1 form a complex, we tested whether NY-ESO-1 could also bind to Mcl-1. Immunoprecipitation was performed in SK-MEL-37 cells, which express both MAGE-C1 and NY-ESO-1, but whereas the binding between MAGE-C1 and Mcl-1 was confirmed, no binding with NY-ESO-1 was observed, even after MG132 treatment (Figure 5.9A). The binding between MAGE-C1 and NY-ESO-1 was promptly detected as a positive control of the efficiency of the immunoprecipitation.

We then performed the same experiment in H1299, which express NY-ESO-1 but not MAGE-C1, to investigate whether the binding between MAGE-C1 and NY-ESO-1 could be mutually exclusive with the NY-ESO-1/Mcl-1 binding, however also in this cell line no interaction between NY-ESO-1 and Mcl-1 was found (Figure 5.9B).

Finally, we tested whether NY-ESO-1 could affect the binding of MAGE-C1 with Mcl-1 by depleting NY-ESO-1 via RNAi in SK-MEL-37 and subsequently performing

immunoprecipitation experiments. However, no significant change was observed (Figure 5.9C), leading to the conclusion that NY-ESO-1 does not affect the binding of MAGE-C1 with Mcl-1.

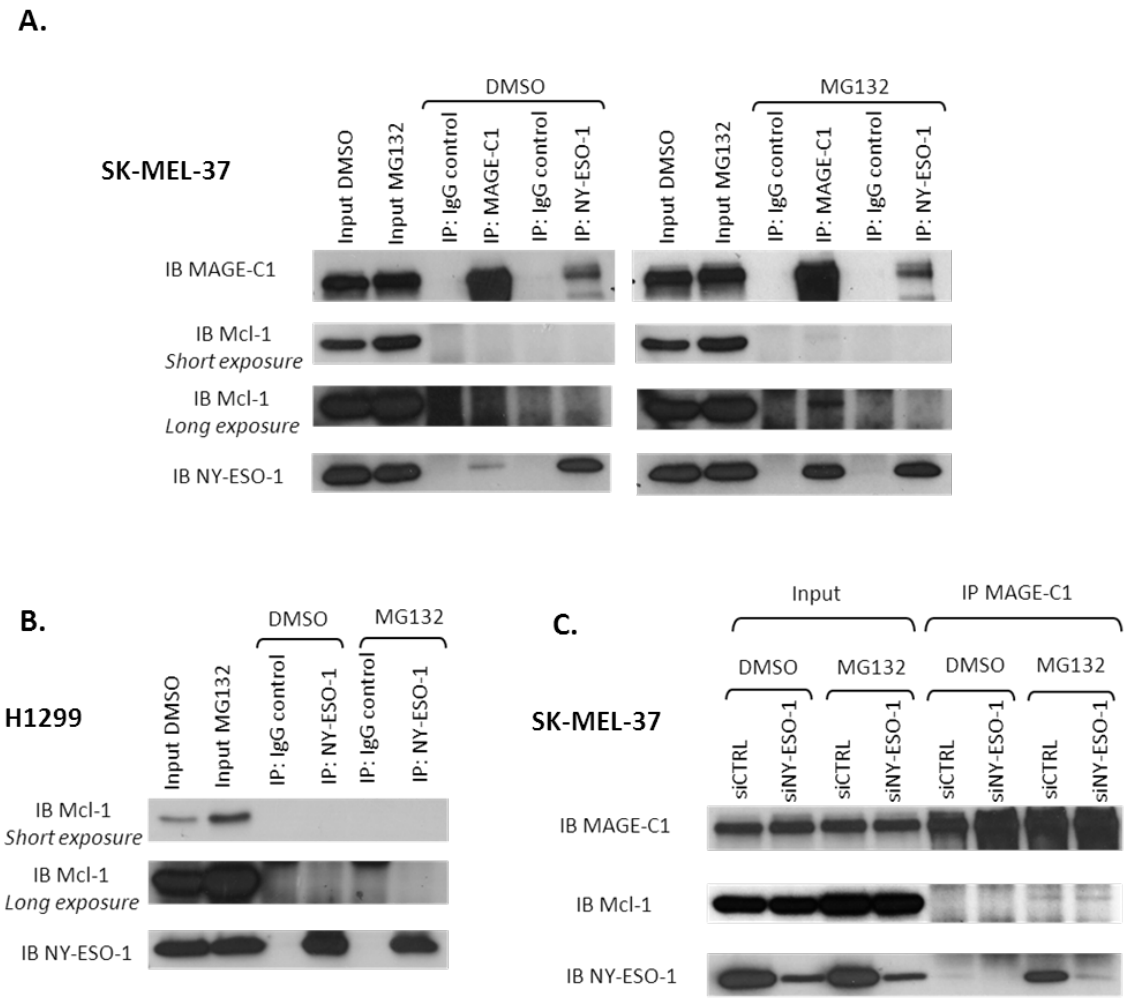

Figure 5.9 MAGE-C1 binding with Mcl-1 is independent of NY-ESO-1. A. MAGE-C1 and NY-ESO-1 were immunoprecipitated with CT7.33 mouse monoclonal antibody and E978 mouse monoclonal antibody respectively in cell lysate from SK-MEL-37 cell line after treatment with 40 µM MG132 or DMSO (negative control) for 4h. The protein complexes were then analysed by SDS-PAGE and immunoblotted for MAGE-C1 (CT7.33 antibody), NY-ESO-1 (E978 antibody) or Mcl-1 (rabbit polyclonal antibody). B. NY-ESO-1 was immunoprecipitated with E978 mouse monoclonal antibody in cell lysate from H1299 cell line after treatment with 40 µM MG132 or DMSO (negative control) for 4h. The protein complexes were then analysed by SDS-PAGE and immunoblotted for NY-ESO-1 (E978 antibody) or Mcl-1 (rabbit polyclonal antibody). C. MAGE-C1 was immunoprecipitated with CT7.33 mouse monoclonal antibody in cell lysate from SK-MEL-37 cell line depleted by RNAi of NY-ESO-1 after treatment with 40 µM MG132 or DMSO (negative control) for 4h. The protein complexes were then analysed by SDS-PAGE and immunoblotted for MAGE-C1 (CT7.33 antibody), NY-ESO-1 (E978 antibody) or Mcl-1 (rabbit polyclonal antibody).

5.2.7 MAGE-C1 binds to the N-terminus of Mcl-1.

The binding between MAGE-C1 and Mcl-1 was mapped using two Myc-tagged deletion mutants for Mcl-1, covering its N-terminus (amino acids 1-127) and C-terminus (amino acids 128-350) (Figure 5.10A).

U2OS cells were transfected with a Myc-tagged full length Mcl-1 plasmid ($Mcl\text{-}1_{F.L.}$) or with these deletion mutants ($Mcl\text{-}1_{1\text{-}127}$ and $Mcl\text{-}1_{128\text{-}350}$), after which endogenous MAGE-C1 was immunoprecipitated. Since the interaction is strengthened by inhibition of the proteasome, MG132 treatment was also utilised. $Mcl\text{-}1_{F.L.}$ and the N-terminal $Mcl\text{-}1_{1\text{-}127}$ deletion mutant were stabilised by MG132 treatment and bound MAGE-C1 upon treatment. The C-terminal fragment $Mcl\text{-}1_{128\text{-}350}$ was not affected by MG132 treatment, suggesting that the N-terminal part of the PEST sequence is the one responsible for proteasome targeting, and did not bind MAGE-C1 (Figure 5.10B).

These results lead to two main observations: first, the BH domains of Mcl-1, which are shared by all the Bcl-2 family members and map at the C-terminus of the protein, are not involved in the binding, therefore the interaction with MAGE-C1 is not likely to be a feature of the entire Bcl-2 family; second, the portion of Mcl-1 which is sensitive to MG132 treatment and therefore responsible for proteasome degradation, namely the N-terminus, is also the one that bind to MAGE-C1, consistent with the fact that MAGE-C1 affects the stability of this protein.

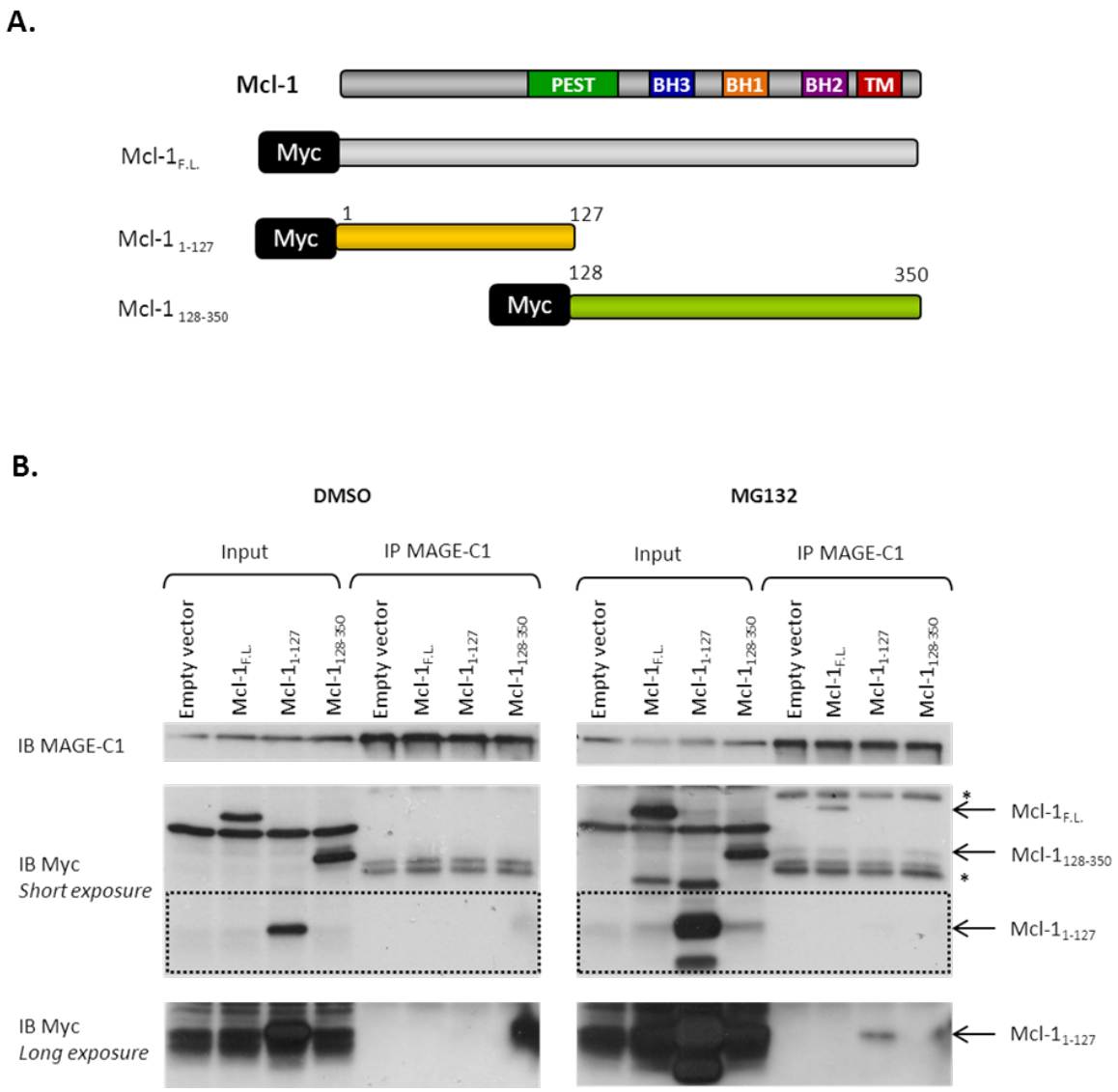

Figure 5.10 MAGE-C1 binds to the N-terminus of Mcl-1. Schematic representation of Mcl-$1_{F.L.}$ (full lenght) construct and deletion mutants Mcl-1_{1-127} and Mcl-$1_{128-350}$. All the fragments were subcloned in a pcDNA3.1/Myc plasmid. B. U2OS cells were transfected with Mcl-$1_{F.L.}$, Mcl-1_{1-127} and Mcl-$1_{128-350}$ vectors according to the Fugene6 protocol and treated with MG132 40µM or DMSO (negative control) for 4h. After treatment, MAGE-C1 was immunoprecipitated with CT7.33 mouse monoclonal antibody. The protein complexes were then analysed by SDS-PAGE and immunoblotted for MAGE-C1 (CT7.33 antibody) or Myc tag (9E10 mouse monoclonal antibody).* indicates IgG heavy and light chains.

5.2.8 MAGE-C1 is modified in mitosis.

As previously mentioned, Mcl-1 stability is strictly controlled through several post-translational modifications; recent publications revealed that, during mitotic arrest, phosphorylation of Mcl-1 by CDK1-cyclin B1 triggers its destruction in a Cdc20-dependent fashion (Harley et al., 2010). We observed that the pool of Mcl-1 that interacts with MAGE-C1 has a slightly higher molecular weight, possibly indicating post-translational modifications; therefore, we decided to test whether MAGE-C1 could influence Mcl-1 degradation in mitosis.

First of all we tested MAGE-C1 expression pattern: U2OS cells were treated with nocodazole, a drug that induces cell cycle arrest in the prometaphase of mitosis by interfering with the polymerisation of microtubules; mitotic cells (floating) were separated by shake-off from adherent cells. Interestingly, western blot analysis following treatment revealed that MAGE-C1 is post-translationally modified during mitosis, as a shift in the protein could be observed partially in the adherent cells and strikingly in the cells collected by shake-off (Figure 5.11A). This result was confirmed in SK-MEL-37 melanoma cell line (Figure 5.11B). After nocodazole treatment Mcl-1 was phosphorylated, as demonstrated by the shift in the western blot, and its levels decreased due to proteasome degradation as expected.

MAGE-C1 expression was then silenced in U2OS cells, which were treated with nocodazole and collected by shake-off. No difference in Mcl-1 levels or migration pattern was observed between normal and MAGE-C1 depleted cells (Figure 5.11C). Immunoprecipitation experiments performed in U2OS cells collecting mitotic vs. adherent cells showed that the binding between MAGE-C1 and Mcl-1 is not affected by nocodazole treatment. The amount of co-immunoprecipitated Mcl-1 in mitotic cells was lower than in untreated cells in agreement with the decrease in Mcl-1 due to its destruction (Figure 5.11D).

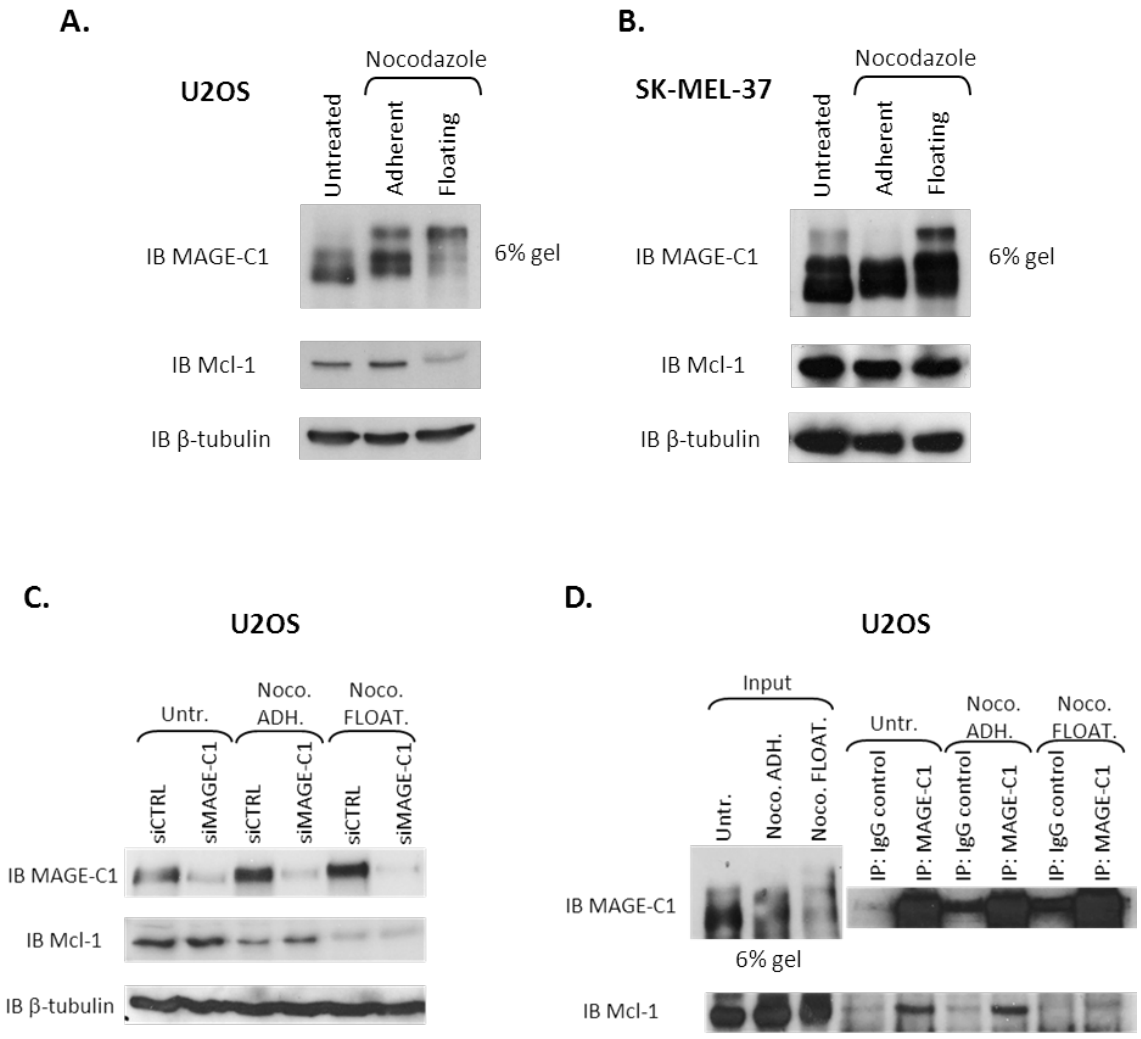

Figure 5.11 MAGE-C1 is modified in mitosis. U2OS cells (A) and SK-MEL-37 cells (B) were treated with nocodazole 10μM for 24h and the mitotic cells were separated by shake off (floating). Cells were lysed in urea buffer, analysed by SDS-PAGE, and immunoblotted for MAGE-C1 using mouse monoclonal CT7.33 antibody, with Mcl-1 rabbit polyclonal antibody or with β-tubulin mouse monoclonal antibody (as a loading control). C. U2OS cells were transfected with a MAGE-C1 specific siRNA (siMAGEC1) or a scrambled siRNA (siCTRL) according to the lipofectamine2000 protocol. 72h after transfection cells were treated with nocodazole 10μM for 24h and the mitotic cells were separated by shake off. Cells were lysed in urea buffer, analysed by SDS-PAGE, and immunoblotted for MAGE-C1 using mouse monoclonal CT7.33 antibody, with Mcl-1 rabbit polyclonal antibody or with β-tubulin mouse monoclonal antibody (as a loading control). D. U2OS cells were treated with nocodazole 10μM for 24h and the mitotic cells were separated by shake off. MAGE-C1 was immunoprecipitated with CT7.33 mouse monoclonal antibody. The protein complexes were then analysed by SDS-PAGE and immunoblotted for MAGE-C1 (CT7.33 antibody) or Mcl-1 (rabbit polyclonal antibody). Where indicated, 6% gels were utilised. In all other cases, 12% gels were used.

5.3 Summary and discussion

Several CT-X antigens have been described as oncogenes as they are able to favour tumourigenesis; on the other hand MAGE-A4 has been shown to inhibit gankyrin, which is an oncogene, and therefore to act as a tumour suppressor. This suggests extreme diversification and complexity in CT antigen role in cancer, which is further complicated by the fact that the function of many members of this family is poorly characterised or totally unknown, including the objects of our study, MAGE-C1 and NY-ESO-1.

To investigate the biological significance of the CT antigens MAGE-C1 and NY-ESO-1 we depleted their expression in U2OS and H1299 cancer cell lines respectively. We then gave the cells a range of different apoptotic stresses and finally analysed their apoptotic response. While we did not observe any effect of NY-ESO-1 depletion on cell survival, MAGE-C1 knockdown caused a significant increase of cell death in response to certain types of stress, namely heat shock, endoplasmic reticulum (ER) stress and UV irradiation.

Both heat shock and ER stress induce protein unfolding and degradation and cause transcriptional activation of molecular chaperones and elements of the ubiquitin–proteasome system (Kopito, 1997; Parsell et al., 1993). Interestingly, a genomic analysis has revealed targets of Hsf1, the main transcription factor mediating heat shock response (HSR), in the secretory pathway that are also induced by the unfolded protein response (UPR), such as GRP78 (Kohno et al., 1993) and ERV29 (Caldwell et al., 2001; Hahn et al., 2004). A more recent study of HSR targets revealed that more than 25% have function in common with UPR target. These findings suggest a role for HSR in ER quality control; indeed, HSR is activated by ER stress and can relieve ER stress-caused damage in UPR-deficient cells (Liu and Chang, 2008); conversely, heat stress can activate ER stress in the cortex of rats (Liu et al., 2012) and the ER stress pathway is also induced by mild heat shock (40ºC) in mammalian cells (Xu et al., 2011).

The link between UV irradiation and ER stress response has not been as thoroughly investigated, but it has been shown that UV light can inhibit protein synthesis through activation of PERK, a

UPR kinase localised to the endoplasmic reticulum (Wu et al., 2002); furthermore UV irradiation induces CHOP transcription factor in the skin of hairless mice, but not in cultured keratinocytes, suggesting a mechanism specific to intact skin (Anand et al., 2005). Additionally, UV irradiation, ER stress and heat shock all induce JNK, a member of the MAP kinase family that influence the cell-death machinery by phosphorylating some members of the Bcl-2 family, including Bcl-2 itself, Mcl-1, Bcl-xL and the BH3-only member Bim (Davis, 2000; Szegezdi et al., 2006). JNK mediated cell death upon heat shock can be inhibited by Heat shock protein 70 (Hsp70), which suppresses its phosphorylation and activation (Meriin et al., 1999; Mosser et al., 2000). It is therefore possible that the apoptotic responses observed after ER stress, heat shock and UV irradiation when silencing MAGE-C1 expression share common mediators.

Many different cell death signals result in induction of p53; this tumour suppressor is regulated among others by some member of the MAGE family of CT antigens, mainly through post-translation modification. Therefore we tested whether p53 was affected by MAGE-C1 RNAi, but we did not observe any alteration in p53 protein levels upon the induction of stress.

Then we proceeded to analyse the Bcl-2 family, which is essential for the intrinsic apoptotic pathway. We focused our attention on the apoptotic effect induced by ER stress, since it appeared consistent and specific, being observed with two drugs, tunicamycin and thapsigargin, which affect the ER through different mechanisms, i.e. impairing glycosylation and Ca^{2+} storage at the ER respectively.

Bcl-2 and Mcl-1 pro-survival proteins are particularly important for the ER stress-induced apoptotic response, therefore we checked their expression after tunicamycin treatment in cells depleted for MAGE-C1. Although Bcl-2 protein levels did not change, a decrease in Mcl-1 was observed upon treatment.

As mentioned above, Mcl-1 levels are tightly regulated through multiple mechanisms (Craig, 2002). We tested *Mcl-1* mRNA levels upon MAGE-C1 RNAi and tunicamycin treatment but no change was observed, therefore we ruled out an influence of MAGE-C1 on *Mcl-1* gene transcription.

Furthermore, our western blot analyses did not reveal any change in the migration pattern of Mcl-1 that could suggest the production of different isoforms or a caspase-dependent cleavage of Mcl-1 as a cause of MAGE-C1 RNAi-induced cell death (data not shown).

So we proceeded to examine the post-translational regulation of Mcl-1. This protein has a remarkably short half-life and is targeted for proteasome degradation upon ubiquitination by several E3 ligases. Its rapid turnover allows a prompt response of the cell to death signals, therefore it represents a fundamental mechanism for tuning Mcl-1 activity in stress conditions.

Being degraded by the proteasome pathway, Mcl-1 is stabilised by proteasome inhibitors like MG132. Therefore we decided to test whether MAGE-C1 could affect Mcl-1 protein stability by silencing its expression and analysing Mcl-1 accumulation upon MG132 treatment in ER stressed cells: indeed, we showed that MAGE-C1 depletion affects Mcl-1 stabilisation in tunicamycin-treated cells, suggesting a regulation at the post-translational level.

Immunoprecipitation experiments also showed that MAGE-C1 and Mcl-1 form a complex, especially upon MG132 treatment, and that MAGE-C1 binding partner NY-ESO-1 is not a member of this complex; moreover, the pool of Mcl-1 that binds MAGE-C1 runs in a gel at a higher molecular weight than the total Mcl-1, suggesting post-translational modifications. Mapping of the binding between MAGE-C1 and Mcl-1 performed using Mcl-1 deletion mutants revealed that the portion of Mcl-1 that binds to the CT antigen, namely the N-terminus fragment 1-127, is stabilised by MG132 treatment, strengthening the link of this interaction with Mcl-1 protein stabilisation.

It was previously shown that Mcl-1 is phosphorylated and degraded during mitotic arrest induced by drugs such as nocodazole and taxol. This promotes apoptosis if such arrest is irreversible, possibly by the release of Bak from sequestration (Chu et al., 2012; Harley et al., 2010; Tunquist et al., 2010; Wertz et al., 2011). We tested whether MAGE-C1 was involved in this process. Despite no changes were observed in the binding between the two proteins and in Mcl-1 degradation upon nocodazole treatment, suggesting that MAGE-C1 is not involved in regulating

Mcl-1 stability upon mitotic arrest, the experiment led to the interesting observation that MAGE-C1 itself is post-translational modified upon nocodazole treatment.

As a whole, we demonstrated that MAGE-C1 inhibits apoptosis induced by specific types of cellular stress and that, at least in response to ER stress, this effect could be mediated by binding to the N-terminus and stabilisation of the pro-survival protein Mcl-1.

Chapter VI: Conclusions and future perspectives

6.1 CT antigens are heterogeneously expressed in human cancer cell lines

The expression of most CT antigens is famously limited to the germ cells of the testis and to tumour cells. Furthermore, extensive immunohistochemical analyses of several CT proteins carried out in different cancer types highlighted a frequent heterogeneity in their pattern, with only a subpopulation of tumour cells showing CT gene expression (Figure 1.9). The reason for such a peculiar pattern has not been elucidated yet.

In the present study, we show that the CT antigens NY-ESO-1, MAGE-C1 and MAGE-C2 are heterogeneously expressed in cancer cell lines. Thus, we may have established an *in vitro* system for investigating CT antigen heterogeneity in cancer.

By screening a panel of 21 cancer cell lines (derived from melanoma, small cell lung cancer and multiple myeloma) we were able to observe expression of at least one of these genes in more than 85% of the cell lines (18 out of 21). Additionally, 67% of the cell lines (14 out of 21) expressed more than one CT antigen, and of these, all showed co-expression of the binding partners NY-ESO-1 and MAGE-C1. These results are in agreement with the fact that melanoma, lung cancer and myeloma are high CT expressers (Table 1.3) and that CT genes are frequently expressed in clusters (Sahin et al., 1998; Sugita et al., 2002). We also investigated the subcellular localisation of the three CT proteins in the various cell lines and we observed a heterogeneous pattern for one or more antigens in multiple cell lines (57%, 12 out of 21), resembling the one observed in tumour samples.

Intra-tumour heterogeneity has been an object of study for many decades (Fidler, 1978), although the lack of suitable technical tools prevented a thorough characterisation and a functional

exploration of this phenomenon. Recent advances showed that this variability is the result of both changes in the genome and non-genetic modifications. The former are facilitated by the large number of cell divisions and the genomic instability required for tumour formation, and can be identified via full genome or exome sequencing, as was recently demonstrated for renal carcinoma (Gerlinger et al., 2012). Instead, the origin of non-genetic heterogeneity is still under debate and has led to the concept of 'cancer stem cells' (CSC). It has been suggested that differences in the differentiation status are the main source of phenotypic variations in a tumour cell; only a small subset of less differentiated cancer cells, or CSCs, have the ability to initiate new tumour growth, while most tumour cells have only limited proliferative potential (Bapat et al., 2005; Collins et al., 2005; Singh et al., 2004; Wang and Dick, 2005). According to this theory, the relapse of cancer and the emergence of metastasis would also be attributed to these cells (Brabletz et al., 2005), therefore eradication of the stem cell compartment of a tumour might be the essential and most effective way of curing cancer and allowing long-lasting remission. One of the main challenges in the field is to unequivocally define CSCs, and the inclusion of additional biomarkers could not only improve the existent knowledge on CSCs, but also impinge on patient stratification and choice of therapy (Marusyk et al., 2012).

Some recent evidence link CT gene expression with 'stemness' in cancer (Costa et al., 2007). CT antigen expression was found in stem cells isolated from melanoma and glioma, as well as in human embryonic stem cells and mesenchymal stem cells; a downregulation was observed after the induction of differentiation (Cronwright et al., 2005; Lifantseva et al., 2011; Sigalotti et al., 2008; Yawata et al., 2010). Moreover, expression in the placenta has been detected (Jungbluth et al., 2007), and there is evidence for foetal and embryonic expression in somatic tissues for some CT antigens (Hofmann et al., 2008). It is also important to point out that most of these proteins have only been found in the spermatogonia in testis, and that their expression is silenced in later stages of sperm cell differentiation, suggesting that they might play a role in the maintenance of an undifferentiated state of the cell. As a consequence, a possible explanation for CT antigens

heterogeneous expression in some cell lines and tumour samples could be an association with a stem cell-like/undifferentiated status of the cancer cell.

Another hypothesis that might explain the intratumoural heterogeneity of CT antigens is a connection of their expression with the cell cycle. The pattern of expression observed could be related to a cell cycle phase-specific function of these proteins.

The poor understanding of CT antigen heterogeneity is strictly connected with a general lack of knowledge about their regulation, and linking their expression to a specific cell type/status could significantly enhance their usage as diagnostic, prognostic and therapeutic biomarkers. The heterogeneous cell lines we identified in our screening represent a new model that can be utilised to clarify the underlying mechanisms that cause ad control CT antigens expression in cancer cells.

6.2 Modulating MAGE-C1 stability: a novel potential function for NY-ESO-1

Previous studies showed that CT genes are normally silenced by methylation on their CpG rich promoters and that demethylation on such regions, as well as histone acetylation, is partially responsible for their aberrant re-expression in cancer (Scanlan et al., 2002b); however, this phenomenon does not explain, for example, the lack of expression of CT in some tumour types characterised by global hypomethylation (e.g. colon cancer) (Goelz et al., 1985), nor the heterogeneity observed in tumour samples and cancer cell lines. Moreover, we noticed that in heterogeneous cell lines different CT antigens are not always co-expressed in the same cell, and that within the same cell line the subcellular localisation of a CT protein can vary, i.e. be more nuclear or more cytoplasmic. Such complexity requires multiple levels of regulation that cannot be only ascribable to transcriptional mechanisms, but so far the post-translational regulation of CT antigens has not been addressed.

Our study revealed that the protein levels and the localisation of MAGE-C1 and its binding protein NY-ESO-1 are regulated by proteasome degradation, and that the stability of MAGE-C1 is modulated by NY-ESO-1.

We investigated the degradation of NY-ESO-1, MAGE-C1 and MAGE-C2 because these tumour antigens are cleaved to be presented by MHC class I molecules on the surface of tumour cells, a process that involves proteasome-mediated degradation (Kloetzel, 2004). Therefore, defining the role of the proteasome pathway in CT protein processing could potentially provide ways of influencing the immune response against CT-expressing tumour cells, as well as help elucidating their expression pattern and function.

We utilised the proteasome inhibitor MG132 to assess NY-ESO-1, MAGE-C1 and MAGE-C2 antigens degradation. Interestingly, we observed that inhibition of the proteasome causes accumulation of these three proteins in the insoluble cellular fraction. This suggests that their stabilisation could result in the formation of insoluble aggregates. Furthermore, the treatment caused an accumulation of NY-ESO-1 and MAGE-C1 at the centrosome, a structure that has a key role in cell division, being an area in the cell where microtubules are produced (Badano et al., 2005). In addition to its cell-cycle related functions, the centrosome is a site of proteasome concentration, as well as microtubule-dependent protein aggresome accumulation (Anton et al., 1999; Fabunmi et al., 2000; Wigley et al., 1999). Hence, NY-ESO-1 and MAGE-C1 could constitute insoluble aggregates in proximity of the centrosome upon increase in their intracellular levels due to inhibition of the proteasome or to transfection. This process could be utilised by the cell in physiological conditions as well, as we observed centrosome staining for NY-ESO-1 in an untreated cell line (H146).

MAGE-C1 and NY-ESO-1 were the first CT proteins shown to form a complex in cancer cells (Cho et al., 2006), but the role of this interaction has not been elucidated yet. Since MG132 induces accumulation of both proteins at the centrosome, we tested the effect of such treatment on their binding; intriguingly, we observed an enhancement in the interaction. Despite this, we proved via RNAi experiments that depletion of one or the other CT antigen does not affect the

localisation of the remaining member of the complex after MG132 treatment, suggesting that their co-expression is not a necessary requirement for centrosome accumulation.

We then identified the regions of sensitivity to proteasome inhibitors on MAGE-C1 and NY-ESO-1 by means of several deletion mutants for the two proteins. The MAGE homology domain (MHD) of MAGE-C1 was the only portion of the protein stabilised by MG132 treatment, in particular in the insoluble fraction. This result is interesting as this domain is shared by all the MAGE family members, therefore this feature of MAGE-C1 could potentially be extended to other MAGE proteins.

For NY-ESO-1, we were able to restrict the region of MG132 sensitivity to the fragment included between amino acids 91 and 150. The deletion mutants containing this part of sequence were also detected at the centrosome after MG132 treatment in SK-MEL-37 cells, strengthening the link between centrosome location and protein stabilisation.

Interestingly, the regions of sensitivity we identified for both MAGE-C1 and NY-ESO-1 correspond to previously characterised epitopes that are able to induce the CTL-mediated immune response (Anderson et al., 2011; Gnjatic et al., 2006). This corroborates our results, since these types of epitopes are the products of proteasome-dependent degradation.

Immunofluorescence staining showed that these deletion mutants of MAGE-C1 and NY-ESO-1 are more cytoplasmic than the proteasome-insensitive deletion mutants. Along the same line, we noticed that the staining of endogenous MAGE-C1 becomes more cytoplasmic upon MG132 treatment. These observations are particularly interesting in the context of multiple myeloma (MM): in fact a previous study showed that myelomas with nuclear-cytoplasmic or nuclear only staining of MAGE-C1 have a worse prognosis if compared with myelomas with cytoplasmic only MAGE-C1 (Tinguely et al., 2008). This tumour type frequently expresses MAGE-C1 and NY-ESO-1 (66% and 22% of cases respectively, Table 1.3) and 93% of MAGE-C1-positive myelomas elicit a detectable humoral and cellular immune response against this antigen (Curioni-Fontecedro et al., 2008; Lendvai et al., 2010). MM accounts for more than 10% of all haematological malignancies and, despite use of autologous stem cell transplantation and other

therapy combinations, the disease recurs in almost all patients and median survival has not improved beyond 4–5 years. The introduction of the proteasome inhibitor bortezomib for the therapy of post-transplant relapsed patients has been a major breakthrough in the treatment of multiple myeloma due to increased progression-free and overall survival. This drug showed several anti-myeloma effects including disruption of the cell cycle, alteration of the bone marrow microenvironment and inhibition of nuclear factor kappa B (NFκB) (Mahindra et al., 2012). According to our results, bortezomib should also induce accumulation of insoluble MAGE-C1 in multiple myeloma cells, which could result in toxicity and contribute to apoptosis. Moreover, bortezomib could potentially cause a partial translocation of MAGE-C1 from the nucleus to the cytoplasm, which as mentioned is correlated with a better prognosis.

We also observed a mobility shift in MAGE-C1 protein upon MG132 treatment, probably corresponding to a post-translational modification. The first hypothesis we tested was ubiquitination, as it is well established that MG132 blocks the degradation of ubiquitin-labelled proteins. Our results showed that the modification is not abolished by incubation with the purified de-ubiquitinating enzyme USP2, which is able to remove ubiquitin from a wide range of target proteins. Nevertheless, MAGE-C1 might not be one of these targets, therefore stronger evidence is needed to exclude MAGE-C1 ubiquitination. Similar experiments were performed with a de-glycosylating enzyme (PNGase F), which did not affect MAGE-C1 mobility shift. Instead, we showed that MAGE-C1 is modified by SUMO-1 conjugation, both after MG132 treatment and in steady state. This post-translational modification is fundamental for cell viability and is involved in a wide variety of processes including transcription and protein nuclear-cytoplasmic translocation (Hay, 2005). Interestingly, the two putative SUMOylation sites we identified on MAGE-C1 are conserved within the MAGE proteins, meaning that other members of the family could also be SUMO-1 modified. An exception is the nuclear protein MAGE-C2, whose sequence does not present these two sites. Differently from MAGE-C2, MAGE-C1 is localised both in the nucleus and in the cytoplasm, with diverse patterns in different cell lines as well as within the same cell line, suggesting it might shuttle between the two compartments. Moreover, preliminary

results showed that the nuclear fraction of MAGE-C1 presents a mobility shift if compared to the cytoplasmic fraction. Therefore, we could speculate that SUMOylation of MAGE-C1 causes its retention in the nucleus and possibly influences its function.

Once we demonstrated that MAGE-C1 and NY-ESO-1 binding is affected by proteasome inhibitors, we wondered whether this phenomenon could have a functional outcome on the complex. Indeed, co-transfection experiments of MAGE-C1 deletion mutants with full length NY-ESO-1 demonstrated that upon MG132 treatment MAGE-C1 MHD stabilisation in the insoluble fraction is increased in the presence of NY-ESO-1, whereas the N-terminus of MAGE-C1 is not affected. The MHD also mediates the interaction between MAGE-C1 and NY-ESO-1 (Cho et al., 2006) and corresponds to the portion stabilised by proteasome inhibitors. Therefore we can hypothesise that NY-ESO-1 binding to the MHD of MAGE-C1 causes a stabilisation of MAGE-C1 protein. It is possible that MAGE-C1 also has an effect on NY-ESO-1 stability, although the lack of a full length plasmid for MAGE-C1 prevented us from investigating this with the same approach we used with full length NY-ESO-1. More evidence is needed to clarify whether these two proteins protect each other from proteasome degradation.

In the future, we will further investigate the role of proteasome inhibitors in regulating MAGE-C1 and NY-ESO-1 in human tumour samples. This will be tested via immunohistochemical examination of MM samples treated with bortezomib vs. untreated samples, which would provide a significant *in vivo* validation of our cellular data.

Furthermore, the SUMO-1 modification of MAGE-C1 will be analysed more in depth. First of all we will confirm that the SUMOylation site is located in the MHD and we will identify the residue responsible for the modification by mutating the lysines highlighted by the prediction programmes. Such mutations will also allow us to determine whether MAGE-C1 subcellular localisation is dependent on SUMO-conjugation.

Another important question to address is whether the stabilisation of MAGE-C1 due to NY-ESO-1 could influence their biological function. The role of these two proteins in tumour cells has not

been thoroughly investigated yet; a better understanding of the cellular pathways they are involved in would help establishing whether the modulation of their expression, for instance with proteasome inhibitors or demethylating agents, could affect the molecular properties of the tumour and represent a tool for cancer therapy.

6.3 MAGE-C1 and Mcl-1: a role in ER stress-induced apoptosis

Previous studies showed that MAGE-C1 exerts a pro-survival function in multiple myeloma cells (Atanackovic et al., 2010; Jungbluth et al., 2005). This neoplasm is characterised by abnormal proliferation of plasma cells and overproduction and secretion of monoclonal antibodies, which require a fully functional endoplasmic reticulum. As a consequence, myeloma cells are very sensitive to endoplasmic reticulum stress. As mentioned above, MM is often treated with proteasome inhibitors that, among other effects, cause accumulation of newly synthesised immunoglobulins in the endoplasmic reticulum of tumour cells, ER stress and apoptosis (Mahindra et al., 2012).

We demonstrated that MAGE-C1 inhibits ER stress-induced apoptosis; furthermore, we showed that depletion of this CT antigen results in decreased stabilisation of Mcl-1 oncogene in ER stress conditions.

Our analysis revealed that MAGE-C1 transient knockdown causes an increase in apoptosis in response to two drugs, tunicamycin and thapsigargin, which induce ER stress through different mechanisms. An enhancement in cell death was also observed in steady state and in response to heat shock and UV irradiation. Considering MAGE-C1 biological role in MM and the ER stress importance for this pathology, we decided to focus our attention on the role of MAGE-C1 in ER stress-induced apoptosis and to try and elucidate the underlying molecular mechanism.

Intriguingly, we observed that MAGE-C1 RNAi impacts on the levels of the pro-survival Mcl-1 protein in tunicamycin treated cells. Mcl-1 belongs to the Bcl-2 family of proteins, which are key

players in regulating apoptosis. It is target of proteasome degradation and its short half-life makes it an ideal mediator of stress-induced cell death, as it allows a rapid response that can be promptly turned off when the stress stimulus stops (Craig, 2002). As a consequence, Mcl-1 plays a role in a variety of stress-induced pathways, including ER stress (Jiang et al., 2008; Jiang et al., 2009).
Upon tunicamycin treatment, MAGE-C1 depleted cells presented significantly lower levels of Mcl-1 protein. Quantitative RT-PCR analysis did not highlight differences in *Mcl-1* mRNA levels, suggesting that MAGE-C1 enhances Mcl-1 protein stability rather than *Mcl-1* transcription. Consistent with this, MAGE-C1 depletion decreased Mcl-1 stabilisation by MG132 proteasome inhibitor. Such effect could be mediated by the interaction of the two proteins, as we were able to co-immunoprecipitate MAGE-C1 and Mcl-1 and their binding was enhanced by MG132 treatment. Mapping of the interaction utilising Mcl-1 deletion mutants revealed that MAGE-C1 binds to the N-terminus of Mcl-1, which also corresponds to the portion of the protein that is stabilised by MG132 treatment.

The mechanism through which MAGE-C1 influences Mcl-1 stability in response to ER stress needs further investigation. One possibility is that MAGE-C1 impairs the binding of Mcl-1 with one of the E3 ubiquitin ligases that have been reported to target Mcl-1 for degradation. This is a potentially interesting hypothesis to test since a recent study showed that several MAGE proteins, including the MAGE-C1-homologue MAGE-C2, act as co-factors of E3 ubiquitin ligases (Doyle et al., 2010). Most E3 ligases that bind Mcl-1, including $SCF^{\beta TrCP}$, SCF^{Fbw7} and APC/C^{Cdc20}, require phosphorylation to recognise their target (Harley et al., 2010; Inuzuka et al., 2011b; Maurer et al., 2006). Intriguingly, the fraction of Mcl-1 that binds MAGE-C1 shows a molecular weight which is slightly higher than Mcl-1, possibly corresponding to a phosphorylated form. APC/C^{Cdc20} and SCF^{Fbw7} ubiquitinate phosphorylated Mcl-1 during mitotic arrest, so we tested MAGE-C1 effect on Mcl-1 upon nocodazole treatment. Despite no difference was observed in Mcl-1 levels and binding with MAGE-C1, we detected a post-translational modification of MAGE-C1 in nocodazole-treated cells yet to be identified; so it is possible that this protein also

plays a role in nocodazole-induced cell cycle arrest and apoptosis. Another interesting Mcl-1 E3 ligase is Mule, which is expressed in early germ cells of the testis but not in spermatids (Liu et al., 2007; Zhong et al., 2005), a pattern that resembles that of MAGE-C1.

Alternatively, MAGE-C1 could affect the interaction of Mcl-1 with the other Bcl-2 family members; for example, binding of Mcl-1 with Bim or Puma enhances its stability (Mei et al., 2005; Wuilleme-Toumi et al., 2007). If this is the case, the inhibitory effect of MAGE-C1 on ER stress-induced apoptosis could also be the result of a disruption of the balance in the oligomerisation of Mcl-1 with pro-apoptotic Bcl-2 proteins.

Again, multiple myeloma represents an attractive system to extend our functional analysis in the future, for several reasons. First of all, Mcl-1 has a central regulatory role as a proliferation checkpoint in this tumour type; among the Bcl-2 family proteins, Mcl-1, rather than Bcl-2 or Bcl-xL, promotes MM cell survival (Derenne et al., 2002; Zhang et al., 2002) and is required for VEGF and IL-6-induced proliferation (Jourdan et al., 2000; Le Gouill et al., 2004). Secondly, as mentioned above this malignancy heavily relies on the ER to cope with the extremely high rate of antibody synthesis and secretion. Accordingly, early work demonstrated that myeloma cell lines frequently overexpress XBP1 transcription factor (Claudio et al., 2002). This protein regulates many genes of the unfolded protein response (UPR) in metazoans, including chaperones, genes related to the proteasome degradation machinery and genes involved in generation of the ER membrane (Sriburi et al., 2004). New therapeutic agents being developed to treat myeloma may exploit the dependence of this neoplasm on UPR activation and clarifying the role of MAGE-C1 could provide new tools to target this pathway that potentially have wide applicability, considering the high frequency of MAGE-C1 expression in MM.

The impact of NY-ESO-1 on MAGE-C1 function will also be an interesting point to address in the future: we have showed that NY-ESO-1 can influence the stability of MAGE-C1 protein; the next step will be to test whether such stabilisation impinges on MAGE-C1 inhibition of ER stress-induced cell death.

In conclusion, we have showed that CT antigens present a heterogeneous pattern of expression in cancer cell lines which resembles the one observed in tumours. Moreover, we have described three different post-translational mechanisms that regulate MAGE-C1 protein, namely proteasome degradation, binding with NY-ESO-1 and SUMOylation Finally, we have reported a novel, inhibitory function of MAGE-C1 on ER stress-induced apoptosis in cancer cells that could be mediated by Mcl-1 oncogene stabilisation (Figure 6.1). Our findings expand the limited biological knowledge about these CT antigens and provide new insights for their manipulation in cancer for therapeutic purposes.

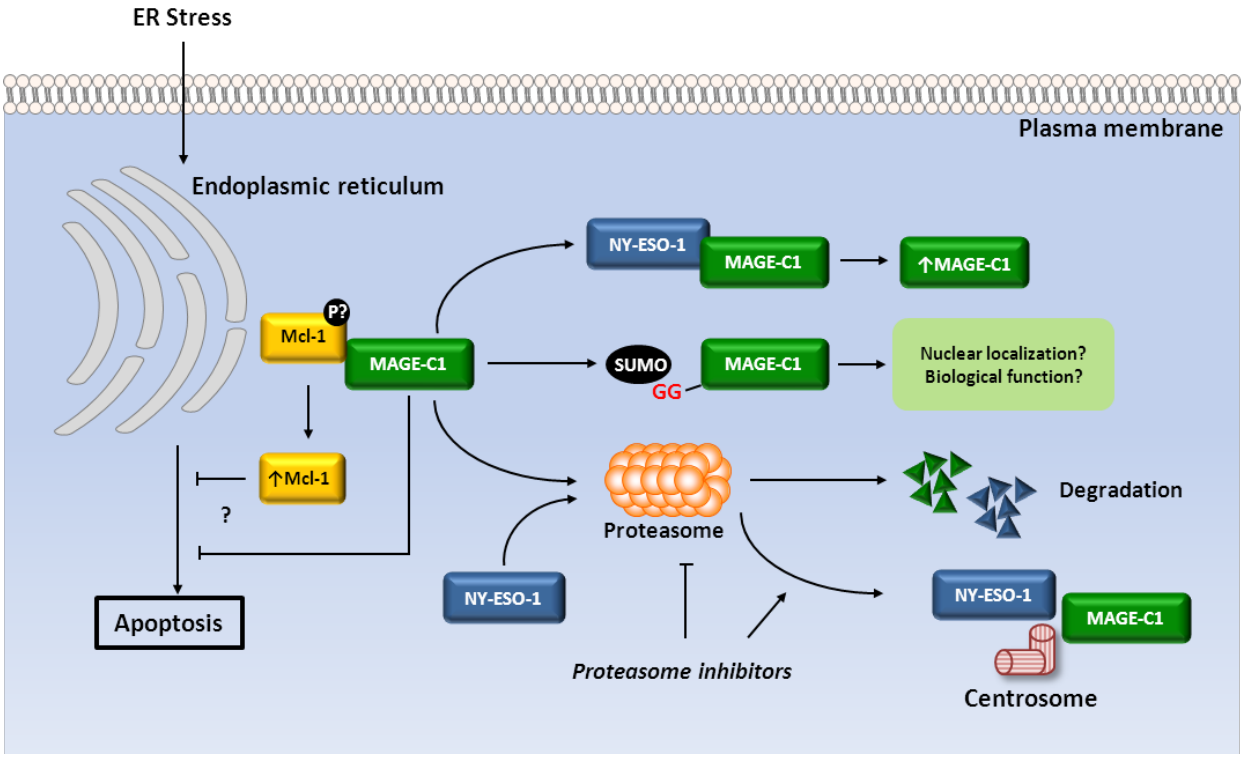

Figure 6.1 Model illustrating MAGE-C1 inhibition of ER stress-induced apoptosis and MAGE-C1 protein regulation. Upon ER stress, MAGE-C1 stabilises Mcl-1 protein, possibly by binding to a phosphorylated form of Mcl-1. Inhibition of apoptosis could occur through Mcl-1 stabilisation and via other still uncharacterised mechanisms. MAGE-C1 is stabilised by NY-ESO-1 whereas both MAGE-C1 and NY-ESO-1 are degraded by the proteasome pathway. Inhibition of proteasome degradation leads to accumulation of MAGE-C1 and NY-ESO-1 at the centrosome. Finally, MAGE-C1 is post-translationally modified by SUMOylation.

References

Aarnoudse, C.A., van den Doel, P.B., Heemskerk, B., and Schrier, P.I. (1999). Interleukin-2-induced, melanoma-specific T cells recognize CAMEL, an unexpected translation product of LAGE-1. Int J Cancer *82*, 442-448.

Aebischer, J., Sturny, R., Andrieu, D., Rieusset, A., Schaller, F., Geib, S., Raoul, C., and Muscatelli, F. (2011). Necdin protects embryonic motoneurons from programmed cell death. PLoS One *6*, e23764.

Almeida, L.G., Sakabe, N.J., deOliveira, A.R., Silva, M.C., Mundstein, A.S., Cohen, T., Chen, Y.T., Chua, R., Gurung, S., Gnjatic, S.*, et al.* (2009). CTdatabase: a knowledge-base of high-throughput and curated data on cancer-testis antigens. Nucleic Acids Res *37*, D816-819.

Alnemri, E.S., Livingston, D.J., Nicholson, D.W., Salvesen, G., Thornberry, N.A., Wong, W.W., and Yuan, J. (1996). Human ICE/CED-3 protease nomenclature. Cell *87*, 171.

Alpen, B., Gure, A.O., Scanlan, M.J., Old, L.J., and Chen, Y.T. (2002). A new member of the NY-ESO-1 gene family is ubiquitously expressed in somatic tissues and evolutionarily conserved. Gene *297*, 141-149.

Anand, S., Chakrabarti, E., Kawamura, H., Taylor, C.R., and Maytin, E.V. (2005). Ultraviolet light (UVB and UVA) induces the damage-responsive transcription factor CHOP/gadd153 in murine and human epidermis: evidence for a mechanism specific to intact skin. J Invest Dermatol *125*, 323-333.

Anderson, L.D., Jr., Cook, D.R., Yamamoto, T.N., Berger, C., Maloney, D.G., and Riddell, S.R. (2011). Identification of MAGE-C1 (CT-7) epitopes for T-cell therapy of multiple myeloma. Cancer Immunol Immunother *60*, 985-997.

Andrade, V.C., Vettore, A.L., Felix, R.S., Almeida, M.S., Carvalho, F., Oliveira, J.S., Chauffaille, M.L., Andriolo, A., Caballero, O.L., Zago, M.A.*, et al.* (2008). Prognostic impact of cancer/testis antigen expression in advanced stage multiple myeloma patients. Cancer Immun *8*, 2.

Anelli, T., and Sitia, R. (2008). Protein quality control in the early secretory pathway. EMBO J *27*, 315-327.

Anthoney, D.A., McIlwrath, A.J., Gallagher, W.M., Edlin, A.R., and Brown, R. (1996). Microsatellite instability, apoptosis, and loss of p53 function in drug-resistant tumor cells. Cancer Res *56*, 1374-1381.

Anton, L.C., Schubert, U., Bacik, I., Princiotta, M.F., Wearsch, P.A., Gibbs, J., Day, P.M., Realini, C., Rechsteiner, M.C., Bennink, J.R.*, et al.* (1999). Intracellular localization of proteasomal degradation of a viral antigen. J Cell Biol *146*, 113-124.

Aoyama, J., Akazawa, Y., Kasahara, K., Higashiyama, Y., Kikuchi, I., Fukumoto, Y., Saburi, S., Nakayama, Y., Fukuda, M.N., and Yamaguchi, N. (2008). Nuclear localization of magphinins, alternative splicing products of the human trophinin gene. J Cell Biochem *103*, 765-777.

Aprelikova, O., Pandolfi, S., Tackett, S., Ferreira, M., Salnikow, K., Ward, Y., Risinger, J.I., Barrett, J.C., and Niederhuber, J. (2009). Melanoma antigen-11 inhibits the hypoxia-inducible factor prolyl hydroxylase 2 and activates hypoxic response. Cancer Res *69*, 616-624.

Ardley, H.C., Scott, G.B., Rose, S.A., Tan, N.G., Markham, A.F., and Robinson, P.A. (2003). Inhibition of proteasomal activity causes inclusion formation in neuronal and non-neuronal cells overexpressing Parkin. Mol Biol Cell *14*, 4541-4556.

Asher, G., Lotem, J., Tsvetkov, P., Reiss, V., Sachs, L., and Shaul, Y. (2003). P53 hot-spot mutants are resistant to ubiquitin-independent degradation by increased binding to NAD(P)H:quinone oxidoreductase 1. Proc Natl Acad Sci U S A *100*, 15065-15070.

Ashkenazi, A. (2002). Targeting death and decoy receptors of the tumour-necrosis factor superfamily. Nat Rev Cancer *2*, 420-430.

Askew, E.B., Bai, S., Blackwelder, A.J., and Wilson, E.M. (2010). Transcriptional synergy between melanoma antigen gene protein-A11 (MAGE-11) and p300 in androgen receptor signaling. J Biol Chem *285*, 21824-21836.

Askew, E.B., Bai, S., Hnat, A.T., Minges, J.T., and Wilson, E.M. (2009). Melanoma antigen gene protein-A11 (MAGE-11) F-box links the androgen receptor NH2-terminal transactivation domain to p160 coactivators. J Biol Chem *284*, 34793-34808.

Atanackovic, D., Hildebrandt, Y., Jadczak, A., Cao, Y., Luetkens, T., Meyer, S., Kobold, S., Bartels, K., Pabst, C., Lajmi, N.*, et al.* (2010). Cancer-testis antigens MAGE-C1/CT7 and MAGE-A3 promote the survival of multiple myeloma cells. Haematologica *95*, 785-793.

Atanackovic, D., Luetkens, T., Hildebrandt, Y., Arfsten, J., Bartels, K., Horn, C., Stahl, T., Cao, Y., Zander, A.R., Bokemeyer, C.*, et al.* (2009). Longitudinal analysis and prognostic effect of cancer-testis antigen expression in multiple myeloma. Clin Cancer Res *15*, 1343-1352.

Aubry, F., Satie, A.P., Rioux-Leclercq, N., Rajpert-De Meyts, E., Spagnoli, G.C., Chomez, P., De Backer, O., Jegou, B., and Samson, M. (2001). MAGE-A4, a germ cell specific marker, is expressed differentially in testicular tumors. Cancer *92*, 2778-2785.

Azuma, T., Makita, M., Ninomiya, K., Fujita, S., Harada, M., and Yasukawa, M. (2002). Identification of a novel WT1-derived peptide which induces human leucocyte antigen-A24-restricted anti-leukaemia cytotoxic T lymphocytes. Br J Haematol *116*, 601-603.

Badano, J.L., Teslovich, T.M., and Katsanis, N. (2005). The centrosome in human genetic disease. Nat Rev Genet *6*, 194-205.

Bai, S., He, B., and Wilson, E.M. (2005). Melanoma antigen gene protein MAGE-11 regulates androgen receptor function by modulating the interdomain interaction. Mol Cell Biol *25*, 1238-1257.

Bai, S., and Wilson, E.M. (2008). Epidermal-growth-factor-dependent phosphorylation and ubiquitinylation of MAGE-11 regulates its interaction with the androgen receptor. Mol Cell Biol *28*, 1947-1963.

Bainton, D.F. (1981). The discovery of lysosomes. J Cell Biol *91*, 66s-76s.

Ballestrero, A., Boy, D., Moran, E., Cirmena, G., Brossart, P., and Nencioni, A. (2008). Immunotherapy with dendritic cells for cancer. Adv Drug Deliv Rev *60*, 173-183.

Bandic, D., Juretic, A., Sarcevic, B., Separovic, V., Kujundzic-Tiljak, M., Hudolin, T., Spagnoli, G.C., Covic, D., and Samija, M. (2006). Expression and possible prognostic role of MAGE-A4,

NY-ESO-1, and HER-2 antigens in women with relapsing invasive ductal breast cancer: retrospective immunohistochemical study. Croat Med J *47*, 32-41.

Bapat, S.A., Mali, A.M., Koppikar, C.B., and Kurrey, N.K. (2005). Stem and progenitor-like cells contribute to the aggressive behavior of human epithelial ovarian cancer. Cancer research *65*, 3025-3029.

Barker, P.A., and Salehi, A. (2002). The MAGE proteins: emerging roles in cell cycle progression, apoptosis, and neurogenetic disease. J Neurosci Res *67*, 705-712.

Bartek, J., and Lukas, J. (2007). DNA damage checkpoints: from initiation to recovery or adaptation. Curr Opin Cell Biol *19*, 238-245.

Bartel, D.P. (2004). MicroRNAs: genomics, biogenesis, mechanism, and function. Cell *116*, 281-297.

Baumeister, W., Walz, J., Zuhl, F., and Seemuller, E. (1998). The proteasome: paradigm of a self-compartmentalizing protease. Cell *92*, 367-380.

Bence, N.F., Sampat, R.M., and Kopito, R.R. (2001). Impairment of the ubiquitin-proteasome system by protein aggregation. Science *292*, 1552-1555.

Bernardi, P., Scorrano, L., Colonna, R., Petronilli, V., and Di Lisa, F. (1999). Mitochondria and cell death. Mechanistic aspects and methodological issues. Eur J Biochem *264*, 687-701.

Bertram, J., Palfner, K., Hiddemann, W., and Kneba, M. (1998). Elevated expression of S100P, CAPL and MAGE 3 in doxorubicin-resistant cell lines: comparison of mRNA differential display reverse transcription-polymerase chain reaction and subtractive suppressive hybridization for the analysis of differential gene expression. Anticancer Drugs *9*, 311-317.

Bertrand, M.J., Kenchappa, R.S., Andrieu, D., Leclercq-Smekens, M., Nguyen, H.N., Carter, B.D., Muscatelli, F., Barker, P.A., and De Backer, O. (2008). NRAGE, a p75NTR adaptor protein, is required for developmental apoptosis in vivo. Cell Death Differ *15*, 1921-1929.

Bestor, T.H. (1998). Gene silencing. Methylation meets acetylation. Nature *393*, 311-312.

Bhan, S., Negi, S.S., Shao, C., Glazer, C.A., Chuang, A., Gaykalova, D.A., Sun, W., Sidransky, D., Ha, P.K., and Califano, J.A. (2011). BORIS binding to the promoters of cancer testis antigens, MAGEA2, MAGEA3, and MAGEA4, is associated with their transcriptional activation in lung cancer. Clin Cancer Res *17*, 4267-4276.

Bhatia, N., Yang, B., Xiao, T.Z., Peters, N., Hoffmann, M.F., and Longley, B.J. (2011). Identification of novel small molecules that inhibit protein-protein interactions between MAGE and KAP-1. Arch Biochem Biophys *508*, 217-221.

Bhattacharya, A., Deng, J.M., Zhang, Z., Behringer, R., de Crombrugghe, B., and Maity, S.N. (2003). The B subunit of the CCAAT box binding transcription factor complex (CBF/NF-Y) is essential for early mouse development and cell proliferation. Cancer Res *63*, 8167-8172.

Black, R.A., Kronheim, S.R., and Sleath, P.R. (1989). Activation of interleukin-1 beta by a co-induced protease. FEBS Lett *247*, 386-390.

Boatright, K.M., Renatus, M., Scott, F.L., Sperandio, S., Shin, H., Pedersen, I.M., Ricci, J.E., Edris, W.A., Sutherlin, D.P., Green, D.R.*, et al.* (2003). A unified model for apical caspase activation. Mol Cell *11*, 529-541.

Boel, P., Wildmann, C., Sensi, M.L., Brasseur, R., Renauld, J.C., Coulie, P., Boon, T., and van der Bruggen, P. (1995). BAGE: a new gene encoding an antigen recognized on human melanomas by cytolytic T lymphocytes. Immunity *2*, 167-175.

Bolli, M., Schultz-Thater, E., Zajac, P., Guller, U., Feder, C., Sanguedolce, F., Carafa, V., Terracciano, L., Hudolin, T., Spagnoli, G.C.*, et al.* (2005). NY-ESO-1/LAGE-1 coexpression with MAGE-A cancer/testis antigens: a tissue microarray study. International journal of cancer *115*, 960-966.

Boon, T., Cerottini, J.C., Van den Eynde, B., van der Bruggen, P., and Van Pel, A. (1994). Tumor antigens recognized by T lymphocytes. Annu Rev Immunol *12*, 337-365.

Bos, J.L. (1989). ras oncogenes in human cancer: a review. Cancer Res *49*, 4682-4689.

Boyce, M., and Yuan, J. (2006). Cellular response to endoplasmic reticulum stress: a matter of life or death. Cell Death Differ *13*, 363-373.

Brabletz, T., Jung, A., Spaderna, S., Hlubek, F., and Kirchner, T. (2005). Opinion: migrating cancer stem cells - an integrated concept of malignant tumour progression. Nat Rev Cancer *5*, 744-749.

Brasseur, F., Rimoldi, D., Lienard, D., Lethe, B., Carrel, S., Arienti, F., Suter, L., Vanwijck, R., Bourlond, A., Humblet, Y.*, et al.* (1995). Expression of MAGE genes in primary and metastatic cutaneous melanoma. Int J Cancer *63*, 375-380.

Brenner, S. (1974). The genetics of Caenorhabditis elegans. Genetics *77*, 71-94.

Brichard, V., Van Pel, A., Wolfel, T., Wolfel, C., De Plaen, E., Lethe, B., Coulie, P., and Boon, T. (1993). The tyrosinase gene codes for an antigen recognized by autologous cytolytic T lymphocytes on HLA-A2 melanomas. J Exp Med *178*, 489-495.

Brinkmann, U., Vasmatzis, G., Lee, B., and Pastan, I. (1999). Novel genes in the PAGE and GAGE family of tumor antigens found by homology walking in the dbEST database. Cancer Res *59*, 1445-1448.

Brinkmann, U., Vasmatzis, G., Lee, B., Yerushalmi, N., Essand, M., and Pastan, I. (1998). PAGE-1, an X chromosome-linked GAGE-like gene that is expressed in normal and neoplastic prostate, testis, and uterus. Proc Natl Acad Sci U S A *95*, 10757-10762.

Brossart, P., Heinrich, K.S., Stuhler, G., Behnke, L., Reichardt, V.L., Stevanovic, S., Muhm, A., Rammensee, H.G., Kanz, L., and Brugger, W. (1999). Identification of HLA-A2-restricted T-cell epitopes derived from the MUC1 tumor antigen for broadly applicable vaccine therapies. Blood *93*, 4309-4317.

Brunelli, S., Tagliafico, E., De Angelis, F.G., Tonlorenzi, R., Baesso, S., Ferrari, S., Niinobe, M., Yoshikawa, K., Schwartz, R.J., Bozzoni, I.*, et al.* (2004). Msx2 and necdin combined activities are required for smooth muscle differentiation in mesoangioblast stem cells. Circ Res *94*, 1571-1578.

Bruno, B., Rotta, M., Patriarca, F., Mordini, N., Allione, B., Carnevale-Schianca, F., Giaccone, L., Sorasio, R., Omede, P., Baldi, I.*, et al.* (2007). A comparison of allografting with autografting for newly diagnosed myeloma. N Engl J Med *356*, 1110-1120.

Bush, J.R., and Wevrick, R. (2012). Loss of the Prader-Willi obesity syndrome protein necdin promotes adipogenesis. Gene.

Busso, D., Cohen, D.J., Hayashi, M., Kasahara, M., and Cuasnicu, P.S. (2005). Human testicular protein TPX1/CRISP-2: localization in spermatozoa, fate after capacitation and relevance for gamete interaction. Mol Hum Reprod *11*, 299-305.

Caballero, O.L., Zhao, Q., Rimoldi, D., Stevenson, B.J., Svobodova, S., Devalle, S., Rohrig, U.F., Pagotto, A., Michielin, O., Speiser, D.*, et al.* (2010). Frequent MAGE mutations in human melanoma. PLoS One *5*.

Caldwell, S.R., Hill, K.J., and Cooper, A.A. (2001). Degradation of endoplasmic reticulum (ER) quality control substrates requires transport between the ER and Golgi. J Biol Chem *276*, 23296-23303.

Calin, G.A., Dumitru, C.D., Shimizu, M., Bichi, R., Zupo, S., Noch, E., Aldler, H., Rattan, S., Keating, M., Rai, K.*, et al.* (2002). Frequent deletions and down-regulation of micro- RNA genes miR15 and miR16 at 13q14 in chronic lymphocytic leukemia. Proc Natl Acad Sci U S A *99*, 15524-15529.

Carrasco, D.R., Sukhdeo, K., Protopopova, M., Sinha, R., Enos, M., Carrasco, D.E., Zheng, M., Mani, M., Henderson, J., Pinkus, G.S.*, et al.* (2007). The differentiation and stress response factor XBP-1 drives multiple myeloma pathogenesis. Cancer Cell *11*, 349-360.

Carrillo-Infante, C., Abbadessa, G., Bagella, L., and Giordano, A. (2007). Viral infections as a cause of cancer (review). Int J Oncol *30*, 1521-1528.

Chapman, E.J., Kelly, G., and Knowles, M.A. (2008). Genes involved in differentiation, stem cell renewal, and tumorigenesis are modulated in telomerase-immortalized human urothelial cells. Mol Cancer Res *6*, 1154-1168.

Chen, L., Willis, S.N., Wei, A., Smith, B.J., Fletcher, J.I., Hinds, M.G., Colman, P.M., Day, C.L., Adams, J.M., and Huang, D.C. (2005). Differential targeting of prosurvival Bcl-2 proteins by their BH3-only ligands allows complementary apoptotic function. Mol Cell *17*, 393-403.

Chen, Q., Jackson, H., Parente, P., Luke, T., Rizkalla, M., Tai, T.Y., Zhu, H.C., Mifsud, N.A., Dimopoulos, N., Masterman, K.A.*, et al.* (2004). Immunodominant CD4+ responses identified in a patient vaccinated with full-length NY-ESO-1 formulated with ISCOMATRIX adjuvant. Proc Natl Acad Sci U S A *101*, 9363-9368.

Chen, Y.T., Boyer, A.D., Viars, C.S., Tsang, S., Old, L.J., and Arden, K.C. (1997a). Genomic cloning and localization of CTAG, a gene encoding an autoimmunogenic cancer-testis antigen NY-ESO-1, to human chromosome Xq28. Cytogenet Cell Genet *79*, 237-240.

Chen, Y.T., Ross, D.S., Chiu, R., Zhou, X.K., Chen, Y.Y., Lee, P., Hoda, S.A., Simpson, A.J., Old, L.J., Caballero, O.*, et al.* (2011). Multiple cancer/testis antigens are preferentially expressed in hormone-receptor negative and high-grade breast cancers. PLoS One *6*, e17876.

Chen, Y.T., Scanlan, M.J., Sahin, U., Tureci, O., Gure, A.O., Tsang, S., Williamson, B., Stockert, E., Pfreundschuh, M., and Old, L.J. (1997b). A testicular antigen aberrantly expressed in human cancers detected by autologous antibody screening. Proc Natl Acad Sci U S A *94*, 1914-1918.

Cheng, Y., Buffone, M.G., Kouadio, M., Goodheart, M., Page, D.C., Gerton, G.L., Davidson, I., and Wang, P.J. (2007). Abnormal sperm in mice lacking the Taf7l gene. Mol Cell Biol *27*, 2582-2589.

Chitale, D.A., Jungbluth, A.A., Marshall, D.S., Leitao, M.M., Hedvat, C.V., Kolb, D., Spagnoli, G.C., Iversen, K., and Soslow, R.A. (2005). Expression of cancer-testis antigens in endometrial carcinomas using a tissue microarray. Mod Pathol *18*, 119-126.

Chng, W.J., and Fonseca, R. (2009). Centrosomes and myeloma; aneuploidy and proliferation. Environ Mol Mutagen *50*, 697-707.

Cho, B., Lim, Y., Lee, D.Y., Park, S.Y., Lee, H., Kim, W.H., Yang, H., Bang, Y.J., and Jeoung, D.I. (2002). Identification and characterization of a novel cancer/testis antigen gene CAGE. Biochem Biophys Res Commun *292*, 715-726.

Cho, H.J., Caballero, O.L., Gnjatic, S., Andrade, V.C., Colleoni, G.W., Vettore, A.L., Outtz, H.H., Fortunato, S., Altorki, N., Ferrera, C.A.*, et al.* (2006). Physical interaction of two cancer-testis antigens, MAGE-C1 (CT7) and NY-ESO-1 (CT6). Cancer Immun *6*, 12.

Chomez, P., De Backer, O., Bertrand, M., De Plaen, E., Boon, T., and Lucas, S. (2001). An overview of the MAGE gene family with the identification of all human members of the family. Cancer Res *61*, 5544-5551.

Chu, R., Terrano, D.T., and Chambers, T.C. (2012). Cdk1/cyclin B plays a key role in mitotic arrest-induced apoptosis by phosphorylation of Mcl-1, promoting its degradation and freeing Bak from sequestration. Biochem Pharmacol *83*, 199-206.

Cilensek, Z.M., Yehiely, F., Kular, R.K., and Deiss, L.P. (2002). A member of the GAGE family of tumor antigens is an anti-apoptotic gene that confers resistance to Fas/CD95/APO-1, Interferon-gamma, taxol and gamma-irradiation. Cancer Biol Ther *1*, 380-387.

Cimmino, A., Calin, G.A., Fabbri, M., Iorio, M.V., Ferracin, M., Shimizu, M., Wojcik, S.E., Aqeilan, R.I., Zupo, S., Dono, M.*, et al.* (2005). miR-15 and miR-16 induce apoptosis by targeting BCL2. Proc Natl Acad Sci U S A *102*, 13944-13949.

Claudio, J.O., Masih-Khan, E., Tang, H., Goncalves, J., Voralia, M., Li, Z.H., Nadeem, V., Cukerman, E., Francisco-Pabalan, O., Liew, C.C.*, et al.* (2002). A molecular compendium of genes expressed in multiple myeloma. Blood *100*, 2175-2186.

Collins, A.T., Berry, P.A., Hyde, C., Stower, M.J., and Maitland, N.J. (2005). Prospective identification of tumorigenic prostate cancer stem cells. Cancer research *65*, 10946-10951.

Cook, W.D., and McCaw, B.J. (2000). Accommodating haploinsufficient tumor suppressor genes in Knudson's model. Oncogene *19*, 3434-3438.

Cooper, C.D., Liggins, A.P., Ait-Tahar, K., Roncador, G., Banham, A.H., and Pulford, K. (2006). PASD1, a DLBCL-associated cancer testis antigen and candidate for lymphoma immunotherapy. Leukemia *20*, 2172-2174.

Coral, S., Sigalotti, L., Altomonte, M., Engelsberg, A., Colizzi, F., Cattarossi, I., Maraskovsky, E., Jager, E., Seliger, B., and Maio, M. (2002). 5-aza-2'-deoxycytidine-induced expression of functional cancer testis antigens in human renal cell carcinoma: immunotherapeutic implications. Clin Cancer Res *8*, 2690-2695.

Corman, J.M., Sercarz, E.E., and Nanda, N.K. (1998). Recognition of prostate-specific antigenic peptide determinants by human CD4 and CD8 T cells. Clin Exp Immunol *114*, 166-172.

Cory, S., Huang, D.C., and Adams, J.M. (2003). The Bcl-2 family: roles in cell survival and oncogenesis. Oncogene *22*, 8590-8607.

Costa, F.F., Le Blanc, K., and Brodin, B. (2007). Concise review: cancer/testis antigens, stem cells, and cancer. Stem Cells *25*, 707-711.

Costessi, A., Mahrour, N., Tijchon, E., Stunnenberg, R., Stoel, M.A., Jansen, P.W., Sela, D., Martin-Brown, S., Washburn, M.P., Florens, L.*, et al.* (2011). The tumour antigen PRAME is a subunit of a Cul2 ubiquitin ligase and associates with active NFY promoters. EMBO J *30*, 3786-3798.

Coulie, P.G., Karanikas, V., Colau, D., Lurquin, C., Landry, C., Marchand, M., Dorval, T., Brichard, V., and Boon, T. (2001). A monoclonal cytolytic T-lymphocyte response observed in a melanoma patient vaccinated with a tumor-specific antigenic peptide encoded by gene MAGE-3. Proc Natl Acad Sci U S A *98*, 10290-10295.

Coux, O., Tanaka, K., and Goldberg, A.L. (1996). Structure and functions of the 20S and 26S proteasomes. Annu Rev Biochem *65*, 801-847.

Cox, D.N., Chao, A., Baker, J., Chang, L., Qiao, D., and Lin, H. (1998). A novel class of evolutionarily conserved genes defined by piwi are essential for stem cell self-renewal. Genes Dev *12*, 3715-3727.

Craig, R.W. (2002). MCL1 provides a window on the role of the BCL2 family in cell proliferation, differentiation and tumorigenesis. Leukemia *16*, 444-454.

Cronwright, G., Le Blanc, K., Gotherstrom, C., Darcy, P., Ehnman, M., and Brodin, B. (2005). Cancer/testis antigen expression in human mesenchymal stem cells: down-regulation of SSX impairs cell migration and matrix metalloproteinase 2 expression. Cancer Res *65*, 2207-2215.

Cruz, C.R., Gerdemann, U., Leen, A.M., Shafer, J.A., Ku, S., Tzou, B., Horton, T.M., Sheehan, A., Copeland, A., Younes, A.*, et al.* (2011). Improving T-cell therapy for relapsed EBV-negative Hodgkin lymphoma by targeting upregulated MAGE-A4. Clin Cancer Res *17*, 7058-7066.

Curioni-Fontecedro, A., Knights, A.J., Tinguely, M., Nuber, N., Schneider, C., Thomson, C.W., von Boehmer, L., Bossart, W., Pahlich, S., Gehring, H.*, et al.* (2008). MAGE-C1/CT7 is the dominant cancer-testis antigen targeted by humoral immune responses in patients with multiple myeloma. Leukemia *22*, 1646-1648.

Curioni-Fontecedro, A., Nuber, N., Mihic-Probst, D., Seifert, B., Soldini, D., Dummer, R., Knuth, A., van den Broek, M., and Moch, H. (2011). Expression of MAGE-C1/CT7 and MAGE-C2/CT10 predicts lymph node metastasis in melanoma patients. PLoS One *6*, e21418.

Davis, I.D., Chen, W., Jackson, H., Parente, P., Shackleton, M., Hopkins, W., Chen, Q., Dimopoulos, N., Luke, T., Murphy, R.*, et al.* (2004). Recombinant NY-ESO-1 protein with

ISCOMATRIX adjuvant induces broad integrated antibody and CD4(+) and CD8(+) T cell responses in humans. Proc Natl Acad Sci U S A *101*, 10697-10702.

Davis, R.J. (2000). Signal transduction by the JNK group of MAP kinases. Cell *103*, 239-252.

De Carvalho, D.D., Binato, R., Pereira, W.O., Leroy, J.M., Colassanti, M.D., Proto-Siqueira, R., Bueno-Da-Silva, A.E., Zago, M.A., Zanichelli, M.A., Abdelhay, E.*, et al.* (2011). BCR-ABL-mediated upregulation of PRAME is responsible for knocking down TRAIL in CML patients. Oncogene *30*, 223-233.

De Plaen, E., Arden, K., Traversari, C., Gaforio, J.J., Szikora, J.P., De Smet, C., Brasseur, F., van der Bruggen, P., Lethe, B., Lurquin, C.*, et al.* (1994). Structure, chromosomal localization, and expression of 12 genes of the MAGE family. Immunogenetics *40*, 360-369.

De Smet, C., Courtois, S.J., Faraoni, I., Lurquin, C., Szikora, J.P., De Backer, O., and Boon, T. (1995). Involvement of two Ets binding sites in the transcriptional activation of the MAGE1 gene. Immunogenetics *42*, 282-290.

De Smet, C., De Backer, O., Faraoni, I., Lurquin, C., Brasseur, F., and Boon, T. (1996). The activation of human gene MAGE-1 in tumor cells is correlated with genome-wide demethylation. Proc Natl Acad Sci U S A *93*, 7149-7153.

De Smet, C., Lurquin, C., Lethe, B., Martelange, V., and Boon, T. (1999). DNA methylation is the primary silencing mechanism for a set of germ line- and tumor-specific genes with a CpG-rich promoter. Mol Cell Biol *19*, 7327-7335.

Deng, W., and Lin, H. (2002). miwi, a murine homolog of piwi, encodes a cytoplasmic protein essential for spermatogenesis. Dev Cell *2*, 819-830.

Derenne, S., Monia, B., Dean, N.M., Taylor, J.K., Rapp, M.J., Harousseau, J.L., Bataille, R., and Amiot, M. (2002). Antisense strategy shows that Mcl-1 rather than Bcl-2 or Bcl-x(L) is an essential survival protein of human myeloma cells. Blood *100*, 194-199.

Deshaies, R.J., and Joazeiro, C.A. (2009). RING domain E3 ubiquitin ligases. Annu Rev Biochem *78*, 399-434.

Dhar, S., Thota, A., and Rao, M.R. (2012). Insights into the role of Bromodomain, testis-specific (Brdt) in acetylated histone H4 dependent chromatin remodeling in mammalian spermiogenesis. J Biol Chem.

Dhodapkar, M.V., Osman, K., Teruya-Feldstein, J., Filippa, D., Hedvat, C.V., Iversen, K., Kolb, D., Geller, M.D., Hassoun, H., Kewalramani, T.*, et al.* (2003). Expression of cancer/testis (CT) antigens MAGE-A1, MAGE-A3, MAGE-A4, CT-7, and NY-ESO-1 in malignant gammopathies is heterogeneous and correlates with site, stage and risk status of disease. Cancer Immun *3*, 9.

Dice, J.F. (1987). Molecular determinants of protein half-lives in eukaryotic cells. FASEB J *1*, 349-357.

Didier, C., Merdes, A., Gairin, J.E., and Jabrane-Ferrat, N. (2008). Inhibition of proteasome activity impairs centrosome-dependent microtubule nucleation and organization. Mol Biol Cell *19*, 1220-1229.

Ding, Q., He, X., Hsu, J.M., Xia, W., Chen, C.T., Li, L.Y., Lee, D.F., Liu, J.C., Zhong, Q., Wang, X.*, et al.* (2007). Degradation of Mcl-1 by beta-TrCP mediates glycogen synthase kinase 3-induced tumor suppression and chemosensitization. Mol Cell Biol *27*, 4006-4017.

Domina, A.M., Vrana, J.A., Gregory, M.A., Hann, S.R., and Craig, R.W. (2004). MCL1 is phosphorylated in the PEST region and stabilized upon ERK activation in viable cells, and at additional sites with cytotoxic okadaic acid or taxol. Oncogene *23*, 5301-5315.

Dong, L., Jiang, C.C., Thorne, R.F., Croft, A., Yang, F., Liu, H., de Bock, C.E., Hersey, P., and Zhang, X.D. (2011). Ets-1 mediates upregulation of Mcl-1 downstream of XBP-1 in human melanoma cells upon ER stress. Oncogene *30*, 3716-3726.

dos Santos, N.R., de Bruijn, D.R., Balemans, M., Janssen, B., Gartner, F., Lopes, J.M., de Leeuw, B., and Geurts van Kessel, A. (1997). Nuclear localization of SYT, SSX and the synovial sarcoma-associated SYT-SSX fusion proteins. Hum Mol Genet *6*, 1549-1558.

dos Santos, N.R., de Bruijn, D.R., Kater-Baats, E., Otte, A.P., and van Kessel, A.G. (2000). Delineation of the protein domains responsible for SYT, SSX, and SYT-SSX nuclear localization. Exp Cell Res *256*, 192-202.

Downward, J. (2003). Targeting RAS signalling pathways in cancer therapy. Nat Rev Cancer *3*, 11-22.

Doyle, J.M., Gao, J., Wang, J., Yang, M., and Potts, P.R. (2010). MAGE-RING protein complexes comprise a family of E3 ubiquitin ligases. Mol Cell *39*, 963-974.

Drexler, H.C. (1997). Activation of the cell death program by inhibition of proteasome function. Proc Natl Acad Sci U S A *94*, 855-860.

Druker, B.J., Talpaz, M., Resta, D.J., Peng, B., Buchdunger, E., Ford, J.M., Lydon, N.B., Kantarjian, H., Capdeville, R., Ohno-Jones, S.*, et al.* (2001). Efficacy and safety of a specific inhibitor of the BCR-ABL tyrosine kinase in chronic myeloid leukemia. N Engl J Med *344*, 1031-1037.

Duan, Z., Duan, Y., Lamendola, D.E., Yusuf, R.Z., Naeem, R., Penson, R.T., and Seiden, M.V. (2003). Overexpression of MAGE/GAGE genes in paclitaxel/doxorubicin-resistant human cancer cell lines. Clin Cancer Res *9*, 2778-2785.

Duan, Z., Feller, A.J., Toh, H.C., Makastorsis, T., and Seiden, M.V. (1999). TRAG-3, a novel gene, isolated from a taxol-resistant ovarian carcinoma cell line. Gene *229*, 75-81.

Egger, G., Liang, G., Aparicio, A., and Jones, P.A. (2004). Epigenetics in human disease and prospects for epigenetic therapy. Nature *429*, 457-463.

Ehrhardt, A.G., and Sluder, G. (2005). Spindle pole fragmentation due to proteasome inhibition. J Cell Physiol *204*, 808-818.

Ehrlich, M. (2002). DNA methylation in cancer: too much, but also too little. Oncogene *21*, 5400-5413.

Ellis, H.M., and Horvitz, H.R. (1986). Genetic control of programmed cell death in the nematode C. elegans. Cell *44*, 817-829.

Epping, M.T., Wang, L., Edel, M.J., Carlee, L., Hernandez, M., and Bernards, R. (2005). The human tumor antigen PRAME is a dominant repressor of retinoic acid receptor signaling. Cell *122*, 835-847.

Espantman, K.C., and O'Shea, C.C. (2010). aMAGEing new players enter the RING to promote ubiquitylation. Mol Cell *39*, 835-837.

Esteller, M., and Herman, J.G. (2002). Cancer as an epigenetic disease: DNA methylation and chromatin alterations in human tumours. J Pathol *196*, 1-7.

Fabunmi, R.P., Wigley, W.C., Thomas, P.J., and DeMartino, G.N. (2000). Activity and regulation of the centrosome-associated proteasome. J Biol Chem *275*, 409-413.

Fidler, I.J. (1978). Tumor heterogeneity and the biology of cancer invasion and metastasis. Cancer Res *38*, 2651-2660.

Finn, O.J. (2003). Cancer vaccines: between the idea and the reality. Nat Rev Immunol *3*, 630-641.

Finn, O.J., and Forni, G. (2002). Prophylactic cancer vaccines. Curr Opin Immunol *14*, 172-177.

Fratta, E., Sigalotti, L., Colizzi, F., Covre, A., Nicolay, H.J., Danielli, R., Fonsatti, E., Altomonte, M., Calabro, L., Coral, S.*, et al.* (2010). Epigenetically regulated clonal heritability of CTA expression profiles in human melanoma. J Cell Physiol *223*, 352-358.

Fujimoto, T., Onda, M., Nagai, H., Nagahata, T., Ogawa, K., and Emi, M. (2003). Upregulation and overexpression of human X-box binding protein 1 (hXBP-1) gene in primary breast cancers. Breast Cancer *10*, 301-306.

Fujimoto, T., Yoshimatsu, K., Watanabe, K., Yokomizo, H., Otani, T., Matsumoto, A., Osawa, G., Onda, M., and Ogawa, K. (2007). Overexpression of human X-box binding protein 1 (XBP-1) in colorectal adenomas and adenocarcinomas. Anticancer Res *27*, 127-131.

Fujiwara, K., Hasegawa, K., Ohkumo, T., Miyoshi, H., Tseng, Y.H., and Yoshikawa, K. (2012). Necdin controls proliferation of white adipocyte progenitor cells. PLoS One *7*, e30948.

Garzon, R., Marcucci, G., and Croce, C.M. (2010). Targeting microRNAs in cancer: rationale, strategies and challenges. Nat Rev Drug Discov *9*, 775-789.

Geiss-Friedlander, R., and Melchior, F. (2007). Concepts in sumoylation: a decade on. Nat Rev Mol Cell Biol *8*, 947-956.

Geller, S.A. (2002). Hepatitis B and hepatitis C. Clin Liver Dis *6*, 317-334, v.

Gerard, M., Hernandez, L., Wevrick, R., and Stewart, C.L. (1999). Disruption of the mouse necdin gene results in early post-natal lethality. Nat Genet *23*, 199-202.

Gerlinger, M., Rowan, A.J., Horswell, S., Larkin, J., Endesfelder, D., Gronroos, E., Martinez, P., Matthews, N., Stewart, A., Tarpey, P.*, et al.* (2012). Intratumor heterogeneity and branched evolution revealed by multiregion sequencing. N Engl J Med *366*, 883-892.

Germain, M., and Duronio, V. (2007). The N terminus of the anti-apoptotic BCL-2 homologue MCL-1 regulates its localization and function. J Biol Chem *282*, 32233-32242.

Gjerstorff, M.F., Harkness, L., Kassem, M., Frandsen, U., Nielsen, O., Lutterodt, M., Mollgard, K., and Ditzel, H.J. (2008). Distinct GAGE and MAGE-A expression during early human development indicate specific roles in lineage differentiation. Hum Reprod *23*, 2194-2201.

Gjerstorff, M.F., Kock, K., Nielsen, O., and Ditzel, H.J. (2007). MAGE-A1, GAGE and NY-ESO-1 cancer/testis antigen expression during human gonadal development. Hum Reprod *22*, 953-960.

Glynn, S.A., Gammell, P., Heenan, M., O'Connor, R., Liang, Y., Keenan, J., and Clynes, M. (2004). A new superinvasive in vitro phenotype induced by selection of human breast carcinoma cells with the chemotherapeutic drugs paclitaxel and doxorubicin. Br J Cancer *91*, 1800-1807.

Gnjatic, S., Nagata, Y., Jager, E., Stockert, E., Shankara, S., Roberts, B.L., Mazzara, G.P., Lee, S.Y., Dunbar, P.R., Dupont, B*., et al.* (2000). Strategy for monitoring T cell responses to NY-ESO-1 in patients with any HLA class I allele. Proc Natl Acad Sci U S A *97*, 10917-10922.

Gnjatic, S., Nishikawa, H., Jungbluth, A.A., Gure, A.O., Ritter, G., Jager, E., Knuth, A., Chen, Y.T., and Old, L.J. (2006). NY-ESO-1: review of an immunogenic tumor antigen. Adv Cancer Res *95*, 1-30.

Goelz, S.E., Vogelstein, B., Hamilton, S.R., and Feinberg, A.P. (1985). Hypomethylation of DNA from benign and malignant human colon neoplasms. Science *228*, 187-190.

Goodyear, O., Agathanggelou, A., Novitzky-Basso, I., Siddique, S., McSkeane, T., Ryan, G., Vyas, P., Cavenagh, J., Stankovic, T., Moss, P*., et al.* (2010). Induction of a CD8+ T-cell response to the MAGE cancer testis antigen by combined treatment with azacitidine and sodium valproate in patients with acute myeloid leukemia and myelodysplasia. Blood *116*, 1908-1918.

Gostissa, M., Hengstermann, A., Fogal, V., Sandy, P., Schwarz, S.E., Scheffner, M., and Del Sal, G. (1999). Activation of p53 by conjugation to the ubiquitin-like protein SUMO-1. EMBO J *18*, 6462-6471.

Graff-Dubois, S., Faure, O., Gross, D.A., Alves, P., Scardino, A., Chouaib, S., Lemonnier, F.A., and Kosmatopoulos, K. (2002). Generation of CTL recognizing an HLA-A*0201-restricted epitope shared by MAGE-A1, -A2, -A3, -A4, -A6, -A10, and -A12 tumor antigens: implication in a broad-spectrum tumor immunotherapy. J Immunol *169*, 575-580.

Grah, J., Samija, M., Juretic, A., Sarcevic, B., and Sobat, H. (2008). Immunohystochemical expression of cancer/testis antigens (MAGE-A3/4, NY-ESO-1) in non-small cell lung cancer: the relationship with clinical-pathological features. Collegium antropologicum *32*, 731-736.

Grassmann, R., Aboud, M., and Jeang, K.T. (2005). Molecular mechanisms of cellular transformation by HTLV-1 Tax. Oncogene *24*, 5976-5985.

Grigoriadis, A., Caballero, O.L., Hoek, K.S., da Silva, L., Chen, Y.T., Shin, S.J., Jungbluth, A.A., Miller, L.D., Clouston, D., Cebon, J*., et al.* (2009). CT-X antigen expression in human breast cancer. Proc Natl Acad Sci U S A *106*, 13493-13498.

Grizzi, F., Chiriva-Internati, M., Franceschini, B., Hermonat, P.L., Soda, G., Lim, S.H., and Dioguardi, N. (2003). Immunolocalization of sperm protein 17 in human testis and ejaculated spermatozoa. J Histochem Cytochem *51*, 1245-1248.

Gronostajski, R.M., Pardee, A.B., and Goldberg, A.L. (1985). The ATP dependence of the degradation of short- and long-lived proteins in growing fibroblasts. J Biol Chem *260*, 3344-3349.

Grskovic, M., Chaivorapol, C., Gaspar-Maia, A., Li, H., and Ramalho-Santos, M. (2007). Systematic identification of cis-regulatory sequences active in mouse and human embryonic stem cells. PLoS Genet *3*, e145.

Gupta, S.K., Alves, K., Palladino, L.O., Mark, G.E., and Hollis, G.F. (1996). Molecular cloning of the human fertilin beta subunit. Biochem Biophys Res Commun *224*, 318-326.

Gure, A.O., Wei, I.J., Old, L.J., and Chen, Y.T. (2002). The SSX gene family: characterization of 9 complete genes. Int J Cancer *101*, 448-453.

Gurtner, A., Fuschi, P., Magi, F., Colussi, C., Gaetano, C., Dobbelstein, M., Sacchi, A., and Piaggio, G. (2008). NF-Y dependent epigenetic modifications discriminate between proliferating and postmitotic tissue. PLoS One *3*, e2047.

Hahn, J.S., Hu, Z., Thiele, D.J., and Iyer, V.R. (2004). Genome-wide analysis of the biology of stress responses through heat shock transcription factor. Mol Cell Biol *24*, 5249-5256.

Hammarstrom, S. (1999). The carcinoembryonic antigen (CEA) family: structures, suggested functions and expression in normal and malignant tissues. Semin Cancer Biol *9*, 67-81.

Hanahan, D., and Weinberg, R.A. (2000). The hallmarks of cancer. Cell *100*, 57-70.

Hanahan, D., and Weinberg, R.A. (2011). Hallmarks of cancer: the next generation. Cell *144*, 646-674.

Harley, M.E., Allan, L.A., Sanderson, H.S., and Clarke, P.R. (2010). Phosphorylation of Mcl-1 by CDK1-cyclin B1 initiates its Cdc20-dependent destruction during mitotic arrest. EMBO J *29*, 2407-2420.

Harris, A.L. (2002). Hypoxia--a key regulatory factor in tumour growth. Nat Rev Cancer *2*, 38-47.

Hasegawa, K., and Yoshikawa, K. (2008). Necdin regulates p53 acetylation via Sirtuin1 to modulate DNA damage response in cortical neurons. J Neurosci *28*, 8772-8784.

Haviland, R., Eschrich, S., Bloom, G., Ma, Y., Minton, S., Jove, R., and Cress, W.D. (2011). Necdin, a negative growth regulator, is a novel STAT3 target gene down-regulated in human cancer. PLoS One *6*, e24923.

Hay, R.T. (2005). SUMO: a history of modification. Mol Cell *18*, 1-12.

Hayashi, T., Seki, M., Maeda, D., Wang, W., Kawabe, Y., Seki, T., Saitoh, H., Fukagawa, T., Yagi, H., and Enomoto, T. (2002). Ubc9 is essential for viability of higher eukaryotic cells. Exp Cell Res *280*, 212-221.

Hayashi, Y., Matsuyama, K., Takagi, K., Sugiura, H., and Yoshikawa, K. (1995). Arrest of cell growth by necdin, a nuclear protein expressed in postmitotic neurons. Biochem Biophys Res Commun *213*, 317-324.

Hayward, W.S., Neel, B.G., and Astrin, S.M. (1981). Activation of a cellular onc gene by promoter insertion in ALV-induced lymphoid leukosis. Nature *290*, 475-480.

Healy, S.J., Gorman, A.M., Mousavi-Shafaei, P., Gupta, S., and Samali, A. (2009). Targeting the endoplasmic reticulum-stress response as an anticancer strategy. Eur J Pharmacol *625*, 234-246.

Heidecker, L., Brasseur, F., Probst-Kepper, M., Gueguen, M., Boon, T., and Van den Eynde, B.J. (2000). Cytolytic T lymphocytes raised against a human bladder carcinoma recognize an antigen encoded by gene MAGE-A12. J Immunol *164*, 6041-6045.

Hellman, M., Tossavainen, H., Rappu, P., Heino, J., and Permi, P. (2011). Characterization of intrinsically disordered prostate associated gene (PAGE5) at single residue resolution by NMR spectroscopy. PLoS One *6*, e26633.

Hendriksen, P.J. (1999). Do X and Y spermatozoa differ in proteins? Theriogenology *52*, 1295-1307.

Hengartner, M.O., and Horvitz, H.R. (1994a). Activation of C. elegans cell death protein CED-9 by an amino-acid substitution in a domain conserved in Bcl-2. Nature *369*, 318-320.

Hengartner, M.O., and Horvitz, H.R. (1994b). C. elegans cell survival gene ced-9 encodes a functional homolog of the mammalian proto-oncogene bcl-2. Cell *76*, 665-676.

Herrant, M., Jacquel, A., Marchetti, S., Belhacene, N., Colosetti, P., Luciano, F., and Auberger, P. (2004). Cleavage of Mcl-1 by caspases impaired its ability to counteract Bim-induced apoptosis. Oncogene *23*, 7863-7873.

Hershko, A., and Ciechanover, A. (1998). The ubiquitin system. Annu Rev Biochem *67*, 425-479.

Hetz, C.A. (2007). ER stress signaling and the BCL-2 family of proteins: from adaptation to irreversible cellular damage. Antioxid Redox Signal *9*, 2345-2355.

Hicke, L. (2001). Protein regulation by monoubiquitin. Nat Rev Mol Cell Biol *2*, 195-201.

Hoek, K., Rimm, D.L., Williams, K.R., Zhao, H., Ariyan, S., Lin, A., Kluger, H.M., Berger, A.J., Cheng, E., Trombetta, E.S.*, et al.* (2004). Expression profiling reveals novel pathways in the transformation of melanocytes to melanomas. Cancer Res *64*, 5270-5282.

Hoeller, D., and Dikic, I. (2009). Targeting the ubiquitin system in cancer therapy. Nature *458*, 438-444.

Hofmann, O., Caballero, O.L., Stevenson, B.J., Chen, Y.T., Cohen, T., Chua, R., Maher, C.A., Panji, S., Schaefer, U., Kruger, A.*, et al.* (2008). Genome-wide analysis of cancer/testis gene expression. Proc Natl Acad Sci U S A *105*, 20422-20427.

Hong, J.A., Kang, Y., Abdullaev, Z., Flanagan, P.T., Pack, S.D., Fischette, M.R., Adnani, M.T., Loukinov, D.I., Vatolin, S., Risinger, J.I.*, et al.* (2005). Reciprocal binding of CTCF and BORIS to the NY-ESO-1 promoter coincides with derepression of this cancer-testis gene in lung cancer cells. Cancer Res *65*, 7763-7774.

Hu, J., Dang, N., Menu, E., De Bryune, E., Xu, D., Van Camp, B., Van Valckenborgh, E., and Vanderkerken, K. (2012). Activation of ATF4 mediates unwanted Mcl-1 accumulation by proteasome inhibition. Blood *119*, 826-837.

Huang, K., and Lin, S. (2000). Nationwide vaccination: a success story in Taiwan. Vaccine *18 Suppl 1*, S35-38.

Hung, C.F., Wu, T.C., Monie, A., and Roden, R. (2008). Antigen-specific immunotherapy of cervical and ovarian cancer. Immunol Rev *222*, 43-69.

Ikeda, H., Lethe, B., Lehmann, F., van Baren, N., Baurain, J.F., de Smet, C., Chambost, H., Vitale, M., Moretta, A., Boon, T.*, et al.* (1997). Characterization of an antigen that is recognized on a melanoma showing partial HLA loss by CTL expressing an NK inhibitory receptor. Immunity *6*, 199-208.

Inoshita, S., Takeda, K., Hatai, T., Terada, Y., Sano, M., Hata, J., Umezawa, A., and Ichijo, H. (2002). Phosphorylation and inactivation of myeloid cell leukemia 1 by JNK in response to oxidative stress. J Biol Chem *277*, 43730-43734.

Inuzuka, H., Fukushima, H., Shaik, S., Liu, P., Lau, A.W., and Wei, W. (2011a). Mcl-1 ubiquitination and destruction. Oncotarget *2*, 239-244.

Inuzuka, H., Shaik, S., Onoyama, I., Gao, D., Tseng, A., Maser, R.S., Zhai, B., Wan, L., Gutierrez, A., Lau, A.W.*, et al.* (2011b). SCF(FBW7) regulates cellular apoptosis by targeting MCL1 for ubiquitylation and destruction. Nature *471*, 104-109.

Jackson, H.M., Dimopoulos, N., Chen, Q., Luke, T., Yee Tai, T., Maraskovsky, E., Old, L.J., Davis, I.D., Cebon, J., and Chen, W. (2004). A robust human T-cell culture method suitable for monitoring CD8+ and CD4+ T-cell responses from cancer clinical trial samples. J Immunol Methods *291*, 51-62.

Jagadish, N., Rana, R., Mishra, D., Garg, M., Selvi, R., and Suri, A. (2006). Characterization of immune response in mice to plasmid DNA encoding human sperm associated antigen 9 (SPAG9). Vaccine *24*, 3695-3703.

Jagadish, N., Rana, R., Mishra, D., Kumar, M., and Suri, A. (2005). Sperm associated antigen 9 (SPAG9): a new member of c-Jun NH2 -terminal kinase (JNK) interacting protein exclusively expressed in testis. Keio J Med *54*, 66-71.

Jager, E., Chen, Y.T., Drijfhout, J.W., Karbach, J., Ringhoffer, M., Jager, D., Arand, M., Wada, H., Noguchi, Y., Stockert, E.*, et al.* (1998). Simultaneous humoral and cellular immune response against cancer-testis antigen NY-ESO-1: definition of human histocompatibility leukocyte antigen (HLA)-A2-binding peptide epitopes. J Exp Med *187*, 265-270.

Jager, E., Gnjatic, S., Nagata, Y., Stockert, E., Jager, D., Karbach, J., Neumann, A., Rieckenberg, J., Chen, Y.T., Ritter, G.*, et al.* (2000a). Induction of primary NY-ESO-1 immunity: CD8+ T lymphocyte and antibody responses in peptide-vaccinated patients with NY-ESO-1+ cancers. Proc Natl Acad Sci U S A *97*, 12198-12203.

Jager, E., Nagata, Y., Gnjatic, S., Wada, H., Stockert, E., Karbach, J., Dunbar, P.R., Lee, S.Y., Jungbluth, A., Jager, D.*, et al.* (2000b). Monitoring CD8 T cell responses to NY-ESO-1: correlation of humoral and cellular immune responses. Proc Natl Acad Sci U S A *97*, 4760-4765.

Jager, E., Stockert, E., Zidianakis, Z., Chen, Y.T., Karbach, J., Jager, D., Arand, M., Ritter, G., Old, L.J., and Knuth, A. (1999). Humoral immune responses of cancer patients against "Cancer-Testis" antigen NY-ESO-1: correlation with clinical events. Int J Cancer *84*, 506-510.

Jaini, R., Kesaraju, P., Johnson, J.M., Altuntas, C.Z., Jane-Wit, D., and Tuohy, V.K. (2010). An autoimmune-mediated strategy for prophylactic breast cancer vaccination. Nat Med *16*, 799-803.

Jang, M.S., Ryu, S.W., and Kim, E. (2002). Modification of Daxx by small ubiquitin-related modifier-1. Biochem Biophys Res Commun *295*, 495-500.

Jaramillo, A., Majumder, K., Manna, P.P., Fleming, T.P., Doherty, G., Dipersio, J.F., and Mohanakumar, T. (2002). Identification of HLA-A3-restricted CD8+ T cell epitopes derived from mammaglobin-A, a tumor-associated antigen of human breast cancer. Int J Cancer *102*, 499-506.

Jariel-Encontre, I., Bossis, G., and Piechaczyk, M. (2008). Ubiquitin-independent degradation of proteins by the proteasome. Biochim Biophys Acta *1786*, 153-177.

Jay, P., Rougeulle, C., Massacrier, A., Moncla, A., Mattei, M.G., Malzac, P., Roeckel, N., Taviaux, S., Lefranc, J.L., Cau, P.*, et al.* (1997). The human necdin gene, NDN, is maternally imprinted and located in the Prader-Willi syndrome chromosomal region. Nat Genet *17*, 357-361.

Jiang, C.C., Lucas, K., Avery-Kiejda, K.A., Wade, M., deBock, C.E., Thorne, R.F., Allen, J., Hersey, P., and Zhang, X.D. (2008). Up-regulation of Mcl-1 is critical for survival of human melanoma cells upon endoplasmic reticulum stress. Cancer Res *68*, 6708-6717.

Jiang, C.C., Wroblewski, D., Yang, F., Hersey, P., and Zhang, X.D. (2009). Human melanoma cells under endoplasmic reticulum stress are more susceptible to apoptosis induced by the BH3 mimetic obatoclax. Neoplasia *11*, 945-955.

Jiang, Y., Tsai, T.F., Bressler, J., and Beaudet, A.L. (1998). Imprinting in Angelman and Prader-Willi syndromes. Curr Opin Genet Dev *8*, 334-342.

Jin, L., Hu, W.L., Jiang, C.C., Wang, J.X., Han, C.C., Chu, P., Zhang, L.J., Thorne, R.F., Wilmott, J., Scolyer, R.A.*, et al.* (2011). MicroRNA-149*, a p53-responsive microRNA, functions as an oncogenic regulator in human melanoma. Proc Natl Acad Sci U S A *108*, 15840-15845.

Johnston, J.A., Ward, C.L., and Kopito, R.R. (1998). Aggresomes: a cellular response to misfolded proteins. J Cell Biol *143*, 1883-1898.

Jones, M.H., Numata, M., and Shimane, M. (1997). Identification and characterization of BRDT: A testis-specific gene related to the bromodomain genes RING3 and Drosophila fsh. Genomics *45*, 529-534.

Jordan, B.W., Dinev, D., LeMellay, V., Troppmair, J., Gotz, R., Wixler, L., Sendtner, M., Ludwig, S., and Rapp, U.R. (2001). Neurotrophin receptor-interacting mage homologue is an inducible inhibitor of apoptosis protein-interacting protein that augments cell death. J Biol Chem *276*, 39985-39989.

Jourdan, M., De Vos, J., Mechti, N., and Klein, B. (2000). Regulation of Bcl-2-family proteins in myeloma cells by three myeloma survival factors: interleukin-6, interferon-alpha and insulin-like growth factor 1. Cell Death Differ *7*, 1244-1252.

Jungbluth, A.A., Busam, K.J., Kolb, D., Iversen, K., Coplan, K., Chen, Y.T., Spagnoli, G.C., and Old, L.J. (2000a). Expression of MAGE-antigens in normal tissues and cancer. Int J Cancer *85*, 460-465.

Jungbluth, A.A., Chen, Y.T., Busam, K.J., Coplan, K., Kolb, D., Iversen, K., Williamson, B., Van Landeghem, F.K., Stockert, E., and Old, L.J. (2002). CT7 (MAGE-C1) antigen expression in normal and neoplastic tissues. Int J Cancer *99*, 839-845.

Jungbluth, A.A., Chen, Y.T., Stockert, E., Busam, K.J., Kolb, D., Iversen, K., Coplan, K., Williamson, B., Altorki, N., and Old, L.J. (2001). Immunohistochemical analysis of NY-ESO-1 antigen expression in normal and malignant human tissues. Int J Cancer *92*, 856-860.

Jungbluth, A.A., Ely, S., DiLiberto, M., Niesvizky, R., Williamson, B., Frosina, D., Chen, Y.T., Bhardwaj, N., Chen-Kiang, S., Old, L.J.*, et al.* (2005). The cancer-testis antigens CT7 (MAGE-C1) and MAGE-A3/6 are commonly expressed in multiple myeloma and correlate with plasma-cell proliferation. Blood *106*, 167-174.

Jungbluth, A.A., Silva, W.A., Jr., Iversen, K., Frosina, D., Zaidi, B., Coplan, K., Eastlake-Wade, S.K., Castelli, S.B., Spagnoli, G.C., Old, L.J.*, et al.* (2007). Expression of cancer-testis (CT) antigens in placenta. Cancer Immun *7*, 15.

Jungbluth, A.A., Stockert, E., Chen, Y.T., Kolb, D., Iversen, K., Coplan, K., Williamson, B., Altorki, N., Busam, K.J., and Old, L.J. (2000b). Monoclonal antibody MA454 reveals a heterogeneous expression pattern of MAGE-1 antigen in formalin-fixed paraffin embedded lung tumours. Br J Cancer *83*, 493-497.

Juretic, A., Spagnoli, G.C., Schultz-Thater, E., and Sarcevic, B. (2003). Cancer/testis tumour-associated antigens: immunohistochemical detection with monoclonal antibodies. The lancet oncology *4*, 104-109.

Kaneda, A., Tsukamoto, T., Takamura-Enya, T., Watanabe, N., Kaminishi, M., Sugimura, T., Tatematsu, M., and Ushijima, T. (2004). Frequent hypomethylation in multiple promoter CpG islands is associated with global hypomethylation, but not with frequent promoter hypermethylation. Cancer Sci *95*, 58-64.

Karbach, J., Gnjatic, S., Bender, A., Neumann, A., Weidmann, E., Yuan, J., Ferrara, C.A., Hoffmann, E., Old, L.J., Altorki, N.K.*, et al.* (2010). Tumor-reactive CD8+ T-cell responses after vaccination with NY-ESO-1 peptide, CpG 7909 and Montanide ISA-51: association with survival. Int J Cancer *126*, 909-918.

Karpf, A.R., Bai, S., James, S.R., Mohler, J.L., and Wilson, E.M. (2009). Increased expression of androgen receptor coregulator MAGE-11 in prostate cancer by DNA hypomethylation and cyclic AMP. Mol Cancer Res *7*, 523-535.

Karpf, A.R., Lasek, A.W., Ririe, T.O., Hanks, A.N., Grossman, D., and Jones, D.A. (2004). Limited gene activation in tumor and normal epithelial cells treated with the DNA methyltransferase inhibitor 5-aza-2'-deoxycytidine. Mol Pharmacol *65*, 18-27.

Kaufmann, S.H., and Earnshaw, W.C. (2000). Induction of apoptosis by cancer chemotherapy. Exp Cell Res *256*, 42-49.

Kawada, J., Wada, H., Isobe, M., Gnjatic, S., Nishikawa, H., Jungbluth, A.A., Okazaki, N., Uenaka, A., Nakamura, Y., Fujiwara, S.*, et al.* (2012). Heteroclitic serological response in esophageal and prostate cancer patients after NY-ESO-1 protein vaccination. Int J Cancer *130*, 584-592.

Kawakami, Y., Eliyahu, S., Delgado, C.H., Robbins, P.F., Rivoltini, L., Topalian, S.L., Miki, T., and Rosenberg, S.A. (1994a). Cloning of the gene coding for a shared human melanoma antigen recognized by autologous T cells infiltrating into tumor. Proc Natl Acad Sci U S A *91*, 3515-3519.

Kawakami, Y., Eliyahu, S., Delgado, C.H., Robbins, P.F., Sakaguchi, K., Appella, E., Yannelli, J.R., Adema, G.J., Miki, T., and Rosenberg, S.A. (1994b). Identification of a human melanoma antigen recognized by tumor-infiltrating lymphocytes associated with in vivo tumor rejection. Proc Natl Acad Sci U S A *91*, 6458-6462.

Kendall, S.E., Battelli, C., Irwin, S., Mitchell, J.G., Glackin, C.A., and Verdi, J.M. (2005). NRAGE mediates p38 activation and neural progenitor apoptosis via the bone morphogenetic protein signaling cascade. Mol Cell Biol *25*, 7711-7724.

Kim, I., Xu, W., and Reed, J.C. (2008). Cell death and endoplasmic reticulum stress: disease relevance and therapeutic opportunities. Nat Rev Drug Discov *7*, 1013-1030.

Kim, Y., Park, H., Park, D., Lee, Y.S., Choe, J., Hahn, J.H., Lee, H., Kim, Y.M., and Jeoung, D. (2010). Cancer/testis antigen CAGE exerts negative regulation on p53 expression through HDAC2 and confers resistance to anti-cancer drugs. J Biol Chem *285*, 25957-25968.

Kinzler, K.W., and Vogelstein, B. (1996). Lessons from hereditary colorectal cancer. Cell *87*, 159-170.

Kinzler, K.W., and Vogelstein, B. (1998). Landscaping the cancer terrain. Science *280*, 1036-1037.

Kisseleva-Romanova, E., Lopreiato, R., Baudin-Baillieu, A., Rousselle, J.C., Ilan, L., Hofmann, K., Namane, A., Mann, C., and Libri, D. (2006). Yeast homolog of a cancer-testis antigen defines a new transcription complex. EMBO J *25*, 3576-3585.

Kloetzel, P.M. (2004). The proteasome and MHC class I antigen processing. Biochim Biophys Acta *1695*, 225-233.

Kmiecik, T.E., and Shalloway, D. (1987). Activation and suppression of pp60c-src transforming ability by mutation of its primary sites of tyrosine phosphorylation. Cell *49*, 65-73.

Knuth, A., Wolfel, T., Klehmann, E., Boon, T., and Meyer zum Buschenfelde, K.H. (1989). Cytolytic T-cell clones against an autologous human melanoma: specificity study and definition of three antigens by immunoselection. Proc Natl Acad Sci U S A *86*, 2804-2808.

Kobayashi, S., Lee, S.H., Meng, X.W., Mott, J.L., Bronk, S.F., Werneburg, N.W., Craig, R.W., Kaufmann, S.H., and Gores, G.J. (2007). Serine 64 phosphorylation enhances the antiapoptotic function of Mcl-1. J Biol Chem *282*, 18407-18417.

Kocher, T., Zheng, M., Bolli, M., Simon, R., Forster, T., Schultz-Thater, E., Remmel, E., Noppen, C., Schmid, U., Ackermann, D.*, et al.* (2002). Prognostic relevance of MAGE-A4 tumor antigen expression in transitional cell carcinoma of the urinary bladder: a tissue microarray study. Int J Cancer *100*, 702-705.

Kohno, K., Normington, K., Sambrook, J., Gething, M.J., and Mori, K. (1993). The promoter region of the yeast KAR2 (BiP) gene contains a regulatory domain that responds to the presence of unfolded proteins in the endoplasmic reticulum. Mol Cell Biol *13*, 877-890.

Konishi, J., Toyooka, S., Aoe, M., Omura, Y., Washio, K., Tsukuda, K., and Shimizu, N. (2004). The relationship between NY-ESO-1 mRNA expression and clinicopathological features in non-small cell lung cancer. Oncology reports *11*, 1063-1067.

Kopito, R.R. (1997). ER quality control: the cytoplasmic connection. Cell *88*, 427-430.

Kosaka-Suzuki, N., Suzuki, T., Pugacheva, E.M., Vostrov, A.A., Morse, H.C., 3rd, Loukinov, D., and Lobanenkov, V. (2011). Transcription factor BORIS (Brother of the Regulator of Imprinted Sites) directly induces expression of a cancer-testis antigen, TSP50, through regulated binding of BORIS to the promoter. J Biol Chem *286*, 27378-27388.

Kozopas, K.M., Yang, T., Buchan, H.L., Zhou, P., and Craig, R.W. (1993). MCL1, a gene expressed in programmed myeloid cell differentiation, has sequence similarity to BCL2. Proc Natl Acad Sci U S A *90*, 3516-3520.

Kubota, Y., Osawa, M., Jakt, L.M., Yoshikawa, K., and Nishikawa, S. (2009). Necdin restricts proliferation of hematopoietic stem cells during hematopoietic regeneration. Blood *114*, 4383-4392.

Kular, R.K., Yehiely, F., Kotlo, K.U., Cilensek, Z.M., Bedi, R., and Deiss, L.P. (2009). GAGE, an antiapoptotic protein binds and modulates the expression of nucleophosmin/B23 and interferon regulatory factor 1. J Interferon Cytokine Res *29*, 645-655.

Kumar, S.K., Rajkumar, S.V., Dispenzieri, A., Lacy, M.Q., Hayman, S.R., Buadi, F.K., Zeldenrust, S.R., Dingli, D., Russell, S.J., Lust, J.A.*, et al.* (2008). Improved survival in multiple myeloma and the impact of novel therapies. Blood *111*, 2516-2520.

Kuramochi-Miyagawa, S., Kimura, T., Ijiri, T.W., Isobe, T., Asada, N., Fujita, Y., Ikawa, M., Iwai, N., Okabe, M., Deng, W.*, et al.* (2004). Mili, a mammalian member of piwi family gene, is essential for spermatogenesis. Development *131*, 839-849.

Kurashige, T., Noguchi, Y., Saika, T., Ono, T., Nagata, Y., Jungbluth, A., Ritter, G., Chen, Y.T., Stockert, E., Tsushima, T.*, et al.* (2001). Ny-ESO-1 expression and immunogenicity associated with transitional cell carcinoma: correlation with tumor grade. Cancer Res *61*, 4671-4674.

Kuwajima, T., Nishimura, I., and Yoshikawa, K. (2006). Necdin promotes GABAergic neuron differentiation in cooperation with Dlx homeodomain proteins. J Neurosci *26*, 5383-5392.

Kuwajima, T., Taniura, H., Nishimura, I., and Yoshikawa, K. (2004). Necdin interacts with the Msx2 homeodomain protein via MAGE-D1 to promote myogenic differentiation of C2C12 cells. J Biol Chem *279*, 40484-40493.

Kuwako, K., Taniura, H., and Yoshikawa, K. (2004). Necdin-related MAGE proteins differentially interact with the E2F1 transcription factor and the p75 neurotrophin receptor. J Biol Chem *279*, 1703-1712.

Kuwana, T., Bouchier-Hayes, L., Chipuk, J.E., Bonzon, C., Sullivan, B.A., Green, D.R., and Newmeyer, D.D. (2005). BH3 domains of BH3-only proteins differentially regulate Bax-mediated mitochondrial membrane permeabilization both directly and indirectly. Mol Cell *17*, 525-535.

Laduron, S., Deplus, R., Zhou, S., Kholmanskikh, O., Godelaine, D., De Smet, C., Hayward, S.D., Fuks, F., Boon, T., and De Plaen, E. (2004). MAGE-A1 interacts with adaptor SKIP and the deacetylase HDAC1 to repress transcription. Nucleic Acids Res *32*, 4340-4350.

Lai, D., Sakkas, D., and Huang, Y. (2006). The fragile X mental retardation protein interacts with a distinct mRNA nuclear export factor NXF2. RNA *12*, 1446-1449.

Lajer, C.B., and von Buchwald, C. (2010). The role of human papillomavirus in head and neck cancer. APMIS *118*, 510-519.

Lamkanfi, M., Kalai, M., and Vandenabeele, P. (2004). Caspase-12: an overview. Cell Death Differ *11*, 365-368.

Le Gouill, S., Podar, K., Amiot, M., Hideshima, T., Chauhan, D., Ishitsuka, K., Kumar, S., Raje, N., Richardson, P.G., Harousseau, J.L.*, et al.* (2004). VEGF induces Mcl-1 up-regulation and protects multiple myeloma cells against apoptosis. Blood *104*, 2886-2892.

Lea, I.A., Adoyo, P., and O'Rand, M.G. (1997). Autoimmunogenicity of the human sperm protein Sp17 in vasectomized men and identification of linear B cell epitopes. Fertil Steril *67*, 355-361.

Lee, A.S. (2007). GRP78 induction in cancer: therapeutic and prognostic implications. Cancer Res *67*, 3496-3499.

Lee, D.H., and Goldberg, A.L. (1998). Proteasome inhibitors: valuable new tools for cell biologists. Trends Cell Biol *8*, 397-403.

Lee, J.H., Schutte, D., Wulf, G., Fuzesi, L., Radzun, H.J., Schweyer, S., Engel, W., and Nayernia, K. (2006a). Stem-cell protein Piwil2 is widely expressed in tumors and inhibits apoptosis through activation of Stat3/Bcl-XL pathway. Hum Mol Genet *15*, 201-211.

Lee, M.H., Lee, S.W., Lee, E.J., Choi, S.J., Chung, S.S., Lee, J.I., Cho, J.M., Seol, J.H., Baek, S.H., Kim, K.I.*, et al.* (2006b). SUMO-specific protease SUSP4 positively regulates p53 by promoting Mdm2 self-ubiquitination. Nat Cell Biol *8*, 1424-1431.

Lee, S.Y., Williamson, B., Caballero, O.L., Chen, Y.T., Scanlan, M.J., Ritter, G., Jongeneel, C.V., Simpson, A.J., and Old, L.J. (2004). Identification of the gonad-specific anion transporter SLCO6A1 as a cancer/testis (CT) antigen expressed in human lung cancer. Cancer Immun *4*, 13.

Lendvai, N., Gnjatic, S., Ritter, E., Mangone, M., Austin, W., Reyner, K., Jayabalan, D., Niesvizky, R., Jagannath, S., Bhardwaj, N.*, et al.* (2010). Cellular immune responses against CT7 (MAGE-C1) and humoral responses against other cancer-testis antigens in multiple myeloma patients. Cancer Immun *10*, 4.

Lethe, B., Lucas, S., Michaux, L., De Smet, C., Godelaine, D., Serrano, A., De Plaen, E., and Boon, T. (1998). LAGE-1, a new gene with tumor specificity. Int J Cancer *76*, 903-908.

Li, M., Yuan, Y.H., Han, Y., Liu, Y.X., Yan, L., Wang, Y., and Gu, J. (2005). Expression profile of cancer-testis genes in 121 human colorectal cancer tissue and adjacent normal tissue. Clin Cancer Res *11*, 1809-1814.

Li, P., Nijhawan, D., Budihardjo, I., Srinivasula, S.M., Ahmad, M., Alnemri, E.S., and Wang, X. (1997). Cytochrome c and dATP-dependent formation of Apaf-1/caspase-9 complex initiates an apoptotic protease cascade. Cell *91*, 479-489.

Lifantseva, N., Koltsova, A., Krylova, T., Yakovleva, T., Poljanskaya, G., and Gordeeva, O. (2011). Expression patterns of cancer-testis antigens in human embryonic stem cells and their cell derivatives indicate lineage tracks. Stem Cells Int *2011*, 795239.

Liggins, A.P., Brown, P.J., Asker, K., Pulford, K., and Banham, A.H. (2004). A novel diffuse large B-cell lymphoma-associated cancer testis antigen encoding a PAS domain protein. Br J Cancer *91*, 141-149.

Lin, C., Mak, S., Meitner, P.A., Wolf, J.M., Bluman, E.M., Block, J.A., and Terek, R.M. (2002). Cancer/testis antigen CSAGE is concurrently expressed with MAGE in chondrosarcoma. Gene *285*, 269-278.

Linley, A.J., Ahmad, M., and Rees, R.C. (2011). Tumour-associated antigens: considerations for their use in tumour immunotherapy. Int J Hematol *93*, 263-273.

Liu, W., Cheng, S., Asa, S.L., and Ezzat, S. (2008). The melanoma-associated antigen A3 mediates fibronectin-controlled cancer progression and metastasis. Cancer Res *68*, 8104-8112.

Liu, Y., and Chang, A. (2008). Heat shock response relieves ER stress. EMBO J *27*, 1049-1059.

Liu, Y., Elf, S.E., Miyata, Y., Sashida, G., Huang, G., Di Giandomenico, S., Lee, J.M., Deblasio, A., Menendez, S., Antipin, J.*, et al.* (2009). p53 regulates hematopoietic stem cell quiescence. Cell Stem Cell *4*, 37-48.

Liu, Y., Sakamoto, H., Adachi, M., Zhao, S., Ukai, W., Hashimoto, E., Hareyama, M., Ishida, T., Imai, K., and Shinomura, Y. (2012). Heat stress activates ER stress signals which suppress the heat shock response, an effect occurring preferentially in the cortex in rats. Mol Biol Rep *39*, 3987-3993.

Liu, Z., Miao, D., Xia, Q., Hermo, L., and Wing, S.S. (2007). Regulated expression of the ubiquitin protein ligase, E3(Histone)/LASU1/Mule/ARF-BP1/HUWE1, during spermatogenesis. Dev Dyn *236*, 2889-2898.

Loeffler, M., and Kroemer, G. (2000). The mitochondrion in cell death control: certainties and incognita. Exp Cell Res *256*, 19-26.

Loukinov, D.I., Pugacheva, E., Vatolin, S., Pack, S.D., Moon, H., Chernukhin, I., Mannan, P., Larsson, E., Kanduri, C., Vostrov, A.A.*, et al.* (2002). BORIS, a novel male germ-line-specific protein associated with epigenetic reprogramming events, shares the same 11-zinc-finger domain with CTCF, the insulator protein involved in reading imprinting marks in the soma. Proc Natl Acad Sci U S A *99*, 6806-6811.

Lu, Y., Zhang, K., Li, C., Yao, Y., Tao, D., Liu, Y., Zhang, S., and Ma, Y. (2012). Piwil2 suppresses p53 by inducing phosphorylation of signal transducer and activator of transcription 3 in tumor cells. PLoS One *7*, e30999.

Lucas, S., De Plaen, E., and Boon, T. (2000). MAGE-B5, MAGE-B6, MAGE-C2, and MAGE-C3: four new members of the MAGE family with tumor-specific expression. Int J Cancer *87*, 55-60.

Lucas, S., De Smet, C., Arden, K.C., Viars, C.S., Lethe, B., Lurquin, C., and Boon, T. (1998). Identification of a new MAGE gene with tumor-specific expression by representational difference analysis. Cancer Res *58*, 743-752.

Luo, X., Budihardjo, I., Zou, H., Slaughter, C., and Wang, X. (1998). Bid, a Bcl2 interacting protein, mediates cytochrome c release from mitochondria in response to activation of cell surface death receptors. Cell *94*, 481-490.

Ma, Y., and Hendershot, L.M. (2004). ER chaperone functions during normal and stress conditions. J Chem Neuroanat *28*, 51-65.

Madsen, B., Tarsounas, M., Burchell, J.M., Hall, D., Poulsom, R., and Taylor-Papadimitriou, J. (2003). PLU-1, a transcriptional repressor and putative testis-cancer antigen, has a specific expression and localisation pattern during meiosis. Chromosoma *112*, 124-132.

Mahindra, A., Laubach, J., Raje, N., Munshi, N., Richardson, P.G., and Anderson, K. (2012). Latest advances and current challenges in the treatment of multiple myeloma. Nat Rev Clin Oncol *9*, 135-143.

Marcar, L., Maclaine, N.J., Hupp, T.R., and Meek, D.W. (2010). Mage-A cancer/testis antigens inhibit p53 function by blocking its interaction with chromatin. Cancer Res *70*, 10362-10370.

Marchand, M., van Baren, N., Weynants, P., Brichard, V., Dreno, B., Tessier, M.H., Rankin, E., Parmiani, G., Arienti, F., Humblet, Y.*, et al.* (1999). Tumor regressions observed in patients with metastatic melanoma treated with an antigenic peptide encoded by gene MAGE-3 and presented by HLA-A1. Int J Cancer *80*, 219-230.

Martelange, V., De Smet, C., De Plaen, E., Lurquin, C., and Boon, T. (2000). Identification on a human sarcoma of two new genes with tumor-specific expression. Cancer Res *60*, 3848-3855.

Marusyk, A., Almendro, V., and Polyak, K. (2012). Intra-tumour heterogeneity: a looking glass for cancer? Nat Rev Cancer *12*, 323-334.

Maruyama, K., Usami, M., Aizawa, T., and Yoshikawa, K. (1991). A novel brain-specific mRNA encoding nuclear protein (necdin) expressed in neurally differentiated embryonal carcinoma cells. Biochem Biophys Res Commun *178*, 291-296.

Masuda, Y., Sasaki, A., Shibuya, H., Ueno, N., Ikeda, K., and Watanabe, K. (2001). Dlxin-1, a novel protein that binds Dlx5 and regulates its transcriptional function. J Biol Chem *276*, 5331-5338.

Matsumoto, K., Taniura, H., Uetsuki, T., and Yoshikawa, K. (2001). Necdin acts as a transcriptional repressor that interacts with multiple guanosine clusters. Gene *272*, 173-179.

Maurer, U., Charvet, C., Wagman, A.S., Dejardin, E., and Green, D.R. (2006). Glycogen synthase kinase-3 regulates mitochondrial outer membrane permeabilization and apoptosis by destabilization of MCL-1. Mol Cell *21*, 749-760.

McCurdy, D.K., Tai, L.Q., Nguyen, J., Wang, Z., Yang, H.M., Udar, N., Naiem, F., Concannon, P., and Gatti, R.A. (1998). MAGE Xp-2: a member of the MAGE gene family isolated from an expression library using systemic lupus erythematosus sera. Mol Genet Metab *63*, 3-13.

McCurrach, M.E., Connor, T.M., Knudson, C.M., Korsmeyer, S.J., and Lowe, S.W. (1997). bax-deficiency promotes drug resistance and oncogenic transformation by attenuating p53-dependent apoptosis. Proc Natl Acad Sci U S A *94*, 2345-2349.

Mei, Y., Du, W., Yang, Y., and Wu, M. (2005). Puma(*)Mcl-1 interaction is not sufficient to prevent rapid degradation of Mcl-1. Oncogene *24*, 7224-7237.

Meng, L., Mohan, R., Kwok, B.H., Elofsson, M., Sin, N., and Crews, C.M. (1999). Epoxomicin, a potent and selective proteasome inhibitor, exhibits in vivo antiinflammatory activity. Proc Natl Acad Sci U S A *96*, 10403-10408.

Menoret, E., Gomez-Bougie, P., Surget, S., Trichet, V., Oliver, L., Pellat-Deceunynck, C., and Amiot, M. (2010). Mcl-1(128-350) fragment induces apoptosis through direct interaction with Bax. FEBS Lett *584*, 487-492.

Meriin, A.B., Gabai, V.L., Yaglom, J., Shifrin, V.I., and Sherman, M.Y. (1998). Proteasome inhibitors activate stress kinases and induce Hsp72. Diverse effects on apoptosis. J Biol Chem *273*, 6373-6379.

Meriin, A.B., Yaglom, J.A., Gabai, V.L., Zon, L., Ganiatsas, S., Mosser, D.D., and Sherman, M.Y. (1999). Protein-damaging stresses activate c-Jun N-terminal kinase via inhibition of its dephosphorylation: a novel pathway controlled by HSP72. Mol Cell Biol *19*, 2547-2555.

Meuwissen, R.L., Offenberg, H.H., Dietrich, A.J., Riesewijk, A., van Iersel, M., and Heyting, C. (1992). A coiled-coil related protein specific for synapsed regions of meiotic prophase chromosomes. EMBO J *11*, 5091-5100.

Michels, J., Johnson, P.W., and Packham, G. (2005). Mcl-1. Int J Biochem Cell Biol *37*, 267-271.

Michels, J., O'Neill, J.W., Dallman, C.L., Mouzakiti, A., Habens, F., Brimmell, M., Zhang, K.Y., Craig, R.W., Marcusson, E.G., Johnson, P.W.*, et al.* (2004). Mcl-1 is required for Akata6 B-lymphoma cell survival and is converted to a cell death molecule by efficient caspase-mediated cleavage. Oncogene *23*, 4818-4827.

Mimura, N., Fulciniti, M., Gorgun, G., Tai, Y.T., Cirstea, D., Santo, L., Hu, Y., Fabre, C., Minami, J., Ohguchi, H.*, et al.* (2012). Blockade of XBP1 splicing by inhibition of IRE1alpha is a promising therapeutic option in multiple myeloma. Blood *119*, 5772-5781.

Mizejewski, G.J. (2002). Biological role of alpha-fetoprotein in cancer: prospects for anticancer therapy. Expert Rev Anticancer Ther *2*, 709-735.

Moenner, M., Pluquet, O., Bouchecareilh, M., and Chevet, E. (2007). Integrated endoplasmic reticulum stress responses in cancer. Cancer Res *67*, 10631-10634.

Monte, M., Simonatto, M., Peche, L.Y., Bublik, D.R., Gobessi, S., Pierotti, M.A., Rodolfo, M., and Schneider, C. (2006). MAGE-A tumor antigens target p53 transactivation function through histone deacetylase recruitment and confer resistance to chemotherapeutic agents. Proc Natl Acad Sci U S A *103*, 11160-11165.

Moon, H.E., Ahn, M.Y., Park, J.A., Min, K.J., Kwon, Y.W., and Kim, K.W. (2005). Negative regulation of hypoxia inducible factor-1alpha by necdin. FEBS Lett *579*, 3797-3801.

Moriniere, J., Rousseaux, S., Steuerwald, U., Soler-Lopez, M., Curtet, S., Vitte, A.L., Govin, J., Gaucher, J., Sadoul, K., Hart, D.J.*, et al.* (2009). Cooperative binding of two acetylation marks on a histone tail by a single bromodomain. Nature *461*, 664-668.

Morishima, N., Nakanishi, K., Takenouchi, H., Shibata, T., and Yasuhiko, Y. (2002). An endoplasmic reticulum stress-specific caspase cascade in apoptosis. Cytochrome c-independent activation of caspase-9 by caspase-12. J Biol Chem *277*, 34287-34294.

Mosser, D.D., Caron, A.W., Bourget, L., Meriin, A.B., Sherman, M.Y., Morimoto, R.I., and Massie, B. (2000). The chaperone function of hsp70 is required for protection against stress-induced apoptosis. Mol Cell Biol *20*, 7146-7159.

Mott, J.L., Kobayashi, S., Bronk, S.F., and Gores, G.J. (2007). mir-29 regulates Mcl-1 protein expression and apoptosis. Oncogene *26*, 6133-6140.

Muraoka, M., Konishi, M., Kikuchi-Yanoshita, R., Tanaka, K., Shitara, N., Chong, J.M., Iwama, T., and Miyaki, M. (1996). p300 gene alterations in colorectal and gastric carcinomas. Oncogene *12*, 1565-1569.

Muscatelli, F., Abrous, D.N., Massacrier, A., Boccaccio, I., Le Moal, M., Cau, P., and Cremer, H. (2000). Disruption of the mouse Necdin gene results in hypothalamic and behavioral alterations reminiscent of the human Prader-Willi syndrome. Hum Mol Genet *9*, 3101-3110.

Muscatelli, F., Walker, A.P., De Plaen, E., Stafford, A.N., and Monaco, A.P. (1995). Isolation and characterization of a MAGE gene family in the Xp21.3 region. Proc Natl Acad Sci U S A *92*, 4987-4991.

Nacerddine, K., Lehembre, F., Bhaumik, M., Artus, J., Cohen-Tannoudji, M., Babinet, C., Pandolfi, P.P., and Dejean, A. (2005). The SUMO pathway is essential for nuclear integrity and chromosome segregation in mice. Dev Cell *9*, 769-779.

Nagao, T., Higashitsuji, H., Nonoguchi, K., Sakurai, T., Dawson, S., Mayer, R.J., Itoh, K., and Fujita, J. (2003). MAGE-A4 interacts with the liver oncoprotein gankyrin and suppresses its tumorigenic activity. The Journal of biological chemistry *278*, 10668-10674.

Naismith, J.H., and Sprang, S.R. (1998). Modularity in the TNF-receptor family. Trends Biochem Sci *23*, 74-79.

Nakada, Y., Taniura, H., Uetsuki, T., Inazawa, J., and Yoshikawa, K. (1998). The human chromosomal gene for necdin, a neuronal growth suppressor, in the Prader-Willi syndrome deletion region. Gene *213*, 65-72.

Nakagawa, T., Zhu, H., Morishima, N., Li, E., Xu, J., Yankner, B.A., and Yuan, J. (2000). Caspase-12 mediates endoplasmic-reticulum-specific apoptosis and cytotoxicity by amyloid-beta. Nature *403*, 98-103.

Nardiello, T., Jungbluth, A.A., Mei, A., Diliberto, M., Huang, X., Dabrowski, A., Andrade, V.C., Wasserstrum, R., Ely, S., Niesvizky, R.*, et al.* (2011). MAGE-A inhibits apoptosis in proliferating myeloma cells through repression of Bax and maintenance of survivin. Clin Cancer Res *17*, 4309-4319.

Narod, S., Lynch, H., Conway, T., Watson, P., Feunteun, J., and Lenoir, G. (1993). Increasing incidence of breast cancer in family with BRCA1 mutation. Lancet *341*, 1101-1102.

Neckers, L. (2002). Hsp90 inhibitors as novel cancer chemotherapeutic agents. Trends Mol Med *8*, S55-61.

Nelson, P.T., Zhang, P.J., Spagnoli, G.C., Tomaszewski, J.E., Pasha, T.L., Frosina, D., Caballero, O.L., Simpson, A.J., Old, L.J., and Jungbluth, A.A. (2007). Cancer/testis (CT) antigens are expressed in fetal ovary. Cancer Immun *7*, 1.

Nencioni, A., and Brossart, P. (2004). Cellular immunotherapy with dendritic cells in cancer: current status. Stem Cells *22*, 501-513.

Nicholaou, T., Ebert, L., Davis, I.D., Robson, N., Klein, O., Maraskovsky, E., Chen, W., and Cebon, J. (2006). Directions in the immune targeting of cancer: lessons learned from the cancer-testis Ag NY-ESO-1. Immunol Cell Biol *84*, 303-317.

Nicholaou, T., Ebert, L.M., Davis, I.D., McArthur, G.A., Jackson, H., Dimopoulos, N., Tan, B., Maraskovsky, E., Miloradovic, L., Hopkins, W.*, et al.* (2009). Regulatory T-cell-mediated attenuation of T-cell responses to the NY-ESO-1 ISCOMATRIX vaccine in patients with advanced malignant melanoma. Clin Cancer Res *15*, 2166-2173.

Nicoletti, I., Migliorati, G., Pagliacci, M.C., Grignani, F., and Riccardi, C. (1991). A rapid and simple method for measuring thymocyte apoptosis by propidium iodide staining and flow cytometry. J Immunol Methods *139*, 271-279.

Nijhawan, D., Fang, M., Traer, E., Zhong, Q., Gao, W., Du, F., and Wang, X. (2003). Elimination of Mcl-1 is required for the initiation of apoptosis following ultraviolet irradiation. Genes Dev *17*, 1475-1486.

Norbury, C., and Nurse, P. (1992). Animal cell cycles and their control. Annual review of biochemistry *61*, 441-470.

Oba-Shinjo, S.M., Caballero, O.L., Jungbluth, A.A., Rosemberg, S., Old, L.J., Simpson, A.J., and Marie, S.K. (2008). Cancer-testis (CT) antigen expression in medulloblastoma. Cancer Immun *8*, 7.

Obeng, E.A., Carlson, L.M., Gutman, D.M., Harrington, W.J., Jr., Lee, K.P., and Boise, L.H. (2006). Proteasome inhibitors induce a terminal unfolded protein response in multiple myeloma cells. Blood *107*, 4907-4916.

Oberthuer, A., Hero, B., Spitz, R., Berthold, F., and Fischer, M. (2004). The tumor-associated antigen PRAME is universally expressed in high-stage neuroblastoma and associated with poor outcome. Clin Cancer Res *10*, 4307-4313.

Oehler, V.G., Guthrie, K.A., Cummings, C.L., Sabo, K., Wood, B.L., Gooley, T., Yang, T., Epping, M.T., Shou, Y., Pogosova-Agadjanyan, E.*, et al.* (2009). The preferentially expressed antigen in melanoma (PRAME) inhibits myeloid differentiation in normal hematopoietic and leukemic progenitor cells. Blood *114*, 3299-3308.

Ohlsson, R., Renkawitz, R., and Lobanenkov, V. (2001). CTCF is a uniquely versatile transcription regulator linked to epigenetics and disease. Trends Genet *17*, 520-527.

Ohminami, H., Yasukawa, M., and Fujita, S. (2000). HLA class I-restricted lysis of leukemia cells by a CD8(+) cytotoxic T-lymphocyte clone specific for WT1 peptide. Blood *95*, 286-293.

Oi, S., Natsume, A., Ito, M., Kondo, Y., Shimato, S., Maeda, Y., Saito, K., and Wakabayashi, T. (2009). Synergistic induction of NY-ESO-1 antigen expression by a novel histone deacetylase inhibitor, valproic acid, with 5-aza-2'-deoxycytidine in glioma cells. J Neurooncol *92*, 15-22.

Okura, T., Gong, L., Kamitani, T., Wada, T., Okura, I., Wei, C.F., Chang, H.M., and Yeh, E.T. (1996). Protection against Fas/APO-1- and tumor necrosis factor-mediated cell death by a novel protein, sentrin. J Immunol *157*, 4277-4281.

Old, L.J. (2001). Cancer/testis (CT) antigens - a new link between gametogenesis and cancer. Cancer Immun *1*, 1.

Ono, T., Kurashige, T., Harada, N., Noguchi, Y., Saika, T., Niikawa, N., Aoe, M., Nakamura, S., Higashi, T., Hiraki, A.*, et al.* (2001). Identification of proacrosin binding protein sp32 precursor as a human cancer/testis antigen. Proc Natl Acad Sci U S A *98*, 3282-3287.

Palumbo, A., and Anderson, K. (2011). Multiple myeloma. N Engl J Med *364*, 1046-1060.

Pan, J., Eckardt, S., Leu, N.A., Buffone, M.G., Zhou, J., Gerton, G.L., McLaughlin, K.J., and Wang, P.J. (2009). Inactivation of Nxf2 causes defects in male meiosis and age-dependent depletion of spermatogonia. Dev Biol *330*, 167-174.

Panelli, M.C., Bettinotti, M.P., Lally, K., Ohnmacht, G.A., Li, Y., Robbins, P., Riker, A., Rosenberg, S.A., and Marincola, F.M. (2000). A tumor-infiltrating lymphocyte from a melanoma metastasis with decreased expression of melanoma differentiation antigens recognizes MAGE-12. J Immunol *164*, 4382-4392.

Pardee, A.B. (1989). G1 events and regulation of cell proliferation. Science *246*, 603-608.

Park, H.J., Yu, E., and Shim, Y.H. (2006). DNA methyltransferase expression and DNA hypermethylation in human hepatocellular carcinoma. Cancer Lett *233*, 271-278.

Park, J.H., Kong, G.H., and Lee, S.W. (2002). hMAGE-A1 overexpression reduces TNF-alpha cytotoxicity in ME-180 cells. Mol Cells *14*, 122-129.

Parsell, D.A., Taulien, J., and Lindquist, S. (1993). The role of heat-shock proteins in thermotolerance. Philos Trans R Soc Lond B Biol Sci *339*, 279-285; discussion 285-276.

Patard, J.J., Brasseur, F., Gil-Diez, S., Radvanyi, F., Marchand, M., Francois, P., Abi-Aad, A., Van Cangh, P., Abbou, C.C., Chopin, D.*, et al.* (1995). Expression of MAGE genes in transitional-cell carcinomas of the urinary bladder. Int J Cancer *64*, 60-64.

Pattle, S.B., and Farrell, P.J. (2006). The role of Epstein-Barr virus in cancer. Expert Opin Biol Ther *6*, 1193-1205.

Peche, L.Y., Scolz, M., Ladelfa, M.F., Monte, M., and Schneider, C. (2011). MageA2 restrains cellular senescence by targeting the function of PMLIV/p53 axis at the PML-NBs. Cell Death Differ.

Peikert, T., Specks, U., Farver, C., Erzurum, S.C., and Comhair, S.A. (2006). Melanoma antigen A4 is expressed in non-small cell lung cancers and promotes apoptosis. Cancer research *66*, 4693-4700.

Peng, D.F., Kanai, Y., Sawada, M., Ushijima, S., Hiraoka, N., Kitazawa, S., and Hirohashi, S. (2006). DNA methylation of multiple tumor-related genes in association with overexpression of DNA methyltransferase 1 (DNMT1) during multistage carcinogenesis of the pancreas. Carcinogenesis *27*, 1160-1168.

Peoples, G.E., Goedegebuure, P.S., Smith, R., Linehan, D.C., Yoshino, I., and Eberlein, T.J. (1995). Breast and ovarian cancer-specific cytotoxic T lymphocytes recognize the same HER2/neu-derived peptide. Proc Natl Acad Sci U S A *92*, 432-436.

Perez, D., Hauswirth, F., Jager, D., Metzger, U., Samartzis, E.P., Went, P., and Jungbluth, A. (2011). Protein expression of cancer testis antigens predicts tumor recurrence and treatment response to imatinib in gastrointestinal stromal tumors. Int J Cancer *128*, 2947-2952.

Pessina, P., Conti, V., Tonlorenzi, R., Touvier, T., Meneveri, R., Cossu, G., and Brunelli, S. (2011). Necdin enhances muscle reconstitution of dystrophic muscle by vessel-associated progenitors, by promoting cell survival and myogenic differentiation. Cell Death Differ.

Pickart, C.M. (2001). Mechanisms underlying ubiquitination. Annu Rev Biochem *70*, 503-533.

Pivot-Pajot, C., Caron, C., Govin, J., Vion, A., Rousseaux, S., and Khochbin, S. (2003). Acetylation-dependent chromatin reorganization by BRDT, a testis-specific bromodomain-containing protein. Mol Cell Biol *23*, 5354-5365.

Pizzo, P., and Pozzan, T. (2007). Mitochondria-endoplasmic reticulum choreography: structure and signaling dynamics. Trends Cell Biol *17*, 511-517.

Plummer, M., and Franceschi, S. (2002). Strategies for HPV prevention. Virus Res *89*, 285-293.

Pointud, J.C., Mengus, G., Brancorsini, S., Monaco, L., Parvinen, M., Sassone-Corsi, P., and Davidson, I. (2003). The intracellular localisation of TAF7L, a paralogue of transcription factor TFIID subunit TAF7, is developmentally regulated during male germ-cell differentiation. J Cell Sci *116*, 1847-1858.

Por, E., Byun, H.J., Lee, E.J., Lim, J.H., Jung, S.Y., Park, I., Kim, Y.M., Jeoung, D.I., and Lee, H. (2010). The cancer/testis antigen CAGE with oncogenic potential stimulates cell proliferation by up-regulating cyclins D1 and E in an AP-1- and E2F-dependent manner. J Biol Chem *285*, 14475-14485.

Primakoff, P., and Myles, D.G. (2000). The ADAM gene family: surface proteins with adhesion and protease activity. Trends Genet *16*, 83-87.

Rajagopalan, K., Mooney, S.M., Parekh, N., Getzenberg, R.H., and Kulkarni, P. (2011). A majority of the cancer/testis antigens are intrinsically disordered proteins. J Cell Biochem *112*, 3256-3267.

Rao, M., Chinnasamy, N., Hong, J.A., Zhang, Y., Zhang, M., Xi, S., Liu, F., Marquez, V.E., Morgan, R.A., and Schrump, D.S. (2011). Inhibition of histone lysine methylation enhances cancer-testis antigen expression in lung cancer cells: implications for adoptive immunotherapy of cancer. Cancer Res *71*, 4192-4204.

Rao, R.V., Castro-Obregon, S., Frankowski, H., Schuler, M., Stoka, V., del Rio, G., Bredesen, D.E., and Ellerby, H.M. (2002). Coupling endoplasmic reticulum stress to the cell death program. An Apaf-1-independent intrinsic pathway. J Biol Chem *277*, 21836-21842.

Rao, R.V., Ellerby, H.M., and Bredesen, D.E. (2004). Coupling endoplasmic reticulum stress to the cell death program. Cell Death Differ *11*, 372-380.

Reis, C.A., Osorio, H., Silva, L., Gomes, C., and David, L. (2010). Alterations in glycosylation as biomarkers for cancer detection. J Clin Pathol *63*, 322-329.

Ren, J., Gao, X., Jin, C., Zhu, M., Wang, X., Shaw, A., Wen, L., Yao, X., and Xue, Y. (2009). Systematic study of protein sumoylation: Development of a site-specific predictor of SUMOsp 2.0. Proteomics *9*, 3409-3412.

Ren, R. (2005). Mechanisms of BCR-ABL in the pathogenesis of chronic myelogenous leukaemia. Nat Rev Cancer *5*, 172-183.

Ribas, A., Butterfield, L.H., Glaspy, J.A., and Economou, J.S. (2003). Current developments in cancer vaccines and cellular immunotherapy. J Clin Oncol *21*, 2415-2432.

Richter, K., Haslbeck, M., and Buchner, J. (2010). The heat shock response: life on the verge of death. Mol Cell *40*, 253-266.

Riener, M.O., Wild, P.J., Soll, C., Knuth, A., Jin, B., Jungbluth, A., Hellerbrand, C., Clavien, P.A., Moch, H., and Jochum, W. (2009). Frequent expression of the novel cancer testis antigen MAGE-C2/CT-10 in hepatocellular carcinoma. Int J Cancer *124*, 352-357.

Rimoldi, D., Salvi, S., Reed, D., Coulie, P., Jongeneel, V.C., De Plaen, E., Brasseur, F., Rodriguez, A.M., Boon, T., and Cerottini, J.C. (1999). cDNA and protein characterization of human MAGE-10. Int J Cancer *82*, 901-907.

Rinkenberger, J.L., Horning, S., Klocke, B., Roth, K., and Korsmeyer, S.J. (2000). Mcl-1 deficiency results in peri-implantation embryonic lethality. Genes Dev *14*, 23-27.

Robertson, K.D., and Wolffe, A.P. (2000). DNA methylation in health and disease. Nat Rev Genet *1*, 11-19.

Rock, K.L., Gramm, C., Rothstein, L., Clark, K., Stein, R., Dick, L., Hwang, D., and Goldberg, A.L. (1994). Inhibitors of the proteasome block the degradation of most cell proteins and the generation of peptides presented on MHC class I molecules. Cell *78*, 761-771.

Rodriguez, M.S., Desterro, J.M., Lain, S., Midgley, C.A., Lane, D.P., and Hay, R.T. (1999). SUMO-1 modification activates the transcriptional response of p53. EMBO J *18*, 6455-6461.

Roesch, A., Fukunaga-Kalabis, M., Schmidt, E.C., Zabierowski, S.E., Brafford, P.A., Vultur, A., Basu, D., Gimotty, P., Vogt, T., and Herlyn, M. (2010). A temporarily distinct subpopulation of slow-cycling melanoma cells is required for continuous tumor growth. Cell *141*, 583-594.

Roldan, E.R. (1998). Role of phospholipases during sperm acrosomal exocytosis. Front Biosci *3*, D1109-1119.

Romanienko, P.J., and Camerini-Otero, R.D. (1999). Cloning, characterization, and localization of mouse and human SPO11. Genomics *61*, 156-169.

Rosenberg, S.A., and Dudley, M.E. (2009). Adoptive cell therapy for the treatment of patients with metastatic melanoma. Curr Opin Immunol *21*, 233-240.

Rosenberg, S.A., Restifo, N.P., Yang, J.C., Morgan, R.A., and Dudley, M.E. (2008). Adoptive cell transfer: a clinical path to effective cancer immunotherapy. Nat Rev Cancer *8*, 299-308.

Rosenberg, S.A., Yang, J.C., and Restifo, N.P. (2004). Cancer immunotherapy: moving beyond current vaccines. Nat Med *10*, 909-915.

Ross, M.T., Grafham, D.V., Coffey, A.J., Scherer, S., McLay, K., Muzny, D., Platzer, M., Howell, G.R., Burrows, C., Bird, C.P.*, et al.* (2005). The DNA sequence of the human X chromosome. Nature *434*, 325-337.

Saburi, S., Nadano, D., Akama, T.O., Hirama, K., Yamanouchi, K., Naito, K., Tojo, H., Tachi, C., and Fukuda, M.N. (2001). The trophinin gene encodes a novel group of MAGE proteins, magphinins, and regulates cell proliferation during gametogenesis in the mouse. J Biol Chem *276*, 49378-49389.

Saelens, X., Festjens, N., Vande Walle, L., van Gurp, M., van Loo, G., and Vandenabeele, P. (2004). Toxic proteins released from mitochondria in cell death. Oncogene *23*, 2861-2874.

Sahin, U., Tureci, O., Chen, Y.T., Seitz, G., Villena-Heinsen, C., Old, L.J., and Pfreundschuh, M. (1998). Expression of multiple cancer/testis (CT) antigens in breast cancer and melanoma: basis for polyvalent CT vaccine strategies. Int J Cancer *78*, 387-389.

Sahota, S.S., Goonewardena, C.M., Cooper, C.D., Liggins, A.P., Ait-Tahar, K., Zojer, N., Stevenson, F.K., Banham, A.H., and Pulford, K. (2006). PASD1 is a potential multiple myeloma-associated antigen. Blood *108*, 3953-3955.

Sakurai, E., Maesawa, C., Shibazaki, M., Yasuhira, S., Oikawa, H., Sato, M., Tsunoda, K., Ishikawa, Y., Watanabe, A., Takahashi, K.*, et al.* (2011). Downregulation of microRNA-211 is involved in expression of preferentially expressed antigen of melanoma in melanoma cells. Int J Oncol *39*, 665-672.

Sakurai, T., Itoh, K., Higashitsuji, H., Nagao, T., Nonoguchi, K., Chiba, T., and Fujita, J. (2004). A cleaved form of MAGE-A4 binds to Miz-1 and induces apoptosis in human cells. The Journal of biological chemistry *279*, 15505-15514.

Salehi, A.H., Roux, P.P., Kubu, C.J., Zeindler, C., Bhakar, A., Tannis, L.L., Verdi, J.M., and Barker, P.A. (2000). NRAGE, a novel MAGE protein, interacts with the p75 neurotrophin receptor and facilitates nerve growth factor-dependent apoptosis. Neuron *27*, 279-288.

Salehi, A.H., Xanthoudakis, S., and Barker, P.A. (2002). NRAGE, a p75 neurotrophin receptor-interacting protein, induces caspase activation and cell death through a JNK-dependent mitochondrial pathway. J Biol Chem *277*, 48043-48050.

Sang, M., Wang, L., Ding, C., Zhou, X., Wang, B., Lian, Y., and Shan, B. (2011). Melanoma-associated antigen genes - an update. Cancer Lett *302*, 85-90.
Sarge, K.D., and Park-Sarge, O.K. (2009). Sumoylation and human disease pathogenesis. Trends Biochem Sci *34*, 200-205.

Satie, A.P., Rajpert-De Meyts, E., Spagnoli, G.C., Henno, S., Olivo, L., Jacobsen, G.K., Rioux-Leclercq, N., Jegou, B., and Samson, M. (2002). The cancer-testis gene, NY-ESO-1, is expressed in normal fetal and adult testes and in spermatocytic seminomas and testicular carcinoma in situ. Laboratory investigation; a journal of technical methods and pathology *82*, 775-780.

Savill, J., and Fadok, V. (2000). Corpse clearance defines the meaning of cell death. Nature *407*, 784-788.

Scaffidi, C., Fulda, S., Srinivasan, A., Friesen, C., Li, F., Tomaselli, K.J., Debatin, K.M., Krammer, P.H., and Peter, M.E. (1998). Two CD95 (APO-1/Fas) signaling pathways. EMBO J *17*, 1675-1687.

Scanlan, M.J., Altorki, N.K., Gure, A.O., Williamson, B., Jungbluth, A., Chen, Y.T., and Old, L.J. (2000). Expression of cancer-testis antigens in lung cancer: definition of bromodomain testis-specific gene (BRDT) as a new CT gene, CT9. Cancer Lett *150*, 155-164.

Scanlan, M.J., Gordon, C.M., Williamson, B., Lee, S.Y., Chen, Y.T., Stockert, E., Jungbluth, A., Ritter, G., Jager, D., Jager, E.*, et al.* (2002a). Identification of cancer/testis genes by database mining and mRNA expression analysis. Int J Cancer *98*, 485-492.

Scanlan, M.J., Gure, A.O., Jungbluth, A.A., Old, L.J., and Chen, Y.T. (2002b). Cancer/testis antigens: an expanding family of targets for cancer immunotherapy. Immunol Rev *188*, 22-32.

Scanlan, M.J., Simpson, A.J., and Old, L.J. (2004). The cancer/testis genes: review, standardization, and commentary. Cancer Immun *4*, 1.

Schiffman, M., Castle, P.E., Jeronimo, J., Rodriguez, A.C., and Wacholder, S. (2007). Human papillomavirus and cervical cancer. Lancet *370*, 890-907.

Schroder, M., and Kaufman, R.J. (2005). The mammalian unfolded protein response. Annu Rev Biochem *74*, 739-789.

Schultz, J. (2003). Success of vaccine offers promise of cervical cancer prevention. J Natl Cancer Inst *95*, 102-104.

Schuster, M., Nechansky, A., and Kircheis, R. (2006). Cancer immunotherapy. Biotechnol J *1*, 138-147.

Schwickart, M., Huang, X., Lill, J.R., Liu, J., Ferrando, R., French, D.M., Maecker, H., O'Rourke, K., Bazan, F., Eastham-Anderson, J.*, et al.* (2010). Deubiquitinase USP9X stabilizes MCL1 and promotes tumour cell survival. Nature *463*, 103-107.

Seiter, S., Monsurro, V., Nielsen, M.B., Wang, E., Provenzano, M., Wunderlich, J.R., Rosenberg, S.A., and Marincola, F.M. (2002). Frequency of MART-1/MelanA and gp100/PMel17-specific T cells in tumor metastases and cultured tumor-infiltrating lymphocytes. J Immunother *25*, 252-263.

Serrano, A., Tanzarella, S., Lionello, I., Mendez, R., Traversari, C., Ruiz-Cabello, F., and Garrido, F. (2001). Rexpression of HLA class I antigens and restoration of antigen-specific CTL response in melanoma cells following 5-aza-2'-deoxycytidine treatment. Int J Cancer *94*, 243-251.

Seufert, W., Futcher, B., and Jentsch, S. (1995). Role of a ubiquitin-conjugating enzyme in degradation of S- and M-phase cyclins. Nature *373*, 78-81.

Shan, J., Yuan, L., Xiao, Q., Chiorazzi, N., Budman, D., Teichberg, S., and Xu, H.P. (2002). TSP50, a possible protease in human testes, is activated in breast cancer epithelial cells. Cancer Res *62*, 290-294.

Shan, J., Zhao, W., and Gu, W. (2009). Suppression of cancer cell growth by promoting cyclin D1 degradation. Mol Cell *36*, 469-476.

Shang, E., Nickerson, H.D., Wen, D., Wang, X., and Wolgemuth, D.J. (2007). The first bromodomain of Brdt, a testis-specific member of the BET sub-family of double-bromodomain-containing proteins, is essential for male germ cell differentiation. Development *134*, 3507-3515.

Sharma, A., Bode, B., Wenger, R.H., Lehmann, K., Sartori, A.A., Moch, H., Knuth, A., Boehmer, L., and Broek, M. (2011). gamma-radiation promotes immunological recognition of cancer cells through increased expression of cancer-testis antigens in vitro and in vivo. PLoS One *6*, e28217.

Shim, H., Lee, H., and Jeoung, D. (2006). Cancer/testis antigen cancer-associated gene (CAGE) promotes motility of cancer cells through activation of focal adhesion kinase (FAK). Biotechnol Lett *28*, 2057-2063.

Shore, G.C., Papa, F.R., and Oakes, S.A. (2011). Signaling cell death from the endoplasmic reticulum stress response. Curr Opin Cell Biol *23*, 143-149.

Shuda, M., Kondoh, N., Imazeki, N., Tanaka, K., Okada, T., Mori, K., Hada, A., Arai, M., Wakatsuki, T., Matsubara, O.*, et al.* (2003). Activation of the ATF6, XBP1 and grp78 genes in

human hepatocellular carcinoma: a possible involvement of the ER stress pathway in hepatocarcinogenesis. J Hepatol *38*, 605-614.

Sigalotti, L., Coral, S., Altomonte, M., Natali, L., Gaudino, G., Cacciotti, P., Libener, R., Colizzi, F., Vianale, G., Martini, F.*, et al.* (2002a). Cancer testis antigens expression in mesothelioma: role of DNA methylation and bioimmunotherapeutic implications. Br J Cancer *86*, 979-982.

Sigalotti, L., Coral, S., Nardi, G., Spessotto, A., Cortini, E., Cattarossi, I., Colizzi, F., Altomonte, M., and Maio, M. (2002b). Promoter methylation controls the expression of MAGE2, 3 and 4 genes in human cutaneous melanoma. J Immunother *25*, 16-26.

Sigalotti, L., Covre, A., Zabierowski, S., Himes, B., Colizzi, F., Natali, P.G., Herlyn, M., and Maio, M. (2008). Cancer testis antigens in human melanoma stem cells: expression, distribution, and methylation status. J Cell Physiol *215*, 287-291.

Simon, J.A., and Kingston, R.E. (2009). Mechanisms of polycomb gene silencing: knowns and unknowns. Nat Rev Mol Cell Biol *10*, 697-708.

Simpson, A.J., Caballero, O.L., Jungbluth, A., Chen, Y.T., and Old, L.J. (2005). Cancer/testis antigens, gametogenesis and cancer. Nat Rev Cancer *5*, 615-625.

Singh, S.K., Hawkins, C., Clarke, I.D., Squire, J.A., Bayani, J., Hide, T., Henkelman, R.M., Cusimano, M.D., and Dirks, P.B. (2004). Identification of human brain tumour initiating cells. Nature *432*, 396-401.

Sjoblom, T., Jones, S., Wood, L.D., Parsons, D.W., Lin, J., Barber, T.D., Mandelker, D., Leary, R.J., Ptak, J., Silliman, N.*, et al.* (2006). The consensus coding sequences of human breast and colorectal cancers. Science *314*, 268-274.

Slee, E.A., Harte, M.T., Kluck, R.M., Wolf, B.B., Casiano, C.A., Newmeyer, D.D., Wang, H.G., Reed, J.C., Nicholson, D.W., Alnemri, E.S.*, et al.* (1999). Ordering the cytochrome c-initiated caspase cascade: hierarchical activation of caspases-2, -3, -6, -7, -8, and -10 in a caspase-9-dependent manner. J Cell Biol *144*, 281-292.

Smith, H.A., Cronk, R.J., Lang, J.M., and McNeel, D.G. (2011). Expression and immunotherapeutic targeting of the SSX family of cancer-testis antigens in prostate cancer. Cancer Res *71*, 6785-6795.

Smith, H.A., and McNeel, D.G. (2010). The SSX family of cancer-testis antigens as target proteins for tumor therapy. Clin Dev Immunol *2010*, 150591.

Smith, M.L., Ford, J.M., Hollander, M.C., Bortnick, R.A., Amundson, S.A., Seo, Y.R., Deng, C.X., Hanawalt, P.C., and Fornace, A.J., Jr. (2000). p53-mediated DNA repair responses to UV radiation: studies of mouse cells lacking p53, p21, and/or gadd45 genes. Mol Cell Biol *20*, 3705-3714.

Smith, M.L., and Fornace, A.J., Jr. (1997). p53-mediated protective responses to UV irradiation. Proc Natl Acad Sci U S A *94*, 12255-12257.

Smits, V.A., and Medema, R.H. (2001). Checking out the G(2)/M transition. Biochim Biophys Acta *1519*, 1-12.

Song, Z.B., Bao, Y.L., Zhang, Y., Mi, X.G., Wu, P., Wu, Y., Yu, C.L., Sun, Y., Zheng, L.H., Huang, Y.X.*, et al.* (2011). Testes-specific protease 50 (TSP50) promotes cell proliferation

through the activation of the nuclear factor kappaB (NF-kappaB) signalling pathway. Biochem J *436*, 457-467.

Soulez, M., Saurin, A.J., Freemont, P.S., and Knight, J.C. (1999). SSX and the synovial-sarcoma-specific chimaeric protein SYT-SSX co-localize with the human Polycomb group complex. Oncogene *18*, 2739-2746.

Sriburi, R., Jackowski, S., Mori, K., and Brewer, J.W. (2004). XBP1: a link between the unfolded protein response, lipid biosynthesis, and biogenesis of the endoplasmic reticulum. J Cell Biol *167*, 35-41.

Stanbridge, E.J. (1990). Human tumor suppressor genes. Annu Rev Genet *24*, 615-657.

Stankiewicz, A.R., Livingstone, A.M., Mohseni, N., and Mosser, D.D. (2009). Regulation of heat-induced apoptosis by Mcl-1 degradation and its inhibition by Hsp70. Cell Death Differ *16*, 638-647.

Steinbach, D., Hermann, J., Viehmann, S., Zintl, F., and Gruhn, B. (2002a). Clinical implications of PRAME gene expression in childhood acute myeloid leukemia. Cancer Genet Cytogenet *133*, 118-123.

Steinbach, D., Viehmann, S., Zintl, F., and Gruhn, B. (2002b). PRAME gene expression in childhood acute lymphoblastic leukemia. Cancer Genet Cytogenet *138*, 89-91.

Sternsdorf, T., Puccetti, E., Jensen, K., Hoelzer, D., Will, H., Ottmann, O.G., and Ruthardt, M. (1999). PIC-1/SUMO-1-modified PML-retinoic acid receptor alpha mediates arsenic trioxide-induced apoptosis in acute promyelocytic leukemia. Mol Cell Biol *19*, 5170-5178.

Stevenson, B.J., Iseli, C., Panji, S., Zahn-Zabal, M., Hide, W., Old, L.J., Simpson, A.J., and Jongeneel, C.V. (2007a). Rapid evolution of cancer/testis genes on the X chromosome. BMC Genomics *8*, 129.

Stevenson, L.F., Sparks, A., Allende-Vega, N., Xirodimas, D.P., Lane, D.P., and Saville, M.K. (2007b). The deubiquitinating enzyme USP2a regulates the p53 pathway by targeting Mdm2. EMBO J *26*, 976-986.

Storlazzi, C.T., Mertens, F., Mandahl, N., Gisselsson, D., Isaksson, M., Gustafson, P., Domanski, H.A., and Panagopoulos, I. (2003). A novel fusion gene, SS18L1/SSX1, in synovial sarcoma. Genes Chromosomes Cancer *37*, 195-200.

Sugita, M., Geraci, M., Gao, B., Powell, R.L., Hirsch, F.R., Johnson, G., Lapadat, R., Gabrielson, E., Bremnes, R., Bunn, P.A.*, et al.* (2002). Combined use of oligonucleotide and tissue microarrays identifies cancer/testis antigens as biomarkers in lung carcinoma. Cancer Res *62*, 3971-3979.

Suyama, T., Ohashi, H., Nagai, H., Hatano, S., Asano, H., Murate, T., Saito, H., and Kinoshita, T. (2002). The MAGE-A1 gene expression is not determined solely by methylation status of the promoter region in hematological malignancies. Leuk Res *26*, 1113-1118.

Suyama, T., Shiraishi, T., Zeng, Y., Yu, W., Parekh, N., Vessella, R.L., Luo, J., Getzenberg, R.H., and Kulkarni, P. (2010). Expression of cancer/testis antigens in prostate cancer is associated with disease progression. Prostate *70*, 1778-1787.

Szegezdi, E., Logue, S.E., Gorman, A.M., and Samali, A. (2006). Mediators of endoplasmic reticulum stress-induced apoptosis. EMBO Rep *7*, 880-885.

Szegezdi, E., Macdonald, D.C., Ni Chonghaile, T., Gupta, S., and Samali, A. (2009). Bcl-2 family on guard at the ER. Am J Physiol Cell Physiol *296*, C941-953.

Tajeddine, N., Gala, J.L., Louis, M., Van Schoor, M., Tombal, B., and Gailly, P. (2005). Tumor-associated antigen preferentially expressed antigen of melanoma (PRAME) induces caspase-independent cell death in vitro and reduces tumorigenicity in vivo. Cancer Res *65*, 7348-7355.

Takano, K., Miki, T., Katahira, J., and Yoneda, Y. (2007). NXF2 is involved in cytoplasmic mRNA dynamics through interactions with motor proteins. Nucleic Acids Res *35*, 2513-2521.

Tan, K., Shaw, A.L., Madsen, B., Jensen, K., Taylor-Papadimitriou, J., and Freemont, P.S. (2003). Human PLU-1 Has transcriptional repression properties and interacts with the developmental transcription factors BF-1 and PAX9. J Biol Chem *278*, 20507-20513.

Taniura, H., Matsumoto, K., and Yoshikawa, K. (1999). Physical and functional interactions of neuronal growth suppressor necdin with p53. J Biol Chem *274*, 16242-16248.

Taniura, H., Taniguchi, N., Hara, M., and Yoshikawa, K. (1998). Necdin, a postmitotic neuron-specific growth suppressor, interacts with viral transforming proteins and cellular transcription factor E2F1. J Biol Chem *273*, 720-728.

Tapparel, C., Reymond, A., Girardet, C., Guillou, L., Lyle, R., Lamon, C., Hutter, P., and Antonarakis, S.E. (2003). The TPTE gene family: cellular expression, subcellular localization and alternative splicing. Gene *323*, 189-199.

Tawa, N.E., Jr., Odessey, R., and Goldberg, A.L. (1997). Inhibitors of the proteasome reduce the accelerated proteolysis in atrophying rat skeletal muscles. J Clin Invest *100*, 197-203.

Taylor, B.L., and Zhulin, I.B. (1999). PAS domains: internal sensors of oxygen, redox potential, and light. Microbiol Mol Biol Rev *63*, 479-506.

Thompson, M.P., and Kurzrock, R. (2004). Epstein-Barr virus and cancer. Clin Cancer Res *10*, 803-821.

Tian, X.X., Rai, D., Li, J., Zou, C., Bai, Y., Wazer, D., Band, V., and Gao, Q. (2005). BRCA2 suppresses cell proliferation via stabilizing MAGE-D1. Cancer Res *65*, 4747-4753.

Tinguely, M., Jenni, B., Knights, A., Lopes, B., Korol, D., Rousson, V., Curioni Fontecedro, A., Cogliatti, S.B., Bittermann, A.G., Schmid, U*., et al.* (2008). MAGE-C1/CT-7 expression in plasma cell myeloma: sub-cellular localization impacts on clinical outcome. Cancer Sci *99*, 720-725.

Todd, R., and Wong, D.T. (1999). Oncogenes. Anticancer Res *19*, 4729-4746.

Tsai, W.L., and Chung, R.T. (2010). Viral hepatocarcinogenesis. Oncogene *29*, 2309-2324.

Tseng, Y.H., Butte, A.J., Kokkotou, E., Yechoor, V.K., Taniguchi, C.M., Kriauciunas, K.M., Cypess, A.M., Niinobe, M., Yoshikawa, K., Patti, M.E*., et al.* (2005). Prediction of preadipocyte differentiation by gene expression reveals role of insulin receptor substrates and necdin. Nat Cell Biol *7*, 601-611.

Tunquist, B.J., Woessner, R.D., and Walker, D.H. (2010). Mcl-1 stability determines mitotic cell fate of human multiple myeloma tumor cells treated with the kinesin spindle protein inhibitor ARRY-520. Mol Cancer Ther *9*, 2046-2056.

Tureci, O., Mack, U., Luxemburger, U., Heinen, H., Krummenauer, F., Sester, M., Sester, U., Sybrecht, G.W., and Sahin, U. (2006). Humoral immune responses of lung cancer patients against tumor antigen NY-ESO-1. Cancer Lett *236*, 64-71.

Tureci, O., Sahin, U., Koslowski, M., Buss, B., Bell, C., Ballweber, P., Zwick, C., Eberle, T., Zuber, M., Villena-Heinsen, C.*, et al.* (2002). A novel tumour associated leucine zipper protein targeting to sites of gene transcription and splicing. Oncogene *21*, 3879-3888.

Tureci, O., Sahin, U., Schobert, I., Koslowski, M., Scmitt, H., Schild, H.J., Stenner, F., Seitz, G., Rammensee, H.G., and Pfreundschuh, M. (1996). The SSX-2 gene, which is involved in the t(X;18) translocation of synovial sarcomas, codes for the human tumor antigen HOM-MEL-40. Cancer Res *56*, 4766-4772.

Tureci, O., Sahin, U., Zwick, C., Koslowski, M., Seitz, G., and Pfreundschuh, M. (1998). Identification of a meiosis-specific protein as a member of the class of cancer/testis antigens. Proc Natl Acad Sci U S A *95*, 5211-5216.

Tyagi, P., and Mirakhur, B. (2009). MAGRIT: the largest-ever phase III lung cancer trial aims to establish a novel tumor-specific approach to therapy. Clin Lung Cancer *10*, 371-374.

Uversky, V.N., and Dunker, A.K. (2010). Understanding protein non-folding. Biochim Biophys Acta *1804*, 1231-1264.

van 't Veer, L.J., Dai, H., van de Vijver, M.J., He, Y.D., Hart, A.A., Mao, M., Peterse, H.L., van der Kooy, K., Marton, M.J., Witteveen, A.T.*, et al.* (2002). Gene expression profiling predicts clinical outcome of breast cancer. Nature *415*, 530-536.

van Baren, N., Brasseur, F., Godelaine, D., Hames, G., Ferrant, A., Lehmann, F., Andre, M., Ravoet, C., Doyen, C., Spagnoli, G.C.*, et al.* (1999). Genes encoding tumor-specific antigens are expressed in human myeloma cells. Blood *94*, 1156-1164.

van Baren, N., Chambost, H., Ferrant, A., Michaux, L., Ikeda, H., Millard, I., Olive, D., Boon, T., and Coulie, P.G. (1998). PRAME, a gene encoding an antigen recognized on a human melanoma by cytolytic T cells, is expressed in acute leukaemia cells. Br J Haematol *102*, 1376-1379.

Van den Eynde, B., Peeters, O., De Backer, O., Gaugler, B., Lucas, S., and Boon, T. (1995). A new family of genes coding for an antigen recognized by autologous cytolytic T lymphocytes on a human melanoma. J Exp Med *182*, 689-698.

van der Bruggen, P., Traversari, C., Chomez, P., Lurquin, C., De Plaen, E., Van den Eynde, B., Knuth, A., and Boon, T. (1991). A gene encoding an antigen recognized by cytolytic T lymphocytes on a human melanoma. Science *254*, 1643-1647.

Van Pel, A., van der Bruggen, P., Coulie, P.G., Brichard, V.G., Lethe, B., van den Eynde, B., Uyttenhove, C., Renauld, J.C., and Boon, T. (1995). Genes coding for tumor antigens recognized by cytolytic T lymphocytes. Immunol Rev *145*, 229-250.

Vatolin, S., Abdullaev, Z., Pack, S.D., Flanagan, P.T., Custer, M., Loukinov, D.I., Pugacheva, E., Hong, J.A., Morse, H., 3rd, Schrump, D.S.*, et al.* (2005). Conditional expression of the CTCF-

paralogous transcriptional factor BORIS in normal cells results in demethylation and derepression of MAGE-A1 and reactivation of other cancer-testis genes. Cancer Res *65*, 7751-7762.

Vaughan, H.A., Svobodova, S., Macgregor, D., Sturrock, S., Jungbluth, A.A., Browning, J., Davis, I.D., Parente, P., Chen, Y.T., Stockert, E.*, et al.* (2004). Immunohistochemical and molecular analysis of human melanomas for expression of the human cancer-testis antigens NY-ESO-1 and LAGE-1. Clin Cancer Res *10*, 8396-8404.

Vaux, D.L., Cory, S., and Adams, J.M. (1988). Bcl-2 gene promotes haemopoietic cell survival and cooperates with c-myc to immortalize pre-B cells. Nature *335*, 440-442.

Velazquez, E.F., Jungbluth, A.A., Yancovitz, M., Gnjatic, S., Adams, S., O'Neill, D., Zavilevich, K., Albukh, T., Christos, P., Mazumdar, M.*, et al.* (2007). Expression of the cancer/testis antigen NY-ESO-1 in primary and metastatic malignant melanoma (MM)--correlation with prognostic factors. Cancer Immun *7*, 11.

Vidaeus, C.M., von Kapp-Herr, C., Golden, W.L., Eddy, R.L., Shows, T.B., and Herr, J.C. (1997). Human fertilin beta: identification, characterization, and chromosomal mapping of an ADAM gene family member. Mol Reprod Dev *46*, 363-369.

Viviani, S., Jack, A., Hall, A.J., Maine, N., Mendy, M., Montesano, R., and Whittle, H.C. (1999). Hepatitis B vaccination in infancy in The Gambia: protection against carriage at 9 years of age. Vaccine *17*, 2946-2950.

von Boehmer, L., Keller, L., Mortezavi, A., Provenzano, M., Sais, G., Hermanns, T., Sulser, T., Jungbluth, A.A., Old, L.J., Kristiansen, G.*, et al.* (2011). MAGE-C2/CT10 protein expression is an independent predictor of recurrence in prostate cancer. PLoS One *6*, e21366.

Vucic, D., Dixit, V.M., and Wertz, I.E. (2011). Ubiquitylation in apoptosis: a post-translational modification at the edge of life and death. Nat Rev Mol Cell Biol *12*, 439-452.

Walboomers, J.M., Jacobs, M.V., Manos, M.M., Bosch, F.X., Kummer, J.A., Shah, K.V., Snijders, P.J., Peto, J., Meijer, C.J., and Munoz, N. (1999). Human papillomavirus is a necessary cause of invasive cervical cancer worldwide. J Pathol *189*, 12-19.

Walensky, L.D. (2006). BCL-2 in the crosshairs: tipping the balance of life and death. Cell Death Differ *13*, 1339-1350.

Walker, N.P., Talanian, R.V., Brady, K.D., Dang, L.C., Bump, N.J., Ferenz, C.R., Franklin, S., Ghayur, T., Hackett, M.C., Hammill, L.D.*, et al.* (1994). Crystal structure of the cysteine protease interleukin-1 beta-converting enzyme: a (p20/p10)2 homodimer. Cell *78*, 343-352.

Wang, D., Rayani, S., and Marshall, J.L. (2008). Carcinoembryonic antigen as a vaccine target. Expert Rev Vaccines *7*, 987-993.

Wang, J.C., and Dick, J.E. (2005). Cancer stem cells: lessons from leukemia. Trends in cell biology *15*, 494-501.

Wang, M., Bao, Y.L., Wu, Y., Yu, C.L., Meng, X.Y., Huang, Y.X., Sun, Y., Zheng, L.H., and Li, Y.X. (2010). Basic FGF downregulates TSP50 expression via the ERK/Sp1 pathway. J Cell Biochem *111*, 75-81.

Wang, Q.E., Han, C., Milum, K., and Wani, A.A. (2011). Stem cell protein Piwil2 modulates chromatin modifications upon cisplatin treatment. Mutat Res *708*, 59-68.

Wang, R.F., Robbins, P.F., Kawakami, Y., Kang, X.Q., and Rosenberg, S.A. (1995). Identification of a gene encoding a melanoma tumor antigen recognized by HLA-A31-restricted tumor-infiltrating lymphocytes. J Exp Med *181*, 799-804.

Warr, M.R., Acoca, S., Liu, Z., Germain, M., Watson, M., Blanchette, M., Wing, S.S., and Shore, G.C. (2005). BH3-ligand regulates access of MCL-1 to its E3 ligase. FEBS Lett *579*, 5603-5608.

Warr, M.R., Mills, J.R., Nguyen, M., Lemaire-Ewing, S., Baardsnes, J., Sun, K.L., Malina, A., Young, J.C., Jeyaraju, D.V., O'Connor-McCourt, M.*, et al.* (2011). Mitochondrion-dependent N-terminal processing of outer membrane Mcl-1 protein removes an essential Mule/Lasu1 protein-binding site. J Biol Chem *286*, 25098-25107.

Watari, K., Tojo, A., Nagamura-Inoue, T., Nagamura, F., Takeshita, A., Fukushima, T., Motoji, T., Tani, K., and Asano, S. (2000). Identification of a melanoma antigen, PRAME, as a BCR/ABL-inducible gene. FEBS Lett *466*, 367-371.

Weber, J., Salgaller, M., Samid, D., Johnson, B., Herlyn, M., Lassam, N., Treisman, J., and Rosenberg, S.A. (1994). Expression of the MAGE-1 tumor antigen is up-regulated by the demethylating agent 5-aza-2'-deoxycytidine. Cancer Res *54*, 1766-1771.

Weeraratne, S.D., Amani, V., Neiss, A., Teider, N., Scott, D.K., Pomeroy, S.L., and Cho, Y.J. (2011). miR-34a confers chemosensitivity through modulation of MAGE-A and p53 in medulloblastoma. Neuro Oncol *13*, 165-175.

Wei, M.C., Zong, W.X., Cheng, E.H., Lindsten, T., Panoutsakopoulou, V., Ross, A.J., Roth, K.A., MacGregor, G.R., Thompson, C.B., and Korsmeyer, S.J. (2001). Proapoptotic BAX and BAK: a requisite gateway to mitochondrial dysfunction and death. Science *292*, 727-730.

Wertz, I.E., Kusam, S., Lam, C., Okamoto, T., Sandoval, W., Anderson, D.J., Helgason, E., Ernst, J.A., Eby, M., Liu, J.*, et al.* (2011). Sensitivity to antitubulin chemotherapeutics is regulated by MCL1 and FBW7. Nature *471*, 110-114.

Westbrook, V.A., Schoppee, P.D., Diekman, A.B., Klotz, K.L., Allietta, M., Hogan, K.T., Slingluff, C.L., Patterson, J.W., Frierson, H.F., Irvin, W.P., Jr.*, et al.* (2004). Genomic organization, incidence, and localization of the SPAN-x family of cancer-testis antigens in melanoma tumors and cell lines. Clin Cancer Res *10*, 101-112.

Weynants, P., Thonnard, J., Marchand, M., Delos, M., Boon, T., and Coulie, P.G. (1999). Derivation of tumor-specific cytolytic T-cell clones from two lung cancer patients with long survival. Am J Respir Crit Care Med *159*, 55-62.

Wigley, W.C., Fabunmi, R.P., Lee, M.G., Marino, C.R., Muallem, S., DeMartino, G.N., and Thomas, P.J. (1999). Dynamic association of proteasomal machinery with the centrosome. J Cell Biol *145*, 481-490.

Williams, M.E., Strickland, P., Watanabe, K., and Hinck, L. (2003). UNC5H1 induces apoptosis via its juxtamembrane region through an interaction with NRAGE. J Biol Chem *278*, 17483-17490.

Wischnewski, F., Friese, O., Pantel, K., and Schwarzenbach, H. (2007). Methyl-CpG binding domain proteins and their involvement in the regulation of the MAGE-A1, MAGE-A2, MAGE-A3, and MAGE-A12 gene promoters. Mol Cancer Res *5*, 749-759.

Wischnewski, F., Pantel, K., and Schwarzenbach, H. (2006). Promoter demethylation and histone acetylation mediate gene expression of MAGE-A1, -A2, -A3, and -A12 in human cancer cells. Mol Cancer Res *4*, 339-349.

Wojcik, C. (1997a). An inhibitor of the chymotrypsin-like activity of the proteasome (PSI) induces similar morphological changes in various cell lines. Folia Histochem Cytobiol *35*, 211-214.

Wojcik, C. (1997b). On the spatial organization of ubiquitin-dependent proteolysis in HeLa cells. Folia Histochem Cytobiol *35*, 117-118.

Woloszynska-Read, A., Mhawech-Fauceglia, P., Yu, J., Odunsi, K., and Karpf, A.R. (2008). Intertumor and intratumor NY-ESO-1 expression heterogeneity is associated with promoter-specific and global DNA methylation status in ovarian cancer. Clin Cancer Res *14*, 3283-3290.

Wong, A.J., Ruppert, J.M., Eggleston, J., Hamilton, S.R., Baylin, S.B., and Vogelstein, B. (1986). Gene amplification of c-myc and N-myc in small cell carcinoma of the lung. Science *233*, 461-464.

Wu, S., Hu, Y., Wang, J.L., Chatterjee, M., Shi, Y., and Kaufman, R.J. (2002). Ultraviolet light inhibits translation through activation of the unfolded protein response kinase PERK in the lumen of the endoplasmic reticulum. J Biol Chem *277*, 18077-18083.

Wuilleme-Toumi, S., Trichet, V., Gomez-Bougie, P., Gratas, C., Bataille, R., and Amiot, M. (2007). Reciprocal protection of Mcl-1 and Bim from ubiquitin-proteasome degradation. Biochem Biophys Res Commun *361*, 865-869.

Wyllie, A.H. (1980a). Glucocorticoid-induced thymocyte apoptosis is associated with endogenous endonuclease activation. Nature *284*, 555-556.

Wyllie, A.H., Kerr, J.F., and Currie, A.R. (1980b). Cell death: the significance of apoptosis. Int Rev Cytol *68*, 251-306.

Xiao, J., and Chen, H.S. (2004). Biological functions of melanoma-associated antigens. World J Gastroenterol *10*, 1849-1853.

Xirodimas, D.P., Chisholm, J., Desterro, J.M., Lane, D.P., and Hay, R.T. (2002). P14ARF promotes accumulation of SUMO-1 conjugated (H)Mdm2. FEBS Lett *528*, 207-211.

Xu, H., Shan, J., Jurukovski, V., Yuan, L., Li, J., and Tian, K. (2007). TSP50 encodes a testis-specific protease and is negatively regulated by p53. Cancer Res *67*, 1239-1245.

Xu, H.P., Yuan, L., Shan, J., and Feng, H. (2004). Localization and expression of TSP50 protein in human and rodent testes. Urology *64*, 826-832.

Xu, X., Gupta, S., Hu, W., McGrath, B.C., and Cavener, D.R. (2011). Hyperthermia induces the ER stress pathway. PLoS One *6*, e23740.

Yamane, K., Tateishi, K., Klose, R.J., Fang, J., Fabrizio, L.A., Erdjument-Bromage, H., Taylor-Papadimitriou, J., Tempst, P., and Zhang, Y. (2007). PLU-1 is an H3K4 demethylase involved in transcriptional repression and breast cancer cell proliferation. Mol Cell *25*, 801-812.

Yang, B., O'Herrin, S., Wu, J., Reagan-Shaw, S., Ma, Y., Nihal, M., and Longley, B.J. (2007a). Select cancer testes antigens of the MAGE-A, -B, and -C families are expressed in mast cell lines and promote cell viability in vitro and in vivo. J Invest Dermatol *127*, 267-275.

Yang, B., O'Herrin, S.M., Wu, J., Reagan-Shaw, S., Ma, Y., Bhat, K.M., Gravekamp, C., Setaluri, V., Peters, N., Hoffmann, F.M.*, et al.* (2007b). MAGE-A, mMage-b, and MAGE-C proteins form complexes with KAP1 and suppress p53-dependent apoptosis in MAGE-positive cell lines. Cancer Res *67*, 9954-9962.

Yang, H.J., Liu, V.W., Wang, Y., Tsang, P.C., and Ngan, H.Y. (2006). Differential DNA methylation profiles in gynecological cancers and correlation with clinico-pathological data. BMC Cancer *6*, 212.

Yang, K., Lui, W.O., Xie, Y., Zhang, A., Skytting, B., Mandahl, N., Larsson, C., and Larsson, O. (2002). Co-existence of SYT-SSX1 and SYT-SSX2 fusions in synovial sarcomas. Oncogene *21*, 4181-4190.

Yawata, T., Nakai, E., Park, K.C., Chihara, T., Kumazawa, A., Toyonaga, S., Masahira, T., Nakabayashi, H., Kaji, T., and Shimizu, K. (2010). Enhanced expression of cancer testis antigen genes in glioma stem cells. Mol Carcinog *49*, 532-544.

Yin, D.T., Wang, Q., Chen, L., Liu, M.Y., Han, C., Yan, Q., Shen, R., He, G., Duan, W., Li, J.J.*, et al.* (2011). Germline stem cell gene PIWIL2 mediates DNA repair through relaxation of chromatin. PLoS One *6*, e27154.

Yoneda, T., Imaizumi, K., Oono, K., Yui, D., Gomi, F., Katayama, T., and Tohyama, M. (2001). Activation of caspase-12, an endoplastic reticulum (ER) resident caspase, through tumor necrosis factor receptor-associated factor 2-dependent mechanism in response to the ER stress. J Biol Chem *276*, 13935-13940.

Yoshida, N., Abe, H., Ohkuri, T., Wakita, D., Sato, M., Noguchi, D., Miyamoto, M., Morikawa, T., Kondo, S., Ikeda, H.*, et al.* (2006). Expression of the MAGE-A4 and NY-ESO-1 cancer-testis antigens and T cell infiltration in non-small cell lung carcinoma and their prognostic significance. Int J Oncol *28*, 1089-1098.

Yuan, J., Gnjatic, S., Li, H., Powel, S., Gallardo, H.F., Ritter, E., Ku, G.Y., Jungbluth, A.A., Segal, N.H., Rasalan, T.S.*, et al.* (2008). CTLA-4 blockade enhances polyfunctional NY-ESO-1 specific T cell responses in metastatic melanoma patients with clinical benefit. Proc Natl Acad Sci U S A *105*, 20410-20415.

Zendman, A.J., van Kraats, A.A., den Hollander, A.I., Weidle, U.H., Ruiter, D.J., and van Muijen, G.N. (2002a). Characterization of XAGE-1b, a short major transcript of cancer/testis-associated gene XAGE-1, induced in melanoma metastasis. Int J Cancer *97*, 195-204.

Zendman, A.J., Van Kraats, A.A., Weidle, U.H., Ruiter, D.J., and Van Muijen, G.N. (2002b). The XAGE family of cancer/testis-associated genes: alignment and expression profile in normal tissues, melanoma lesions and Ewing's sarcoma. Int J Cancer *99*, 361-369.

Zendman, A.J., Zschocke, J., van Kraats, A.A., de Wit, N.J., Kurpisz, M., Weidle, U.H., Ruiter, D.J., Weiss, E.H., and van Muijen, G.N. (2003). The human SPANX multigene family: genomic organization, alignment and expression in male germ cells and tumor cell lines. Gene *309*, 125-133.

Zeng, Y., He, Y., Yang, F., Mooney, S.M., Getzenberg, R.H., Orban, J., and Kulkarni, P. (2011). The cancer/testis antigen prostate-associated gene 4 (PAGE4) is a highly intrinsically disordered protein. J Biol Chem *286*, 13985-13994.

Zhang, B., Gojo, I., and Fenton, R.G. (2002). Myeloid cell factor-1 is a critical survival factor for multiple myeloma. Blood *99*, 1885-1893.

Zhang, C., Cai, T.Y., Zhu, H., Yang, L.Q., Jiang, H., Dong, X.W., Hu, Y.Z., Lin, N.M., He, Q.J., and Yang, B. (2011). Synergistic antitumor activity of gemcitabine and ABT-737 in vitro and in vivo through disrupting the interaction of USP9X and Mcl-1. Mol Cancer Ther *10*, 1264-1275.

Zhang, K., and Dent, S.Y. (2005). Histone modifying enzymes and cancer: going beyond histones. J Cell Biochem *96*, 1137-1148.

Zhang, M., Wang, Q., and Huang, Y. (2007). Fragile X mental retardation protein FMRP and the RNA export factor NXF2 associate with and destabilize Nxf1 mRNA in neuronal cells. Proc Natl Acad Sci U S A *104*, 10057-10062.

Zhao, J., Ren, Y., Jiang, Q., and Feng, J. (2003). Parkin is recruited to the centrosome in response to inhibition of proteasomes. J Cell Sci *116*, 4011-4019.

Zhong, Q., Gao, W., Du, F., and Wang, X. (2005). Mule/ARF-BP1, a BH3-only E3 ubiquitin ligase, catalyzes the polyubiquitination of Mcl-1 and regulates apoptosis. Cell *121*, 1085-1095.

Zhuang, R., Zhu, Y., Fang, L., Liu, X.S., Tian, Y., Chen, L.H., Ouyang, W.M., Xu, X.G., Jian, J.L., Gure, A.O.*, et al.* (2006). Generation of monoclonal antibodies to cancer/testis (CT) antigen CT10/MAGE-C2. Cancer Immun *6*, 7.

Ziegler, A., Jonason, A.S., Leffell, D.J., Simon, J.A., Sharma, H.W., Kimmelman, J., Remington, L., Jacks, T., and Brash, D.E. (1994). Sunburn and p53 in the onset of skin cancer. Nature *372*, 773-776.

Zou, W. (2006). Regulatory T cells, tumour immunity and immunotherapy. Nat Rev Immunol *6*, 295-307.